Rapporter och meddelanden 146

Rare earth elements distribution, mineralisation and exploration potential in Sweden

Editor: Martiya Sadeghi

SGU
Sveriges geologiska undersökning
Geological Survey of Sweden

Rapporter och meddelanden 146

Rare earth elements distribution, mineralisation and exploration potential in Sweden

Editor: Martiya Sadeghi

Sveriges geologiska undersökning
2019

ISSN 0349-2176
ISBN 978-91-7403-459-2

Cover photo: Abundant, coarsely crystallised red eudialyte (*sensu lato*) in outcropping pegmatitic grennaite (“PGT”), Norra Kärr. Hand lenses for scale.
Photographer: Erik Jonsson

Editor: Martiya Sadeghi
Head of unit: Ildikó Antal Lundin

Layout: Lina Rönnåsen

Geological Survey of Sweden
Box 670, 751 28 Uppsala
phone: 018-17 90 00
fax: 018-17 92 10
e-mail: sgu@sgu.se
www.sgu.se

TABLE OF CONTENTS

Sammanfattning **4**

Abstract **5**

Introduction **7**
- Rare earth elements 7
- Classification of rare earth element mineralisations in Europe 9

The geology of Sweden **12**
- Tectonic setting 12
- Mineral resources 17

REE mineralisations in Sweden **20**
- REE mineralisation in granitic pegmatites and granitoids 20
- REE mineralisation in alkaline intrusive rocks 36
- REE mineralisation in carbonatitic and ultramafic rocks 42
- REEs in apatite-iron oxide deposits, Norrbotten, northern Sweden 50
- REE mineralisation in apatite-iron oxide deposits, Bergslagen ore province, south-central Sweden 55
- The REE-Fe mineralisations of the Olserum area, southeastern Sweden 60
- The Fe-REE (Bastnäs-type) deposits of the REE line, Bergslagen ore province, south-central Sweden 66
- REE mineralisation in other iron oxide deposits 94
- Secondary/sedimentary REE deposits 106

Distribution of Rare earth elements in Swedish soils and rocks **112**

Geochemistry of REE mineralisations **120**
- Hydrothermal REE mineralisations 120
- Orthomagmatic REE mineralisations 121
- Placer and phosphorite REE mineralisations 122
- REE chemistry in Sweden 122
- Principal component analysis 132

Conceptual models for rare earth element exploration in Sweden **135**
- Key exploration criteria 135
- Conceptual model for rare earth element exploration in Bergslagen 138
- Prospectivity mapping for REE mineralisation in Bergslagen 144

Summary and conclusions **148**

Acknowledgements **150**

References **151**
- List of unpublished references 168

Appendix 1 .... **169**

Appendix 2 .... **177**

SAMMANFATTNING

Denna rapport är ett resultat av EURARE-projektet, vilket bekostades av Europeiska kommissionen för att utveckla en plan för hållbar exploatering av Europas fyndigheter av sällsynta jordartsmetaller (REE).

Projektets huvudmål var att skapa en grund för att kunna utveckla en hållbar värdekedja som säkerställer kontinuerlig tillgång av råmaterial och produkter innehållande REE. Dessa råmaterial och produkter är kritiska för EU:s industrisektorer, som till exempel bil-, elektronik- och kemiindustri.

EURARE-projektet omfattade verksamhet och uppgifter inom områdena geologi, gruvdrift, anrikning, utvinning och lagstiftning kring REE. Projektet sammanställde dessutom en databas av nu kända REE-fyndigheter i EU. Tillsammans med andra nationella geologiska undersökningar arbetade Sveriges geologiska undersökning (SGU) huvudsakligen med de rent geologiska frågorna.

SGU har levererat uppdaterad geologisk information och resursdata om kända REE-mineraliseringar i Sverige. Bakomliggande arbete omfattade dels litteraturstudier av äldre geologiska publikationer och rapporter, dels fältarbete. Litteraturstudierna ledde till en uppdatering av SGU:s fyndighetsdatabas med nya förekomster och till idéer om vidare undersökningar. Fältarbetet bedrevs i områden med kända REE-förekomster. Fler än 200 bergartsprov från utvalda fyndigheter togs för kemisk och mineralogisk analys. Vid provtagningen användes i några fall en bärbar XRF-utrustning för att spåra eventuella förhöjda halter av REE. SGU har också provat hyperspektral IR-analysteknik på olika provmaterial.

REE-mineraliseringarna i Sverige är spridda över hela landet, även om vissa områden har relativt fler förekomster. De vanligaste typerna finns associerade med apatitjärnmalmerna i Norrbotten och Bergslagen, skarnjärnmalmerna i Riddarhytte-Norbergsområdet, det magmatiska komplexet i Norra Kärr samt i Olserum- och Alnöområdena.

Denna rapport presenterar utvalda resultat från fältarbetet och från mineralogiska och petrologiska studier samt geokemiska data och tolkningen av dessa. Samtliga aktiviteter i EURARE-projektet ledde till ökade kunskaper om ett antal fyndigheter och dessutom till att ett par nya upptäcktes. Det är dock också tydligt att flera mineraliseringar skulle behöva studeras ytterligare. Föreliggande rapport ger en omfattande överblick av och inblick i potentialen för REE-mineraliseringar i Sverige och tillför värde för forskningen genom att lyfta det ekonomiska perspektivet på REE.

ABSTRACT

This report is a result of the EURARE project which was funded by the European Commission to address the “Development of a sustainable exploitation scheme for Europe’s Rare Earth Element ore deposits”.

The main goal of the EURARE project was to set a basis for sustainable development of a European REE value chain to safeguard uninterrupted supply of REE raw materials and products. These materials and products are crucial for the EU economy-driven industrial sectors, such as the automotive, electronics, engineering and chemicals industries.

EURARE included activities and tasks on geological resources, mining and beneficiation, extraction and separation, and regulation in relation to REE. In addition, EURARE provides a database of currently known REE deposits within the EU. Alongside other national geological surveys, the Geological Survey of Sweden (SGU) was mainly involved in the geological work undertaken.

SGU delivered updated geological information and resource data on known REE mineralisations in Sweden. The work included an extensive literature review of previous publications and reports, which led to updates of SGU’s national database with additional occurrences, as well as suggestions for new investigations. Field work activities were carried out in several REE-mineralised areas and were followed by analysis of selected mineralisations, as well as new ore classifications. More than 200 rock samples were taken and analysed for chemical composition, and in part for mineralogy and petrographical features in thin and thick sections. For the collection of samples, portable XRF equipment was in some cases tested for the tracing of elevated REE concentrations, and testing also included the use of hyperspectral imaging techniques on different sample materials.

REE occurrences in Sweden are distributed throughout the country, although some regions are better endowed than others. Major deposit types are the apatite-iron oxide mineralisations in Norrbotten and Bergslagen, the skarns of the Riddarhyttan–Norberg belt, the Norra Kärr complex, and the Olserum and Alnö areas

This report presents a selection of results from field work, mineralogical and petrological studies, as well as geochemical data and interpretation. All activities under the EURARE project resulted in knowledge upgrades for a number of REE mineralisations, as well as the discovery of new ones. Several of the mineralisations clearly require further study. The present report provides a comprehensive overview and introduction to REE potential in the bedrock of Sweden, and adds R&D value by raising the REE economic geology perspective.

INTRODUCTION

Martiya Sadeghi, Nikolaos Arvanitidis, Magnus Ripa

This report presents compiled economic geology data and information on rare earth element (REE) mineral resources in Sweden collected during the EURARE project. This project was carried out under the European Commission (EC) FP7 programme to fund a consortium of 23 partners from Europe. The project included work packages (WPs) on geological resources, mining and beneficiation, extraction and separation of the REE, and related legislation (Sadeghi et al., 2017a). The goals of the project were (i) to characterise potential REE resources in Europe; and (ii) to investigate, develop, optimise and demonstrate technologies for efficient and economically viable exploitation of currently available European REE deposits with minimum impact on the environment (www.eurare.org).

Current state-of-the-art processes for REE extraction use complicated, energy- and resource-intensive technologies. REE mineral processing technologies currently used for representative European REE ores will be investigated under the EURARE project. The project aims to improve these techniques by adopting new approaches for complete ore utilisation, minimal environmental impact and by establishing integrated mineral processing systems, with zero or close to zero tailings.

The EURARE project also seeks to demonstrate new sources for REE exploitation from industrial metallurgical waste. This will not only be lucrative but will minimise the overall environmental footprint of the primary European metallurgical industry. The EURARE project managed to deliver and establish a novel sustainable exploitation scheme for Europe's REE deposits.

The Geological Survey of Sweden (SGU) was involved in WP1 (on geological resources). This work package aimed to describe the potentially exploitable REE resources in Europe, focusing on countries known to be promising REE target areas (i.e. Sweden, Norway, Finland and Greece). Work Package 1 also aimed to identify REE demand in Europe, both as a raw material and as intermediate products.

The data and knowledge compiled and created in WP1 are processed and elaborated through the development of an electronic Integrated Knowledge Management system (IKMS), which will lay the foundations for a roadmap to both sustainable REE exploitation and REE material supply autonomy in Europe.

Rare earth elements

Chemically speaking, the rare earth elements (REEs) comprise the 15 lanthanides plus Sc and Y. In normal geological usage, however, the REEs are confined to the lanthanides, and this approach is adopted here. They form a key group of chemically similar metallic elements that are often used to study earth systems (Taylor & McLennan 1985; Prego et al. 2009). The REEs are commonly divided into the light rare earth elements (LREEs), with lower atomic weights and larger atomic radii (lanthanum to europium), and the heavy rare earth elements (HREEs), with higher atomic weights and smaller atomic radii (gadolinium to lutetium). This gradual decrease of atomic radii with increasing atomic number is a characteristic feature of REEs, and is known as the contraction of lanthanides. Scandium and yttrium are often grouped with the REEs because they are chemically similar (Hedrick 1997; Walters et al. 2011). In particular, yttrium is often grouped with the HREEs because of its similar chemical properties (Samson & Wood 2004).

REEs are not found as native elements but occur in a variety of minerals, e.g. oxides (fergusonite), carbonates (bastnäsite), phosphates (monazite), and silicates (allanite). At least 100 minerals are known to incorporate REEs in their crystal structures, while approximately 10 of these minerals contain significant REE concentrations. Currently, only bastnäsite, monazite, and xenotime are primary REE-bearing minerals of economic importance (Richardson & Birkett 1996).

REEs act incompatibly during most magmatic processes and thus concentrate in the final products of magma differentiation and by low degrees of melting (e.g. evolved granites and pegmatites). REEs have been considered relatively immobile during metamorphism and are not easily affected by alteration in surficial environments (Öhlander et al. 1996). However, some studies have indicated that REEs may be mobile during weathering processes, e.g. in till cover in northern Sweden (Öhlander et al. 1991, 1996) and in hydrothermal systems (MacLean 1988).

REE-bearing mineral deposits occur in a range of igneous, sedimentary, and metamorphic rocks. Geological environments in which REEs are enriched can be broadly divided into two categories (Walters et al. 2011): (i) primary deposits associated with igneous and hydrothermal processes; and (ii) secondary deposits concentrated from primary sources by sedimentary processes and weathering. Primary deposits include REEs associated with carbonatites and/or alkaline igneous rocks, REEs associated with iron oxide-copper-gold (IOCG) deposits and hydrothermal deposits (unrelated to alkaline igneous rocks). Secondary deposits include marine placers (including coastal dune deposits formed by aeolian processes), alluvial placers, palaeoplacers, lateritic deposits, and ion-adsorption clays (Walters et al. 2011).

The most significant economic concentrations of REE-bearing minerals worldwide are hosted in, or associated with, alkaline igneous rocks and carbonatites. Within hydrothermal systems, REE-bearing minerals are associated with quartz- and fluorite-bearing veins and occur as breccia-filling. REE-bearing minerals also occur in skarns, in pegmatite and may be concentrated in placer and laterite clay deposits.

Over the last few decades, rare earth metals have found many applications in metallurgy, electronics, the "high-tech" and "green tech" sectors, medicine, military, and many other areas of modern life. This has greatly increased demand for these commodities (e.g. Haxel et al. 2002). There is therefore a need to define the natural background levels of REEs in order to distinguish their crustal variations related to geology and mineralisation from anthropogenic input and contamination (Fedele et al. 2008).

From an economic viewpoint, another important factor in REE accessibility is the market and current global geopolitical conditions. Earlier REE mines, such as the Mountain Pass Mine in California, produced significant amounts of REE, but these shut down some time ago. At present, China dominates the REE market, controlling over 95% of global supply. Hence, recent reductions in Chinese REE export quotas have created considerable uncertainty about future global supply (Moffett & Palmer 2012). As a result, more research on REEs is being conducted and new REE exploration projects are starting worldwide, including the famous Mountain Pass Mine, which is to be reopened (Wiens 2012).

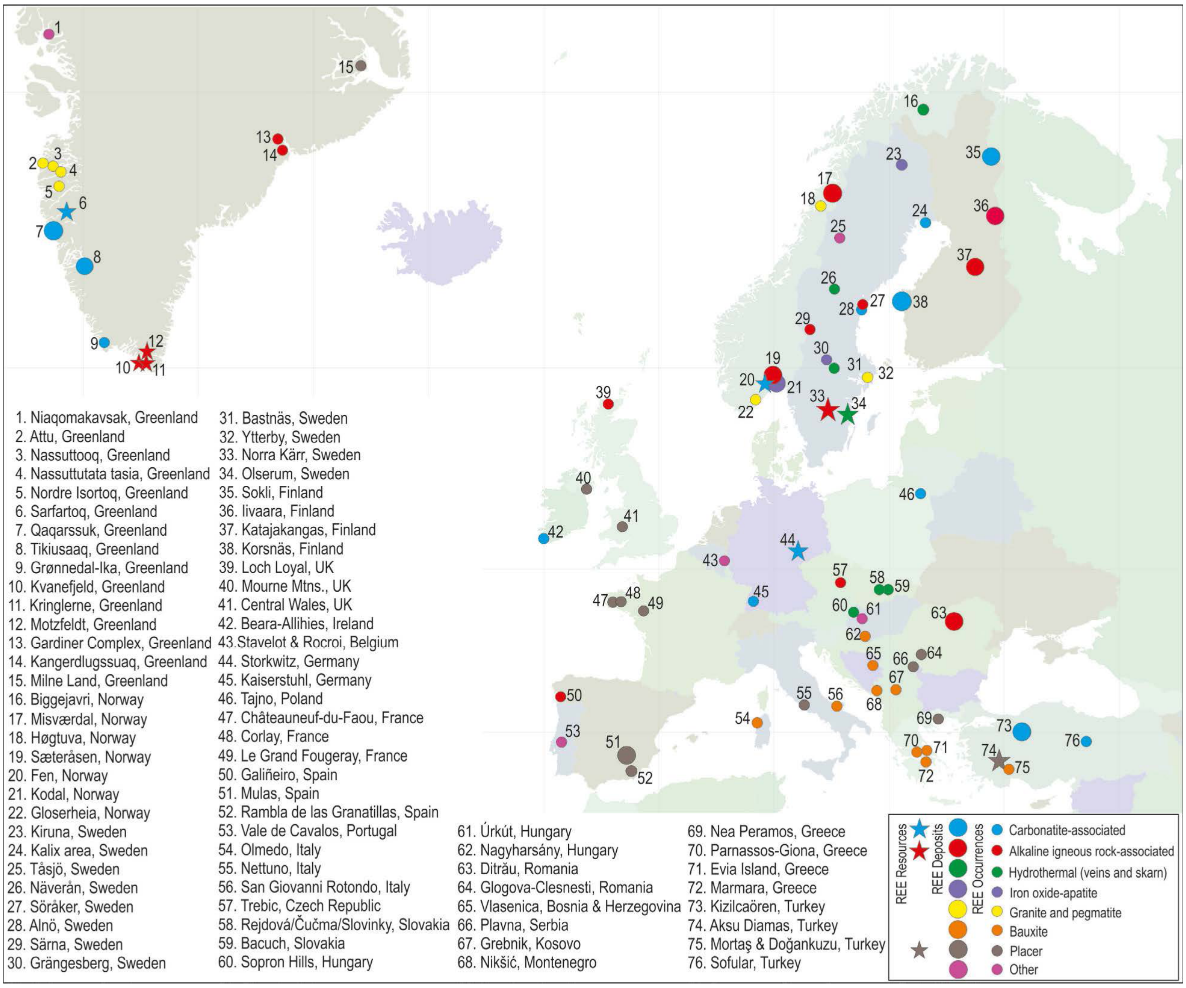

Figure 1. Map of European REE mineral deposits and occurrences in Europe (Source: www.eurare.org).

Classification of rare earth element mineralisations in Europe

A brief summary of the main types of REE deposit is given here, following the definitions agreed to by the EURARE WP1-partners (www.eurare.org):

The EURARE project has recently released a brochure summarising European REE resources, including a map of REE mineral deposits and occurrences in Europe (source: EURARE project, Fig. 1).

- **Alkaline igneous rock deposits:** In the magmatic environment, REE deposits are typically associated with alkaline igneous suites. Highly evolved alkaline/peralkaline igneous rocks host deposits of rare earth elements, including Y, in addition to Zr, Hf, Nb, Ta, U, and Th. In highly peralkaline magmas, REE-rich oxides, phosphates and/or silicates may be concentrated in certain horizons within the magma chamber because of the incompatible behaviour of REEs. Alternatively, REEs may be concentrated by late-stage magmatic-hydrothermal activity. Magmatic deposits/ prospects can be subdivided into three types. The first is hosted by nepheline syenitic rocks of large, layered alkaline intrusions, where the mineralisation commonly occurs in layers rich in REE-bearing minerals, which mostly show cumulate textures (e.g. Thor Lake/Nechalacho, Canada; Ilimaussaq, Greenland; Lovozero, Russia; Kipawa, Canada; Norra Kärr, Sweden; Pilanesberg, South Africa). The second type includes mineralisation in peralkaline granitic rocks where REE-bearing minerals are usually disseminated. The mineralisation is typically hosted by pegmatites (including the Nb-Y-F type), felsic dykes, and minor granitic intrusions (e.g. Strange Lake, Canada; Khaldzan-Buregtey, Mongolia; Ghurayyah, Saudi Arabia; Bokan, Alaska, United States). The third type is disseminated, very fine-grained, and hosted by peralkaline felsic volcanic/volcaniclastic rocks, mostly of trachytic composition (e.g. Dubbo Zirconia and Brockman/Hastings, Australia; Dostal 2016). In general, REE deposits associated with alkaline igneous rocks are rather low grade, but may have large tonnage and be relatively enriched in HREE (hosted in complex silicate REE minerals).

- **Carbonatite deposits:** Carbonatites (unusual magmas with >50% modal carbonate minerals) are most commonly found in continental-rift tectonic environments, and often associated with alkaline igneous rocks. These formed from low-degree mantle melts and may contain high concentrations of REE to crystallise REE carbonates, REE fluorcarbonates (e.g. bastnäsite) and REE phosphates (monazite and xenotime). Carbonatites have been the primary source of niobium and REEs for nearly 50 years. Although there are more than 500 known carbonatites in the world, only four are currently mined for REEs: the Bayan Obo, Maoniuping, and Dalucao deposits in China, and the Mountain Pass deposit in California (Verplanck et al. 2016). The carbonatite-associated deposits predominantly comprise LREE-enriched REE minerals.
- **Granite and pegmatite deposits:** Rare-element granitic pegmatites represent highly concentrated sources of rare metals, including Li, Rb, Cs, Be, Sn, Nb, Ta, Zr, Y, REE, and U. Deposits of this type were among the first sources of REE to be exploited in the early twentieth century, e.g. the Ytterby pegmatite in central Sweden. Whilst historically important, they are rarely promising exploration targets due to their small tonnage and complex mineralogy. However, they often have potential for by-products such as beryllium, fluorine and niobium (London 216).
- **Vein and skarn (hydrothermal) deposits:** Vein and/or skarn REE deposits are characterised by mineralisation processes involving hot aqueous solutions forming REE-bearing veins and replacement ore bodies (e.g. Bastnäs and Riddarhyttan, central Sweden). The Bastnäs (skarn)-type deposits, also referred to locally as Fe oxide-REE-Cu (Co-Au-Bi-Mo; Holtstam et al. 2014), all occur within a belt of mostly significantly altered felsic metavolcanic to metasedimentary rocks in the Nora–Riddarhyttan–Norberg area of Bergslagen, which is called the "REE line" (Jonsson & Högdahl 2013). Carbonatite and/or alkaline magmatic bodies may be spatially associated and act as a metal and/or source. Examples of REE deposits where hydrothermal processes are found to have been important include Bayan Obo (China), Nolans Bore (Australia), and Steenkampskraal (South Africa).
- **Iron oxide-apatite deposits (IOA):** Kiruna-type iron oxide-apatite deposits are generally associated with volcanic and intrusive rocks of acidic to basic composition (Hitzman 2000). Notable examples of Kiruna-type iron oxide-apatite deposits include Kiirunavaara, northern Sweden (Nyström & Henriquez 1994, Harlov et al. 2002a); Grängesberg, central Sweden (Frietsch & Perdahl 1995, Hallberg et al. 2006, Jonsson et al. 2010); and Blötberget (Jansson et al. 2014). In most of these deposits monazite and xenotime inclusions are commonly found in the apatite prominent areas (typically fluorapatite), which have experienced obvious fluid-induced alteration with (Y +REE) + Na + Si + Cl depletion (e.g. Kiirunavaara, northern Sweden; Harlov et al. 2002a), with apatite serving as the source of P + (Y+REE) (Harlov et al. 2005). Some iron-oxide copper gold (IOCG) deposits, such as Olympic Dam, Australia, carry the mineral apatite, which has the potential to produce REE as a by-product. REE-bearing apatite is currently treated as waste during iron ore processing.
- **Placer deposits:** Some REE-bearing minerals, such as monazite and xenotime, are relatively resistant to weathering and can be transported by sedimentary processes. They may then become concentrated in heavy mineral sand deposits, referred to as placers. Ancient and modern types of sedimentary placer deposits formed in both alluvial and coastal environments have been significant sources of the rare earth elements. The REE-bearing minerals in placer-type deposits are primarily monazite [$(Ce,La,Nd,Th)PO_4$], and sometimes xenotime (YPO_4), which are high-density

minerals that accumulate with the suite of heavy minerals (Sengupta & Gosen 2016). Placer deposits can form in rivers, in arid environments (dunes), or in beach and shallow marine environments, e.g. Nea Peramos along the Aegean coast of northern Greece. Mineral sand mining operations in India, Malaysia and Australia, which mine cassiterite (Sn), rutile (Ti), and/or zircon (Zr), currently also stockpile monazite and/or xenotime, from which REEs can be produced as by-products. This deposit type is also known from the geological record (palaeo-placer) where subsequent metamorphic processes may have upgraded the REE resource (e.g. Olserum, Sweden).

- **Bauxite deposits:** Bauxite ores are classified in three ways, based on genetic principles, geological age and mineralogical composition (Valeton 1972). Two main classes of bauxites are: 1) those that form on aluminosilicate lithologies; and 2) those that form on limestone, known as karst bauxites (Bárdossy 1982). The bauxites on carbonate rocks (karst) have higher REE concentrations than do other bauxites (Mordberg 1993). Accumulation of residual clay mineral during the weathering of host rock in a tropical climate has the potential to generate near-surface bauxite deposits due to crystallisation of authigenic REE-bearing minerals, accumulation of residual phases and the adsorption of ions on clays and other mineral surfaces (Deady et al. 2014). The Mediterranean bauxite deposits (e.g. central Greece) have the potential to produce REE as a by-product of aluminium production (Deady et al. 2016).
- **Ion-adsorption deposits:** Ion adsorption-type rare earth element deposits are the world's main source of HREE and yttrium. Economic examples of the deposits are confined almost exclusively to areas underlain by granitic rocks in southern China. These deposits are termed "ion adsorption-type" because the weathered granites contain more than ~50% ion-exchangeable REY (REE + Y), relative to whole-rock REY (Sanematsu & Watanabe 2016). Ion-adsorption deposits in Europe are a specific type of laterite deposit (EURARE 2017). They are formed by in situ chemical weathering of granitic rocks, resulting in adsorption of REE to clay mineral surfaces within the laterite profile. The weatherable REE-bearing minerals, including fluorocarbonates, allanite, and titanite, are the source minerals for the ion adsorption ores (Sanematsu & Watanabe 2016). Such ion-adsorption clay deposits are typified by the occurrences in the Jiangxi, Guangdong, Hunan, and Fujian provinces of southern China and, despite being low-grade, are important sources of the more valuable HREE. These clay deposits are easily mined because the adsorbed REE can be released from the clays by simple acid leaching methods using leachates such as ammonium sulphate.
- **Rare earth elements in sedimentary phosphorite deposits:** Sedimentary marine phosphorites are the world's principal source of phosphorus for the fertiliser industry, and thus an essential ingredient of modern agriculture. The availability of low-cost phosphorus has been fundamental to the "Green Revolution," which has allowed modern agricultural systems to meet increasing food demands resulting from global population growth. Phosphate, a non-renewable commodity, resides in "francolite" (an informal name for a carbonate-rich fluorapatite mineral) that has been periodically deposited as a constituent of seafloor sediment in areas covering thousands of square kilometres at continental and sedimentary basin margins, forming enormous deposits in the process. The REE assessment described here relates to marine phosphorite deposits formed along passive and convergent continental ocean-basin margins and marginal to cratonic epeiric ocean basins; it does not include marine insular and seamount deposits. Phosphorite is a marine sedimentary rock in which phosphate minerals are the major constituents (more than ~18% P_2O_5; Cathcart 1980b). The principal gangue or diluent minerals in all marine phosphorite deposits are quartz, carbonate minerals (calcite and dolomite), clay minerals (i.e. montmorillonite, illite, chlorite, and kaolinite), and Fe oxide minerals (goethite, hematite, limonite). Organic matter is a further constituent of many deposits. These diluents affect processing and chemical uses of the phosphorite (Cathcart 1980a).

THE GEOLOGY OF SWEDEN

Magnus Ripa

The following description of the geology of Sweden is modified from Stephens (1988), Lindström et al. (2000) and Stephens & Weihed (2013).

The Fennoscandian Shield (Koistinen et al. 2001) is overlain by mostly platformal sedimentary rocks and the Palaeozoic Caledonian orogen, and these form the three major tectonic components in the bedrock of northern Europe, including Sweden (Stephens et al. 1997). In its northeastern part, predominantly outside Sweden, the shield is composed of a collage of Archaean cratons (Gaal & Gorbatschev 1987; Daly et al. 2006; Hölttä et al. 2008) with Palaeoproterozoic cover rocks, and to the southwest, including Sweden, accreted magmatic domains and sedimentary basinal material (Gaal & Gorbatschev 1987; Bingen et al. 2008; Lahtinen et al. 2008). All these tectonic components were progressively amalgamated over a period of more than one billion years during the Proterozoic.

The Fennoscandian Shield contains abundant mineral resources and several ore districts, and Palaeoproterozoic assemblages in particular are host to many major mineral deposits of various types. The rocks of the Caledonides also contain various mineral deposits.

Tectonic setting

The Fennoscandian Shield in Sweden predominantly comprises three orogens: the Svecokarelian orogen in the north and east of the country and the Blekinge–Bornholm and Sveconorwegian orogens in the far southeast and southwest, respectively (Fig. 2). The bedrock in the largest orogenic system – the Svecokarelian orogen at 2.0–1.8 Ga – ceased to be affected by ductile deformation, metamorphism and associated magmatic activity, and started to react to crustal deformation in a brittle manner around 1.8–1.7 Ga (Viola et al. 2009; Saintot et al. 2011). The bedrock inside the other orogens approached a cratonic condition at 1.5–1.4 Ga (Danopolonian orogeny) and at 1.1–0.9 Ga (Sveconorwegian orogeny), respectively. Rocks and structures belonging to older orogenic systems are preserved in the far north of Sweden inside the Svecokarelian orogen (c. 2.7 Ga orogenic event), inside the Blekinge–Bornholm orogen (1.8 Ga) and inside the Sveconorwegian orogen (1.9–1.8 Ga, 1.7 Ga, 1.6–1.5 Ga, referred to as Gothian, and 1.5–1.4 Ga, referred to as Danopolonian and Hallandian). The rocks and structures formed during these older orogenic events were more or less reworked by the deformation and metamorphism associated with each of the younger orogenic systems.

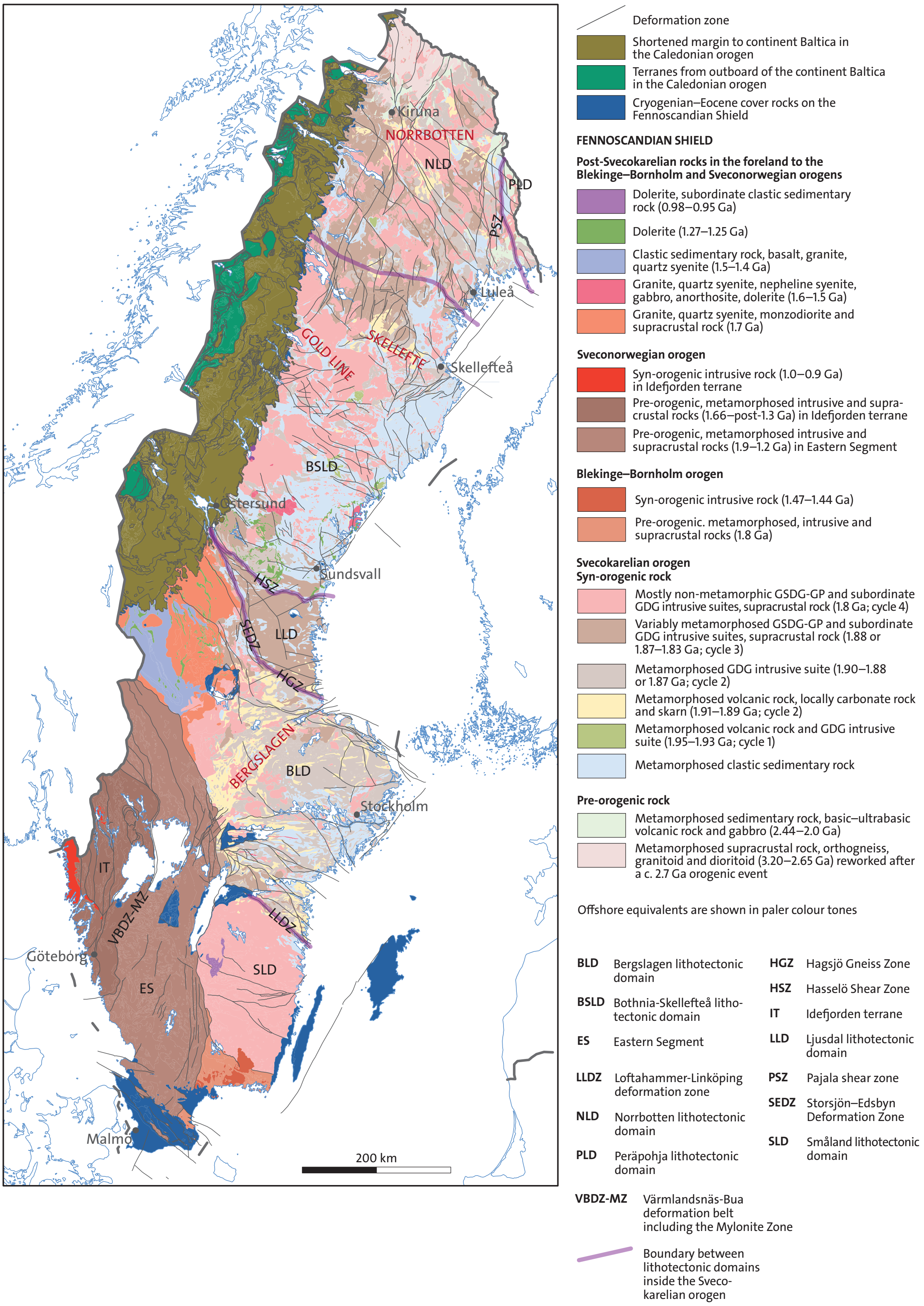

Figure 2. Simplified bedrock geological map of Sweden (modified from Stephens & Weihed 2013). The image was generated using the 1:1 million national bedrock database for Sweden at the Geological Survey of Sweden (SGU). GDG = granitoid-dioritoid-gabbroid, GP = granite-pegmatite, GSDG = granite-syenitoid-dioritoid-gabbroid. The position of the major ore districts (Bergslagen, Caledonides, Skellefte, Norrbotten) and the "Gold Line" of the Svecokarelian orogen are indicated.

Well-preserved, magmatic and sedimentary rocks, formed around 1.7 Ga, 1.6–1.4 Ga, 1.27–1.25 Ga and 0.98–0.95 Ga, represent a volumetrically subordinate component in the Fennoscandian Shield in eastern Sweden (Fig. 2). These rocks intrude or lie unconformably on top of the rocks belonging to the Svecokarelian orogen, and are situated tectonically in the foreland to both the Blekinge–Bornholm and Sveconorwegian orogens.

The Svecokarelian orogen (2.0–1.8 Ga)

Syn-orogenic rocks that formed at 2.0–1.8 Ga, included in the Svecofennian Domain by Gaal & Gorbatschev (1987), predominate inside the Svecokarelian orogen in Sweden (Fig. 2). In the far north of the country, deformation and metamorphism at 2.0–1.8 Ga also affected pre-orogenic (with respect to the Svecokarelian orogeny), Archaean gneissic and granitic basement as well as Palaeoproterozoic (2.4–2.0 Ga), predominantly supracrustal cover rocks (Fig. 2), all included in the Karelian Province by Gaal & Gorbatschev (1987).

Synorogenic Svecokarelian volcanic (1.91–1.89 Ga) and older supracrustal rocks were intruded by several different suites of igneous rocks that can be distinguished using a combination of compositional trend, intrusion-deformation relationships and absolute age (Fig. 2). Three compositional suites have been identified, referred to as the granitoid-dioritoid-gabbroid (GDG), granite-syenitoid-dioritoid-gabbroid (GSDG) and granite-pegmatite (GP) intrusive rock suites by Stephens et al. (2009). Mingling relationships between rocks with felsic composition and rocks with more primitive compositions are a conspicuous feature of the intrusive rocks in the GDG and GSDG suites. The GP plutonic rocks are mainly granitic in composition.

The Pajala shear zone (Kärki et al. 1993; Bergman et al. 2006a) in the far northeast of Sweden is a deformation belt that is up to 40 km wide at the ground surface and trends in a north–south direction. It marks a distinctive lithological boundary inside the Svecokarelian orogen. The bedrock to the west of the zone predominantly comprises syn-orogenic, Palaeoproterozoic (2.0–1.8 Ga) rocks overlying pre-orogenic, Archaean basement and Palaeoproterozoic (2.4–2.0 Ga) cover rocks (Fig. 2). In contrast, the bedrock to the east of this zone, in Finland, Norway and northwestern Russia, belongs to the part of the orogen dominated by pre-orogenic rocks.

Further to the southwest in northernmost Sweden, Öhlander et al. (1993) and Mellqvist et al. (1999) identified a boundary separating Palaeoproterozoic rocks derived in part from Archaean crust to the northeast from juvenile Palaeoproterozoic crust without an Archaean input to the southwest. The character and spatial position of this boundary are poorly constrained. However, its occurrence is conceptually consistent with the interpretation of reflection seismic data from beneath the Bothnian Bay (BABEL Working Group 1990, 1993; Korja & Heikkinen 2005, 2008). On the basis of these considerations, the Svecokarelian orogen north of the Hasselö Shear Zone (Fig. 2) has been divided into three lithotectonic domains: the Norrbotten lithotectonic domain (NLD), the Peräpohja lithotectonic domain (PLD), and the Bothnia-Skellefteå lithotectonic domain (BSLD), respectively. Since Archaean material at deeper crustal levels has been inferred to be present in the southern part of the BSLD (Andersson et al. 2011), some care is needed in interpreting the broader tectonic significance of this division.

The Svecokarelian orogen in the near-surface realm south of the Hasselö Shear Zone is composed entirely of syn-orogenic, Palaeoproterozoic (1.9–1.8 Ga) rocks (Fig. 2), whereas slightly older, juvenile Palaeoproterozoic crust has been inferred to predominate at deeper crustal levels (Andersson et al. 2011). The rocks are transected by several ductile shear zones or combinations of zones that form broader shear belts up to several tens of kilometres thick in places (Fig. 2). The shear zones are generally steeply dipping and trend predominantly west-northwest–east-southeast. Together with major folds between these zones, they contribute to a significant transposition of bedrock units into a predominantly west-northwest to east-southeast direction (Fig. 2). The Svecokarelian orogen in the southern half of the country has been divided into three separate lithotectonic domains (Fig. 2), the boundaries between which are defined by ductile shear zones. These are the Ljusdal lithotectonic domain (LLD), the Bergslagen lithotectonic domain (BLD) and the Småland lithotectonic domain (SLD).

Cyclic magmatic activity, sedimentation and deformational–metamorphic events

The syn-orogenic rocks in the various lithotectonic domains in the Svecokarelian orogen share many characteristics, but the proportions of the different rock types change inside the different domains (Fig. 2). Cycles of magmatic activity and sedimentation, lasting up to 40–50 million years, are a characteristic feature of the orogenic development. These cycles include and are separated by short periods of ductile transpressive deformation. Metamorphism under low pressure and, in large areas, amphibolite and even granulite facies conditions prevailed during and after crustal shortening.

The oldest cycle with magmatic activity is dated at 1.95–1.93 Ga, and occurs in a small area southwest of Skellefteå in the BSLD (Fig. 2). The volumetrically most conspicuous cycle consists of predominantly rhyolitic or dacitic, 1.91–1.89 Ga volcanic and subvolcanic rocks. These are sandwiched between siliciclastic sedimentary rocks and intruded by a calc-alkaline GDG suite at 1.89–1.88 Ga north of the Hasselö Shear Zone (Fig. 2) and at 1.90–1.87 Ga south of this zone. Many of the mineral deposits in Sweden are spatially associated with the magmatic activity during this cycle when a transtensional or extensional tectonic environment prevailed (Allen et al. 1996a, 1996b; Stephens et al. 2009). All these rocks were affected by a short pulse of transpressional ductile deformation and the initial stages of metamorphism at 1.88–1.87 Ga north of the Hasselö Shear Zone (Bergman et al. 2001; Kathol & Weihed 2005; Skyttä et al. 2012) and a little later at 1.87–1.86 Ga in the domains along and south of this zone (Hermansson et al. 2008a; Högdahl et al. 2009).

A part of a third cycle of magmatic activity and deposition of siliciclastic sedimentary rocks is conspicuous in the BSLD and NLD at 1.88–1.86 Ga and, more extensively, at 1.87–1.83 Ga in the LLD south of the Hasselö Shear Zone (Fig. 2). Magmatic activity belonging to this cycle is also present further south. It is apparent that the rocks in this cycle started to form during the 1.88–1.86 Ga transpressional event and, at least in the LLD, continued during a second period of transtension or extension between 1.86 and 1.83 Ga (Bergman et al. 2008). The intrusive rocks in this cycle are locally discordant to structures formed during the earlier deformational evolution but, at least in the domains south of the Hasselö Shear Zone, were affected by deformation and metamorphism around 1.83–1.82 Ga. Ductile strain also formed around 1.8 Ga along the shear belts (e.g. Beunk & Page 2001; Högdahl & Sjöström 2001; Hermansson et al. 2008b). The intrusive (and equivalent volcanic) rocks in the third cycle belong predominantly to a GSDG suite showing an alkali-calcic trend and a shoshonitic composition. Locally, rocks belonging to a calc-alkaline GDG intrusive suite are also present.

A fourth cycle of magmatic activity and deposition of siliciclastic sedimentary rocks, included in the older group of rocks in the Transscandinavian Igneous Belt (Patchett et al. 1987; Larson & Berglund 1992; Högdahl et al. 2004), marks the final phase in the Svecokarelian orogenic evolution at 1.83–1.78 Ga. This cycle is conspicuous at the ground surface in the Småland lithotectonic domain, but similar magmatic activity occupies large areas in the near-surface realm in most of the other lithotectonic domains (Fig. 2). Many of the intrusive rocks that belong to this cycle are isotropic and contacts are discordant to structures formed during earlier deformational events. However, ductile deformation and metamorphism under greenschist facies conditions occur along a broad belt with a west-northwest to east-southeast or northeast to southwest trend in the central part of the SLD. The intrusive (and equivalent volcanic) rocks in the fourth cycle are similar in composition to the rocks in the third cycle.

The Svecokarelian orogen in Sweden is inferred to have formed along an active continental margin in a convergent plate boundary setting between 2.0 and 1.8 Ga. Accretionary orogenic activity related to ongoing subduction processes (Cawood et al. 2009) prevailed, involving both longer periods of retreating and shorter periods of advancing, easterly-directed subduction (Hermansson et al. 2008a;

Stephens et al. 2009). The palaeotectonic setting corresponds to the current circum-Pacific orogenic system (Brown 2009) and builds on earlier pioneering work on the Fennoscandian Shield by Hietanen (1975), Gaal (1982) and Park (1985), for example. Alternative tectonic models invoking both accretionary and terminal (1.8 Ga) continental collisional tectonics, in a setting equivalent to the current Alpine–Himalayan–Indonesian orogenic system (Brown 2009), have also been proposed (e.g. Nironen 1997; Lahtinen et al. 2005, 2008; Korja & Heikkinen 2008), but are not adopted here.

The Blekinge–Bornholm orogen (1.5–1.4 Ga)

The bedrock in the Blekinge–Bornholm orogen (Fig. 2) predominantly comprises magmatic rocks that formed along a 1.8 Ga active continental margin in a convergent plate boundary setting. However, it differs from the bedrock further north in the SLD, since it was affected by a younger orogenic event at 1.5–1.4 Ga (Čečys 2004), referred to as Danopolonian. This younger event is expressed by ductile deformation and amphibolite facies metamorphism as well as by synorogenic magmatic activity, with the crystallisation of a suite of granites and syenitoids around 1.45 Ga. Some uncertainty remains concerning the presence of earlier deformation and metamorphism at 1.8–1.7 Ga similar in age to the main bedrock component (e.g. Johansson et al. 2006).

The Sveconorwegian orogen (1.1–0.9 Ga)

In southwestern Scandinavia the bedrock shows evidence of an accretionary to terminal collisional tectonic events at 1.1–0.9 Ga (Fig. 2). In Sweden these events involved subduction of continental lithosphere, with the development of eclogite and high-P granulite. The different tectonic events in this time interval belong to the Sveconorwegian orogeny (Berthelsen 1980; Bingen et al. 2008), and the volume of bedrock affected by them is referred to as the Sveconorwegian orogen (Fig. 2). A significant feature of this orogen in Sweden is the predominance of pre-orogenic crustal material, including not only magmatic rocks formed at 1.3–1.2 Ga and sedimentary cover rocks formed after 1.3 Ga in the Idefjorden terrane (Fig. 2), but also reworked basement from older accretionary orogenies. Orogenies active at 1.9–1.8 Ga (Svecokarelian), around 1.7 Ga and at 1.5–1.4 Ga (Danopolonian and Hallandian) have been reworked in the Eastern Segment and at 1.6–1.5 Ga (Gothian) in the Idefjorden terrane (Fig. 2).

Post-Svecokarelian rocks in the foreland to the Blekinge–Bornholm and Sveconorwegian orogensWW

Well-preserved volcanic and sub-volcanic rocks, interlayered siliciclastic sedimentary rock and an alkali-calcic intrusive suite containing granite, quartz syenite and monzodiorite, which all formed around 1.7 Ga, occur in west-central Sweden (Fig. 2). These rocks belong to the younger group of rocks in the Transscandinavian Igneous Belt. The boundary between these rocks and the surrounding bedrock in the Svecokarelian orogen is either a primary intrusive contact or an angular unconformity. Locally, deformation along a ductile shear zone affected this rock suite during the development of the magmatic rocks (Bergman et al. 2006b). Otherwise, the rocks are unaffected by ductile strain. Geochemical data indicate formation along an active continental margin in a convergent plate boundary setting (Nyström 1982, 2004), and the 1.7 Ga suite represents a high crustal level inside a spatially, poorly constrained accretionary orogenic system with, once again, an inferred easterly-directed sense of subduction (Bergman et al. 2006b).

Mesoproterozoic magmatic rocks, formed at 1.6–1.5 Ga, are conspicuous in central Sweden (Fig. 2). They consist of granite with rapakivi texture and quartz syenite, spatially associated with gabbro, anorthosite and monzodiorite (Andersson 2001). These rocks are overlain by siliciclastic sedimentary rock and basalt (Fig. 2), the latter inferred to have formed around 1.48–1.46 Ga (Söderlund et al. 2005). Predominantly basic dykes with a west-northwest to east-southeast trend that formed at 1.6 Ga (Söderlund et al. 2005; Stephens et al. 2009), as well as isolated intrusive bodies of nepheline syenite, probably Mesoproterozoic in age, and 1.45 Ga granite (Kresten & Chyssler 1976; Friese et al. 2012) are also present in the southeast of the country (Fig. 2). A far-field intracratonic response to the Gothian orogenic event, preserved to the west inside the Sveconorwegian orogen, has been proposed for the 1.6–1.5 Ga magmatic activity (Åhäll et al. 2000). A similar foreland response to the Danopolonian orogenic event in the Blekinge-Bornholm orogen can also be inferred for the formation of the 1.5–1.4 Ga rocks.

Mesoproterozoic (1.27–1.25 Ga) dolerite sills and dykes as well as Neoproterozoic (0.98–0.95 Ga) dykes and subordinate clastic sedimentary rock (Söderlund et al. 2005) completed the tectonic evolution in the Fennoscandian Shield in Sweden (Fig. 2). These rock suites are related to separate intracratonic rifting events in the foreland to the Blekinge–Bornholm and Sveconorwegian orogens.

The Caledonian orogen (0.5–0.3 Ga)

The Scandinavian Caledonides (Fig. 2) are characterised by mostly flat-lying thrust sheets or nappes. The rocks of these sheets are dominated by original sedimentary, late Proterozoic to early Palaeozoic successions that formed on the margin of the Fennoscandian Shield and in the Iapetus Ocean. The thrust sheets also include mafic dykes, ultramafic (largely sepentinised) intrusive bodies and pieces of crystalline basement of the Fennoscandian Shield and of exotic terranes. During closure of the Iapetus Ocean the thrust sheets were transported eastwards (present day coordinates) onto the Shield and each other.

Mineral resources

Sweden has had an extensive mining and mineral processing industry for over 1,000 years, and documented mining dates back to the 8th century AD. Important types of ore deposit include volcanogenic massive sulphide deposits (Cu-Zn-Pb-Au-Ag or Zn-Pb-Ag), volcanic- and carbonate- or skarn-hosted, replacement-type Zn-Pb-Ag-(Cu-Au) sulphide and Fe oxide deposits, Fe oxide-apatite deposits, Cu-Au deposits hosted by intrusive rock, and orogenic Au deposits. Alongside these well-documented deposits, new types of deposit are being explored, e.g. Fe oxide-Cu-Au (IOCG) deposits and REE, Li, Te and other deposit types (Weihed et al. 2005).

No economic or major mineral deposits have been discovered in the Archaean rocks in Sweden. The major ore deposits are hosted by Palaeoproterozoic assemblages belonging to the BLD, BSLD and NLD in the Svecokarelian orogen. Each of these domains is dominated by one or more of the important ore types identified above, and mineral resources in Sweden are described below according to their location in the lithotectonic framework and ore type.

Volcanogenic massive sulphide (VMS) deposits are currently the most mined base metal ore type in Sweden. Four deposits are currently mined in the Skellefte ore district (Kankberg, Maurliden, Kristineberg and Renström), which is situated inside the BSLD (Fig. 2). The VMS deposits in the Skellefte ore district are composed of lenses of semi-massive to massive sulphides with Cu, Zn, Pb, Au and Ag, hosted mainly in the upper part of predominantly felsic, submarine volcanic arc rocks (Allen et al. 1996a). Recent studies (unpublished Boliden AB report, Bauer et al. 2013) have shown that the ores display a close spatial relationship with early syn-volcanic faults. The most recently opened mine in this area, Kankberg, is an Au-Te deposit, the first Te mine in Sweden. The famous Au-rich, VMS Boliden deposit is also located in the Skellefte District (Bergman, Weihed et al. 1996; Mercier-Langevin et al. 2013). Apart from the VMS deposits, Au deposits hosted by intrusive rock, including the operating mine at Björkdal (Weihed et al. 2003), Cu-Mo-Au porphyry-style deposits and Cu-Ni deposits hosted by mafic intrusive rock are also present. Intrusion-hosted porphyry and Au deposits formed approximately 10 million years after the VMS deposits, during basin inversion (Skyttä et al. 2012) and a shift from general extension to compression of the volcanic arc at 1.88–1.87 Ga (Bejgarn et al. 2013).

Various types of ore deposit are present in the Bergslagen ore district in south-central Sweden (Fig. 2), including several thousand Fe oxide and polymetallic base metal sulphide deposits (Stephens et al. 2009). The district is situated predominantly inside the BLD (Fig. 2). However, the westernmost part of it shows ductile strain along Sveconorwegian shear zones and has been included in the frontal part of the Sveconorwegian orogen (Fig. 2). Three deposits are currently mined in this district: Zn-Pb-Ag-(Cu-Au) sulphide deposits at Garpenberg, a Zn-Pb-Ag sulphide deposit with subordinate Cu at Zinkgruvan and a Zn-Pb-Ag sulphide at Lovisagruvan.

Stratiform, tabular-shaped Zn-Pb-Ag ore at the Zinkgruvan operating mine is hosted by felsic ash-siltstone volcanic rock with intercalations of carbonate rock, skarn, chemical sediment and mafic rock, all affected by upper amphibolite facies metamorphism (Hedström et al. 1989; Allen et al. 1996b; Stephens et al. 2009). Veins and disseminations of Cu mineralisation are hosted by the carbonate rock. The underlying felsic volcanic rocks are hydrothermally altered and metamorphosed, and the ore deposit is overlain by migmatitic paragneiss. In contrast, a more typical feature of the Bergslagen district is a spatial association between Zn-Pb-Ag-(Cu-Au) sulphide deposits and Fe oxide deposits, all hosted by crystalline carbonate rock or skarn in extensive successions of metamorphosed and hydrothermally altered felsic volcanic rock (Allen et al. 1996b; Stephens et al. 2009). Examples include Garpenberg, Stollberg and Dannemora. Kiruna-type Fe oxide-apatite deposits are also present (e.g. Grängesberg).

A variety of processes have been inferred to explain the formation of the sulphide and Fe oxide deposits in Bergslagen, all of which have a common spatial association with magmatic activity around 1.91–1.89 Ga. Volcanogenic exhalative and synvolcanic replacement-type sulphide and Fe oxide skarn deposits, and contact metasomatic Fe oxide skarn deposits have all been identified (e.g. Geijer 1917; Geijer & Magnusson 1944; Hedström et al. 1989; Ripa 1988, 2012; Jansson & Allen 2011, 2013; Jansson et al. 2013). A magmatic or magmatic-hydrothermal origin for the magnetite in the Fe oxide-apatite deposit at Grängesberg has been proposed (Jonsson et al. 2013).

Important Fe oxide and Cu-Au ore deposits occur in a major ore district inside the NLD in northernmost Sweden (Fig. 1). Based on the style of Fe oxide and Cu-Au mineralisation and the extensive albite and scapolite alteration, the region has been regarded as a typical IOCG province (e.g. Martinsson 2001; Niiranen et al. 2007). Five major types of deposit occur: iron formations including typical BIF deposits (e.g. Tornefors); stratiform Cu-Fe deposits (e.g. Viscaria); Kiruna-type Fe oxide-apatite ores (e.g. Kiirunavaara, Malmberget); intrusion-related Cu-Au mineralisation (e.g. Aitik, cf. Wanhainen et al. 2003); and shear- and vein-style Cu-Au deposits (e.g. Nautanen). In strictly genetic terms, only some of these ore types can be classified as typical Fe oxide-Cu-Au (IOCG) deposits; others only share a few characteristic features with this rather loosely defined ore class (cf. Hitzman et al. 1992; Hitzman 2000). The Kiruna-type, Fe oxide-apatite deposits have also been interpreted as magmatic or magmatic-hydrothermal occurrences (Nyström & Henriquez 1994). The smaller Gruvberget, Leveäniemi and Mertainen Fe oxide deposits also recently came into production or are currently at an advanced stage of feasibility studies.

Orogenic gold deposits have been identified in several of the lithotectonic domains in the Svecokarelian orogen north of the Hasselö Shear Zone. Recent discoveries of orogenic gold deposits southwest of the Skellefte District (Fig. 2) in the BSLD have focused much attention on the “Gold Line” (Bark & Weihed 2012), with one mine (Svartliden) recently closed and several prospects at varying degrees of maturity. Age data on orogenic gold mineralising events are scarce, but it is possible to constrain two major periods of mineralisation at 1.90–1.86 Ga and 1.85– 1.79 Ga (Eilu & Weihed 2005). The age data appear to define a rough zonation from northeast to southwest, which seems to be related to the apparent progressive growth of the Fennoscandian Shield over time in this direction. In northernmost Sweden, Pahtohavare (Lindblom et al. 1996) has been described as an orogenic gold deposit, although the high Cu content and saline mineralising fluids are more akin to IOCG deposits (Weihed 2001; Weihed et al. 2005).

Some gold deposits south of the Hasselö Shear Zone have been described with alternative genetic models. For example, Enåsen (Hallberg 1994) has been interpreted as a metamorphosed epithermal deposit.

The autochthonous Ediacaran (c. 590–570 Ma) to Lower Cambrian sandstones at the present eastern erosional front of the Scandinavian Caledonian mountains (Fig. 2) host several Pb-Zn deposits, one world-class example of which is at Laisvall (Saintilan et al. 2015). The mineralisations are epigenetic and formed during the Middle Ordovician in response to early far-field Caledonian deformational events (Saintilan et al. 2015).

Allochthonous Ediacaran sedimentary rocks in the Caledonian nappes (Fig. 2) locally contain Ni-bearing serpentinites, some of which are being, or recently have been, evaluated for exploitation (see www.nickelmountain.se).

The uppermost Caledonian nappes (Köli; Fig. 2) are exotic terranes with local mineralisation such as the Ordovician Stekenjokk-Levi Zn-Cu (-Pb) volcanogenic massive sulphide deposit (Stephens 1986). Other types of metal occurrence in Sweden include REE, Li, Mo, Sn, W, Ti-V, Ni-Cu (-PGE) and U. Recent global interest in REE mineralisation has resulted in fairly intense exploration for these metals in Sweden. One of the most promising prospects is the Norra Kärr deposit, with high grades of HREE, in southern Sweden. This deposit is associated with a Mesoproterozoic nepheline syenite.

REE MINERALISATIONS IN SWEDEN

Erik Jonsson, Per Nysten, Torbjörn Bergman, Martiya Sadeghi, Johan Söderhielm & Dick Claeson

The following chapter summarises known mineralisations with "significant" contents (a concept which is rather subjective and variable) of the rare earth elements. Some of these are fairly well known and studied, whereas others have only been noted briefly during earlier exploration work, as well as during this project.

The chapter sections are based on the overall classifications of the deposit types, starting with the direct magmatic (orthomagmatic) types, chiefly represented by intrusive rock-hosted mineralisations, i.e. granitic/granite pegmatitic, alkaline/syenitic, and carbonatitic ones. A contrasting but common general type of occurrence in Sweden are REE mineralisations hosted by, or directly associated with, different types of iron oxide ores. These range from the apatite-iron oxide ores (or Kiruna-type deposits), which are relatively clear-cut in terms of their classification (although still genetically debated and could also be included in the orthomagmatic group), via skarn-hosted iron oxide mineralisations in central Sweden (the Bastnäs-type deposits), to individual deposits or groups of deposits, whose classification and/or origins are somewhat less clear or are undergoing study. The latter include the hydrothermal vein deposits found in the Olserum area in southeastern Sweden, as well as several other deposits, mainly within or near the Bergslagen ore province in south central Sweden. Several occurrences of U-rich, REE-bearing minerals have been identified in quartzite-dominated Palaeoproterozoic metasedimentary successions in southeastern Sweden. These are interpreted to represent palaeoplacer-type original concentrations of heavy mineral sands. There are also occurrences associated with Phanerozoic "alum" shales and phosphorites in Sweden, such as in the Tåsjö area (Fig. 3).

REE mineralisation in granitic pegmatites and granitoids

Granitic pegmatites, typically of a moderately to highly fractionated character, often host variable amounts of minerals rich in rare or uncommon metals, including Be, Li, Nb, Ta, Sn, U, Th and the rare earth elements (REE). Numerous fields of rare metal-enriched pegmatites occur in the Proterozoic bedrock of Sweden, having formed during an extended time interval (around 1 G.y.). Several hundred of these pegmatite dykes have been quarried or mined on small to relatively extensive scales over time, mainly for quartz and feldspar (Fig. 4), but sometimes also for mica, and in a few cases also for other minerals and metals, such as apatite, beryl, bismuth, and REE minerals (cf. Sundius 1952, Lundegårdh 1971).

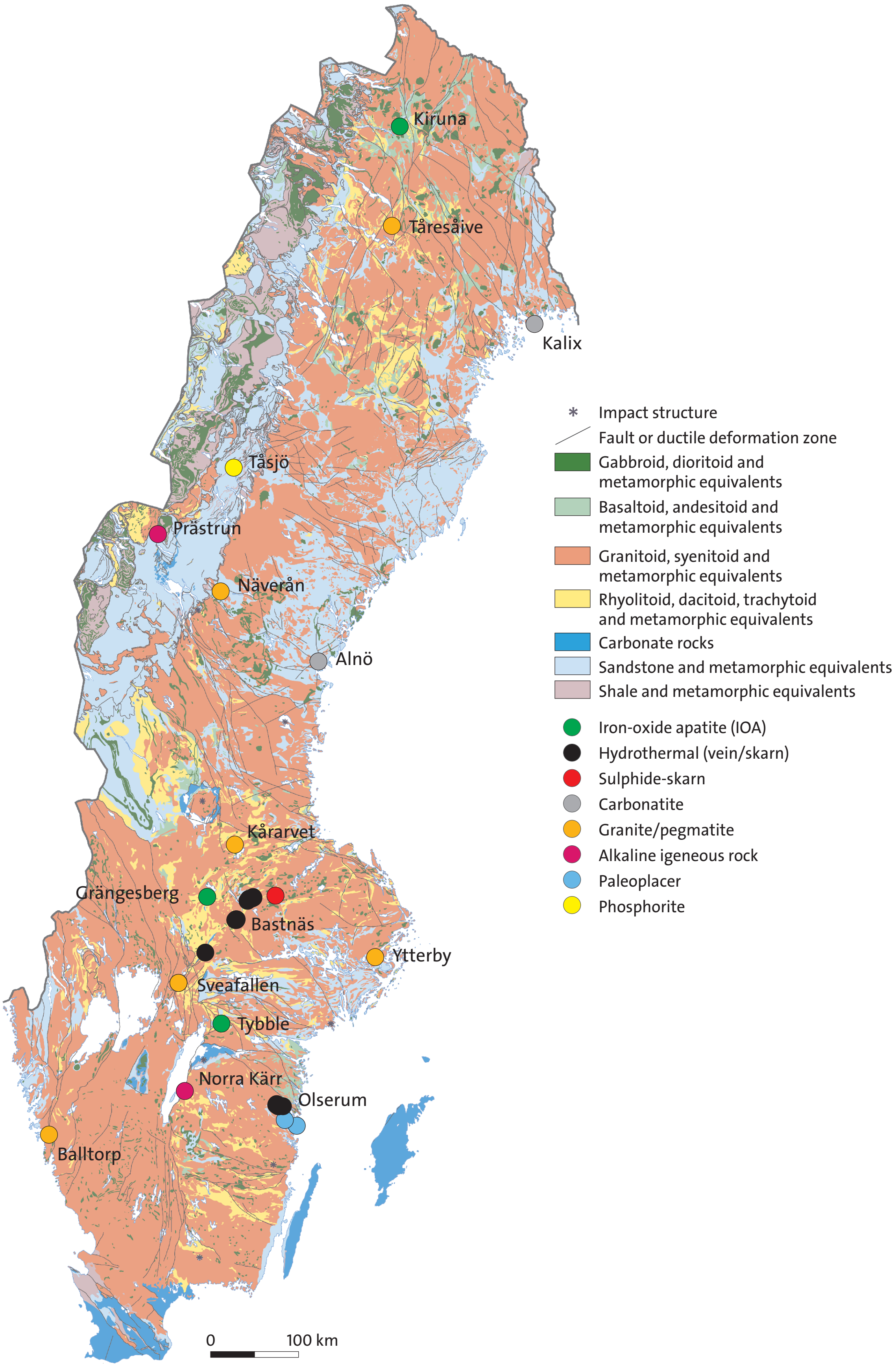

Figure 3. Simplified map of the bedrock geology of Sweden, with a selection of REE deposits, prospects and occurrences.

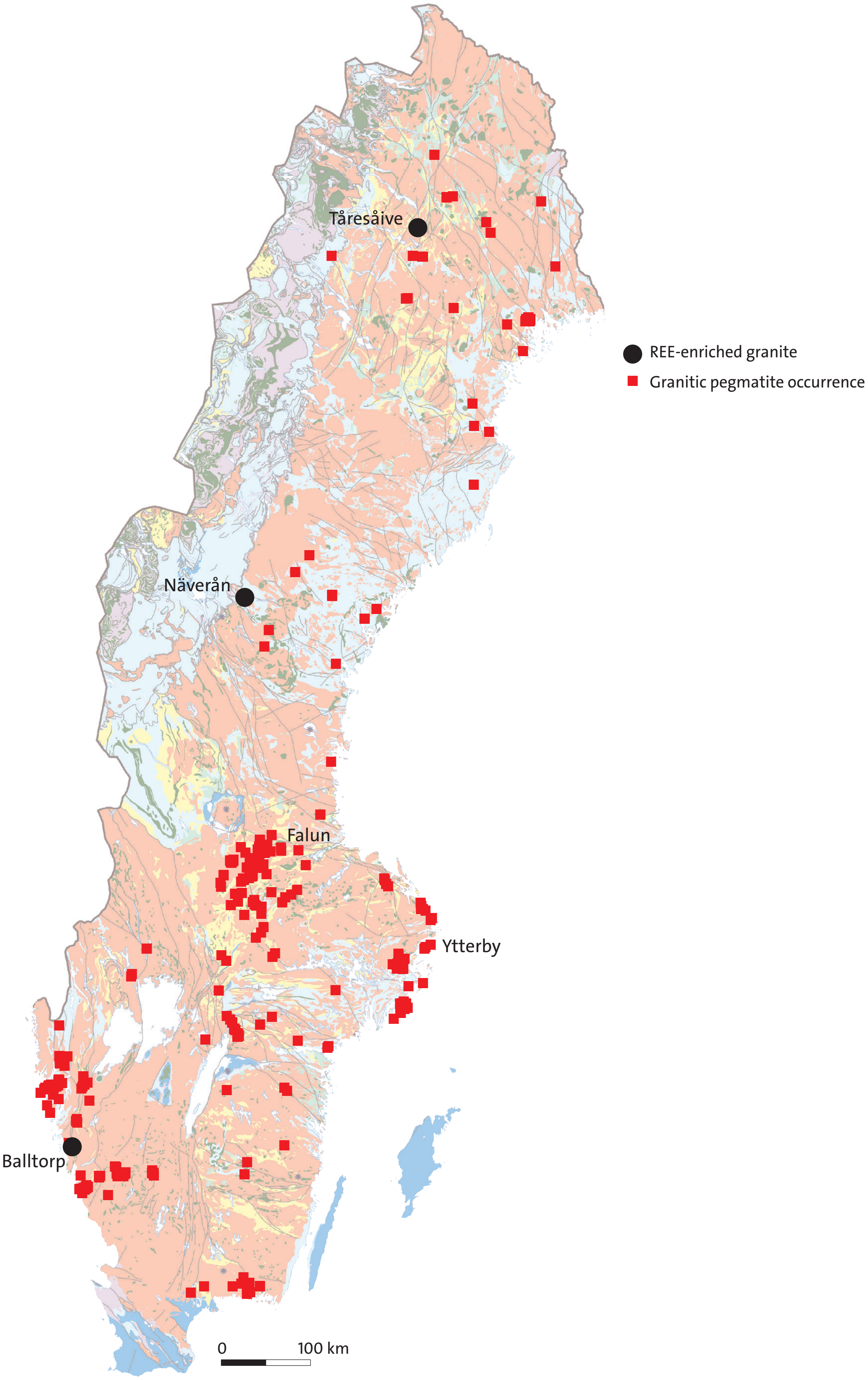

Figure 4. Major granitic pegmatite quarries and occurrences of REE-mineralised granitoids in Sweden.

Study and research on granitic pegmatites and their minerals has a long history in Sweden, featuring, among others, the discoveries leading up to the description of the first known rare earth element ("yttria"; later to be known as a mixture of yttrium and others) from the Ytterby pegmatite (Fig. 4) in the late 18th century (Gadolin 1794), and more extensive and broader studies centred on the Falun pegmatite field (Fig. 4), in the early 19th century (e.g. Hisinger & Berzelius 1806, Hedenberg 1806, Gahn & Berzelius 1815, Berzelius 1815), including the publication of one of the earliest maps of a rare element-bearing granitic pegmatite dyke (Gahn et al. 1818).

Most relevant in the rare earth element context are granitic pegmatites of the abyssal, muscovite, and rare-element classes (based on the benchmark classification by Černý 1991; e.g. also London 2008). The latter class includes dykes and fields belonging to the NYF (Niobium-Yttrium-Fluorine) and LCT (Lithium-Cesium-Tantalum) families (cf. Černý 1991, Černý & Ercit 2005, and references therein). Of these, the NYF family of the rare-element class is overall the most relevant one in terms of potential REE exploitation. Notably, many of these specific pegmatites are particularly enriched in the heavy REEs, including yttrium, and in a few cases, also scandium. However, for the sake of completeness, major LCT fields are also referred to briefly below.

The granitic pegmatites in Sweden have been the focus of quite extensive exploration and exploitation over time, whereas the little-studied (in the context of metal exploration) rare element-enriched granites and granitoids have not. Few occurrences have received much or any attention in terms of their metal potential, and what is known or can be surmised about their overall grades is generally not encouraging. One notable exception to this is the so-called "RA-granite" in Balltorp and the greater Mölndal area, southwestern Sweden (Fig. 4), which locally exhibits relatively high REE content. The RA-granite is a Be-F-Nb-REE-Sn-Ta-Th-U-Zr-anomalous gneissic granite that does show some potential, but which has so far not been systematically explored (cf. Holmqvist 1989, and references therein). Moreover, several other granitic to syenitic rocks in southern Sweden and elsewhere exhibit increased REE contents. A contrasting case to these primary enrichments is the granitoid-hosted but epigenetic, shear zone-related mineralisation at Näverån in Jämtland, central Sweden (Fig. 4).

Although quite variable between different occurrences and fields, important primary host minerals (or mineral groups) for REEs in the rare element pegmatites of Sweden comprise aeschynite-(Y) to polycrase-(Y), allanite-(Ce), allanite-(Y), euxenite-(Y), fergusonite-(Y), Y-dominant thalenite-yttrialite, gadolinite-(Y), monazite-(Ce), samarskite-(Y), yttrotantalite-(Y) (as well as the chemically similar ishikawaite-formanite), and xenotime-(Y)(Table 1). Since many of them often host significant quantities of uranium (and/or thorium), they are typically metamict, and may also have undergone extensive alteration relating to, and post-dating, this process (Fig. 5).

Table 1. Important REE minerals in granitic pegmatites in Sweden

Mineral	General formula	Mineral	General formula
Aeschynite-(Y)	$(Y,HREE,Ca,Fe,Th)(Ti,Nb)_2(O,OH)_6$	Monazite-(Ce)	$(Ce,LREE)(PO_4)$
Allanite-(Ce)	$Ca(Ce,REE)Fe^{2+}Al_2[SiO_4][Si_2O_7]O(OH)$	Polycrase-(Y)	$(Y,HREE,Ca,Ce,U,Th)(Ti,Nb,Ta)_2O_6$
Allanite-(Y)	$Ca(Y,REE)Fe^{2+}Al_2[SiO_4][Si2O_7]O(OH)$	Samarskite-(Y)	$(Y,HREE,Fe,U,Th,Ca)(Nb,Ta,Ti)O4$
Euxenite-(Y)	$(Y,HREE,Ca,Ce,U,Th)(Nb,Ta,Ti)_2O_6$	Tengerite-(Y)	$(Y,REE)_2(CO_3)_2 \cdot 2\text{-}3H_2O$
Fergusonite-(Y)	$(Y,HREE)NbO_4$	Thalenite-(Y)	$(Y,HREE)_3Si_3O_{10}(F,OH)$
Fluocerite-(Ce)	$(Ce,La,LREE)F_3$	Thortveitite	$(Sc,Y)_2Si_2O_7$
Gadolinite-(Y)	$(Y,REE,)_2FeBe_2Si_2O_{10}$	Xenotime-(Y)	$(Y,HREE)(PO_4)$
"Hjelmite"	Heterogeneous mixture, Y+HREE-rich	Yttrialite-(Y)	$(Y,HREE)_2Si_2O_7$
Keiviite-(Y)	$(Y,Yb,HREE)_2Si_2O_7$	Yttrotantalite-(Y)	$(Y,HREE,Ca,Fe)(Ta,Nb)O_4$

High primary content of uranium and/or thorium has thus led to extensive metamictisation of such primary pegmatite minerals. Subsequent alteration and fracturing of both minerals and their surrounding host rocks is also common, on micro to outcrop scale (Figs. 5, 6). Locally, primary REE minerals may also have been affected by one or several stages of later fluids, with effects including alteration and the formation of low-temperature secondary minerals, such as tengerite-(Y), and allied carbonates. The occurrence, distribution and detailed mineralogy of the latter type of phases are little studied and hence poorly known. In a few cases, local co-enrichment of scandium in these pegmatite systems is also evident from the appearance of thortveitite, often intimately associated with HREE-rich oxides or silicates. These represent the only known occurrences to date of minerals with essential scandium in Sweden.

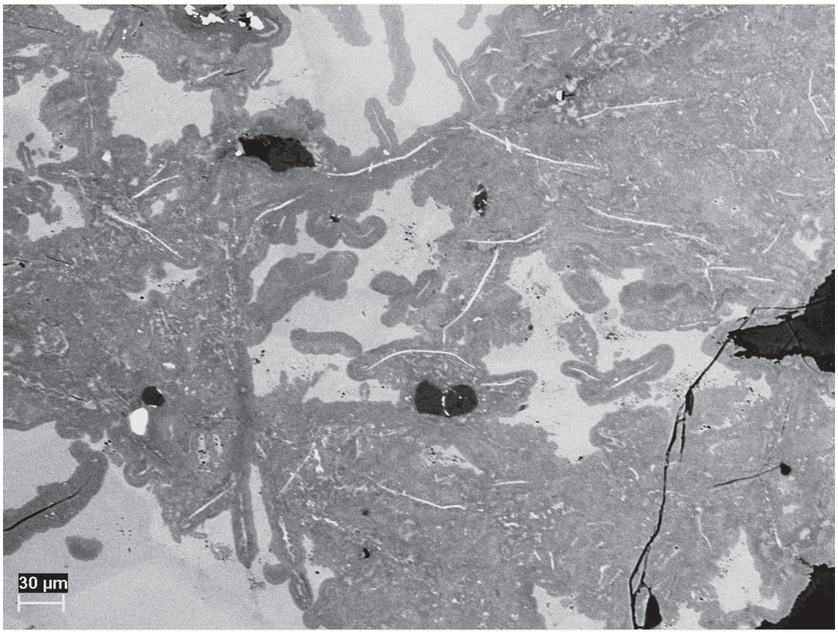

Figure 5. Back-scattered electron (BSE) scanning electron micro scope image of a radioactive and hence metamict Y-HREE-U-Ti-Nb oxide from the Flintgruvan (1) pegmatite, Dalarna (6694334/522455), which has experienced extensive, probably fluid-mediated alteration. The light grey to nearly white fields represent remnants of the metamict “original” mineral, which has been largely replaced by a darker phase along gently curving fracture networks. These are in turn partly infilled with a very BSE-light/white phase, a late-formed radiogenic galena. Photo: Erik Jonsson.

Figure 6. Partly altered metamict and heterogeneous aggregate of highly radioactive REE minerals in the western wall of the uppermost part of the Ytterby pegmatite quarry, near Vaxholm (6592332/690226). The radial fracture pattern in the feldspar-dominated rock surrounding the large, brownish to black radioactive aggregate can be readily seen. The snus box for scale is 70 mm in diameter. Photo: Erik Jonsson.

While most of the known, rare metal-bearing granitic pegmatites in the Swedish part of the Fennoscandian shield are of small to moderate size, and therefore mostly not amenable to metal mining in the modern industrial sense, some dyke systems (or fields) are more extensive, and the potential for new discoveries certainly remains (the very recent discoveries of potentially economic lithium ± tantalum mineralisations in large granitic pegmatites under a modest soil cover in the Bergby area, southeast central Sweden, illustrates this well). It should be noted that the generally small or very small degree of available bedrock exposure in large tracts of Sweden suggests that the prospects of finding new rare element (and other) pegmatites are fairly good, if suitable exploration methods are used. Also, the general mineralogical character of granitic pegmatites, the occurrence of which always offers the potential for actually containing several industrial minerals as well as metal ore minerals, may allow scope for extracting several mineral commodities from a single deposit or group of deposits.

Distribution and REE mineralisation of granitic pegmatites

In central and northern Sweden rare metal pegmatites primarily formed between c. 1.82 and 1.78 Ga (Romer & Smeds 1994, 1997), whereas occurrences with younger ages are found particularly in southern, and not least, southwestern Sweden (down to c. 1 Ga; Romer & Smeds 1996). The groupings into regional clusters (below) have partly been based on the mineral paragenetic and geological synthesis of Smeds (1990). For more detailed information about singular occurrences and fields, in addition to that given here, the reader is referred to references given in the text, including Sundius (1952), Brotzen (1959), Lundegårdh (1971), as well as Smeds (1990), and references therein. Overall, neither figures on average grades of metals including the REEs nor tonnages are available for these occurrences.

Southern Sweden

Several major clusters, as well as more scattered occurrences of rare element pegmatites are found in southern Sweden (Fig. 4). Of these, the more marked clusters are located in the southwesternmost part (Fig. 7). One is mainly associated with metasupracrustal rocks, occurring to the north of Gothenburg and up towards the border with Norway, to a significant extent within the metasedimentary rocks of the c. 1.6–1.5 Ga Stora Le–Marstrand formation. It includes the youngest known rare element pegmatites in the country, associated with similarly young granites (around 0.9 Ga; Eliasson & Schöberg 1991). This pegmatite cluster contains niobium, yttrium, and fluorine (NYF) and lithium, cesium, and tantalum (LCT)-type dykes, with e.g. the locally Y+HREE-Nb mineral-bearing pegmatites in the Nol quarries and other localities belonging to the former type. The other general cluster in the region is located south to southeast of Gothenburg (Göteborg; Fig. 7), mainly within an area dominated by gneisses, including variably metamorphosed and deformed granitoids. These pegmatites represent mainly primitive and NYF types; in this cluster several quarried pegmatites of this type, such as Ytterlida, Gräne, Skillnabo and Derome/Torpa are known to carry locally abundant Y+HREE-Nb oxide minerals (e.g. Sundius 1952). Yttrialite-like minerals may be locally important, such as at Ingelsbo. Additionally, the scandium silicate thortveitite has been found occurring together with Y-HREE-rich oxides in one locality (Ytterlida; Langhof 1996).

A more modest number of granitic pegmatites occur in the southeastern part of Sweden, chiefly in Östergötland and Småland. These are mainly of the NYF type (Fig. 8). A smaller subset occurs in association with rocks predominantly belonging to the c. 1.84–1.80 Ga Vetlanda formation/Oskarshamn-Jönköping belt (OJB), while others primarily occur within or directly associated with TIB intrusives. These pegmatites are typically rich in REE including Y ± Mo ("the Småland type" granitic pegmatites of Smeds 1990).

Characteristically, the REEs occur hosted by both Y+REE oxides and silicates, in some localities also associated with e.g. uraninite. Y+HREE-rich minerals such as euxenite-(Y) occur in several of these pegmatites. Additionally, a chevkinite-like mineral [chevkinite-(Ce), approximately (Ce,REE,Ca,

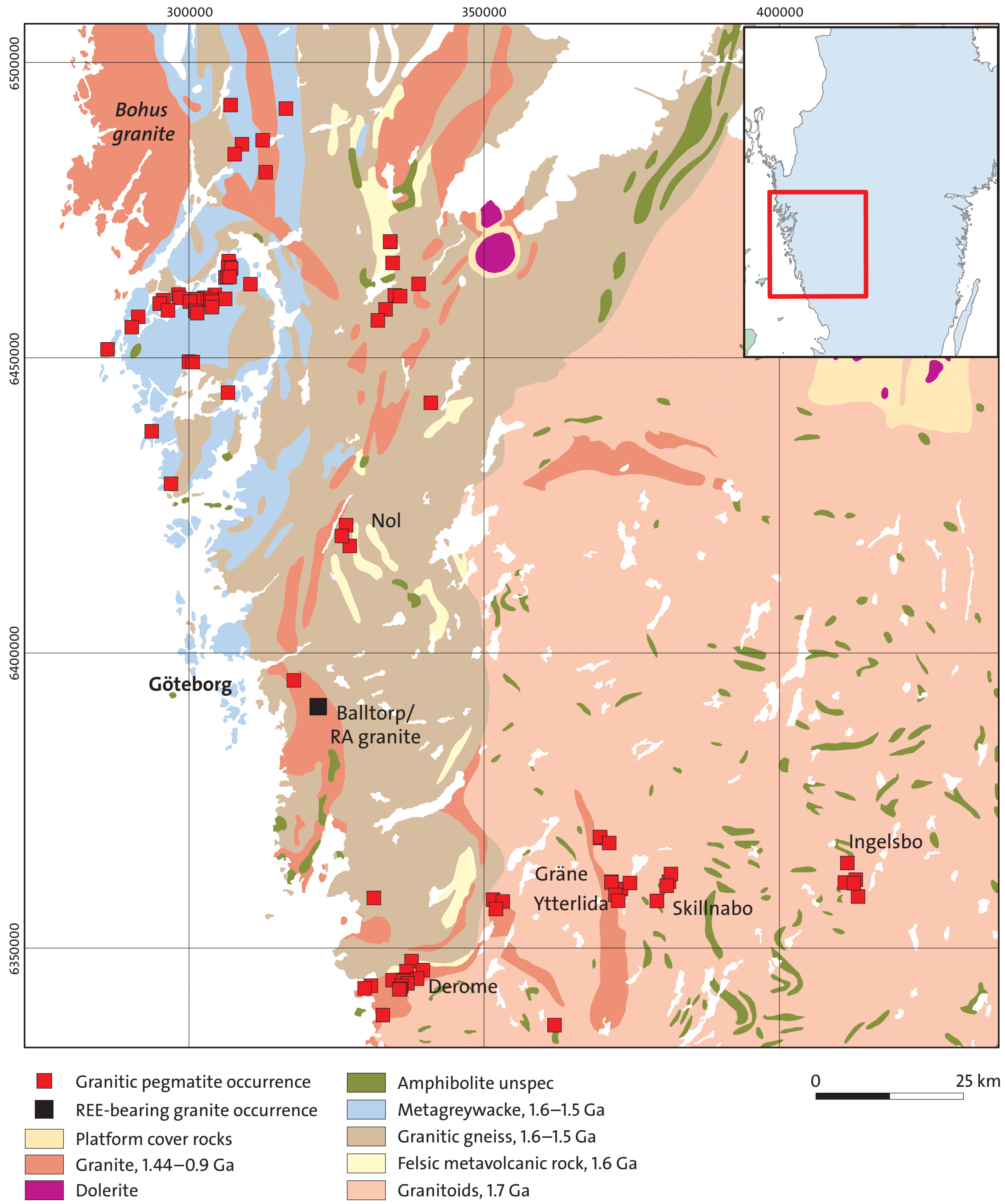

Figure 7. Simplified bedrock geology map showing locations of granitic pegmatites (quarries) and granitoids in southwestern Sweden; REE-enriched occurrences mentioned in the text are named.

Th)$_4$(Fe,Mg)$_2$(Ti,Fe)$_3$Si$_4$O$_{22}$], is an important (L)REE host in at least one locality (Ingridstorp). A good example of the Y+HREE and Mo associations are the dykes formerly quarried at Slättåkra (Fig. 8), featuring locally abundant Y+HREE-Nb-Ti oxides (euxenite and others), Y-enriched titanite ("yttrotitanite"), associated with e.g. molybdenite and its alteration product ferrimolybdite (cf. Langhof 1991).

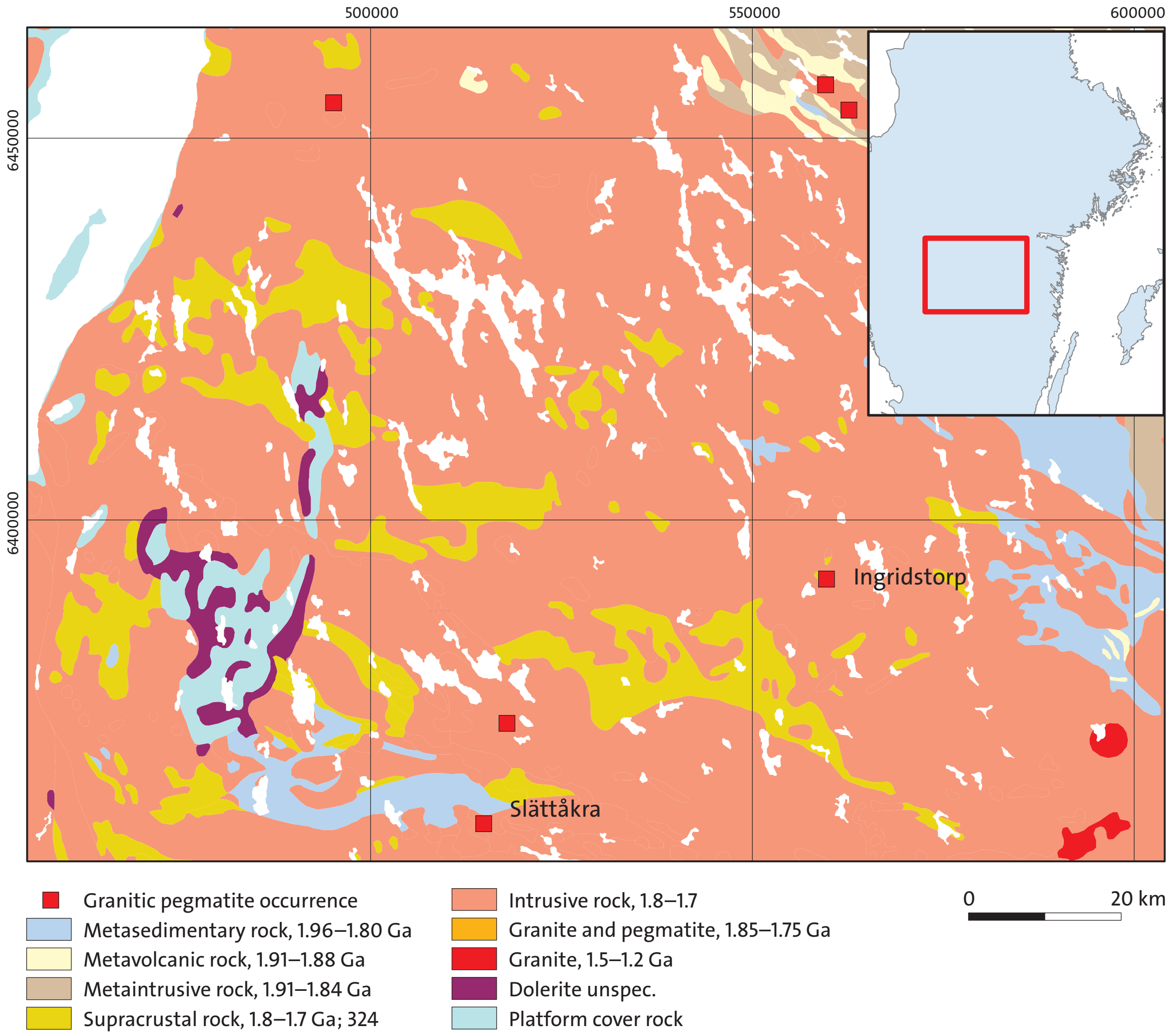

Figure 8. Simplified bedrock geology map showing locations of quarried granitic pegmatites in part of southeastern Sweden; REE-enriched occurrences mentioned in the text are named.

Central Sweden

South-central Sweden (essentially comprising the Bergslagen ore province with surroundings) exhibits several clusters, or fields, of granitic pegmatites of varying character. Within much of Bergslagen, they are predominantly pegmatites of NYF affinity, carrying Y-REE-rich minerals (oxides and silicates) in the northwest-north and (north) east, although LCT-type pegmatite fields are found in the southeast of the region, typically associated with more extensive areas of mainly pelitic metasedimentary rocks (Fig. 9).

Two chemically different suites of granitic pegmatites of NYF and LCT character, respectively, occur in the easternmost part of the region. The pegmatites of the NYF family, including Ytterby, are characteristically strongly enriched in the HREE compared with the LCT-pegmatites. The highest degree of fractionation is observed in lithium-rich, LCT-type pegmatites in the lower-grade metasedimentary rocks of the Stockholm archipelago, and specifically on the island of Utö (Fig. 9).

The well-known, historical pegmatite quarry at Ytterby, north of Stockholm (with abundant Y+HREE-rich minerals such as gadolinite-(Y), fergusonite-(Y) and yttrotantalite/formanite/ichikawaite-(Y); Fig. 10), is part of the easternmost broad grouping of pegmatites in south-central Sweden, which includes a large number of dykes, which can in turn be grouped into four separate clusters (Fig. 9). Two are located in the

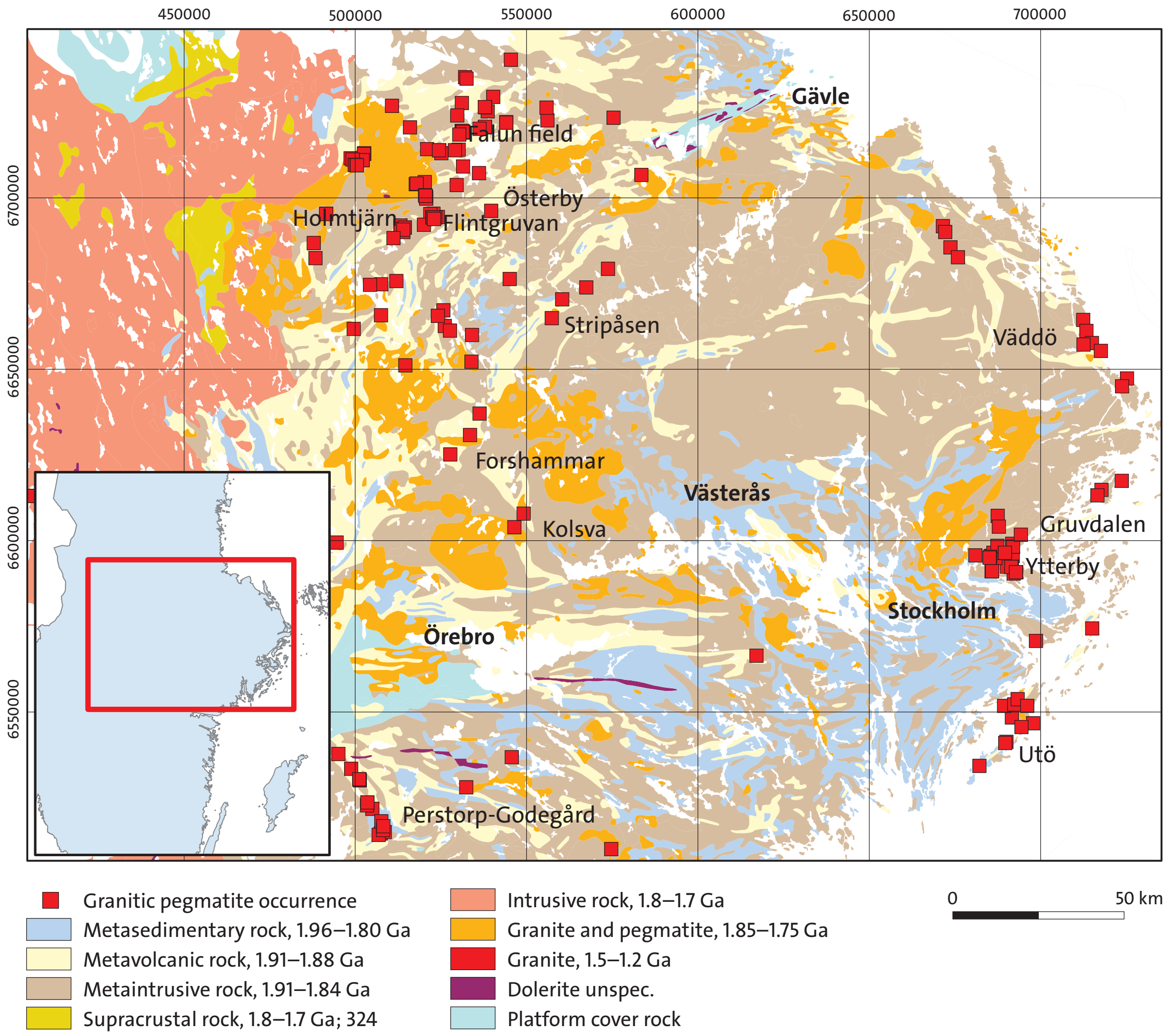

Figure 9. Simplified bedrock geology map showing locations of quarried granitic pegmatites in south-central Sweden, essentially within the Bergslagen ore province; REE-enriched occurrences or clusters mentioned in the text are named.

Figure 10. Hand specimen featuring subhedral black crystals of gadolinite-(Y) up to approximately 2 cm, associated with platy aggregates of biotite (subhorizontal aggregates in the lowermost part of the specimen) and pale feldspar, from the Ytterby pegmatite quarry on the island of Resarö, west of Vaxholm (6592332/690226). Photo: Carl-Erik Alnavik.

northeast of the area, with a significant concentration of quarried dykes on the island of Väddö, including several noted occurrences of HREE-enriched oxide minerals, allanite (*sensu lato*) and REE-phosphates.

An eastern central cluster, north of Stockholm, includes both Ytterby and the Gruvdalen quarry, which exploited a pegmatite dyke similar to that at Ytterby (Smeds 1990, Wik et al. 2004; Fig. 9). Finally, the southern cluster, in the southern part of the Stockholm archipelago, is the most fractionated LCT-type pegmatite system in the region, exemplified by the pollucite-bearing dykes on the island of Utö (Fig. 9). In these occurrences, the relatively sparse REEs that occur are likely to be mainly hosted by pyrochlore-group minerals (microlite *sensu lato*; e.g. Sundius 1952, Frondel 1958, Lumpkin & Ewing 1992, Atencio et al. 2010).

The western to northwestern and northern Bergslagen clusters, as well as dispersed occurrences within the general Bergslagen area, typically host Y+REE as oxides and/or silicates (beside the ubiquitous allanites), which characteristically may include gadolinite-(Y), samarskite *sensu lato*, thalenite-(Y), and yttrialite-(Y) (e.g. Sundius 1952, Brotzen 1959, Škoda et al. 2015; the unspecified Y-REE oxides and silicates of Smeds 1990). The historically important NYF pegmatite field in the Falun region (Fig. 9; Falun field) carries gadolinite-(Y) as a characteristic REE mineral, together with allanite, yttrotantalite-like minerals, and minor REE phosphates, for example (e.g. Smeds 1990). Additional REE carriers here include both "yttrofluorite" and "yttrocerite", REE-enriched fluorites known chiefly from the boulder at Broddbo and the classic pegmatite quarry at Finnbo (e.g. Gahn et al. 1818), as well as sparse fluocerite-(Ce) (Flink 1910). The former two of these minerals also occur in an altered state, with currently unknown mineralogy.

Characteristically, REE hosts such as euxenite-(Y), polycrase-(Y) and samarskite-like minerals are abundant in several occurrences and, as with many of the minerals mentioned above (e.g. yttrialite), are typically associated with increased uranium and/or thorium contents. The latter may occur both as components of the actual REE minerals and as discrete primary phases, as well as in the form of alteration products (cf. above). Fluocerite-(Y) is important only locally, such as at Österby, where thalénite-(Y) also occurs in larger concentrations (Škoda et al. 2015; Fig. 9). The disputed, poorly known, and now discredited Y-Nb-Ta-Sn-U-bearing oxide "hjelmite" (Peacor et al. 1982) occurs in several granitic pegmatites of the province, and may locally be the most important REE carrier, such as in the albite pegmatite at Stripåsen (Tenow 1902; Fig. 9), and also typically occurs in the Falun field pegmatites. Several REE pegmatites have recently been documented by SGU south of Borlänge; e.g. the Flintgruvan 1/Länsmansgruvan and Flintgruvan 2, of which the former locality carries REE minerals in very coarse white plagioclase (albite/oligoclase), and locally high U contents have been recorded (Ripa et al. 2015). A mineral-chemical study showed the major REE host at Flintgruvan (1) to be a heavily altered, Y-dominant aeschynite or polycrase mineral, associated with HREE-enriched thorite and xenotime-(Y) (Orbe 2016; cf. Fig. 5). The Holmtjärn pegmatite, southeast of Idkerberget, carries abundant yttrialite-(Y) and other HREE-enriched minerals (Figs. 9, 11)

Among the largest of the granitic pegmatites quarried in Sweden, the extensive Kolsva dyke (Fig. 9) was mainly mined for feldspar, but was also test-mined for beryllium (from beryl and chrysoberyl), and contained local concentrations of a poorly characterised samarskite-like mineral (Lundegårdh 1971).

The primitive, patchily zoned, mostly graphic pegmatites to pegmatoidal granites at Forshammar in the Riddarhyttan area (Fig. 9; well-known for the nearby REE-rich Bastnäs mines; see separate section in this volume) in west-central Bergslagen, have been quarried for feldspar and quartz on a relatively large scale more or less continuously since the early 1900s. Overall, these pegmatites are mineralogically simple, voluminous, and locally carry andalusite, molybdenite, monazite-(Ce) and allanite-like minerals (cf. Lundegårdh 1971). Notably, crystals of the tourmaline mineral dravite from such a primitive, partly graphic granitic pegmatite cropping out near the Forshammar quarries were found to contain the highest content of REE ever encountered in pegmatite-hosted tourmaline, a dravite with fracture-fillings of hydroxylbastnäsite-(Ce) (Bačík et al. 2012).

The scandium silicate thortveitite has also been found in one of the HREE-rich granitic pegmatites in northwestern Bergslagen (Holmtjärn), as well as in the Ytterby pegmatite (Langhof 1996).

Figure 11. Field image of 10cm-sized lumps of Y-HREE-rich silicates, chiefly yttrialite-(Y) and presumed keiviite-(Y), from the Holmtjärn granitic pegmatite quarry, Dalarna (6691409/514398). Photo: Erik Jonsson.

Northern and north-central Sweden

Broadly speaking, two major areas with pegmatite occurrences can be identified in northern Sweden (Fig. 12); one extensive area in northernmost Sweden, characterised by some regional clusters, and one in north-central Sweden, with minor clusters and singular occurrences in between.

The northern area comprises several variably well-defined clusters, of which the majority do not carry extensive REE mineralisation. Simple, tourmaline-bearing pegmatites are relatively widely distributed, and aplites and pegmatites occasionally also carry weak Mo mineralisation. In northern to northeastern Norrbotten in particular, granitic pegmatites, aplites and pegmatitic granites belonging to the c. 1.8 Ga Lina granite-pegmatite (GP) suite are abundant (Bergman et al. 2001, 2002), although only locally REE-bearing pegmatitic dykes or pods have been observed (Fig. 13).

Others, and in particular the Reunaavare–Flakaberget–Ruoutevare area pegmatites (Fig. 12), exhibit locally substantial amounts of Y+(H)REE oxides and/or silicates, and in one case also the Sc-silicate thortveitite (Langhof 1996). Specifically, the pegmatites quarried in the Ruoutevare area are markedly enriched in (H)REE+Y, carried in allanite, gadolinite, fergusonite, euxenite and "betafite", among others (Dagbo & Martinsson 1981, unpublished thesis; Smeds 1990).

The succession of medium- to high-grade metasedimentary rocks of the Bothnian basin, in north-central Sweden, hosts a significant number of pegmatites. An extensive clustering around Sollefteå is phosphate-rich and of LCT affinity, and collectively bundled together as the "Li-pegmatite horseshoe" by Smeds (1990). These pegmatites are generally poor in REEs, but include one of the largest Sn-mineralised pegmatites in Sweden – the Räggen dyke (e.g. Smeds 1994, and references therein; Fig. 12).

Contrasting with these, and to the north of Räggen, are the Abborrselet and nearby pegmatites (Fig. 12; e.g. Lundegårdh 1971, Kjellman et al. 1999), which carry HREE+Y-rich oxides (fergusonite-(Y), euxenite-samarskite minerals), locally associated with fluocerite-(Ce), as well as allanite, REE fluorocarbonates, and xenotime-(Y). Between the northernmost areas and that of the "Li-pegmatite horseshoe" in the Sollefteå region, are several smaller clusters. One of them comprises the partly well-studied pegmatites of the eastern Skellefte district. Specifically, the complex and mineral-rich, pollucite-bearing Varuträsk pegmatite (Quensel 1956, and references therein) and related smaller dykes in that area (Fig. 12), represent highly fractionated LCT-type pegmatites. These can also be exemplified by the

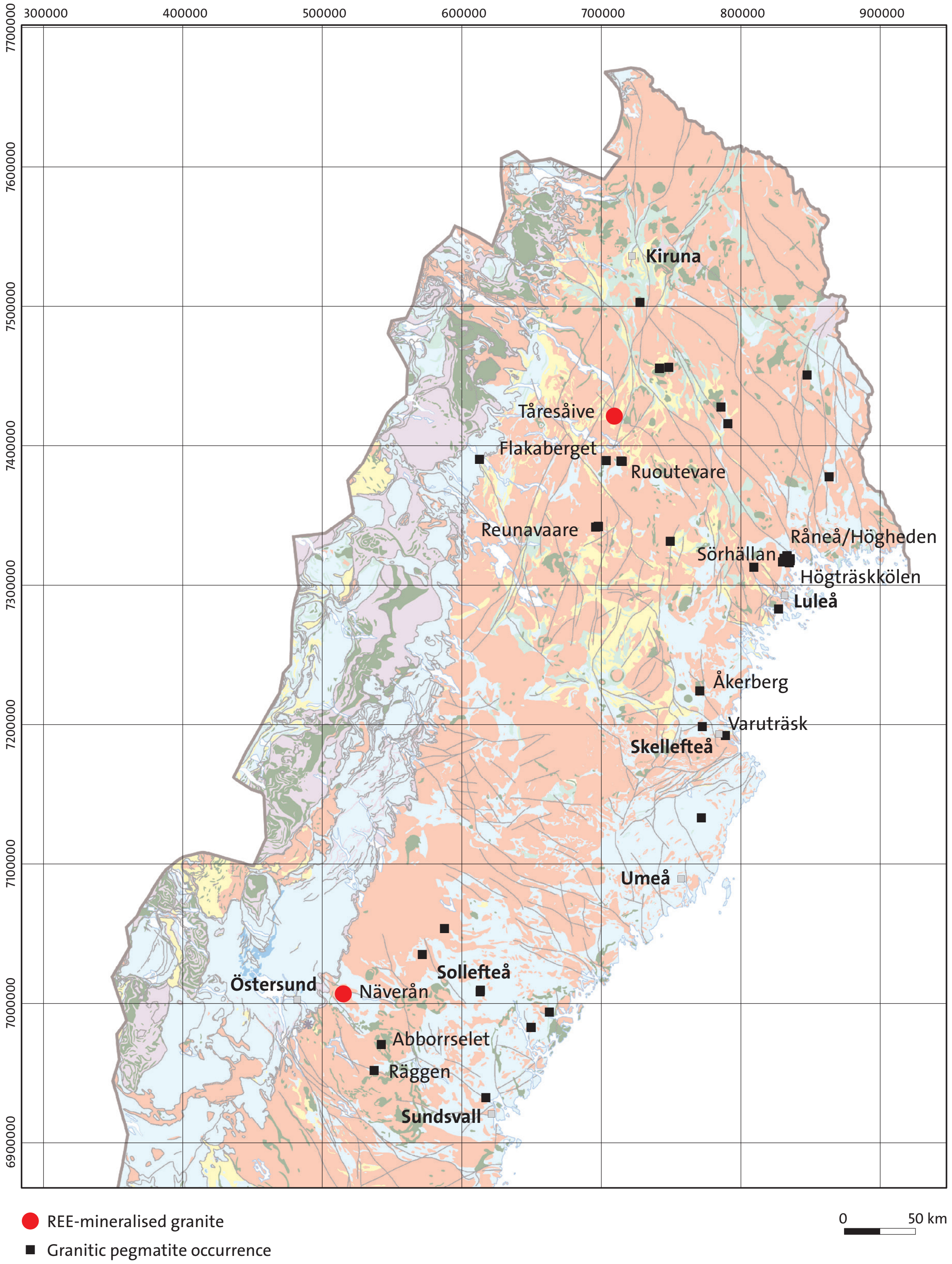

Figure 12. Simplified bedrock geology map showing locations of quarried granitic pegmatites and REE-mineralised granitoids in northern Sweden; occurrences or clusters mentioned in the text are named.

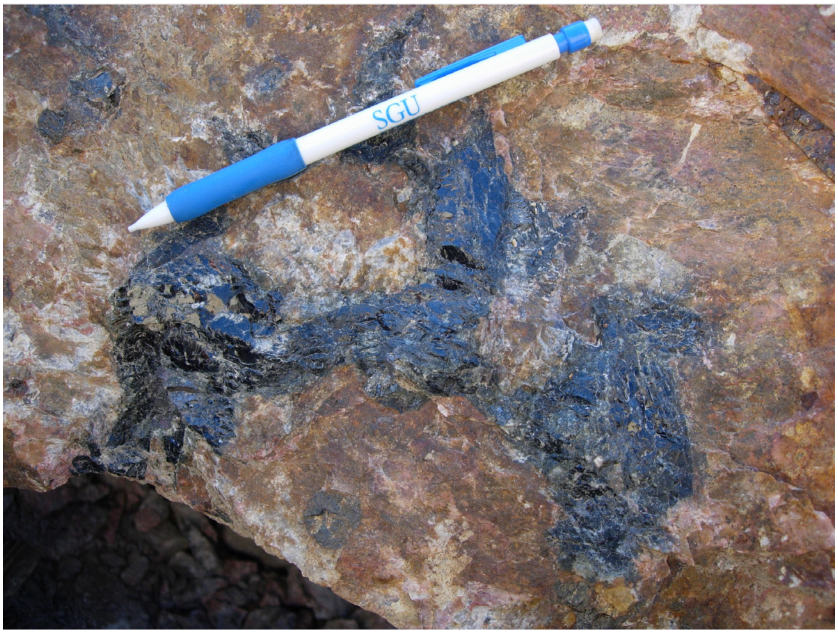

Figure 13. Coarse black masses/aggregates of a metamict REE mineral (allanite?) in a Lina pegmatite dyke/segregation, Övertorneå, Norrbotten (7391663/880957). Photo: Erik Jonsson.

pegmatite occurrence exposed at the Åkerberg mine, featuring a localised, highly fractionated LCT-type unit. In such systems, the relatively low abundances of REEs can be hosted by pyrochlore-group minerals (see above). Yet, all of these more fractionated LCT-type pegmatites only have economic potential for metals such as Ta, Nb, Li, Sn, and Cs, rather than the REEs.

North of the Skellefte district is the pegmatite cluster of the Råneå area (Fig. 12). The Råneå pegmatites mainly seem to belong to the beryl-columbite subtype, and have relatively sparse verified occurrences of REE-rich minerals, such as euxenite (*sensu lato*; A. Österlöv, personal communication). Of these, the Sörhällan dyke is notably rich in monazite-(Ce), and a euxenite-like mineral also occurs; at Högträskkölen HREE oxides have been noted, as well as probable xenotime-(Y) from the Högheden dyke.

REE mineralisation in granites, granitoids and related rocks

The RA-granite in the Balltorp/Mölndal area

Among known granitic rocks with significant enrichment in the REEs, a type called "RA granite", in the Mölndal area of southwestern Sweden (Fig. 4), stands out. This Mesoproterozoic, mostly gneissic, red, and apparently somewhat alkaline granite was initially investigated due to its marked radioactivity. Subsequent analyses showed that, besides U and Th, it was also significantly enriched in a number of other elements, notably Be, F, Nb, REE, Sn, Ta and Zr (Holmqvist 1989, and references therein). Based on the two samples analysed by Holmqvist, it contains between 0.65 and 0.88% total REE+Y, and while it is relatively LREE-enriched, it still shows notable HREE, as well as Y contents between 1000 and 1500 ppm. Additionally, a Zr content of 1.9% was reported, and analyses performed prior to Holmqvist's study yielded 120 ppm U and 380 ppm Th. Subsequent chemical analyses of this rock, performed during an assessment of bedrock quality for aggregate applications, exhibit variable REE contents, with total REE+Y between c. 230 and 1300 ppm (T. Eliasson, personal communication 2016). A transmitted polarised light image of a representative polished thin section of an RA-granite sample shows aggregates of titanite, zircon, chlorite and oxide minerals occurring in a conspicuously fluorite-bearing quartz-feldspar groundmass (Fig. 14).

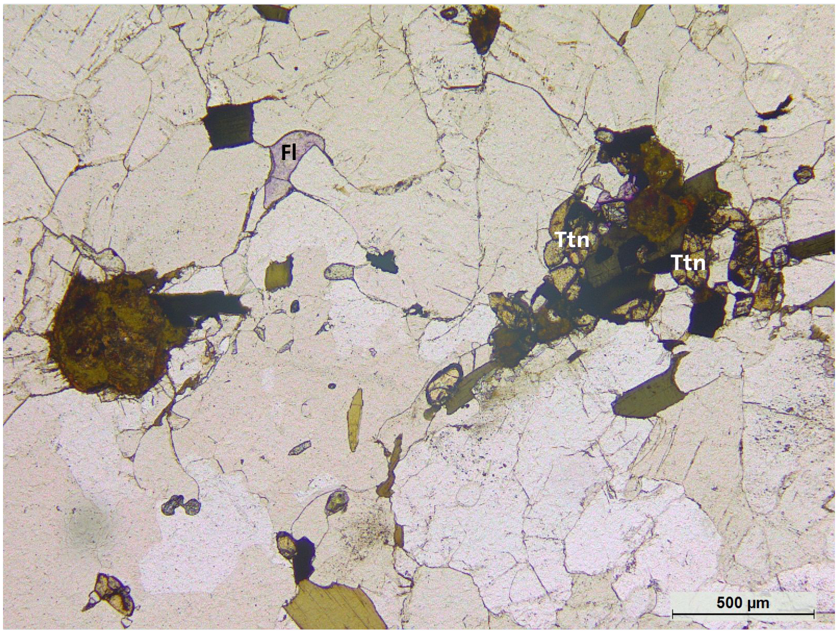

Figure 14. Transmitted polarised light image of a representative polished thin section of the RA-granite sampled for the bedrock quality study of Eliasson et al. Aggregates of titanite (Ttn), zircon, chlorite/biotite and opaque oxide minerals occur in a fluorite-bearing (Fl) quartz-feldspar groundmass. Photo: Thomas Eliasson.

The RA-granite is likely to be related to, and coeval with, the c. 1.3 Ga Kärra granite, belonging to the bimodal Kungsbacka intrusive suite (e.g. Austin Hegardt et al. 2007). The geographical location, partly in a well-populated area, partly in a nature reserve, however, combine to reduce the potential for future exploitation.

The Bohus granite

Also in southwestern Sweden, the c. 920 Ma Bohus granite (Eliasson & Schöberg 1991) exhibits moderately high general REE contents according to available bulk geochemical analyses.

The granitoid-hosted Näverån Th-(U)-REE prospect

The Näverån Th-(U)-REE prospect is situated in central Sweden, approximately 30 kilometres east of Östersund and 100 km east of the Scandinavian Caledonides (7006810/515025; Fig. 15).

The Näverån area predominantly comprises fine- to medium-grained, weakly foliated, light grey granite to granodiorite. Additionally, as observed in drill cores, thin pegmatitic veins and a fine-grained mafic rock occur in subordinate amounts. The granite to granodiorite was dated by the U-Pb-method on monazite to 1.86-1.87 Ga (Lundqvist et al. 2003).

The Näverån prospect was first discovered in the 1970s during a government-funded uranium exploration programme. The area was identified due to a high concentration of boulders of radioactive chlorite-biotite-rich, brecciated granite along an approximately 1.5-km-long and 50-m-wide trail. Analyses showed a generally high content of thorium (up to 2300 ppm) but a relatively low content of uranium (less than 1500 ppm). Besides U and Th, anomalous and significant concentrations of yttrium (up to 1% Y), cerium and lanthanum were detected (Pettersson 1980a; Pettersson, 1980b, unpublished reports). Exploration work continued in the area in the early 1980s, and included 14 diamond drillings totalling 1366 metres of core. A weakly mineralised zone was intersected in two of the cores. The Näverån prospect was abandoned in 1982 due to the meagre results. Tasman Metals AB had a claim of the area between 2011 and 2014 and the company reanalysed several boulder and drill core samples. These analyses showed an average total rare earth oxide (TREO) content of 1.17% (ranging between 0.58 and 2.40%). Chemical analyses of drill core sections from holes NAV80004 and NAV820004 (Fig. 16) are less enriched and contents range between 0.007 and 0.8% TREO, Table 2.

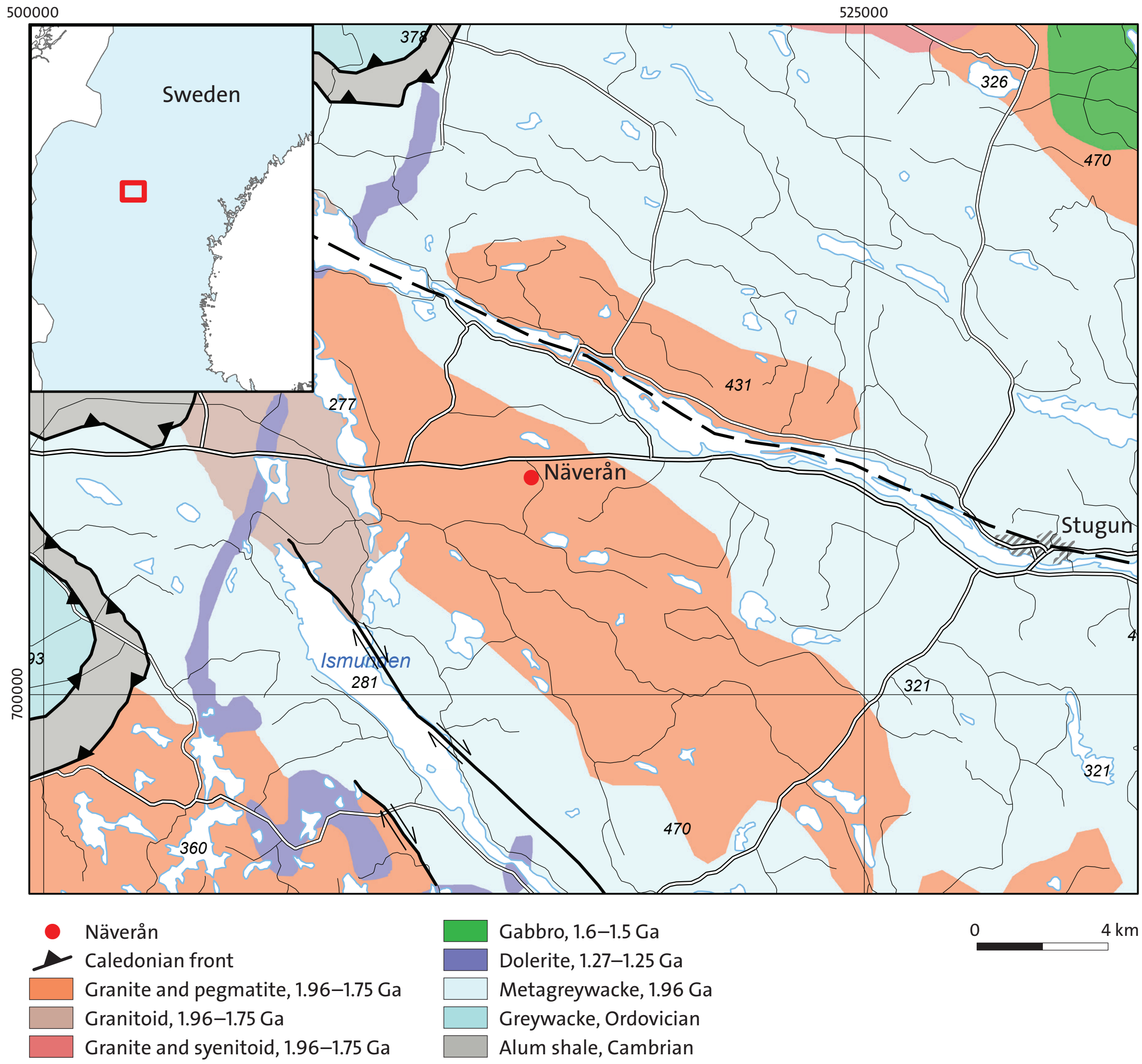

Figure 15. Simplified bedrock geology map showing the location of the Näverån mineralisation (7006810/ 515025), a few kilometres east of the Caledonian front.

The mineralisation is hosted by a highly fractured granitoid rich in chlorite and biotite, interpreted as a brittle-tectonised variety of the granite to granodiorite predominating in the area (Pettersson 1980a, unpublished report). Thin section studies of the mineralised boulders also confirmed the predominance of chlorite and biotite in a strongly schistose texture. Anomalous amounts of other minerals, particularly apatite, xenotime and zircon, are also present, which explains the high contents of Y, Ce and other REE in bulk geochemical analyses (Fig. 17). In addition, minor amounts of galena, uraninite, monazite, allanite, as well as two unidentified minerals, an Y-silicate and an Y-phosphate, occur in the mineralisation. According to Pettersson (1980b; based on SEM-EDS work, unpublished report), Y is mainly hosted by xenotime, but also by the two unidentified Y-minerals, while Ce mainly occurs in monazite and allanite; La in monazite, xenotime and allanite (*sensu lato*), U only in uraninite, and Th mainly in monazite.

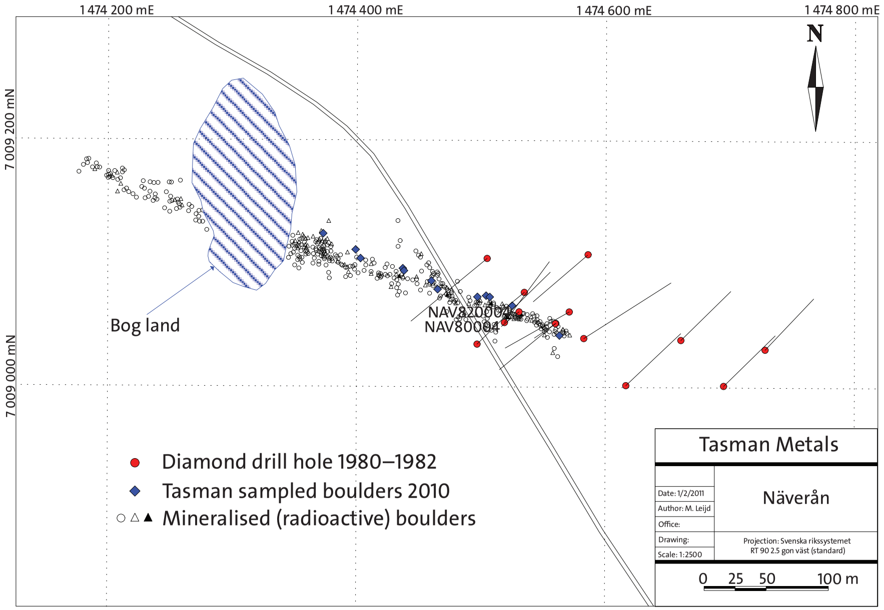

Figure 16. Local map of position of drill cores and boulders in the Näverån area. (Reference: Tasman Metals, drill core protocol NAV80004, 2015).

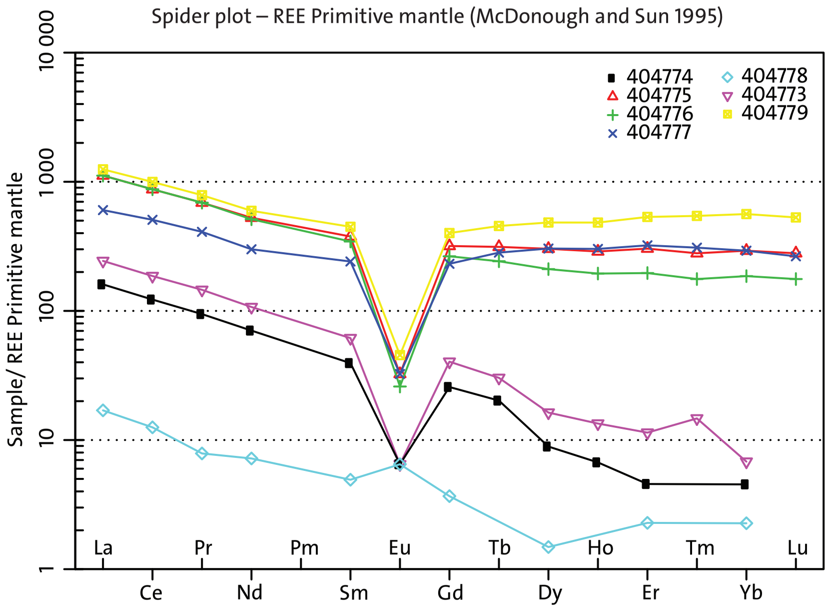

Figure 17. Chondrite-normalised REE data from drill core samples from Näverån. The orange line (sample 404778) is a sample of unaltered granitic pegmatite. The other lines represent samples of strongly altered biotite-chlorite-dominated granite-breccia zones (drillcore report dbh 800004; Source: Tasman Metals AB).

Table 2. Chemical analyses of drill core sections from the Näverån area, drill core NAV800004. All samples consist of chlorite-biotite-dominated granite breccias, except for the sample from section 84.70-85.70, which constitutes unaltered, coarse-grained granite to pegmatite (Tasman Metals, drillcore report NAV80004). All measured values are given in ppm.

Sample id	Location	Type	Section	La	Ce	Pr	Nd	Sm	Eu	Gd	Tb	Dy	Ho	Y	Er	Tm	Yb	Lu	REE-tot
404773	Näverån	Drill core	NAV80004. 9.90-10.85m	158	312	37	134	25	1	22	3	11	2	43	5	1	3	0	756
404774	Näverån	Drill core	NAV80004. 10.85-11.05m	104	205	24	88	16	1	14	2	6	1	24	2	0	2	0	489
404775	Näverån	Drill core	NAV80004. 16.15-16.65m	724	1 465	175	658	153	5	173	31	204	43	1 215	133	19	129	19	5 144
404776	Näverån	Drill core	NAV80004. 16.65-17.10m	723	1 465	175	641	140	4	144	24	142	29	805	86	12	82	12	4 483
404777	Näverån	Drill core	NAV80004. 42.3-42.70m	391	850	104	375	98	5	126	28	205	45	1 190	141	21	129	18	3 724
404778	Näverån	Drill core	NAV80004. 84.70-85.70m	11	21	2	9	2	1	2	0	1	0	8	1	0	1	0	59
404779	Näverån	Drill core	NAV82004. 11.40-12.40m	809	1 670	200	745	182	7	218	45	326	72	2 100	234	37	248	36	6 929

The Tåresåive Mo-REE-(U-Th) mineralisation

The Tåresåive mineralisation in northern Sweden (Figs. 4, 12) was discovered during the "Norrlands mineraljakt" ("northern Sweden mineral hunt") in 1979 (SGU sample ID 79293). Here, molybdenite occurs in hydrothermally altered granite, metarhyolite, and pegmatite. The host granite is c. 1.88 Ga (Claeson et al. 2018); the analysed zircons were significantly metamict, however, and the results therefore of lower quality and with great uncertainties. The molybdenite mineralisation appears to be related to cracks and fissures, but is also disseminated in the host rocks. A few fractures, 10–30 cm wide and more than one metre long, with molybdenite mineralisation occur in the outcrops. An analysis of a mineralised sample from Tåresåive indicates at least 15% Mo and very high contents of rare earth elements (94 900 ppm REE_{tot}, i.e. 9.5%). If yttrium is included, the content increases to >100 600 ppm. The origin of the mineralisation is discussed at some length in Claeson & Antal Lundin (2018). The mineralised sample analysed also exhibits elevated levels of 1490 ppm U, 2430 ppm Th, 396 ppm Nb, 36 ppm Ta, 37 ppm Se, 115 ppm Be, 380 ppm Pb, and 178 ppm W. The economic potential of the mineralisation has not been evaluated.

A reconnaissance scanning electron microscope study of Tåresåive samples performed under the present project revealed a relatively complex mineralogy, with REE mineralisation directly associated with molybdenite, hosted by Th-bearing monazite-(Ce), unidentified, probably mostly altered and heterogeneous U-REE-Pb-Th-rich phases, xenotime-(Y), REE-enriched epidote to allanite-(Ce), unspecified REE fluorocarbonates, aeschynite-(Y), a potential gadolinite-hingganite mineral, and groundmass fluorite (sparse content of Y ± Yb detected; cf. "yttrofluorite"; Fig. 18).

REE mineralisation in alkaline intrusive rocks

Overall, it is well established that evolved alkaline/peralkaline intrusive (± extrusive) rocks may host economic or subeconomic resources of rare metals, including the REEs (e.g. Dostal 2016), and such rocks, together with carbonatites (see below), are therefore among the more relevant ones to explore on a global scale. At present there are several deposits or advanced exploration targets in which REE mineralisation is hosted by, or directly associated with, alkaline/peralkaline igneous rocks (e.g. the Kipawa complex, Strange Lake and Thor Lake, Canada; the Ilimaussaq complex, Greenland; Norra Kärr, Sweden, and Dubbo, Australia). In Sweden, no alkaline-hosted mineralisations have been worked for REEs to date, but one such deposit – Norra Kärr – represents what is currently one of the most advanced

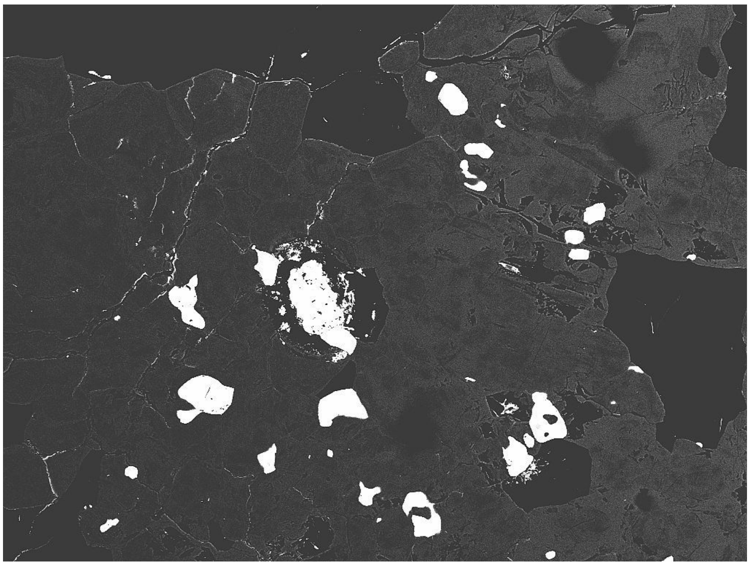

Figure 18. Back-scattered electron (BSE) image of an REE mineralised sample from the Tåresåive mineralisation (7421196/709317). The dark grey to black groundmass predominantly comprises REE epidote/allanite-(Ce), quartz, and mica. The majority of subrounded, white grains are monazite-(Ce), with minor xenotime-(Y) and REE fluorocarbonates. The left central heterogeneous grain/aggregate consists of a core portion of a partially altered U-Pb-Th-U-rich phase, surrounded by two monazite grains. Photo: Erik Jonsson.

and promising REE mining projects in western Europe. In the context of the Fennoscandian Shield, the only recent (and significant) production has been from loparite-mineralised alkaline intrusives on the Kola Peninsula, Russia. The other clans of igneous-hosted REE mineralisation types, granitic (including pegmatitic) intrusives and carbonatites are treated separately (above and below).

Several other alkaline intrusives featuring some potential for REEs (as well as other metals and industrial minerals) are known, such as Särna, Dalarna and Almunge, Uppland. Yet, presently, no clear-cut data showing significant REE mineralisation in either of them are known to us at present.

The Norra Kärr nepheline syenite complex

Among the more advanced REE projects in the Fennoscandian shield, the nepheline syenite-hosted Norra Kärr deposit in southern Sweden, with its NI-43-101-compliant resource of 16.5 Mt at 0.64% TREO (Gates et al. 2013), stands out as one of the more relevant deposits in Europe. This is because of the relatively high proportion of the economically most attractive HREEs, its location in relation to transport and other infrastructure, and the fact that, in contrast to many other similar REE mineralisations, the one at Norra Kärr essentially lacks associated uranium and thorium. The following description is based on that in Jonsson (2013).

The Norra Kärr alkaline complex is a small, Mesoproterozoic intrusion, located east of Lake Vättern, and some 10 km north-northeast of the town of Gränna (Fig. 19). The concentrically zoned intrusion contains several varieties of zirconium and rare earth element-enriched, peralkaline (agpaitic) nepheline syenite rock units (Fig. 20). It is roughly elliptic in outline, with a north–south long axis of approximately 1300 m, and an east–west short axis of about 500 m, and although inwardly dipping, is open at depth (e.g. Sjöqvist et al. 2013b).

The unusual nature of the rocks here was first noted in 1905 and described in more detail by Törnebohm in 1906 as a "katapleiite-syenite", named for its content of the rare alkali-zirconium silicate catapleiite. Norra Kärr was further studied and described by Adamson (1944). An additional "exotic" mineral that is abundant at Norra Kärr is eudialyte (actually eudialyte-group minerals; Sjöqvist et al. 2013a), which is also the main REE ore mineral in the resource.

The geology of the area predominantly consists of 1.81–1.76 Ga magmatic rocks of the Transscandinavian Igneous Belt (TIB), which are made up of mainly felsic plutonic and (lesser amounts of) volcanic rocks (Andersson & Wikström 2004). In the vicinity of Norra Kärr no regional metamorphic overprint is present, yet Norra Kärr is located within a north–south trending corridor of ductile shear zones, which have affected the intrusion significantly, as also suggested by textures and fabrics of the major rock units of the complex (e.g. Sjöqvist et al. 2013b).

The most abundant rock in the Norra Kärr complex is "grennaite" (named after the nearby town of Gränna; Adamson 1944), a foliated, fine-grained nepheline syenitic rock consisting of microcline, albite, nepheline, aegirine, eudialyte (*sensu lato*), and locally abundant catapleiite (hence Törnebohm's original name for it); it is named "GTC" in the nomenclature of Tasman Metals Ltd (Sjöqvist et al. 2013b; Fig. 20). Less abundant rocks are "lakarpite" (an arfvedsonite-albite nepheline syenite), "pulaskite" (microcline-arfvedsonite-albite nepheline syenite), and "kaxtorpite" (a pectolite-eckermannite-aegirine-nepheline syenite; kaxtorpite and lakarpite were both named after nearby farms). Irregularly developed, coarse-grained pegmatitic schlieren with equivalent mineralogy to the grennaite are also common, often hosting coarse-grained REE-zirconium minerals, in particular eudialyte (Fig. 21). This pegmatitic grennaite type is called "PGT" in the Tasman Metals nomenclature (Sjöqvist et al. 2013b; Fig. 20). Lastly, there is another variety of grennaite that is also fine-grained, but differs texturally and chemically from the other fine-grained rock. It contains more hydrated minerals (zeolites), is commonly folded, has a paler colour, and is richer in light rare-earth elements. The rock displays a somewhat veined or migmatitic texture, and has therefore been named "migmatitic" grennaite or "GTM" in Tasman Metals nomenclature (Sjöqvist et al. 2013a, b; Fig. 20). The nepheline syenite variety called lakarpite predominantly comprises sodic amphibole and pyroxene,

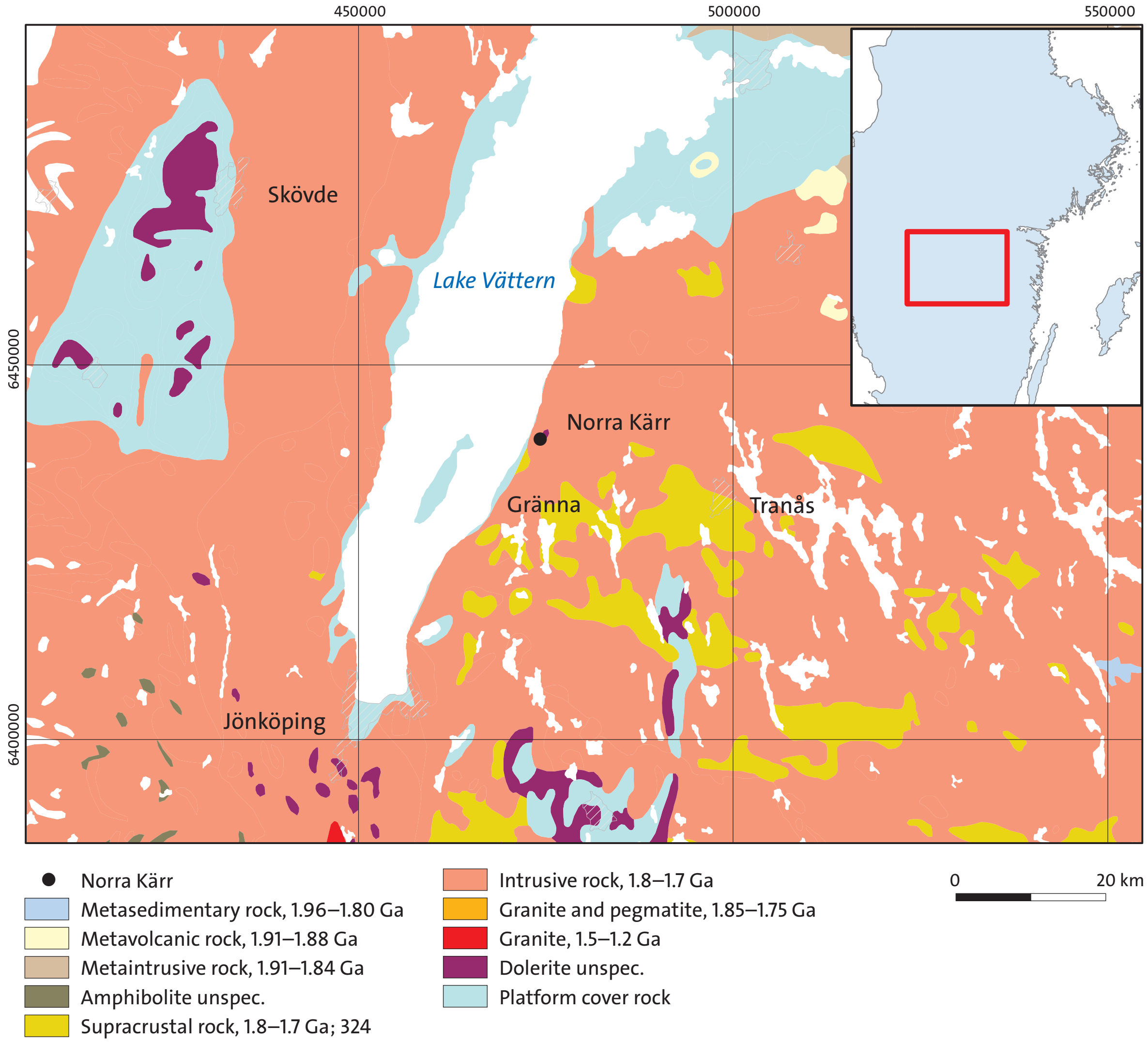

Figure 19. Simplified bedrock map showing the location of the REE-mineralised Norra Kärr nepheline syenite complex (6440266/ 474525) east of Lake Vättern, southern Sweden.

albite, microcline, as well as nepheline, and fluorite. It is by far the most mineralogically varied rock type in the Norra Kärr complex, with associated and accessory minerals including eudialyte, mosandrite, rosenbuschite, pectolite, galena and greenockite (Sjöqvist et al. 2013a, b). The variety called kaxtorpite only occurs near the centre of the intrusion; it is often folded, and consists predominantly of eckermannitic amphibole (fluoro-aluminoleakeite? Cf. Oberti et al. 2009), sodic pyroxene, microcline, albite, and zeolite-altered nepheline, together with accessory pectolite, willemite, and lorenzenite (Sjöqvist et al. 2013a, b).

The Norra Kärr intrusive complex is surrounded by a fenite aureole up to approximately 100 m wide. LA-MC-ICP-MS-dating of fenite-hosted zircons from the hanging-wall to the intrusion, fairly conclusively linked to the intrusion-related fenitisation process, yielded an age of 1.49 ± 0.01 Ga, which is interpreted as equal to a magmatic crystallisation age of the complex (Sjöqvist 2015).

As noted by Sjöqvist et al. (2013), the first stage of exploration in the area was conducted by the Swedish mining company Boliden AB, which investigated the potential for extracting zirconium and nepheline from the grennaite. This was done during and after the Second World War, as Sweden sought self-sufficiency in strategic minerals and energy resources. Following this, in 1948 Boliden AB signed

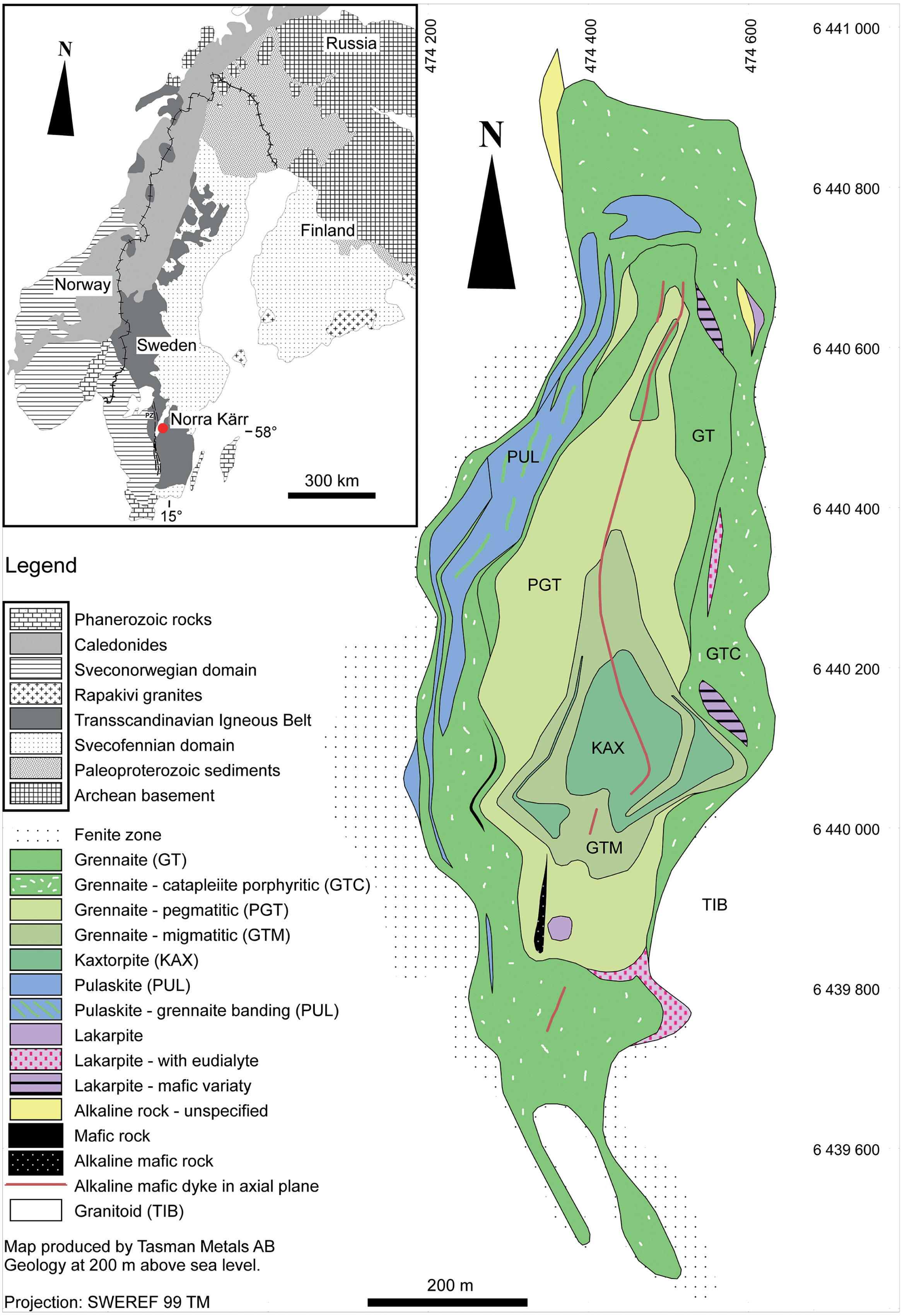

Figure 20. Bedrock geology of the Norra Kärr complex, including unit classification, courtesy of Tasman Metals/Leading Edge Materials (source: Saxon et al. 2015)

Figure 21. Abundant, coarsely crystallised red eudialyte (*sensu lato*) in outcropping pegmatitic grennaite ("PGT"), Norra Kärr. Hand lenses for scale. Photo: Erik Jonsson.

Table 3. Overview of REE and zirconium contents of the main units at Norra Kärr (from Sjöqvist et al. 2013b). The abbreviations PGT, GTM and GTC are explained in the text.

Rock type	TREO%*	HREO%	ZrO2%
PGT domain	0.62	55.4	2.01
GTM domain	0.53	43.1	1.49
GTC domain	0.27	63.5	1.35
Lakarpite	0.23	42.1	0.55
Kaxtorpite	0.18	25.6	0.24
Pulaskite	0.13	40.8	0.35

*TREO%=Rare Earth Elements (La+Ce-Lu +Y) in oxide form. HREO = Eu-Lu +Y.

a contract with the landowners giving the company mining rights. Test mining on a small scale was carried out at two sites in 1949, and included subsequent concentration tests. Using the technology of the day, it was found to be difficult to separate nepheline from feldspar and aegirine, and the iron contents of the nepheline concentrates were therefore too high. In 1974 Boliden AB restarted its exploration for nepheline, zirconium and hafnium at Norra Kärr, and, among other things, sampled two long trenches 400 m apart across the intrusion. This yielded 244 m at 1.9% ZrO_2, 0.37% TREO* in the "north trench", and 149 m at 1.49% ZrO_2, 0.43% TREO; and 52 m at 1.47% ZrO_2, 0.54% TREO in the "south trench" *(TREO = total rare earth oxide + yttrium oxide (Y_{2O3}); Sjöqvist et al. 2013b).*

The eudialyte-group minerals at Norra Kärr exhibit significant chemical variability within the intrusion, including in their REE content (Sjöqvist et al. 2013a). Wavelength-dispersive electron microprobe (WDS-EPMA) analyses of Norra Kärr eudialytes (*sensu lato*), performed for Tasman Metals, and only including Ce_2O_3+La_2O_3+Nd_2O_3+Y_2O_3, yield overall REE totals between 0.85 and 8.49 wt%. The highest and lowest average content reported (from different analytical laboratories) is 6.73 and 5.11 wt%, respectively (Sjöqvist et al. 2013b). Since the REEs that were not analysed should reasonably account for at least an additional 1.5–2.0 wt%, it is inferred that the average total REE content in the

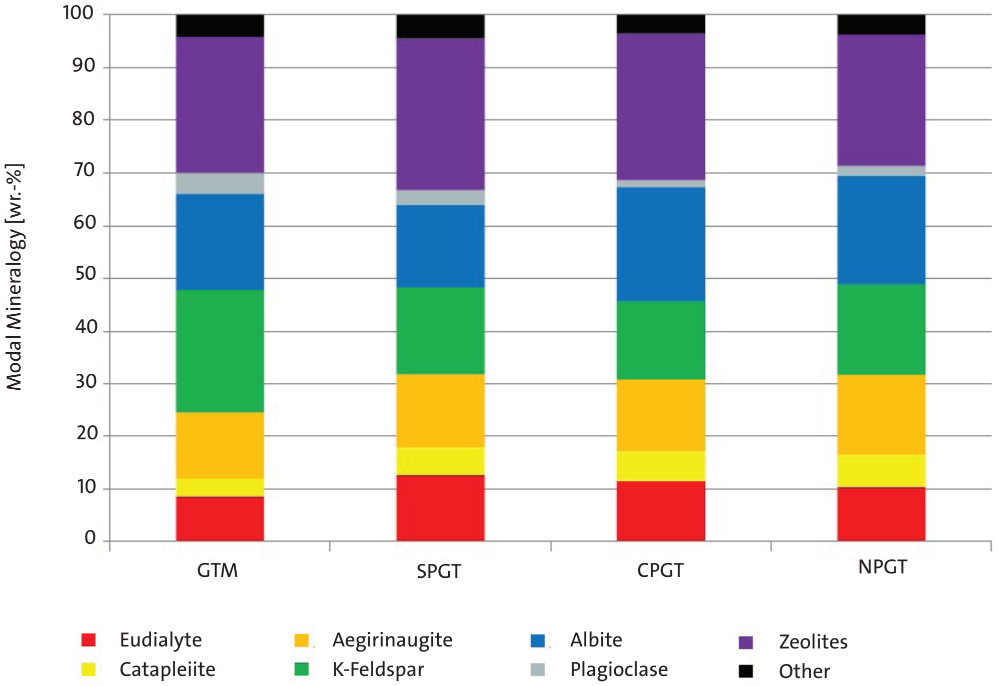

Figure 22. Mineralogical distribution in Norra Kärr mineralised rock types as determined by MLA (Saxon et al. 2015). The abbreviations GTM, SPGT, CPGT, and NPGT are explained in the text and Fig. 20.

Table 4. Norra Kärr Project, NI43-101 Compliant March 2012 "in-pit" mineral resource estimate (from Sjöqvist et al. 2013b).

Classification	Tonnes Mt	TREO%	LREO%	HREO%	HREO/TREO%	ZrO_2%	Tonnes of TREO contained
Indicated	41.6	0.57	0.28	0.29	50.8	1.70	237,120
Inferred	16.5	0.64	0.33	0.31	48.4	1.70	94,050

eudialytes within the Norra Kärr resource ranges between 6 and 9 wt% (Table 3, Sjöqvist et al. 2013b). Although REEs are hosted by several additional minerals present within the complex, the work by Tasman Metals was largely focused on eudialyte. Zirconium has also been looked at as a possible by-product, as have nepheline concentrates.

A resource calculation by Tasman Metals showed REEs to be enriched throughout the Norra Kärr deposit, with the higher value HREEs overall representing more than 50% of total REE content.

Mineralogy is an important factor when it comes to beneficiation test and mineral processing stages. The mineral characterisation of samples from different rock units in Norra Kärr based on mineral liberation analysis (MLA) technology revealed variation and constituents of mineralogy in each domain (Fig. 22).

The Norra Kärr complex thus hosts a significant REE resource featuring a relatively high proportion of the economically most relevant heavy rare earth elements and is one of only a few NI 43-101-compliant REE deposits in the European Union. The mineral resource estimate from March 2012 defined a combined indicated and inferred "in-pit" resource (Table 4) of 58.1 million tonnes grading 0.59% TREO (Total Rare Earth Oxides) and 1.70% ZrO_2, with about 50% of the TREO being the higher value HREO (Heavy Rare Earth Oxides). The resource is defined down to 200 m vertical depth, of which the indicated part comprises the first 120 m, and is based on 49 holes out of a total of 8,016 m drilled in 100 m spaced sections, with an average of 80 m between holes (Sjöqvist et al. 2013b); the resource remains open at depth in most of the drilled sections, and later drilling has also intersected mineralisation above cut-off down to 320 m vertical depth.

REE mineralisation in carbonatitic and ultramafic rocks

The Alnö carbonatite-alkaline intrusive complex

The Alnö complex consists of a main intrusion, and a few separate smaller intrusions on the island of Alnö, in the Bothnian Bay and on the mainland north to northwest of Alnö, all along the coast of east-central Sweden (Kresten 1976, 1979, 1990; Fig. 23).

While no extensive REE mineralisation has been defined on Alnö or in its surroundings, the carbonatites, and specifically the calcite-dominated ones (søvites), contain significantly elevated total REE content,

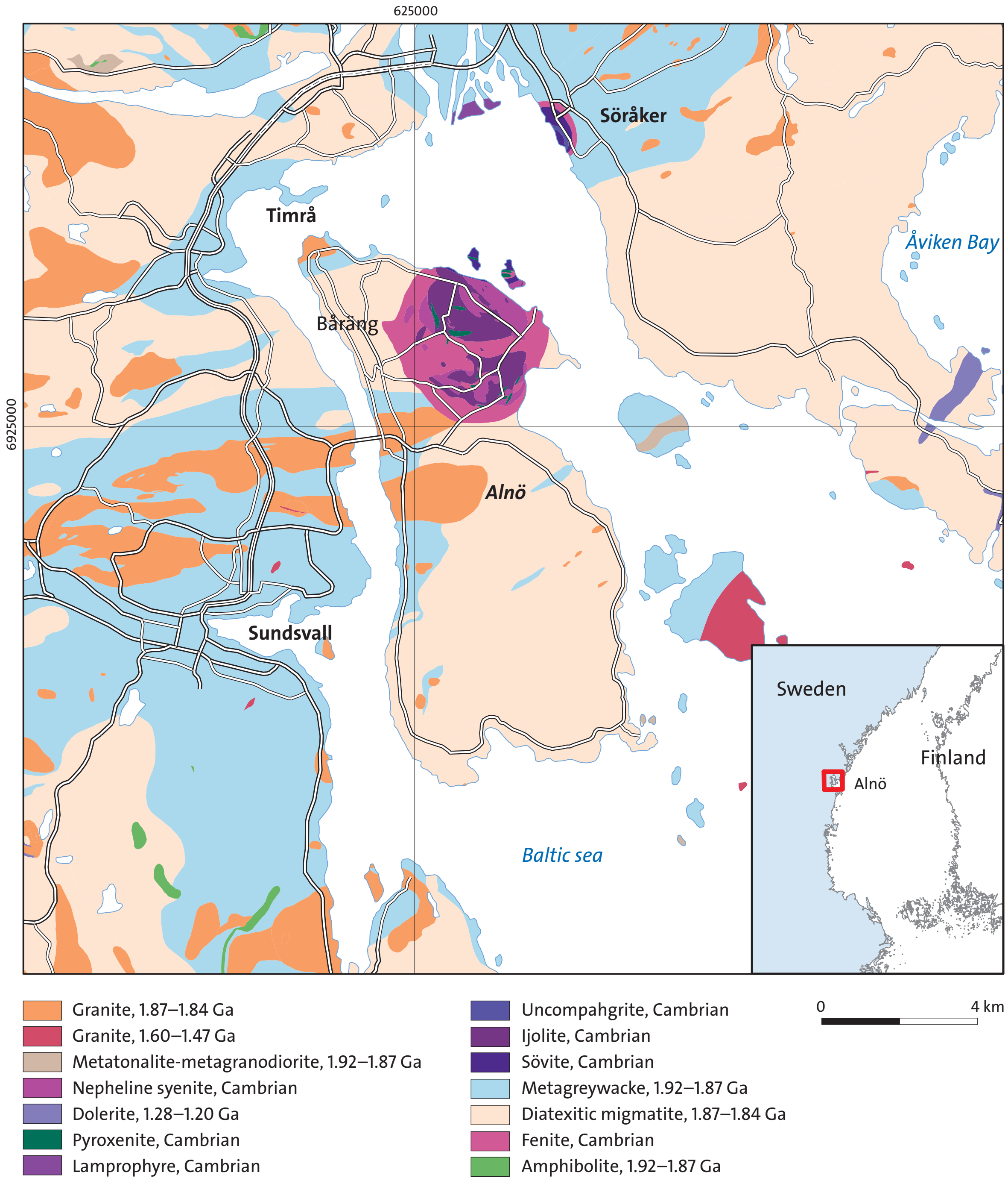

Figure 23. Simplified bedrock geology map of the Alnö complex and surrounding areas.

between approximately 500 and 1500 ppm (Hornig-Kjarsgaard 1998). Alnön and associated rocks on the mainland have also been the focus of exploration for REEs, including that carried out by the Boliden company in the 1970s (Svensson 1972, unpublished report).

The rocks of the main intrusion are ijolite, melteigite, urtite, nepheline syenite, pyroxenite and Ca-carbonatite. Alnöitic, phonolitic and syenitic dykes show cross-cutting relationships with the other rocks of the intrusion (Hode Vuorinen 2005). Fenitisation is a common feature in the surrounding country rocks. The Ca-carbonatite dykes are a few centimetres to several tens of metres wide. One of the largest is the Båräng intrusion, west of the main intrusion.

The Söråker intrusion is located on the mainland north of Alnö and comprises Ca- and Mg-carbonatite dykes and melilitolites (Fig. 24). Melilite occurs in alnöites and kimberlitic alnöites on Alnö and in melilitolites at Söråker. The kimberlitic alnöites contain more olivine and are more primitive than alnöite. Carbonatite dykes, not least Mg-rich ones ("beforsite", named after the locality) also occur in the Bergeforsen–Timrå area, west to west-northwest of Söråker.

The ijolite series rocks are primarily composed of clinopyroxene, nepheline and Ti-andradite. The pyroxenites consist of clinopyroxene and minor amphibole and apatite (Fig. 25). The major constituents of the nepheline syenite are nepheline, K-feldspar and aegirine–augite. Accessory phases in the ijolite series rocks include titanite, apatite, phlogopite, perovskite and magnetite. In the pyroxenites, the accessories include Ti-andradite, titanite, perovskite and nepheline. The nepheline syenites contain accessories such as Ti-andradite, biotite, apatite, titanite, cancrinite, calcite, wöhlerite and pyrochlore (Hode Vuorinen et al. 2005). Clinopyroxenes show enrichment in LREE up to 100 times chondritic values. Ti-andradites show extreme enrichment in all REEs, especially in LREE (La, Ce, Pr, and Nd) and MREE (Sm, Eu, Gd) – more than 2000 times chondritic values (Hode Vuorinen et al. 2005).

The Alnö complex has been dated several times using different methods, yielding ages of between 546 and 590 Ma (Kresten et al. 1977, Brueckner & Rex 1980, Andersen 1996; Walderhaug et al. 2003, Meert et al. 2007).

Melilitolite and ijolite series rocks were formed by fractional crystallisation of olivine, clinopyroxene and melilite in an almost closed system. Crustal contamination took place during late- to post-magmatic stages. Silicate minerals in the carbonatites are either a result of contamination by wall rock or of magmatic origin. Liquid immiscibility may be an important factor in the genesis of the carbonatites on Alnö (Hode Vuorinen 2005).

Figure 24. An approximately 50-cm-wide irregular carbonatite dyke incorporating, dissolving and disseminating high-grade fenite (Stornäset). Photo: Johan Söderhielm

Figure 25. Layered ijolite cross-cut by a fine-grained nepheline syenite at Brännäs. Photo: Johan Söderhielm

Notably, besides Alnön itself, a number of carbonatitic and related dykes on the mainland (such as in the Bergeforsen–Timrå area) as well as smaller massifs (Söråker area) have been reported over time, and also include carbonatites with increased radioactivity (Eckermann 1960). Boulder finds, featuring e.g. apatite mineralisation, and increased REE contents in the vicinity of Söråker also highlight the potential for as yet unknown occurrences in that area (e.g. Sundberg 2005, unpublished report). This, combined with the fairly recent finds of a number of ultramafic diatremes ("kimberlitic"/lamproitic to alnöitic in composition and in part enriched in REEs and other elements), more than 40 km north and northwest, inland from Alnön (e.g. Sundberg 2000, Sjöberg 2004), suggests some remaining potential for new discoveries in the wider region (see below).

Ultramafic and carbonatitic dykes in the Kalix area

Ultramafic rocks occur as up to 1-metre-wide, north–south trending dykes along the coast of the Gulf of Bothnia between Kalix and Luleå (Figs. 26, 27; Larsson 1943, Kresten et al. 1981). The dykes intruded into Palaeoproterozoic igneous and metasedimentary rocks at 1.1 Ga (Kresten et al. 1997). They comprise olivine-rich or micaceous lamprophyres and silico-carbonatites (Kresten et al. 1981). Beforsites, i.e. dolomite-dominated carbonatites, were also described by Kresten et al. (1981).

The lamprophyres are characterised by a porphyritic texture. The most abundant minerals are olivine, phlogopite, spinel (magnetite, hercynite), calcite, serpentine, clinopyroxene and amphibole. Olivine, phlogopite and spinel group minerals occur as phenocrysts (Sundvall 2003). Kresten et al. (1981) reported perovskite and anatase in the olivine-rich lamprophyres. The dykes are co-magmatic, evolving from a low degree of partial melting in the upper mantle by fractional crystallisation of olivine, spinel and phlogopite (Kresten et al., 1981; Sundvall 2003).

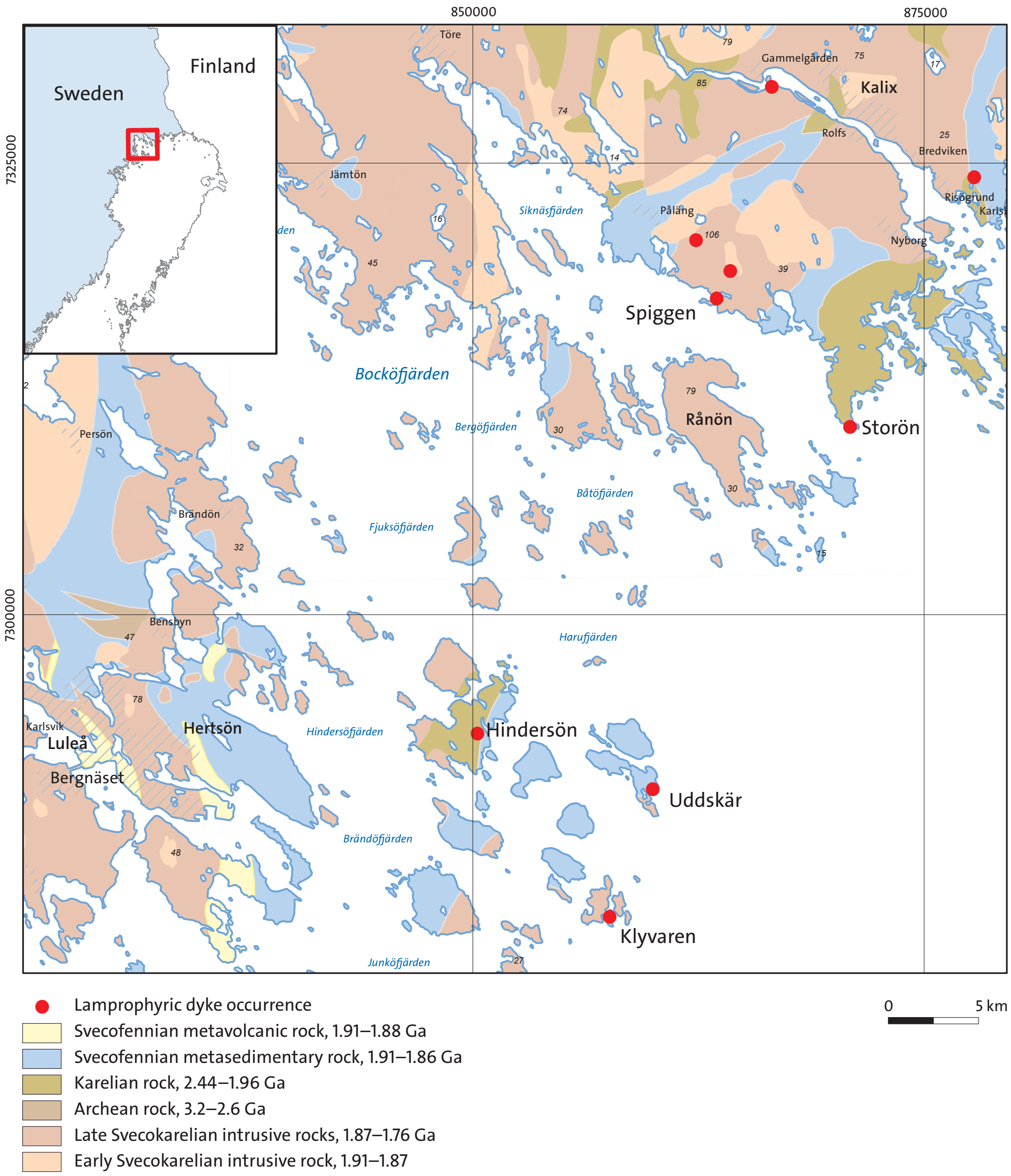

Figure 26. Simplified bedrock geology map showing locations of the Luleå–Kalix section of the northern Swedish coast, including known locations of lamprophyric dykes.

Figure 27. Calcite-rich, zoned lamprophyre dyke at Storön, south of Kalix. Photo: Johan Söderhielm.

Carbonatitic rocks in the Åkersjön area, Jämtland

The Caledonian rocks of the Åkersjön area of Jämtland, west-central Sweden, host a suite of modest exposures of partly REE-mineralised carbonatitic rocks. Intrusive-hosted mineralisation in the region was first noted at Prästrun, west of Åkersjön (Fig. 28) in the 1980s, during the follow up of an airborne radiation anomaly. This was subsequently found to be caused by niobium-mineralised, mostly gneissic, but locally also pegmatitic, alkaline rocks within Caledonian thrust nappes, near the boundary between the Särv and Seve nappe complexes (Löfroth & Pettersson 1982). Additional studies to evaluate the potential for exploiting the niobium mineralisation, hosted by a pyrochlore-group mineral ("betafite") were also carried out (Holmqvist 1989, unpublished report; Hålenius 1990, unpublished report). This was not found to be economically feasible at the time, however. The Åkersjön area is in turn located some 10 km east of Prästrun, in a very similar tectono-stratigraphic position (Fig. 28). Here, the presence of mineralised carbonatitic units was recognised during external contract work by SGU, leading to carbonatitic (to "glimmeritic") rocks carrying local REE-Nb-(U-Th) mineralisation being discovered in both boulders and in situ, seemingly as components of a comagmatic silicic–carbonatitic intrusive system (Jonsson & Stephens 2004, 2006).

The Åkersjön area is predominantly made up of Caledonian thrust sheets; nappes belonging to the Särv Nappes in the Middle Allochthon, and the Seve Nappe Complex in the Upper Allochthon are present (cf. Stephens et al. 2004). Both the alkaline rocks in the Prästrun area (Löfroth & Pettersson 1982) and those exposed at Åkersjön seemingly occur along the contact between the Särv Nappe and the Seve Nappe Complex, and Jonsson & Stephens (2006) suggested that they had intruded along this contact and were subsequently metamorphosed and deformed during the Caledonian orogeny and associated thrusting.

Most of the exposed part of the Åkersjön system consists of variably silicate-bearing carbonate rocks, as well as feldspar-dominated, biotite ± carbonate-silicate rocks, and units consisting almost solely of this ”biotite” are common ("glimmeritic rocks"; Fig. 29). The feldspathoid mineral sodalite occurs locally. The rocks range from fine- to coarse-grained, but are mostly medium-grained, with variably apparent banding/foliation. These rock types are mostly markedly radioactive. In the Prästrun mineralisation, the main host for radioactive elements seems to be a betafite-like mineral of the pyrochlore group, yet at Åkersjön, the host mineral(s) is so far unknown. Mineralisation at Åkersjön is hosted by REE fluorocarbonates (including bastnäsite-(Ce); Jonsson & Stephen 2006).

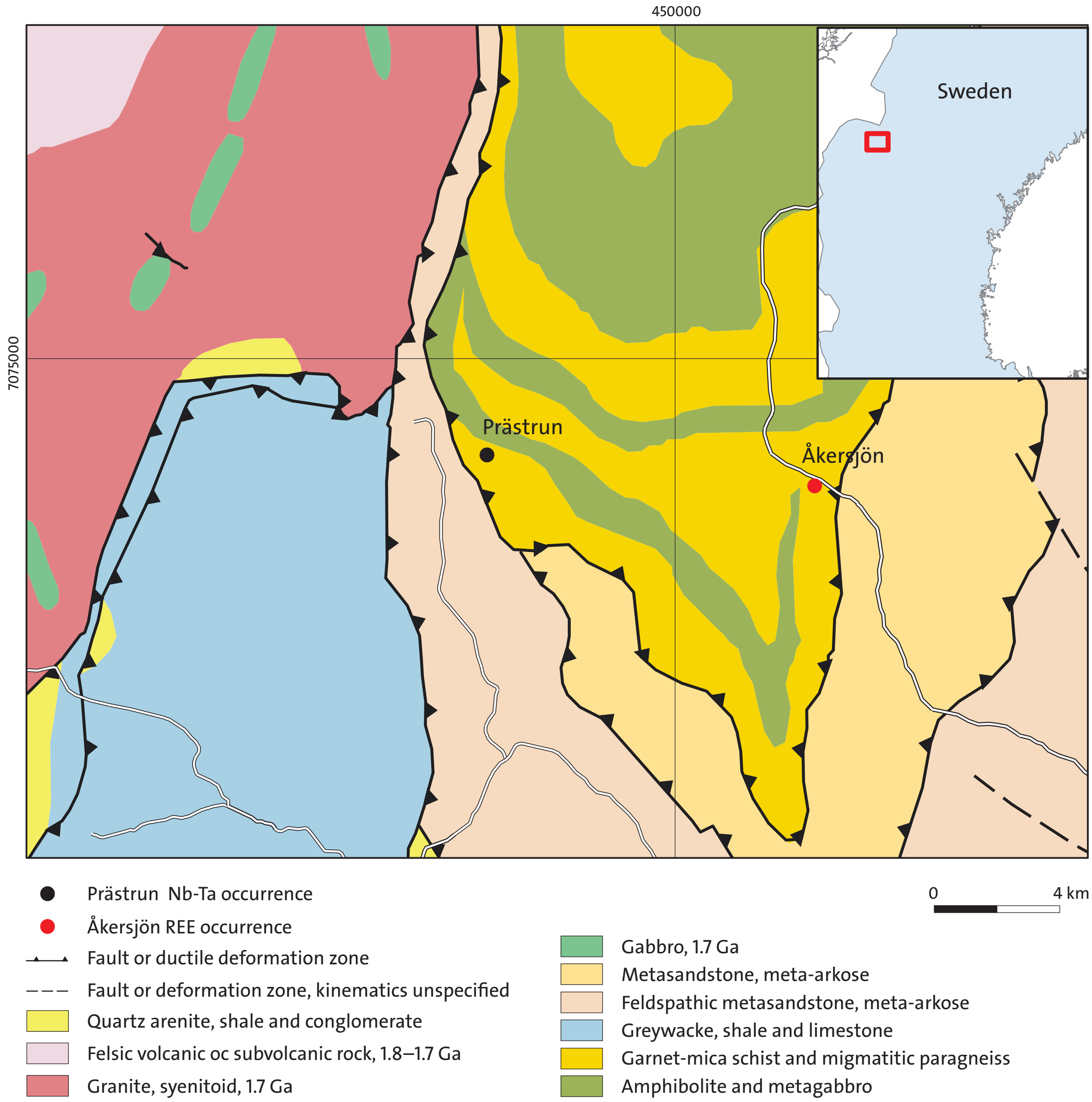

Figure 28. Simplified bedrock geology map showing locations of Åkersjön (7071002/454407) and the Prästrun (7071939/443926) mineralisations in the central Swedish Caledonides.

Figure 29. Medium-grained, calcite-rich carbonatite in contact with black mica-rich ("glimmeritic") unit outcropping at Åkersjön (7071002/454407). Photo: Erik Jonsson.

Other areas of potential future interest for carbonatites and alkaline rocks

The Gävle graben structure, southeast-central Sweden

The Gävle graben is a poorly exposed, west-southwest–east-northeast-oriented structure between Storvik and Gävle, continuing into the southern part of the Bothnian bay. It is filled by c. 1.5 to 1.3 Ga "Jotnian" sandstones, which have been intruded by doleritic sills and stocks and are interlayered by basalt (Fig. 30).

During the Mineraljakten organised public search for minerals, samples of an apatite-calcite rock from boulders found along a forest road near Främlingshem, southwest of Gävle were submitted. Based on studies on these, as well as smaller pieces of rock found subsequently that also carried abundant apatite, Nyström et al. (1985) concluded that they had a carbonatitic character, and suggested the possibility of a covered, unknown carbonatite intrusion within the Gävle graben structure. The occurrence of larger boulders of the soft and easily broken-up apatite-calcite rock (Fig. 31) suggests short glacial transport.

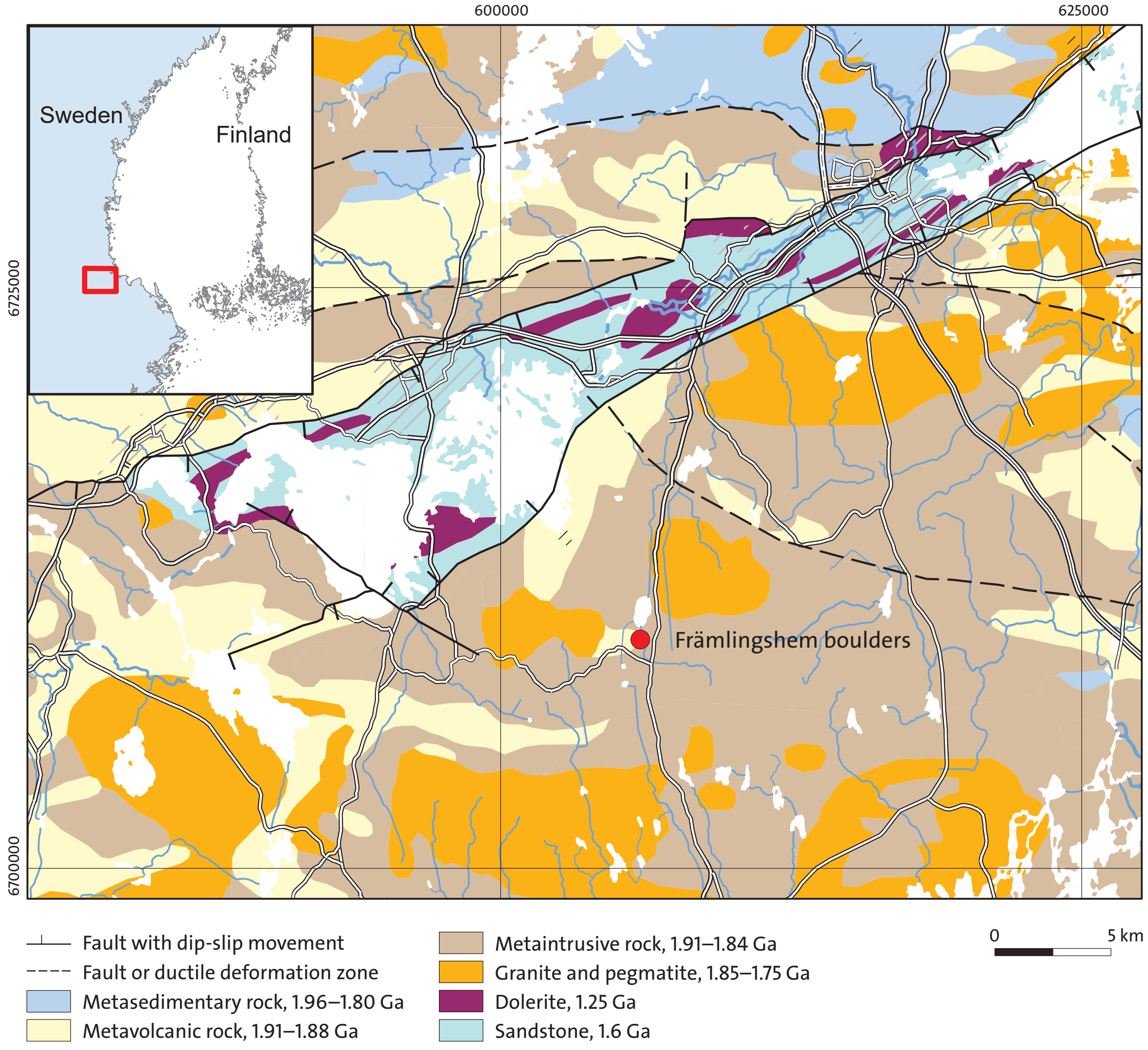

Figure 30. Simplified bedrock geology map showing the location of the Främlingshem boulders (6709872/605974), in relation to the poorly exposed Gävle graben structure.

Mineralogically, the boulder material studied contains fluorapatite, calcite (markedly strontium-enriched at c. 2600 ppm), quartz, fluorite, magnetite, pyrite, chlorite (pseudomorphs after biotite or phlogopite?), and sericite, with accessory hematite, ilmenite, epidote and titanite, and carries abundant xenoliths of what has been interpreted to be Proterozoic country rocks (Nyström et al. 1985). The fluorapatite is reported by these authors to contain around 2000 ppm Ce (notably, as the only REE analysed), and a whole-rock analysis of the apatite-calcite rock yielded over 1000 ppm TREO, with content and proportions very similar to carbonatites from Alnön and Sokli in Finland (Nyström et al. 1985; Möller et al. 1980). These observations, combined with available strontium and carbon isotope data, strongly indicate a carbonatitic affinity for the rock in the Främlingshem boulders. Additionally, as noted by Nyström et al., von Eckermann (1928) discovered a geologically young dyke of a mica lamprophyre at Hamrånge (called "hamrongite" by that author) some 25 km north of Gävle, further indicating young magmatic activity of an alkaline character, potentially allied to carbonatites, in this general area.

All in all, the Gävle graben area seems to have potential for future exploration for what could be economically relevant apatite-REE-mineralised carbonatite occurrences. The low, flat and wet terrain in this area makes both bedrock studies and exploration problematic, but this also increases the likelihood that an occurrence of exotic rocks such as carbonatites has escaped attention.

Figure 31. Apatite- and mica-rich carbonatite-like rock from Främlingshem, south of the Gävle graben; note the approximately 7-mm-wide, euhedral, greenish-grey apatite crystal in the uppermost part of the image. The image width is c. 5 cm. From the mineral collection of the Swedish Museum of Natural History, Stockholm (catalogue number 20040078). Photo: Jörgen Langhof.

The Åvike Bay structure, east-central Sweden

Some 10–15 km northeast of the island of Alnö, with its comparatively well-studied carbonatite-alkaline intrusive complex (Fig. 23) lies the Åvike Bay (Åvikebukten), a markedly semicircular part of the coast, but also extending into the sea(floor). This has been variously interpreted as an igneous centre similar to Alnön, or as a meteorite impact structure (cf. Preeden et al. 2010, and references therein). The occurrence of ultramafic ("kimberlitic") as well as carbonatitic rocks as both in situ dykes and boulders in this area suggests some potential here and in the area between the Åvike Bay and Alnön/Söråker.

An inferred (sub-)seafloor location of the central part of a potential intrusive complex here naturally makes any economic exploitation of such an occurrence unlikely.

REEs in apatite-iron oxide deposits, Norrbotten, northern Sweden

The apatite-iron oxide mines of the Norrbotten region of northernmost Sweden currently produce over 90% of all iron ore mined in Europe. As in other apatite-iron oxide ores (*cf.* description of apatite-iron oxide ores in Bergslagen, Sweden, and references therein), fluorapatite and associated REE-bearing phosphates (and silicates, in the case of REE) in these ores represent variably relevant potential reserves of both REEs and phosphorus.

At present some 40 apatite-iron oxide deposits are known from the far north of Sweden (Fig. 32, Bergman et al. 2001). Outside of the main areas of apatite-iron oxide ore occurrences, late-stage and breccia type iron oxide mineralisations with locally increased REE contents have also been observed (Jonsson 2008, Jonsson & Kero 2013, and references therein). The main (at over 2000 Mt) deposit in Norrbotten is the eponymous Kiruna (Kiirunavaara) mine, the "type locality" of the Kiruna-type ores (cf. Geijer 1931). Second in size and output is the Malmberget mine, also featuring apatite-iron oxide ore, but with a significantly more extensive overprint from both regional metamorphism and deformation. Since mining of these deposits began, their origin has been debated, and there is still controversy over whether they were formed by essentially hydrothermal processes (including replacement), or by a direct (ortho-) magmatic one (e.g. Geijer 1930, Parák 1975, Frietsch 1978, Hitzman et al. 1992, Nyström & Henriquez 1994, Williams et al. 2005, Jonsson et al. 2013, and references therein). The Norrbotten apatite-iron oxide ores are mined by the company LKAB (*Luossavaara-Kirunavaara Aktiebolag*).

Geology and deposits

The host rocks of the Norrbotten apatite-iron oxide ores comprise regionally metamorphosed c. 1.91–1.88 Ga volcanic rocks of the porphyry and porphyrite groups (Fig. 32, cf. Bergman et al. 2001, and references therein). The local feldspar-porphyritic texture of some intermediate and felsic units has given rise to their names. Compositionally, these rocks range from basalt, via andesite or trachyandesite, to rhyolite-dacite, of which a porphyritic trachyandesite ("syenite porphyry") forms the footwall rocks to the Kiruna ore (Bergman et al. 2001). The iron oxide ores characteristically form planar, laterally extensive high-grade magnetite-dominated ore bodies, which are essentially concordant with the host rocks and their contacts. The Kiruna ore itself forms an over 5-km-long, up to 100-m-thick, planar body that dips moderately steeply to the east. Alteration of the host rocks is quite widespread at Kiruna, including albitisation, sericitisation and amphibole alteration. Of these processes, albitisation seems related to a gabbroic to monzonitic sill in the footwall, sericitisation to post-ore deformation; amphibole veining and alteration with associated biotite-chlorite alteration seems associated with ore formation (Bergman et al. 2001). Although most Kiruna ore is massive, some particular textural and structural features occur, such as in the dendritic type of magnetite (cf. Nyström & Henriquez 1994, and references therein). Breccias are also characteristic of the Kiruna deposits, and extensively developed in both the foot and hanging wall contacts (Fig. 33). Amphibole alteration is abundant in and

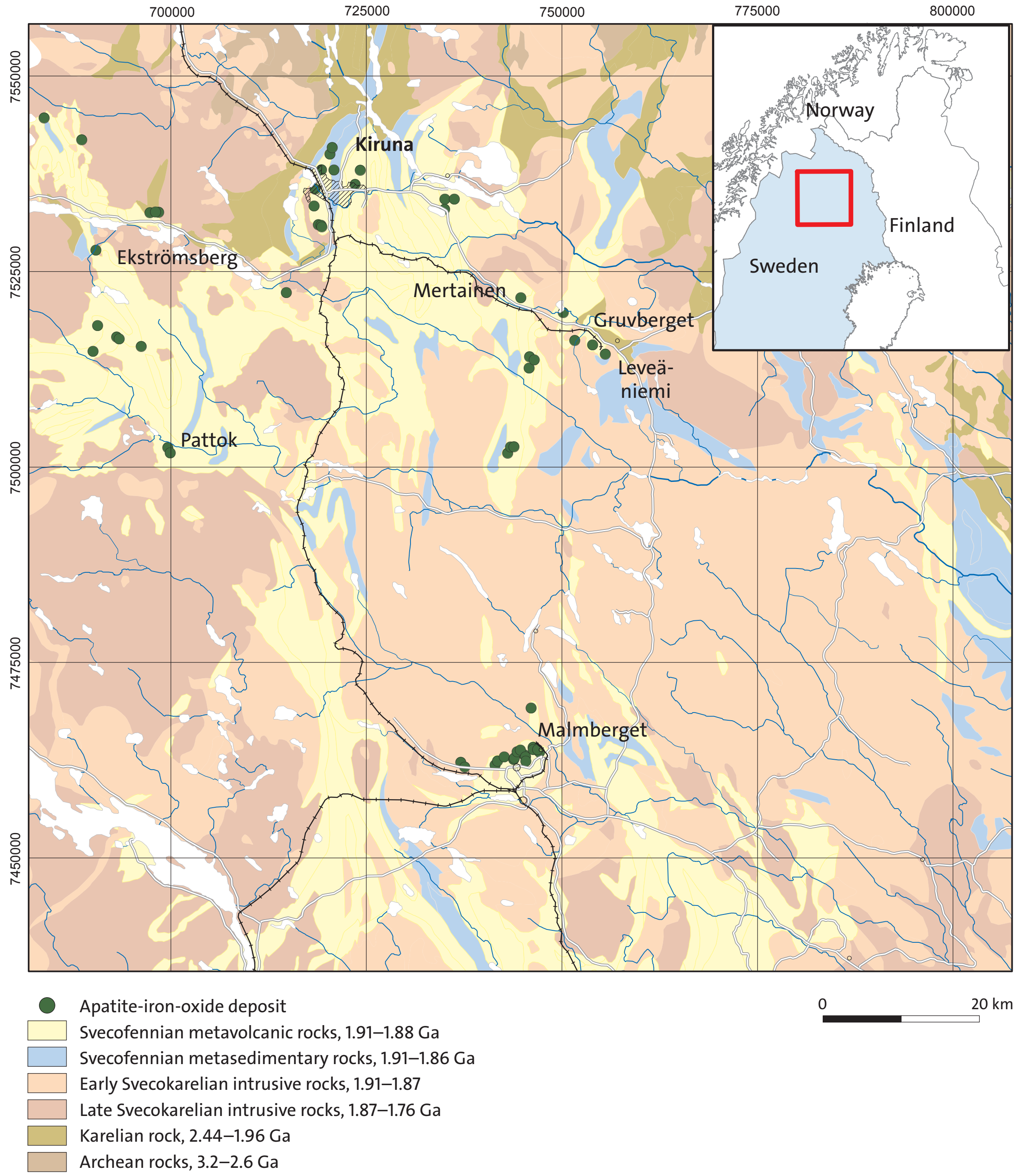

Figure 32. Simplified bedrock geological map of central northern Norrbotten, showing the locations of the Kiruna and Malmberget mines and other significant apatite-iron oxide deposits.

associated with the breccias, and magnetite-amphibole veins can extend tens of metres into the hanging wall (Bergman et al. 2001). The age of mineralisation at Kiruna is suggested to be 1.89–1.88 Ga (cf. Bergman et al. 2001, and references therein), while Smith et al. (2009), based on e.g. in situ LA-ICP-MS analyses of allanite, scapolite and titanite, suggested host rock ages as old as 2.05 Ga, and ages of mineralisation (or potentially related systems) of between 1.92 and 1.79 Ga. Some of these younger ages could represent disturbed isotopic systems, but young ages, down to c. 1.73–1.72 and 1.64–1.62 Ga,

Figure 33. Iron ore breccia exposed at the top of Kirunavaara hill, featuring angular fragments of host rock porphyry cemented by a magnetite-rich groundmass (c. 7534350/7182240). Photo: Erik Jonsson.

related to fluid overprinting of the ores, and formation or growth of monazite and other minerals, were recently reported by Andersson et al. (2016).

As regards the 40 or so known major deposits, the SGU mineral resources database currently contains 80 discrete and named mines, deposits or mineralisations of general apatite-iron oxide character in Norrbotten. Of these, many are individually named mines, sectors or workings within the major mining areas at Kiruna and Malmberget. The occurrence of REEs in these deposits is intimately linked to the presence of apatite (fluorapatite), so in general, high apatite (or phosphorus) content of the discrete ores or ore bodies suggests an increased potential for these metals.

Also in the central Kiruna area, the smaller and more hematite-rich, Per Geijer ores (the Haukivaara, Henry, Rektorn, and Nukutusvaara deposits) are located in the upper part of the porphyry stratigraphy, and are in part apatite-rich; the Rektorn deposit was mined specifically for apatite during 1942–1946 (Geijer 1950).

Malmberget is situated approximately 75 km south-southeast of Kiruna (Fig. 32) and is the second largest of the apatite-iron oxide deposits in Norrbotten, mined since the late 19th century. The deposit comprises 20 ore bodies distributed over an underground area of about 5 × 2.5km, of which 10 are currently mined. The main ore zone has a length of about 5 km (Bergman et al. 2001). In contrast to Kiruna, the Malmberget ores and host rocks are extensively deformed and metamorphosed. Average phosphorus content has been stated as less than 0.8% (Grip & Frietsch 1973).

Leveäniemi, near Svappavaara, some 40 km southeast of Kiruna, is the third largest deposit in Norrbotten. Its magnetite ores exhibit relatively low general phosphorus content, at approximately 0.1%, but can be locally higher, up to 1.1%, and contain apatite veins in the northern part (Bergman et al. 2001). LKAB is currently expanding in the Svappavaara area, and three mines are currently (2017) in operation here, i.e. Mertainen, Gruvberget, Leveäniemi (Fig. 32).

Many of the numerous other, hitherto untouched apatite-bearing iron ore deposits in Norrbotten, may also have potential for REE exploration. One of these is the Pattok (Pattovare) deposit, located about 40 km southwest of Kiruna (Fig. 32), which consists of a hematite and apatite-rich mineralisation, with an average of 2.5% phosphorus, and containing some 40 Mt of ore down to the 200 m level; it was suggested (without references to analyses, etc.) by Hammergren (1988, unpublished eport) to be potentially REE-rich. Grip & Frietsch (1973) noted that Pattok is the only high-phosphorus apatite-iron oxide ore outside the Kiruna area.

REE mineralisation

Apatite, typically as fluorapatite, is obviously a very important mineral in the apatite-iron oxide deposits. It is variably abundant, both within and between deposits; e.g. at Kiruna, the content of phosphorus is bimodal, being either less than 0.05% or higher than 1% in recently mined ores (Bergman et al. 2001); Geijer (1931), on the other hand, stated that the magnetite ore in the upper parts of the Kiruna deposit contained at least 2% phosphorus, equivalent to almost 11% apatite. Characteristic of apatite-iron oxide deposits, Si and (Y+REE) in fluorapatite exhibit a distinct correlation, as opposed to Na and (Y+REE) (cf. Harlov et al. 2002b, Jonsson et al. 2016). This correlation is the result of REE incorporation in the fluorapatite by the coupled substitution Si_{4+} + $(Y+REE)_{3+}$ –> P_{5+} + Ca_{2+} (Pan & Fleet 2002).

The first observation of anomalously high REE content in the Kiruna-type ores was made by Geijer (1931), who reported "0.88 per cent cerium earths in an ore sample from Kiirunavaara, and 0.99 per cent of the same and 0.05 per cent yttria earths in an impure sample from Rektorn on Luossavaara". These analyses were performed as a test, after the publication of Boldyrev (1930), who had presented new analytical results showing high REE content in apatite associated with iron ores in the Urals. Additionally, Geijer (1931) also mentioned "orthite" (i.e. allanite *sensu lato*) occurring in the apatite bands of the Ekströmsberg ore, and in the Hauki hematite ore (Kiruna area).

Landergren (1936, 1948) published some new spectrographic analyses of ores from Kiruna and Malmberget (given as "Gällivare"), which included some rare earths.

Renewed interest in the occurrence of REEs in the Norrbotten ores led to new analyses in the 1960s. Using X-ray spectroscopy, Parák (1973) reported the following "total" REE metal content of apatite-iron oxide ores from northern Sweden: Kiirunavaara 6560 ppm, Malmberget 5760 ppm, Leveäniemi 1545 ppm, Rektorn 3275 ppm, Haukivaara 5295 ppm, Henry 5210 ppm, Nukutusvaara 6730 ppm, and Lappmalmen 5890 ppm. These figures were based solely on the analysed content of cerium, lanthanum and yttrium. Parák also noted the correlation between the occurrence of increased REE and phosphorus contents, as Geijer (1930) had done, and the occurrence of other REE-bearing minerals, and specifically monazite, as inclusions in the apatite. Additionally, the presence of xenotime in the Per Geijer ores was suggested, but not proved.

Andersson (1972) stated that REEs in the Tuollavaara deposit near Kiruna were principally carried by apatite and monazite. Like other deposits of this type, the Kiruna and other deposits of Norrbotten show a pronounced relative abundance of the light REEs, in particular cerium, lanthanum and neodymium, whereas the heavy REEs (except for yttrium) exhibit relatively low abundances (e.g. Parák 1973, Harlov et al. 2002b). Frietsch & Perdahl (1995) supplied more complete REE datasets on apatite and magnetite concentrates from Kiruna and other apatite-iron oxide ores, ranging from 2000 to 7000 ppm total REE; they also noted the similarities in patterns between different ore types, despite variable total content, as well as similarities to mineralised host rocks.

Host rocks of the northern district (Kiruna and Svappavaara) generally show negative Eu and strong enrichment in LREE (Fig. 34). Lundh (2014) demonstrated that samples from the Malmberget district do not show negative Eu anomalies, apart from one sample (Fig. 35).

Thus, like many other apatite-iron oxide ores worldwide, we know that (at least the better studied) Norrbotten deposits (essentially Kiruna) contain partially REE-substituted fluorapatite, from which quite a significant portion of the primary REE content has been remobilised into secondary minerals by means of fluid-mediated processes (Harlov et al. 2002b, Jonsson et al. 2016, and references therein; see also section on the apatite-iron oxide ores in Bergslagen). The major secondary minerals in the Kiruna deposit are monazite-(Ce) and allanite-(Ce) (Harlov et al. 2002b), but xenotime has also been reported (e.g. Andersson et al. 2016). Thorite with a moderate enrichment in heavy REEs was noted by Pålsson et al. (2014)

Harlov et al. (2002b) reported content of a suite of REEs from electron microprobe (EPMA) analyses of ore-hosted fluorapatite from the Kiruna mine, e.g. Y_2O_3 0.01–0.06 wt%, La_2O_3 0.02–0.18

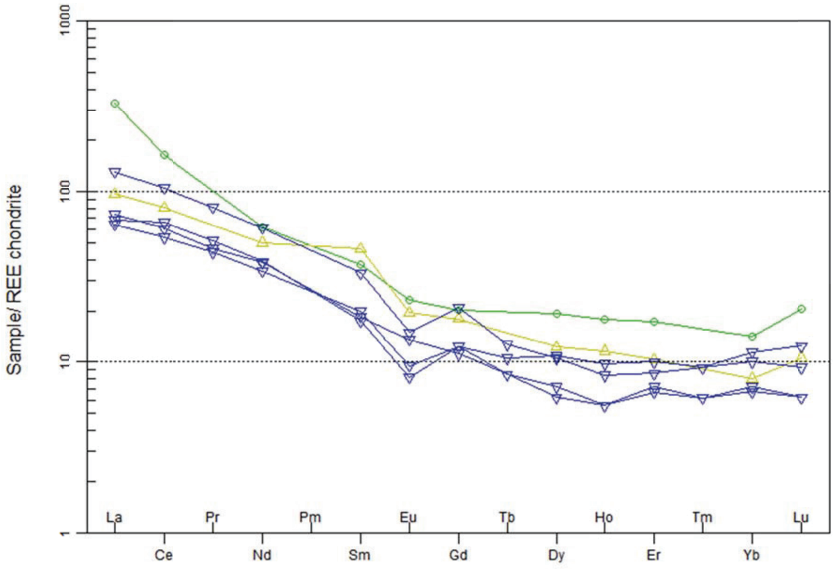

Figure 34. REE plot of host rocks from the northern districts; Kirunavaara (green); Svappavaara (yellow); Vähävaara/Masugnsbyn (blue). Most of the samples display a distinct Eu trough and a relative enrichment in LREE compared to the HREE. All samples are normalised to chondrite values from Boynton (1984). Data source: SGU/Lundh 2014.

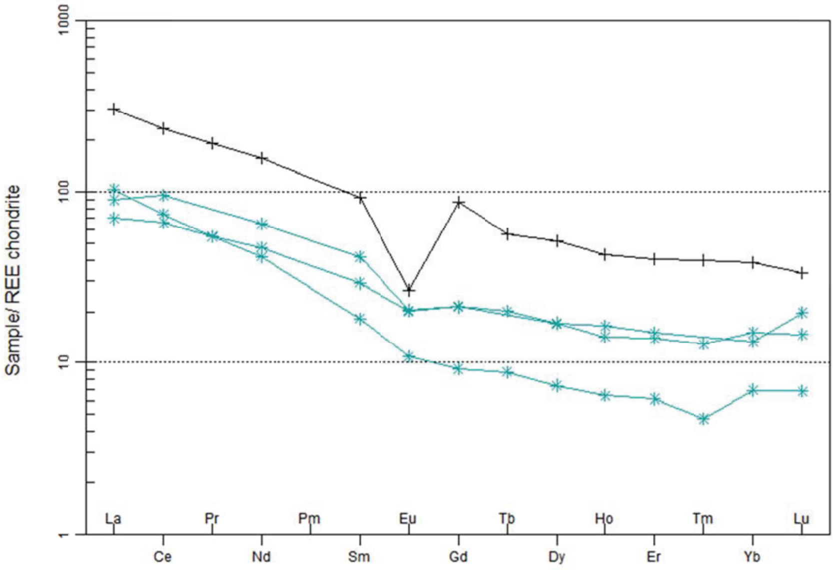

Figure 35. REE plot of host rocks from the Malmberget district (light greenish blue) and Kvikkjokk area (black). Data source: SGU/Lundh 2014.

wt%, Ce_2O_3 0.02-0.46 wt%, and Nd_2O_3 0.02–0.20 wt% (minimum and maximum averages of several, n=4 to 18, point analyses in different zones of fluorapatite grains/crystals from three different ore types), and also EPMA data for monazite-(Ce) and allanite-(Ce). Based on their analyses (including both EPMA and laser-ablation ICP-MS) and textural studies, they concluded that fluid-mediated remobilisation was responsible for variable depletion in the REE content of the Kiruna apatites. With regard to the overall highest content of REEs measured, in a BSE-bright zone in this apatite, Harlov and colleagues suggested that the original (primary) content was likely to have been in the region of at least 7000–8000 ppm total REE+Y.

Processing and extraction

As far back as 1889 small amounts of apatite-rich rocks were test-mined at Malmberget and elsewhere (Berg et al. 1890), albeit with the sole aim of assessing the potential for extraction of phosphorus. Besides the above-mentioned production of apatite from the Rektorn deposit in the 1940s, by-product apatite was also produced at Malmberget during the two world wars and in 1952–1953, in Kiruna between 1942 and 1946, and lastly in 1985–1988, when some 0.5 Mt of apatite concentrate was produced by flotation (Bergman et al. 2001, and references therein). Hammergren (1988, unpublished report) reported that at that point Kiruna produced some 130,000 tonnes of apatite concentrates ("yearly"), which were exported to Norsk Hydro in Norway.

Hammergren also stated that, besides apatite in remnant ore in the mine, some 0.7 Mt of apatite was present in tailing ponds at Kiruna, containing some 3.3 tonnes of REE oxides. Later, Pålsson & Fredriksson (2012) reported the ponded tailings at Kiruna to have average grades of 4–8% P_2O_5 and 1200–1300 g/t REE. Extensive sampling programmes on these tailings, coupled with mineralogical/chemical characterisation as well as flotation tests, have been performed by LKAB/consulting companies, and LTU (cf. Pålsson & Fredriksson 2012).

Andersson (1972) reported total REE content of apatite concentrates from the Tuollavaara mine of between 3000 and 4800 ppm, with an average of 3700 ppm, while a representative sample of waste material for the tailings during one week in 1970 contained 1070 ppm total REE oxides at 1.8% phosphorus.

During more recent assessments of the potential for REE extraction from Kiruna apatite, Sandström & Fredriksson (2012) produced a flotation concentrate with 0.44% total REE oxides that was tested via different routes including acids and solvent extraction to arrive at an REE concentrate. These tests showed the feasibility of REE extraction from Kiruna apatite, specifically when combined with fertiliser production. In a study of apatite and associated minerals from tailing ponds and low as well as high-phosphorus ore from Kiruna, Pålsson et al. (2014) found an average REE content of fluorapatites of 0.25 wt% (taking only Ce, La and Nd into account; EPMA and LA-ICP-MS point analyses), whereas analyses of bulk samples of apatite concentrates gave total content of (complete) REE oxides of between 0.45 and 1.04 wt%. Successive flotation experiments on these materials by Pålsson and colleagues yielded moderate recoveries, and it was noted that REE did not fully follow apatite (or phosphorus content), suggesting the presence of one or more additional host minerals for REE that were lost in the process. Allanite was indicated as the potential (main) culprit, as had also been suggested previously by Pålsson & Fredriksson (2012).

REE mineralisation in apatite-iron oxide deposits, Bergslagen ore province, south-central Sweden

The apatite-iron oxide deposits of central and southern Sweden are represented only by a small number of deposits in the northwestern part of the Palaeoproterozoic Bergslagen ore province, south-central Sweden (Fig. 36). The largest of these – Grängesberg, Blötberget and Idkerberget – have been mined extensively, and constitute the largest iron ore concentration in Sweden, outside of the northernmost province of Norrbotten (which hosts the currently operating Kiruna and Malmberget mines, among others; see that section). Based on their overall mineralogy, geochemistry, geometry and relationships with the host rocks, these Bergslagen deposits clearly represent Kiruna-type deposits (e.g. Jonsson et al. 2010a). Besides iron in the form of magnetite and hematite, fluorapatite and associated rare earth-bearing phosphates and silicates in these ores represent a significant potential reserve of REEs as well as of phosphorus. The following text concentrates on the Grängesberg district, since this is the largest of the deposits (with a past production of 152 Mt iron ore at 58% Fe and 0.81% P; e.g. Hallberg et al. 2006),

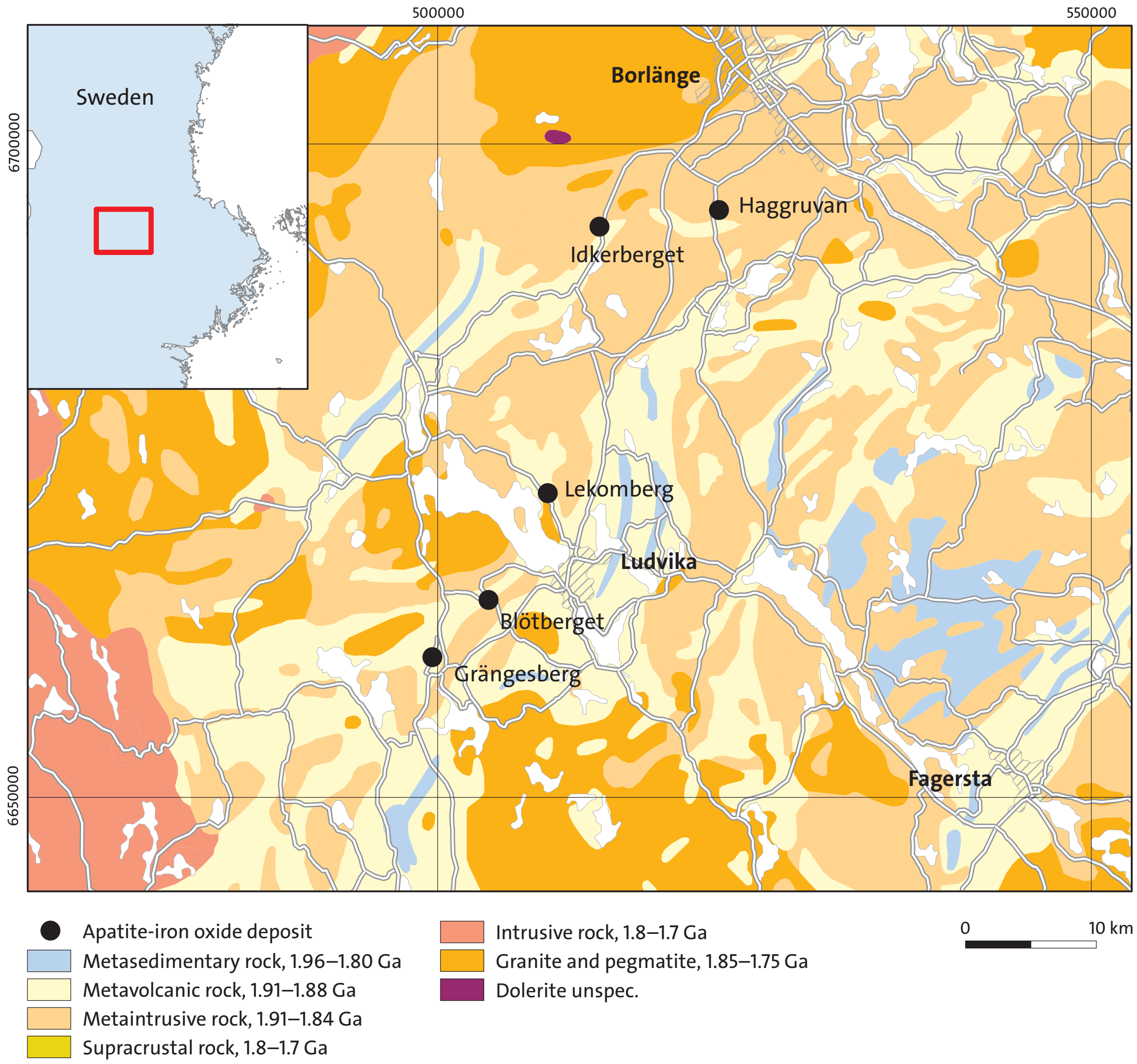

Figure 36. Simplified bedrock geology map of a part of northwestern Bergslagen, showing the locations of the major apatite-iron oxide deposits (and one minor deposit – Haggruvan).

and currently also the most-studied one. Grängesberg was the last of these mines to be in operation and closed in 1989, despite plenty of remaining ore. Recent plans to restart operations are fairly well-advanced (see http://grangesberg.com/index.php).

Even at an early stage of mining and study, the deposits of the Grängesberg district were compared to those of the Kiruna area (e.g. Looström 1929), i.e. the "type locality" of the Kiruna-type ores, and a source of scientific controversy for more than 100 years (e.g. Johansson 1910, Parák 1975, Hitzman et al. 1992, Nyström & Henriquez 1994, Jonsson et al. 2013, and references therein).

Significant rare earth element concentrations are present in the ore-associated apatite in the Grängesberg mines, and although this was noted, and analyses and experimental concentration tests were performed when the mine was in operation (cf. Back 1991), it never led to any full-scale beneficiation.

Geology and deposits

The overall host rocks for most of the Bergslagen ores comprise mainly felsic, regionally metamor phosed c. 1.90–1.87 Ga volcanosedimentary rocks (the *leptite-hälleflinta formation* of old; cf. Stephens et al. 2009; geology section in this report). In the Grängesberg–Ludvika area, the metasupracrustal rocks comprise units of clastic sedimentary origin as well as of direct volcanic and subvolcanic origin, all multiply deformed and metamorphosed to amphibolites facies grade (cf. Strömberg 1988, Strömberg & Sukotjo 1988; Högdahl et al. 2013). The immediate host rocks to the apatite-iron oxide ores, particularly around the Grängesberg deposits, exhibit substantially more intermediate to basic compositions (cf. Geijer & Magnusson 1944; Jonsson et al. 2010b; Jonsson et al. 2011; Nilsson et al. 2013). These metavolcanic rocks are locally feldspar-porphyritic, fine-grained and range between rhyolitic-dacitic to basaltic-andesitic in overall composition. Relative to average crust, the Grängesberg iron oxide ores are typically enriched in Th, U, La, Ce, Nd, P, Fe, Sm, Tb, Y, Tm and Yb, and depleted in Ba, Sr and Ti. K and Zr are variably depleted. The apatite-iron ore is enriched in REE to varying degrees, as is typical of this type of deposit (e.g. Frietsch & Perdahl 1995), particularly so in the LREEs.

Alteration is evident in the host rock metavolcanics, both in the form of regional sodic or potassic alteration and locally, as disseminated and discrete phyllosilicate (mainly biotite + chlorite) and amphibole-rich zones. Localised alteration in these zones and the immediate host rocks is also manifested by their increased REE content, featuring similar REE patterns to the ores and associated apatite-rich assemblages (Jonsson et al. 2011, 2013).

The smaller iron oxide mineralisations in the Kopslahyttan area, and specifically that at Haggruvan (Fig. 36; Geijer & Magnusson 1944) are locally enriched in REE, and most likely represent an eastern continuation of the apatite-iron oxide deposits at Idkerberget (Jonsson et al. 2015), a view also supported by interpretations of the available aeromagnetic maps of the region.

REE mineralisation

As long ago as 1948 Landergren reported some partial rare earth element analyses from the Grängesberg iron ores and others, showing their general REE-enriched nature. Relatively high REE content in the ore-associated apatite in the Grängesberg deposit were found later, with reported total Ce+La+Nd+Y oxides of up to between 5800 and 7700 ppm (Back 1991). Analyses of apatite from the Risberg field in Grängesberg yielded 1340 ppm Ce, 420 ppm La, 980 ppm Nd, and 1270 ppm Y, according to Andersson (1972, unpublished report). It was furthermore noted that REEs were also hosted by allanite and monazite, but despite the presence of allanite (*sensu lato*), the correlation between increased REE and P contents still suggested that the bulk of the REEs were primarily carried by phosphate minerals (Andersson 1972, 1974, unpublished reports; Back 1991).

As noted previously, fluorapatite is a key mineral in the apatite-iron oxide deposits. In the Grängesberg ores it mostly occurs as relatively fine-grained aggregates, bands or subhedral, elongated, bleb-like crystals distributed in the Fe oxide ore. Often the fine-grained apatite, together with associated silicates, exhibits a banded/foliated or schlieren-like structure in the ore (Fig. 37). Characteristic of these deposits, Si and (Y+REE) in fluorapatite exhibit a distinct correlation, as opposed to Na and (Y+REE) (cf. Harlov et al. 2002b; Jonsson et al. 2016). This correlation is the result of REE incorporation in the fluorapatite by the coupled substitution $Si4^+ + (Y+REE)^{3+} = P^{5+} + Ca^{2+}$ (Pan & Fleet 2002).

In the Grängesberg (Export field) ores, the characteristically granular fluorapatite is typically high in Ce, La, Nd, and Y. REEs are also carried by monazite-(Ce), xenotime-(Y), allanite-(Ce) and variably REE-enriched epidotes *sensu stricto*, as well as in Ce-dominant REE fluorocarbonates of the synchysite-bastnäsite-type; a gadolinite-(Ce)-like phase has also been observed (Jonsson et al. 2010b; Majka et al. 2013; Jonsson et al. 2016). Among the immediate and variably altered host rocks that exhibit enrichment in the REEs, these are primarily found concentrated in allanite-(Ce), fluorapatite and monazite-(Ce).

Figure 37. Banded apatite-magnetite ore from the Grängesberg Export field. Section of drill core, image width approximately 5 cm. Photo: Erik Jonsson.

Based on mineralogical and mineral–chemical studies, including high-quality microprobe data, fluorapatites in Grängesberg are generally chemically and texturally variable, and contain between about 0.5 up to almost 2.5 wt% $(Y+REE)_2O_3$ (Jonsson et al. 2016); the most likely interpretation of the variable REE contents and observed textures is that the primary REE content of many of the fluorapatites has been depleted by post-crystallisation fluid overprinting (Figs. 38, 39). Thus, the associated REE-bearing phosphates (monazite, xenotime) and silicates (allanite) primarily formed through fluid-mediated remobilisation of REEs from fluorapatite, and subsequent formation of these secondary, REE-enriched phases (Majka et al. 2013; Jonsson et al. 2016). The REE fluorocarbonates formed under even later, low-temperature geological conditions (e.g. Jonsson et al. 2010b). Bulk geochemical analysis of dump samples, in part carrying megascopically visible apatite, yielded up to 0.7 wt% total REE (Högdahl et al. 2015).

Overall, the Grängesberg fluorapatites exhibit the following ranges in content of discrete REEs (average of 481 electron microprobe point analyses, all in wt% oxide): Ce 0.01–0.6; La 0.01–0.2; Nd 0.03–0.39; Pr 0.02–0.13; Y 0.02–0.24; all others were below the analytical detection levels (Nilsson et al. 2013; Jonsson et al. 2016). Average total REE content for apatite from discrete assemblage types ranges from 0.19 wt% $(Y+REE)_2O_3$ in an altered metavolcanic rock (phyllosilicate-rich alteration assemblage) to between 1.7 and 2.5 wt% $(Y+REE)_2O_3$ in apatite-rich units in magnetite ore (Majka et al. 2013; Jonsson et al. 2016). Allanites occurring in association with the oxide ores are primarily rich in Ce and La. As expected, monazite carries appreciable amounts of REE, mainly Ce, and has been found to be an important accessory REE mineral; however, the abundance of monazite within and associated with fluorapatite varies significantly between samples. Xenotime-(Y) contains significant Y+HREE, but is less common than monazite and allanite.

Initial studies suggest similar general REE mineralogies in the Blötberget and Idkerberget deposits (Jiao 2011, Jiao et al. 2012, Sahlström 2012; Högdahl et al. 2015).

In Blötberget, REEs in the magnetite ore are hosted by fluorapatite, monazite-(Ce), allanite-(Ce) and xenotime-(Y) (Jiao 2011, Jiao et al. 2012). Based on bulk geochemical analyses of drill cores, relatively fluorapatite-rich samples from Blötberget exhibit a total REE content of between approximately 200 and 3000 ppm. Chondrite-normalised plots show a characteristic enrichment in La, Ce, Pr, and Nd, slight to moderate relative depletions in Eu, and flat trends for Gd to Lu. Bulk geochemical analyses of dump samples yielded up to 0.3 wt% total REE (Högdahl et al. 2015).

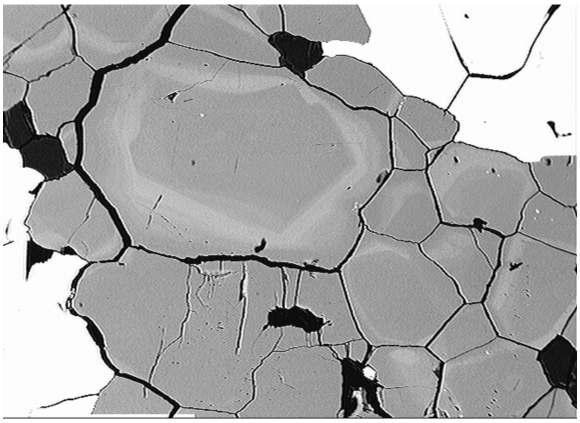

Figure 38. Back-scattered electron (BSE) image of an aggregate of fluorapatite (in different shades of grey) in magnetite-apatite ore from the Export field, Grängesberg (white areas are magnetite). The lighter zones, particularly in the fluorapatite in the centre, have increased REE content; it is suggested that the texture of this variable zoning is due to a similarly variable extent of fluid-mediated remobilisation of REEs at a late-magmatic to regional metamorphic stage. The white scale bar at lower left equals 200 micrometres. Photo: Erik Jonsson.

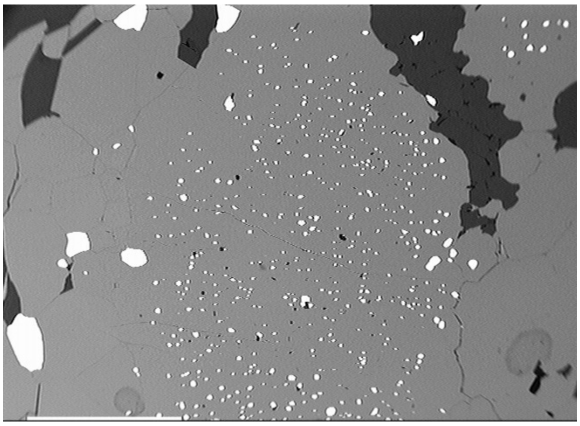

Figure 39. Back-scattered electron (BSE) image of fluorapatite (grey) in magnetite-apatite ore from the Export field, Grängesberg. The small white inclusions in the centre of the image consist of monazite-(Ce) and minor xenotime-(Y). Larger grains or crystals in the outer parts of the fluorapatite are monazite-(Ce). This texture is interpreted to be the result of fluid-mediated remobilisation of the originally fluorapatite-hosted REEs into later-formed REE phosphates, subsequently in part modified by Ostwald ripening-type processes, which led to the growth of fewer and bigger monazites in the outer part of the fluorapatite grains. The white scale bar at lower left equals 200 micrometres. Photo: Erik Jonsson.

At Idkerberget, samples studied show REE-enriched fluorapatite, as well as monazite-(Ce) and allanite-(Ce). The observations here of discrete Th-bearing phases as well as thorium in the form of a substituent in monazite are notable and somewhat unexpected (Sahlström 2012), since monazites formed through REE remobilisation of fluorapatite are normally (very) low in thorium. Bulk geochemical analyses of dump samples from Idkerberget yielded up to 0.1 wt% total REE (Högdahl et al. 2015).

The main carriers of the rare earths in the apatite-iron oxide mineralisation at Haggruvan, Kopslahyttan area, south of Borlänge (Fig. 36), are monazite-(Ce), allanite-(Ce), and REE-enriched epidote, as well as rare xenotime-(Y) (Fig. 40); apparently the fluorapatite does not harbour any REE above the detection limits of the EDS analytical system used (Jonsson et al. 2015). Accessory titanite in the slightly altered host rocks may contain small amounts of yttrium. Bulk geochemical analyses of dump samples yielded up to 1 wt% total REE (Högdahl et al. 2015).

Processing and extraction

Hammergren (1988, unpublished report) stated that 80,000 tonnes of apatite concentrates from Grängesberg were exported "yearly" to Norsk Hydro, in Norway at that time, and that Grängesberg apatite contained an average of 0.75% REE oxides (as compared with 0.5% in Kiruna apatite). He also reported that the remnant apatite in the tailings at Grängesberg was 300,000 tonnes, representing some 2,300 tonnes of REE oxides. Since not much activity took place after this, these are likely to be reasonable estimates of the tailings currently remaining there.

Based on then ongoing separation of apatite, and experimental work including flotation of apatite ores, Andersson (1972) noted that a significant to major proportion of REEs from Grängesberg were

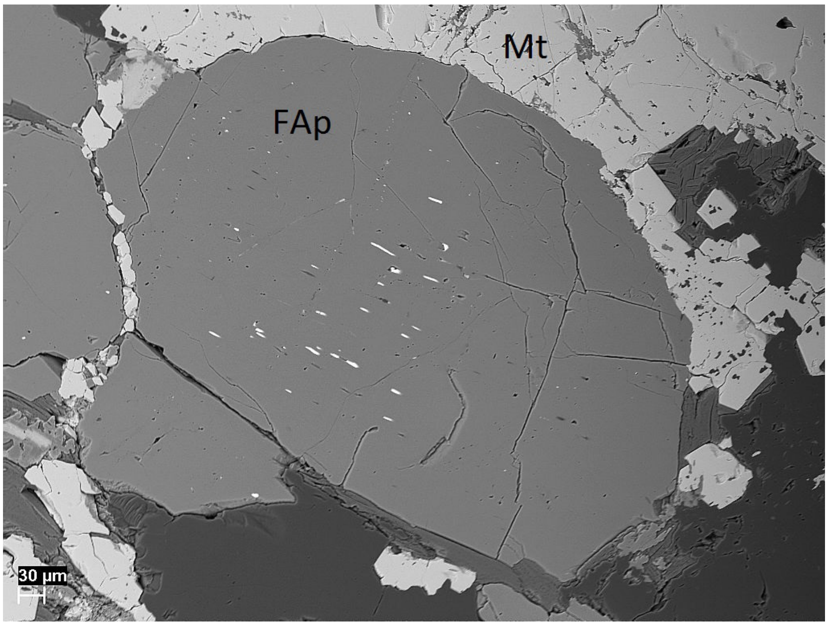

Figure 40. Back-scattered electron (BSE) image showing a rounded-lensoidal fluorapatite (FAp) grain in contact with magnetite (Mt); the fluorapatite exhibits a characteristic texture, containing several BSE-white, epitaxially oriented crystals of monazite-(Ce). The scale bar equals 30 micrometres. Haggruvan, Kopslahyttan area (6694893/ 521413). Photo: Erik Jonsson.

lost in the process, as monazite was separated out of the apatite concentrate, the latter only containing about 35% of the total incoming REEs; if all REE-bearing materials were to remain in the apatite concentrates, it was estimated that the content would be around 1.2 wt% total REE oxides. Similar proportions were found for the Blötberget and Idkerberget mines. In the case of Blötberget, for instance, this meant that about 70% of the REEs in the bulk incoming material ended up in the waste tailings, whereas at Idkerberget, some 63% went into the iron ore concentrate.

It was also noted in comparison that at that point the Typpi Oy Company in Finland was – seemingly successfully – recovering REEs during the process of making phosphoric acid from apatite imported from the Kola peninsula (Russia), with a total REE content similar to that of the Grängesberg apatite.

The REE-Fe mineralisations of the Olserum area, southeastern Sweden

The REE mineralisations of the Olserum area were discovered only fairly recently and represent one of the deposits offering most economic potential in Sweden, after the nepheline syenite-hosted deposit at Norra Kärr. Aside from Norra Kärr, Olserum is the only REE deposit in Sweden with a classified mineral resource.

The Olserum mineralisation is located some 30 km northwest of Västervik in southeastern Sweden (Fig. 41). It represents an unusual type of hydrothermal mineralisation, rich in high-grade REE phosphates.

These mineralisations were in fact first noted with respect to rare metals in the 1950s, when the company Stora Kopparberg AB investigated the presence of uranium in association with iron ores in the area. Several small uranium mineralised areas were discovered, but none was regarded as of economic importance. In the 1970s SGU continued to explore for uranium in the region, during which period several occurrences of apatite with anomalous yttrium content were documented.

Yet, mining of magnetite-dominated iron oxide ores had begun quite some time before, at least as early as 1745, when the Djupedal mine was reported to yield fairly good iron ore (Hoppe 1884). The more important (of these generally small and now abandoned) iron mines in the area are concentrated along a north-northwest–south-southeasterly trend, and mainly comprise Djupedal, Olserum (Olovs-

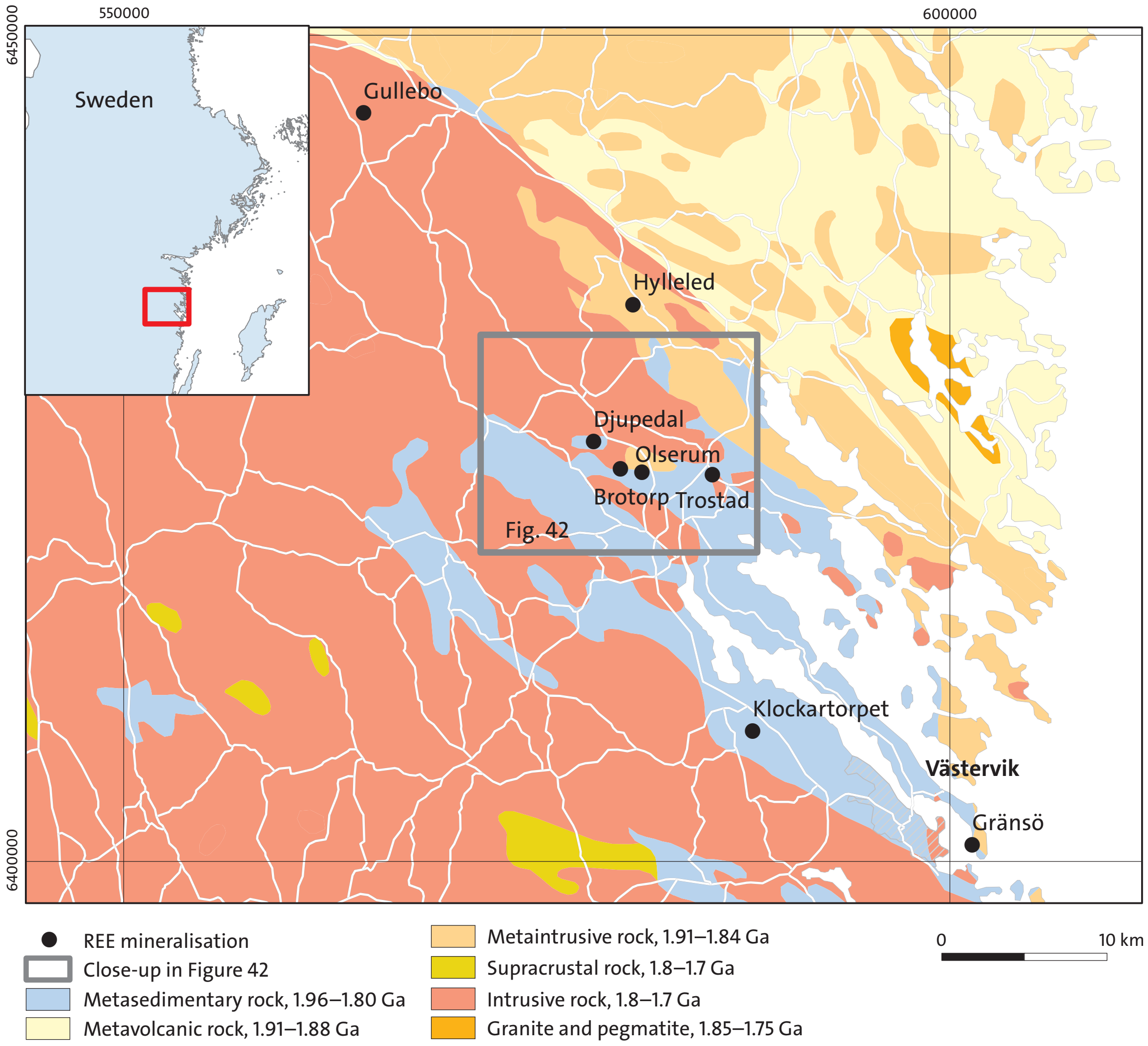

Figure 41. Simplified bedrock geological map showing the locations of Olserum and other REE mineralisations in this area.

rum), and Källhagen (Brotorp), of which the Olserum mines were the largest (Geijer & Magnusson 1944). All of these mines are located within the border zone between Västervik formation metasedimentary rocks in the south, and granitoids belonging to the Transscandinavian Igneous Belt in the north (Figs. 41, 42; TIB; Högdahl et al. 2004). The potential link between TIB magmatism and the formation of the Olserum area REE Fe mineralisations has been somewhat uncertain and debated, and is the topic of ongoing research (cf. Andersson et al. 2018a,b).

The occurrence of REE in sizeable concentrations associated with iron oxide mineralisation in the Olserum area, enough to have economic potential, was realised only relatively recently, however. In the early 1990s, the state-owned company SGAB (*Sveriges Geologiska AB*) followed up earlier SGU-run uranium exploration, but now with the purpose of identifying and classifying rare earth occurrences in Sweden. The anomalous yttrium contents in the area were noted at this point. SGAB followed up with site visits and sampling in the area, confirming the presence of heavy rare earth-enriched mineralisations in the Olserum area, in magnetite-apatite bearing, uranium anomalous mine dump material, as well as veins in outcrops (Gustafsson 1990, 1991, unpublished reports).

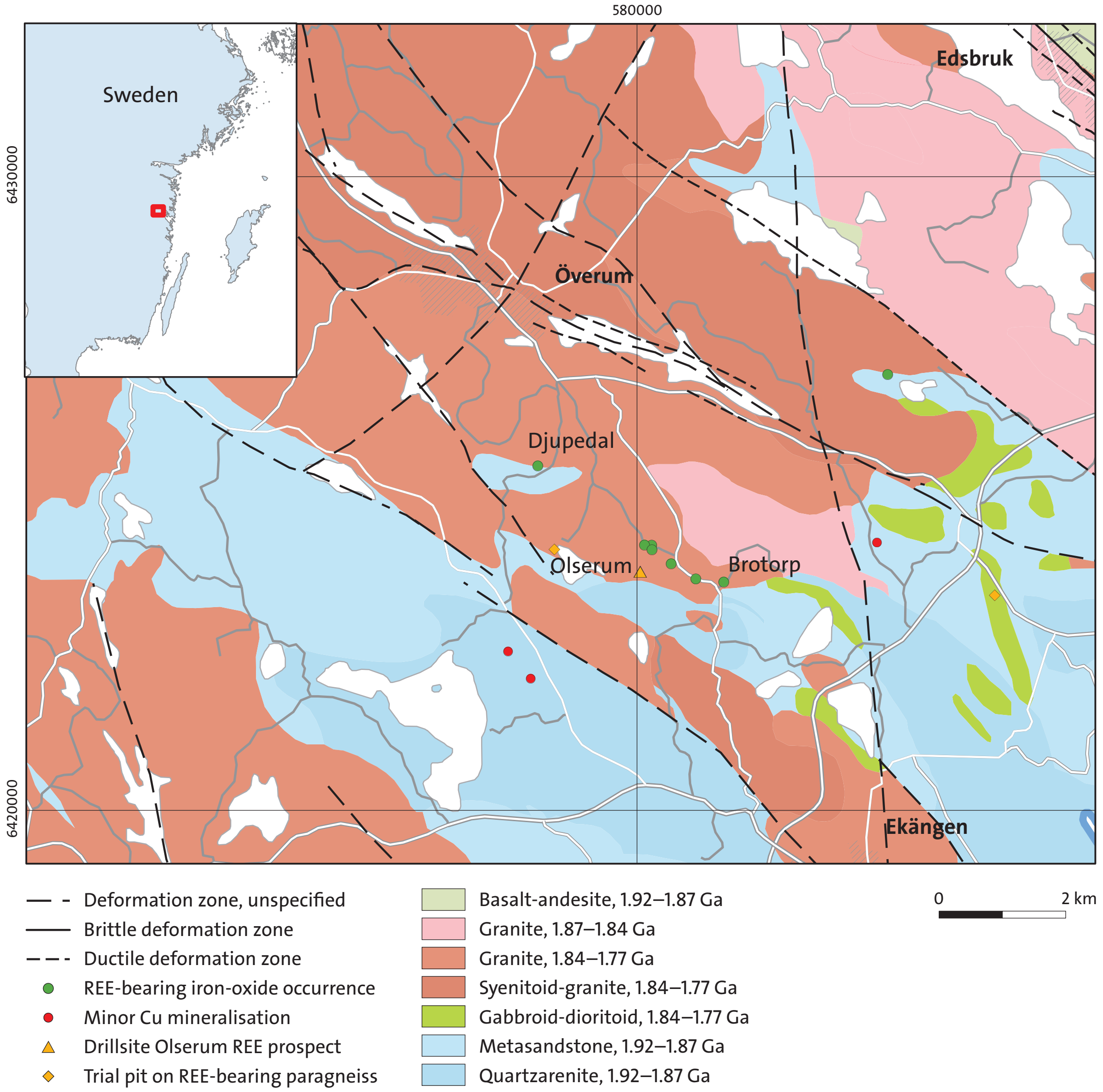

Figure 42. Bedrock geological map of the Olserum area with known mineralisations marked; the most important are named (Brotorp is also known as Källhagen).

The identification by SGAB of a number of iron oxide-magnetite vein-associated targets with high REE content, of which a significant proportion comprised the sought-after HREE (Gustafsson 1991, unpublished report), did not lead to any significant activity at that point. A decade or so later, further exploration and drilling by IGE Nordic, and subsequently Tasman Metals, in the area led to the identification of a mineralised zone open at depth (e.g. Reed 2013, unpublished report,). This, the Olserum deposit as outlined by Tasman Metals, covers only part of the known mineralised area. It has an indicated resource of 4.5 Mt at 0.6% TREO with 33.9% HREO (Reed 2013, unpublished report). In addition, all of the old iron mines mentioned above carry (some) REE mineralisation, and several additional small prospects/pits, along with outcrops that have not been worked, show the same type of REE-enriched apatite-magnetite mineralisation, predominantly comprising fluorapatite, monazite-(Ce) and xenotime-(Y).

The major, megascopic mineral hosts of REE in the Olserum area are monazite-(Ce), xenotime-(Y),

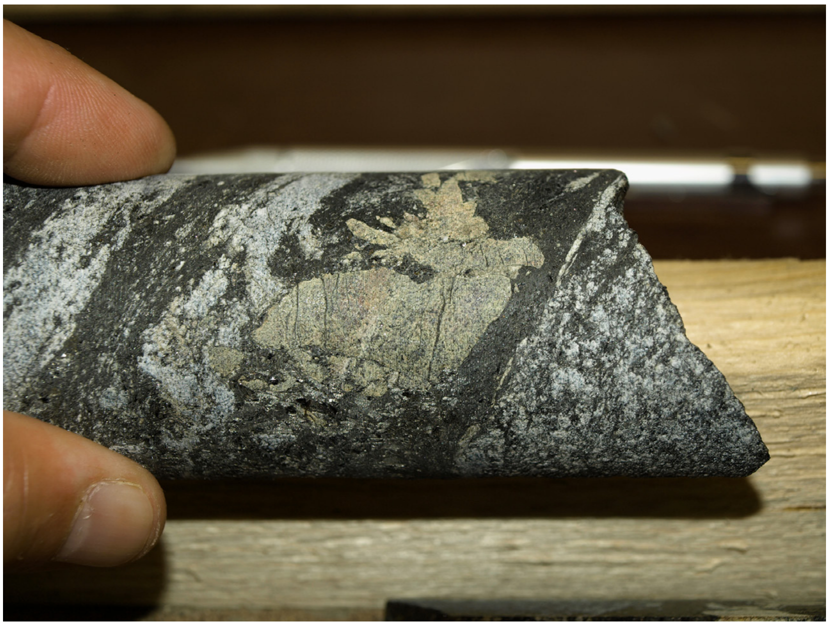

Figure 43. Coarse, subhedral yellowish crystal aggregates of monazite-(Ce) in a biotite-apatite-magnetite vein in a drill core from the former Tasman Metals resource in Olserum. Photo: Erik Jonsson.

Figure 44. Biotite-apatite-magnetite vein(s) with local concentrations of coarse, subhedral brownish crystal aggregates of xenotime-(Y) in the upper central part of the image. Abundant, dull-white fluorapatite is also readily apparent. Outcrop in the former Tasman Metals resource in Olserum (c. 6423926/579862). Photo: Erik Jonsson.

and REE-bearing fluorapatite, whereas allanite-(Ce)/ferriallanite-(Ce) and REE fluorocarbonates are less abundant. Overall, the first-mentioned phosphate minerals predominate, and both the monazite and the xenotime can occur as impressively large individual crystals, up to at least 7 cm in length (Figs. 43–45).

An estimate of the type and proportions of minerals in the Olserum mineralisations based on MLA analysis is shown in Table 5.

Recent studies have revealed new mineralogical details about the Olserum–Djupedal mineralisations, the main associated minerals being biotite, quartz, cordierite, muscovite, magnetite, tourmaline and anthophyllite (most likely the "gedrite" reported in Table 5), and accessory minerals including ilmenite, rutile, hematite, pyrite, chalcopyrite, galena, staurolite, epidote, ferberite, zircon, uraninite, thorite and unidentified REE-Y-Nb-W-U oxides, occurring in a complex and protracted paragenetic sequence (Andersson et al. 2016b, Andersson et al. 2017, 2018a).

Figure 45. Coarse, tectonised crystals of reddish-brown xenotime-(Y) in a magnetite-biotite(-apatite) groundmass, in a dump boulder at the Djupedal mine, Olserum area (6425437/578432). Photo: Erik Jonsson.

Table 5. Modal mineralogy (determined by MLA) of a composite sample representing the mineral resource at Olserum (source: Tasman Metals AB – unpublished data). Marked numbers show common REE-bearing minerals in Olserum.

Mineral	**Wt%**
Quartz	47.89
Biotite	19.66
Albite	11.9
Gedrite	3.96
Cordierite	3.27
Apatite	2.59
Magnetite	2.29
Andalusite	2.12
Staurolite	1.05
Illite	0.92
Cummingtonite	0.9
Clinochlore	0.65
Monazite	**0.61**
K-feldspar	0.54
Xenotime	**0.31**
Muscovite	0.29
Tourmaline	0,25
Allanite	**0.07**
Siderite	0.06
Unclassified	0.06
Calcite	0.04
Ilmenite	0.04
Zircon	0.02

While it has been suggested that a number of REE-bearing iron oxide mineralisations (e.g. Klockartorpet and Södra Gränsö) south of Olserum, within the more homogeneous Västervik formation rocks, represent palaeoplacer (metamorphosed heavy sand) deposits (e.g. Welin 1966; see separate section in this chapter), such an origin has also been loosely suggested for Olserum (e.g. Gustafsson 1990, 1991, unpublished reports). The deformed and partly migmatitic, gneissic nature of much of the rock in the Olserum area makes clear-cut interpretation difficult, but the overall relatively unambiguous vein-type character (Figs. 43 and 42) of the REE-rich magnetite-apatite mineralisations prove their epigenetic nature. That tectonic activity continued after vein formation is evident from the brittle tectonisation of individual minerals (Figs. 43 and 45), as well as the deformation, including faulting, of the actual veins.

It is unclear at present whether the metals that formed these deposits by means of hydrothermal fluids originated from pre-existing palaeoplacer deposits, or from the TIB magmas; yet, the former seems unlikely considering not least the metal flora involved. Trace element studies of magnetites associated with several of these deposits in the Västervik area show significant differences between the Olserum (vein-style) mineralisations and one of the relatively few clear-cut palaeoplacers, Klockartorpet (Andersson et al. 2016a). The most in-depth and recent study suggests that the Olserum area mineralisations formed from a hydrothermal system that was directly caused by the nearby TIB intrusives (Andersson et al. 2018b).

The mineral resource was modelled by Reed Leyton Consulting (2013, unpublished report,), using six different total rare earth oxide (TREO) cut-off grades, with a base-case resource estimated using a TREO cut-off of 0.4% (Tables 6 and 7). At this cut-off, Olserum hosts an indicated mineral resource of 4.5 million tonnes grading 0.60% TREO and an inferred mineral resource of 3.3 million tonnes grading 0.63% TREO, both with 34% of the TREO being the higher value HREO (heavy rare earth oxide). Tables 6 and 7 show the grade averages for rare earth oxides at the various cut-offs (source of table 8 and 7: Tasman Metals AB).

Table 6. Indicated resource estimate for the Olserum deposit (Tasman Metals AB, 2013).

TREO% Cut-off	Million Tonnes	TREO%	% of HREO in TREO	Dy_2O_3 ppm	Y_2O_3 ppm	Nd_2O_3 ppm	Tonnes of TREO contained	
0.7	1.0	0.89	32.3	292	1800	1314	8,620	
0.6	1.7	0.78	32.9	262	1610	1146	13,360	
0.5.	3.0	0.68	33.3	232	1420	996	20,650	
0.4	**4.5**	**0.60**	**33.9**	**209**	**1283**	**878**	**27,260**	**BASE CASE**
0.3	6.3	0.53	34.4	187	1146	769	33,530	
0.2	7.7	0.48	34.5	0.017	1042	700	37,030	

Table 7. Inferred resource estimate for the Olserum deposit (Tasmet Metals AB, 2013).

TREO% Cut-off	Million Tonnes	TREO%	% of HREO in TREO	Dy_2O_3 ppm	Y_2O_3 ppm	Nd_2O_3 ppm	Tonnes of TREO contained	
0.7	0.9	0.85	31.8	288	1667	1294	7,947	
0.6	1.6	0.77	32.5	264	1547	1151	12,088	
0.5.	2.5	0.69	33.6	242	1445	1018	16,960	
0.4	**3.3**	**0.63**	**33.7**	**222**	**1320**	**925**	**20,770**	**BASE CASE**
0.3	4.2	0.57	33.9	202	1205	841	23,820	
0.2	4.7	0.54	33.9	191	1134	790	25,050	

The Fe-REE (Bastnäs-type) deposits of the REE line, Bergslagen ore province, south-central Sweden

The Bastnäs-type Fe-REE deposits are early Proterozoic, skarn-hosted iron oxide (magnetite-dominated), locally polymetallic (± Cu, Au, Co, Bi, Mo…) mineralisations that in part carry very REE-rich assemblages (cf. Geijer 1961; Holtstam & Andersson 2007). They are located in the Bergslagen ore province, and characterised by the occurrence of locally abundant REE-rich silicate minerals such as cerite-(Ce) and allanites (*sensu lato*), but also include REE fluorocarbonates such as bastnäsite-(Ce). Overall, these deposits exhibit a quite complex and diversified REE mineralogy, dominated by silicate minerals (Table 8). The deposit type was named after the Nya Bastnäs mining area (Geijer 1961), the site of the original discovery of cerium (Hisinger & Berzelius 1804), and the type locality for numerous REE minerals (e.g. bastnäsite-(Ce), cerite-(Ce), törnebohmite-(Ce) and several others (cf. Holtstam & Andersson 2007, Holtstam et al. 2014, and references therein). Additionally, the Ceritgruvan mine in the Nya Bastnäs field was most likely the first hard-rock deposit specifically worked for rare earth elements.

Table 8. REE minerals in the Bastnäs-type deposits (REE line) and their chemical formulae.

Mineral	General formula
Allanite-(Ce)	$\mathrm{Ca(Ce,LREE)Fe^{2+}Al_2[SiO_4][Si_2O_7]O(OH)}$
Bastnäsite-(Ce)	$\mathrm{(Ce,LREE)(CO_3)F}$
Bastnäsite-(La)	$\mathrm{(La,LREE)(CO_3)F}$
Cerianite-(Ce)	$\mathrm{(Ce,REE)O_2}$
Cerite-(Ce)	$\mathrm{(Ce,LREE,Ca)_9(Mg,Fe)[SiO_4]_6[SiO_3OH](OH)_3}$
Delhuyarite-(Ce)	$\mathrm{(Ce,LREE)_4Mg(Fe_2W)\square[Si_2O_7]_2O_6(OH)_2}$
Dissakisite-(Ce)	$\mathrm{Ca(Ce,LREE)MgAl_2[SiO_4][Si_2O_7]O(OH)}$
Dollaseite-(Ce)	$\mathrm{Ca(Ce,LREE)Mg_2Al\ [SiO_4][Si2O_7]F(OH)}$
Ferriallanite-(Ce)	$\mathrm{Ca(Ce,LREE)Fe^{3+}AlFe^{2+}[SiO_4][Si_2O_7]O(OH)}$
Ferriperbøeite-(Ce)	$\mathrm{Ca(Ce,LREE)_3(Fe^{3+}Al2Fe^{2+})[Si_2O_7][SiO_4]_3O(OH)_2}$
Fluocerite-(Ce)	$\mathrm{(Ce,LREE)F_3}$
Fluocerite-(La)	$\mathrm{(La,LREE)F_3}$
Fluorbritholite-(Ce)	$\mathrm{Ca_2(Ce,LREE)_3[SiO_4]_3F}$
Fluorbritholite-(Y)	$\mathrm{Ca_2(Y,REE)_3[SiO_4]_3F}$
Gadolinite-(Ce)	$\mathrm{(Ce,LREE,Y)_2FeBe_2Si_2O_{10}}$
Gadolinite-(Nd)	$\mathrm{(Nd,Y,REE,)_2FeBe_2Si_2O_{10}}$
Gadolinite-(Y)	$\mathrm{(Y,REE,)_2FeBe_2Si_2O_{10}}$
Håleniusite-(La)	$\mathrm{(La,LREE)OF}$
Hingganite-(Y)	$\mathrm{(Y,REE,)_2Be_2Si_2O_8(OH)_2}$
Lanthanite-(Ce)	$\mathrm{(Ce,LREE)(CO_3)_3F\cdot 8H_2O}$
Magnesiorowlandite-(Y)	$\mathrm{(Y,REE)_4MgSi_4O_{14}F_2}$
Monazite-(Ce)	$\mathrm{(Ce,LREE)(PO_4)}$
Parisite-(Ce)	$\mathrm{Ca(Ce,LREE)_2(CO_3)_3F_2}$
Percleveite-(Ce)	$\mathrm{(Ce,LREE)_2Si_2O_7}$
Synchysite-(Ce)	$\mathrm{Ca(Ce,LREE)(CO_3)_2F}$
Törnebohmite-(Ce)	$\mathrm{(Ce,LREE)_2Al[SiO_4]_2(OH)}$
Ulfanderssonite-(Ce)	$\mathrm{(Ce,LREE)_{15}CaMg_2[SiO_4]_{10}[SiO_3OH](OH,F)_5Cl_3}$
Västmanlandite-(Ce)	$\mathrm{(Ce,LREE)_3Ca(Mg,Fe)_2Al_2Si_5O_{19}(OH_{)2}(F,OH)}$

Later, several other skarn-hosted iron ore deposits with (at least partly) similar REE mineralisation, had become known, and Geijer (1961) concluded that they ought to be (genetically) related and could be gathered under a common classification and name, i.e. as deposits of the Bastnäs type. The deposits/occurrences he referred to at that time were the Nya Bastnäs mines, together with those of nearby Storgruvan and Högfors fields, and the Lerklockan railway siding, all near Riddarhyttan, together with the Malmkärra, Johanna, Östanmossa, Åsgruvan and Södra Hackspik mines in the Norberg area. Although not clearly classifying them as Bastnäs type, Geijer also remarked on the occurrence of REE minerals at the Stripåsen copper mine (also near Norberg, not to be confused with the HREE-Nb-Ta mineral-bearing granitic pegmatite of the same name that was quarried nearby), as well as at several smaller mines near Knutsbo, further to the northeast.

Notably, in contrast to many other mineralisations with abundant allanite and other REE minerals, the Bastnäs-type deposits (except the Östra Gyttorp mine) are virtually devoid of radioactive elements; hence, all REE-rich minerals so far encountered are non-metamict.

Iron, copper, cobalt and cerium ores were mined intermittently in the Riddarhyttan area for at least 600 years, until 1978, when the last active iron (and copper) mine, Bäckegruvan, was closed (Öhman et al. 2004). The last mine in the Norberg area closed in 1981. Overall, iron was the most important commodity throughout the history of mining in this region, as in most other parts of Bergslagen.

Geology and mineralisation

The Bastnäs type deposits all occur in the western central part of the Palaeoproterozoic Bergslagen ore province, forming a discontinuous, approximately 100-km-long, narrow belt for which the name "the REE line" has been introduced (Jonsson & Högdahl 2013).

This belt (Fig. 46) predominantly comprises variably altered felsic metavolcanic, mostly rhyolitic rocks with carbonate (calcitic and dolomitic marble) interlayers, and is oriented in a northeast–southwest direction, with moderately to steeply dipping foliation. It extends from the Nora area in the southwest to close to Avesta in the northeast, with concentrations of deposits in the Fogdhyttan–Nora, Riddarhyttan–Bastnäs and Fagersta–Norberg areas. The Knutsbo area is somewhat "off" to the northeast, but is thought to represent an extension of the REE line.

These groupings of REE-rich iron oxide skarn deposits occur together with associated BIF occurrences, as well as similar skarn mineralisations without known elevated REE content. The main iron ore horizons, magnetite-dominated skarns and hematite-dominated banded iron formations, are stratiform and generally likely to broadly have a volcano-sedimentary origin (e.g. Andersson 2004). The skarn-hosted mineralisations follow narrow marble horizons within the metavolcanic rocks. Near the actual deposits, the metavolcanic rocks were strongly hydrothermally altered, and subsequently transformed during regional (Svecokarelian) metamorphism into cordierite and/or andalusite-bearing mica schists or "mica quartzites" (e.g. Fig. 47). The main phase of hydrothermal alteration of the volcanic units probably took place during an early syn-volcanic stage, as is also suggested by the close spatial association of extensively altered, originally volcanic rocks with rocks that are essentially unaltered except for a later (regional) metamorphic overprint.

Ductile folding of host rocks as well as REE-mineralised assemblages has been recorded, and many of the mineral assemblages in the deposits studied exhibit recrystallised textures, indicating that they were formed at an early stage of the orogenic evolution (Jonsson & Högdahl 2013; e.g. Figs. 48, 49). Later remobilisation of REEs is also indicated at some localities, such as Högfors, where an older, folded and recrystallised REE silicate (skarn) assemblage containing cerite-(Ce) and the Fe analogue of västmanlandite-(Ce), for example is cross-cut at a high angle by an allanite-(Ce)-bearing quartz vein (Jonsson & Högdahl 2013; Fig. 48).

Similarly, allanite (*sensu lato*)-bearing quartz vein networks cross-cutting an "ore quartzite" (most likely a regionally metamorphosed metasomatic alteration rock) were described from the locality

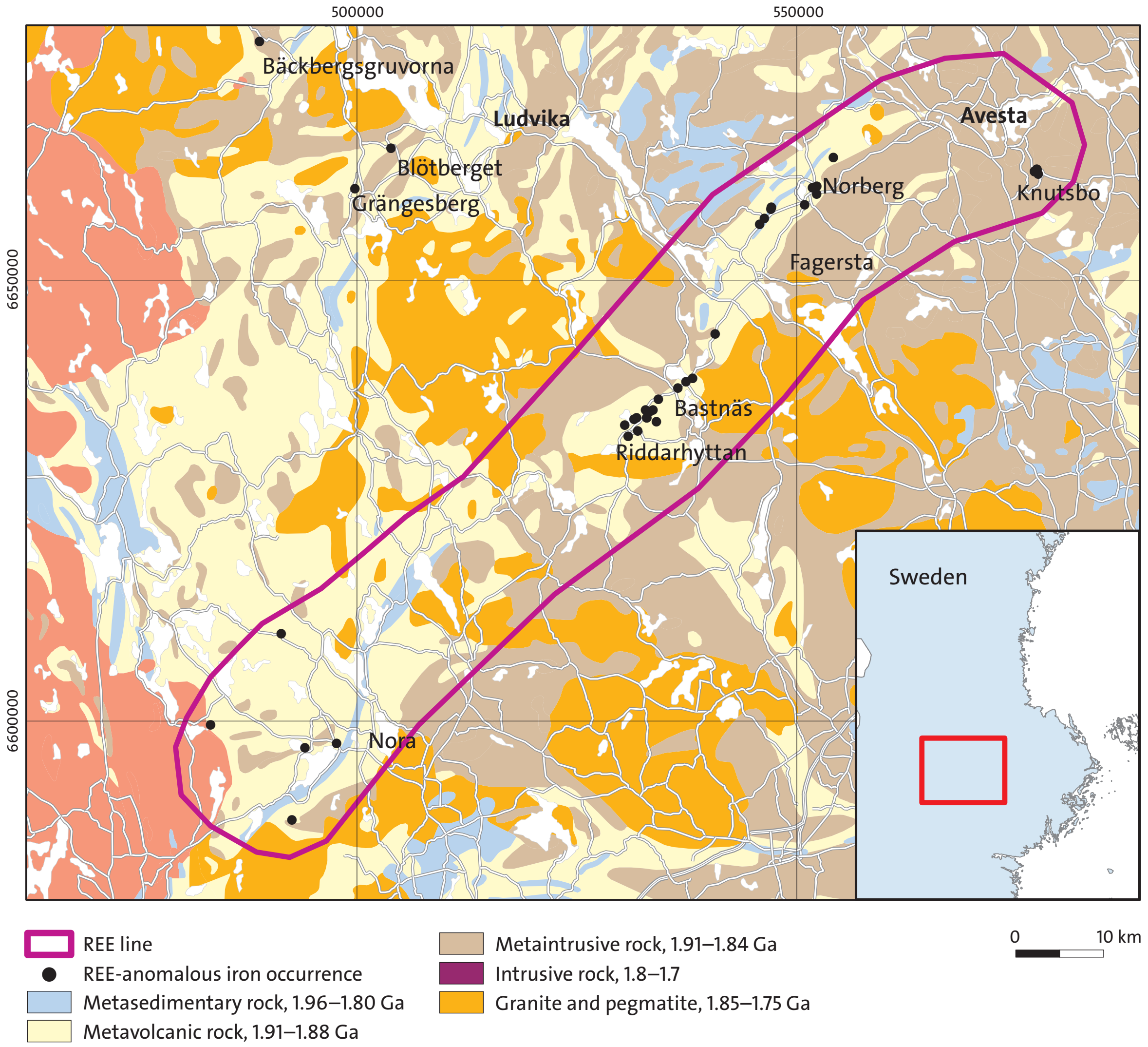

Figure 46. Simplified bedrock geology map showing the main locations or clusters of REE-rich iron-skarn deposits in the REE line.

Lerklockan by Geijer (1961). It is unclear at present whether some of the coarser-crystallised, typically subhedral to euhedral REE minerals (such as one type of bastnäsite-(Ce) and some ferriallanite-(Ce)) in the Nya Bastnäs deposits belong to such a later stage. Both their general morphology and coarseness (of individual crystals) may contrast sharply with the predominant finer-grained and recrystallised appearance of REE mineralisation here and at other Bastnäs-type deposits. Similarly, both minerals usually occur as fine-grained and anhedral grains and masses together with cerite-(Ce), forming the most commonly observed type of REE-mineralised assemblage at Nya Bastnäs.

Within the REE line, at least the central part (Riddarhyttan-Bastnäs) shows LREE enrichment, whereas the northeast (Norberg area) is enriched in LREE and Y + HREE, forming two subtypes of the Bastnäs-type deposits. Subtype 1 is thus represented by the deposits in the central and southern parts, including the Bastnäs mines, and the southwestern part in the Nora area, while subtype 2 is represented by the deposits of the Norberg area in the northeast (Holtstam & Andersson 2007, Holtstam et al. 2014). Silicates are the main hosts of REE in all deposits, although fluorocarbonates such as bastnäsite-(Ce) and synchysite-(Ce) also occur throughout many of them, and may locally be abun-

Figure 47. Cordierite-blastic, altered felsic metavolcanic rock in outcrop at Källfallet, Riddarhyttan (6632184/529935). Photo: Per Nysten.

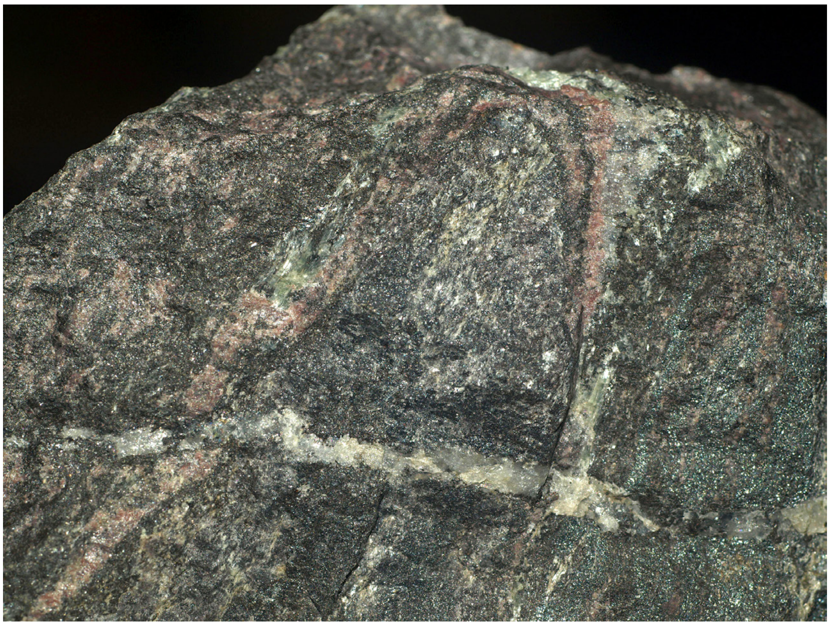

Figure 48. A folded and recrystallised reddish band of REE silicates (reddish tone from abundant cerite-(Ce), in addition to the presumed Fe analogue of västmanlandite-(Ce), for example) within the banded iron formation mined at (Stora) Högfors (6636536/534256), north-northeast of the Bastnäs field. The folded REE silicate band was later cross-cut (and slightly displaced) at a high angle by a quartz vein (subhorizontal in this image), which contains minor ordinary allanite-(Ce). Photo: Erik Jonsson.

dant (as in the case of bastnäsite-(Ce) at Nya Bastnäs). Allanite (*sensu lato*) and cerite-(Ce) associated with tremolite-actinolite dominated skarn is common, particularly in the deposits of the southwestern and central parts of the REE line, whereas dollaseite-(Ce) and fluorbritholite-(Ce) become more important in the northeast. Mo-Bi-Co-Cu-sulphides, together with fluorite, occur disseminated in the skarn, as well as local enrichments of Au-Ag alloys in the deposits of the central part, and most abundantly at Nya Bastnäs.

The origin of the Bastnäs-type deposits has been debated over time, and they are now generally interpreted as being the result of skarn-forming reactions between pre-existing carbonate rocks and medium to high-temperature, metal-rich (including the REEs) hydrothermal fluids (cf. Andersson et al. 2013; Jonsson 2013; Sahlström et al. 2014, 2015; Holtstam et al. 2014, and references therein;

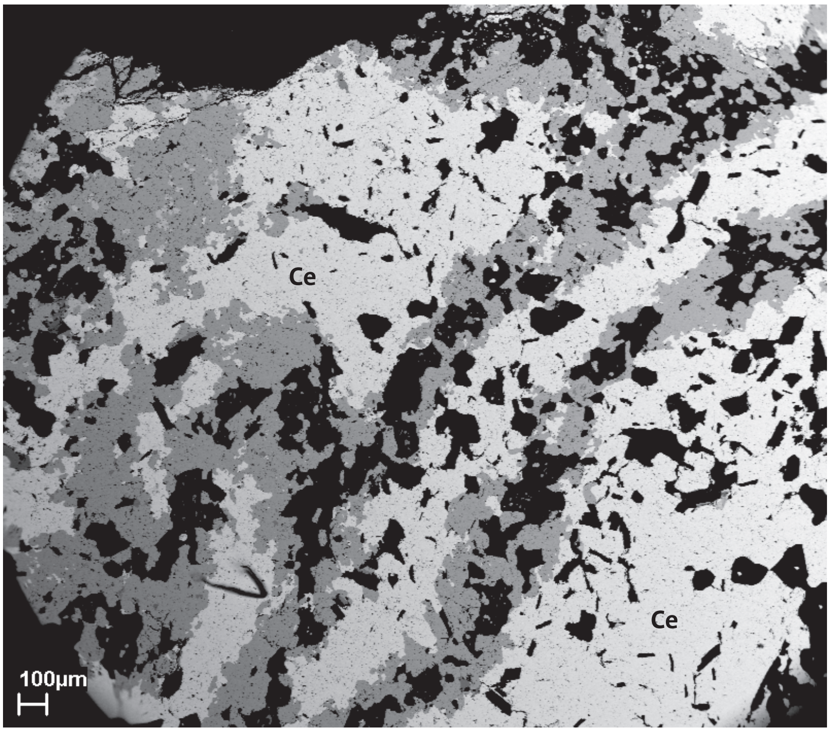

Figure 49. Back-scattered electron (BSE) image of a section from the folded and recrystallised REE silicate bands in the banded iron formation mined at Högfors. Small-scale folding can be seen in the alternating bands of cerite-(Ce) (light grey/white) and a darker grey västmanlandite-like mineral, most likely the unnamed Fe analogue of västmanlandite-(Ce). Black represents silicates, mostly amphibole. Photo: Erik Jonsson.

Jonsson et al. 2014). It has been suggested that the formation of local REE silicate mineralisation in other host rocks, and specifically banded iron formations (BIFs) occurring within the same metasupracrustal package, is potentially related to the same (epigenetic) process, rather than being synchronous with the formation of the BIFs (Jonsson & Högdahl 2013). The age of mineralisation is somewhat contentious, with several indications of an early, syn-volcanic process being responsible (e.g. Sahlström 2014, Sahlström et al. 2014, 2015, Jonsson & Högdahl 2013), although other methods (chiefly Re-Os in molybdenite) yield ages down to c. 1840 Ma (Andersson. 2013, Holtstam et al. 2014). Several recent observations in mine dump material at Nya Bastnäs of molybdenite occurring on late fracture surfaces that cross-cut the REE-mineralised skarn suggest that (numerous observations also exist of molybdenite that is seemingly coeval with the major REE silicate assemblages) this sulphide may in part have formed much later than the REE magnetite skarn assemblage.

New LA-ICP-MS dating of zircons from the variably altered host rocks to the Bastnäs area mineralisations indicate relatively high ages of these felsic metavolcanic rocks, at around and over 1.9 Ga (Linders 2016).

Districts and deposits

The Riddarhyttan district

The district around Riddarhyttan (Fig. 50) is intensely mineralised, and includes the best-known deposit of this type, in the form of the eponymous Bastnäs mines (the Nya Bastnäs, i.e. *New* Bastnäs mine field, in contrast to the *Old* Bastnäs mine field, Gamla Bastnäs, which is situated to the immediate south). However, REE mineralisation in this area occurs at several other locations within the same, in part strongly altered metavolcanic rock unit, e.g. at Stålklockan, Storgruvan (Bastnäs Storgruva), Högfors (Stora Högforsgruvan), and Persgruvan (Fig. 50, Geijer 1923, 1961; Ihre & Sädbom 1986, unpublished report).

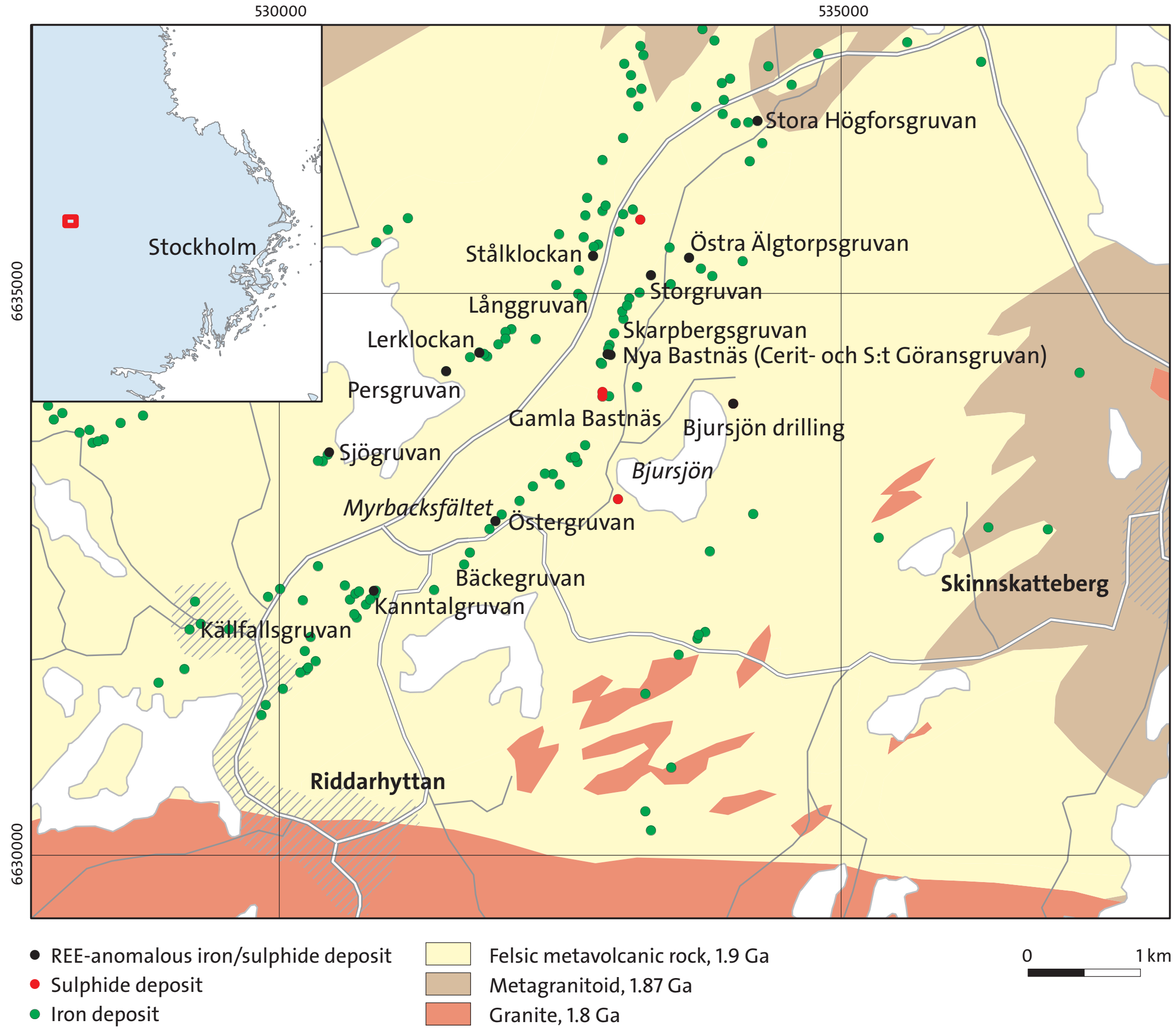

Figure 50. Simplified bedrock geology map showing locations of mines in the Riddarhyttan field, central part of the REE line, highlighting those with REE enrichment.

The first record of what would become known as an REE-bearing mineral from Bastnäs was probably by Axel Fredrik Cronstedt in the 1740s, since the word *tungsten* ("heavy stone" in Swedish, the origin of the name of the metal W in several languages, tungsten) occurs on a Bastnäs specimen labelled 1746 (Nordenskiöld 1873). In 1750 he reported a "dense, reddish rather heavy ironstone and also described "a black *tungsten*" containing iron (Tideström 1890, unpublished manuscript,). This red mineral was subsequently described by Cronstedt (1751) and became known as "Bastnäs tungsten" (one of several "heavy stones" with strange or unknown compositions, at that time). Wilhelm Hisinger and Jacob Berzelius performed analyses on both gadolinite (then known as "ytterbit", the host mineral for the first discovered rare earths, in the form of Johan Gadolin's "yttria" etc. from the Ytterby pegmatite, published in 1794) and the red mineral from Bastnäs. They concluded that a new element with characteristics similar to "yttria" was indeed present in the mineral from Bastnäs. Further analyses performed in 1803–04 confirmed their initial conclusions. Berzelius initially named the element bastium after the locality but renamed it cerium soon afterwards in honour of the newly discovered "planet" Ceres. The cerium-containing mineral thus became cerite following the discovery and publication of the first known light rare earth element cerium by Hisinger & Berzelius in (1804).

The Nya Bastnäs mine field

The Nya Bastnäs field (Fig. 50) comprises a number of discrete mines that worked two parallel ore horizons, featuring skarn-hosted (polymetallic) ores with locally abundant REE minerals, and banded iron formations, respectively. The former are magnetite-dominated, and occur as pods in mainly clinoamphibole-dominated skarn, wholly or partly replacing a carbonate rock (marble) intercalated within the variably altered felsic metavolcanic rock units (cf. also Ambros 1983). Antophyllite-cordierite-bearing assemblages also occur. In the southwestern part of the Nya Bastnäs field, remnant (unreacted) parts of this carbonate horizon are present, according to Geijer (1923). Earlier, Geijer (1921c) had stated that skarn containing remnants of carbonate rock had also been observed in the dumps at Nya Bastnäs. Efforts to find such carbonate rock material have been made recently, but its presence could not be verified in the mine dumps still remaining.

The main ore-bearing horizon, predominantly consisting of magnetite and hematite, has an average width of 8 m and has been traced at the surface for about 400 m. Within this zone the REE-mineralised part was up to 0.6 m thick. Rich REE mineralisation was encountered at S:t Göransgruvan (St Göran mine) and in particular, in Ceritgruvan (the Cerite mine; Fig. 50). The REE deposits here are of a characteristic, amphibole-rich magnetite skarn type, with locally significant Cu-Co-Ni-Bi-Mo sulphides as well as minor Te- and Hg-bearing minerals (Holtstam & Ensterö 2002, Ensterö 2003) and gold-silver alloys. At Bastnäs the most characteristic REE mineralisation type comprises either only "allanite" (mostly ferriallanite-(Ce)), or a typically fairly fine-grained assemblage of cerite-(Ce) and ferriallanite-(Ce), with variable amounts of bastnäsite-(Ce) and törnebohmite-(Ce), for example; a characteristic paragenetic zoning is often present, featuring fine-grained intergrowths of cerite-(Ce) and other minerals rimmed by (and seemingly in part replaced by) coarser-grained ferriallanite-(Ce) (Fig. 51).

Based on information in Tideström (1890, unpublished manuscript,) and others, the Cerite mine was originally known as a copper deposit, as seen on a mine map from 1765. The extent of the ore body was at that time also known from mining compass measurements. In late 1753 A. F. Cronstedt mentioned the find of native gold by assessor Quist, from the St Göran mine, associated with Co-, Cu-, Bi-ore in amphibole skarn. Moreover, Tideström (1890, unpublished manuscript,) described the ore situation in the St Göran mine in 1755 as: "in the western part, copper ore being from 0.15 to 0.9 m thick, is accompanied by asbestos and "Bastnäs tungsten" occurring in pods, to a depth of 30 m. This "heavy stone"

Figure 51. A characteristic REE-rich assemblage from the Nya Bastnäs field: a fine-grained, light-coloured mass of cerite-(Ce), with minor intergrown ferriallanite-(Ce) and bastnäsite-(Ce) is rimmed by coarser-grained ferriallanite-(Ce), within a pale green amphibole-dominated skarn. The cerite-dominated material in the centre has become dull and whitish due to post-mining surface alteration. Photo: Erik Jonsson.

consisted mainly of cerite (and, certainly, minor associated ferriallanite et al.) and was replaced downwards by a less heavy material, reminiscent of hornblende, which proved to be allanite. In 1848 limited efforts were made to extract "cerite ore". During the late 19th century the demand for LREEs increased because of new industrial applications, and therefore mining activity was ramped up in 1886–88, and also included the reworking of the mine dumps for both cerite- and allanite-rich material. At that time the mine was 16.8 m deep. It is mentioned that chalcopyrite always accompanied the cerite ore, albeit "in an erratic manner". Azurite, malachite, chalcocite and bornite were also associated minerals observed at that time. The cobalt mineral linnaeite is also mentioned (linnaeite was originally discovered in Bastnäs, first described by Brandt in 1746, while this specific name was not used until the 1840s, however). Drifts were made towards the St Göran mine and minor amounts of REE ore were found here (Tideström 1890, unpublished manuscript). The St Göran mine produced 287 tonnes of copper ore during 1862–64. This ore was accompanied by magnetite, quartz, amphibole (in part asbestiform), hornblende and minor allanite. Minor cerite was also left in the northeastern part of the mine, which was 45 m deep at that time.

According to Geijer (1921c), the REE mineralisation found at the St Göran mine was a "narrow stripe" associated with the copper sulphide ore, ending at a depth of 30 m; in the Cerite mine, a band of REE minerals was 0.3 to 0.6 m wide and 6–7 m long. Together with a similar but narrower band, it ended at a depth of about 20 m in the mine. About 160 tonnes of cerite-dominated ore were produced between 1860 and 1919 according to Carlborg (1923). However, it is also stated that overall REE ore production from the Cerite mine was approximately 4,500 tonnes, of which cerite alone accounted for "several hundreds of tonnes" (Carlborg 1923, Geijer 1921c). The latter states that "high-grade cerium ore" was mined during the period 1875 to 1888, with a total production of 4,465 tonnes. Additionally, later reworking of the mine dumps at Nya Bastnäs, during and between the world wars, is said to have yielded significant amounts of REE ore (B. Högrelius, personal communication); in 1923 825 tonnes, with an average content of 35% "cerium oxides" was extracted from the mine dumps (Högbom 1930, Hallberg 2012). Hammergren (1988, unpublished report) also noted that subsequent hand-sorting of the old dumps in the 1940s had yielded "some cerite ore".

Somewhat dramatically, Geijer (1921c) stated that "It [Bastnäs] is probably the largest primary deposit of the cerium metals that has ever been discovered"; this was, however, logical at a time when most of the sparse REE world production was known and sourced from monazite placer deposits.

Major REE minerals of the Riddarhyttan district

A typical REE-rich assemblage at Nya Bastnäs is made up of fine-grained cerite-(Ce), often intergrown with variable amounts of other REE minerals, most typically fine-grained bastnäsite-(Ce) and ferriallanite-(Ce), surrounded by a more coarse-grained outer zone or rim of, often platy, ferriallanite-(Ce), all hosted by a medium- to coarse-grained, green clinoamphibole (tremolite to actinolite) skarn. Characteristically, cerite-(Ce) at Bastnäs is reddish to pale reddish-grey when fresh, but alters (mainly) superficially into a dull, chalky white colour, sometimes with a purplish tint. Fine-grained cerite aggregates (with variable amounts of bastnäsite) may also exhibit texturally later veins, or rims, of ferriallanite, (cf. Geijer 1921c; Fig. 51), all features suggesting replacement of an earlier-formed, fine-grained cerite-(Ce) assemblage by ferriallanite-(Ce) ± törnebohmite-(Ce) (cf. Geijer 1921c, Holtstam & Andersson 2007).

Alongside cerite-(Ce), ferriallanite-(Ce) is the most common REE silicate at Nya Bastnäs, whereas "ordinary" allanite-(Ce) is actually quite uncommon (Holtstam et al. 2003b, Holtstam & Andersson 2007). Ferriallanite-(Ce) typically occurs as compact crystalline masses or euhedral platy, unaltered crystals, with other REE silicates and bastnäsite in amphibole skarn. Accessory phases are chalcopyrite, bismuthinite, and molybdenite. Allanite-(Ce) is less common at Bastnäs, and present as a later-formed mineral at Högfors (Jonsson & Högdahl 2013). It also occurs at Rödbergsgruvan and Östra Gyttorp in the Nora area (see descriptions below). In contrast to ferriallanite-(Ce), which commonly occurs in close association with minerals such as cerite-(Ce) etc., allanite-(Ce) seems to occur specifically in assemblages lacking other REE minerals, as observed at both Bastnäs and Rödbergsgruvorna (Holtstam & Andersson 2007).

While västmanlandite-(Ce) is found mainly in the Norberg area, its iron analogue (as yet not fully characterised and hence unnamed) is confined to the subtype 1 deposits, as in Nya Bastnäs, Rödbergsgruvan and Högfors (Holtstam & Andersson 2007, Jonsson & Högdahl 2013).

Bastnäsite was described by Hisinger (1838) under the name of "basiskt fluor-cerium", while Berzelius'steassidenite is (1825a) description of an orange-yellow, fluorine-bearing cerium mineral from Bastnäs was the first record of this mineral. When fine-grained, this yellow-brown mineral is difficult to recognise, whereas the coarsely crystalline type occurring as larger individual, platy crystals, mostly included in ferriallanite-(Ce), is quite apparent. Such crystalline aggregates and crystal sections are known in sizes of up to over 10 cm across. Bastnäsite (*sensu lato*) is also known, in lesser amounts from the Norberg district. Overall, the cerium-dominant mineral is by far the most common, while sparser, lanthanum-dominated ones have also been identified (Holtstam & Andersson 2007).

Törnebohmite-(Ce) was originally described from the Nya Bastnäs field by Geijer (1921c), and although relatively rare in megascopically visible amounts, it is a characteristic constituent of the mineralisation, forming inconspicuous, small green rounded grains, often as aggregates in a fine-grained cerite-bastnäsite-ferriallanite groundmass. It is most typically directly associated with ferriallanite-(Ce) (Holtstam & Andersson 2007).

Fluocerite was first described by Geijer (1921a), and more recent work has verified the presence of both the Ce- and La-dominated species in the Nya Bastnäs deposit (Holtstam & Andersson 2007). From its textural appearance and paragenetic position, it seems to be an early-formed mineral, and characteristically displays some alteration (Geijer 1921a). This alteration, when complete, has led to the formation of a porous mixture, chiefly made up of bastnäsite-(La) and cerianite (Holtstam & Andersson 2007).

Late alteration by essentially oxidising fluids, in part along open fractures, led to the formation of secondary minerals, commonly highlighted by the occurrence of bright green secondary copper minerals. This may also in part include the alteration of REE fluorocarbonates, but more specifically the precipitation of lanthanite-(Ce). This mineral was first described as "kolsyrad ceroxidul" by Berzelius (1825a, b). Its physical properties were later described by Hisinger (1826) and the name lanthanite was given by Haidinger (1845). However, for some reason, the official type locality of lanthanite-(Ce) is now given as the Britannia mine, near Snowdon in Wales (Bevins et al. 1985). The composition of Bastnäs lanthanite, having Ce>La, Nd, Pr, Sm, was verified by means of SEM-EDS analyses by Holtstam & Andersson (2007). Besides the occurrence of beautiful euhedral, pale pink transparent to translucent lanthanite-(Ce) crystals on partly open cracks in cerite-ferriallanite rich assemblages, it is also found in cavities and cracks in ferriallanite-bearing actinolite skarn (Öhman et al. 2004).

Cerianite-(Ce), a rare alteration product of fluocerite, occurs as microscopic grains less than 20 µm in size, in the Nya Bastnäs deposit (Holtstam & Andersson 2007). Håleniusite-(La) is isostructural with cerianite, and also belongs to this late stage of modification of the REE mineralisation, occurring as conspicuously yellow and dull fine-grained masses, often accompanied by secondary copper minerals (Fig. 52). It is suggested that it formed through the alteration of primary La-dominant bastnäsite, most likely by means of a decarbonation reaction (Holtstam et al. 2004). Overall, håleniusite is not uncommon in visibly and more extensively altered cerite-bastnäsite-rich assemblages.

Of the gadolinite-group minerals, gadolinite-(Ce) is reported from a single sample from Nya Bastnäs in which it occurs as anhedral grains up to 0.8 mm in size associated with törnebohmite-Ce), ferriallanite-Ce), cerite-(Ce) and the Fe analogue of västmanlandite-(Ce) (Holtstam & Andersson 2007).

Percleveite-(Ce) is a sorosilicate that occurs in association with cerite-(Ce), bastnäsite-(Ce) and quartz in the Nya Bastnäs deposit. It was first described by Holtstam et al. (2003a) and this mineral must be regarded as rather rare, since it is so far only known from only a few specimens. The host mineral assemblage

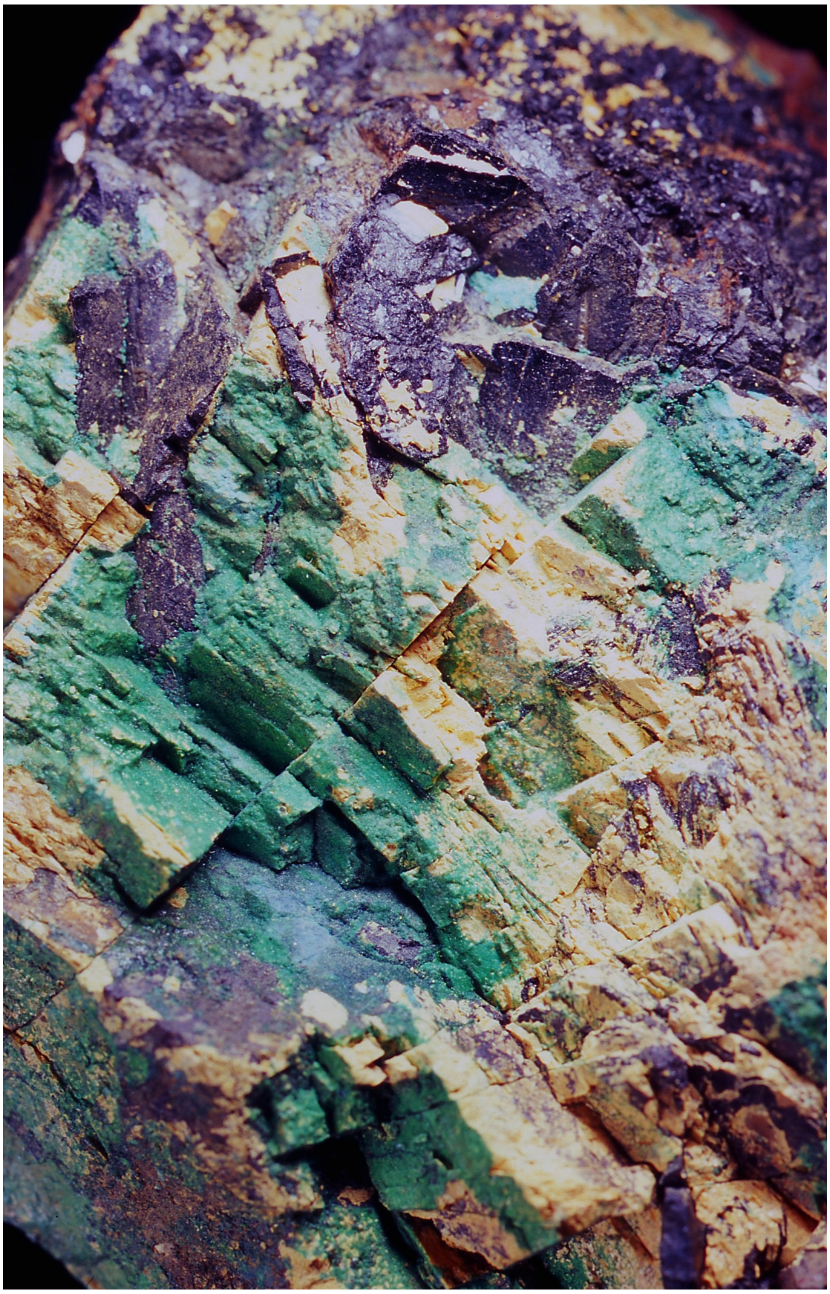

Figure 52. Coarse bastnäsite-(Ce) occurring as a radial crystal aggregate has been extensively replaced by dullish, light yellow håleniusite-(La), and also covered by precipitates of a green secondary copper mineral, probably brochantite. Platy black crystals of ferriallanite-(Ce) border and are partly intergrown with the (former) bastnäsite in the upper part of the image. Nya Bastnäs mines. Specimen from the collection of the Swedish Museum of Natural History (Stockholm). Image width approximately 2.5 cm. Photo: Erik Jonsson.

consists of rich "cerite ore" with minor magnetite, chalcopyrite and clinoamphibole (tremolite-actinolite intermediate *sensu stricto*). Accessory phases are allanite-(Ce), bastnäsite-(Ce) and törnebohmite-(Ce). Percleveite-(Ce) is the first pure lanthanide silicate with major Ce and La. The percleveite obviously formed under (local) conditions featuring slightly higher silicon activity and lower concentrations of Ca and Mg than those favourable for the crystallisation of cerite-(Ce) (Holtstam et al. 2003a).

Although fluorbritholite minerals are a characteristic of the Bastnäs-type deposits in the Norberg area, they have been identified as a likely main component of the REE mineralisation observed in the Stålklockan skarn (see below).

A mineral corresponding to magnesiorowlandite-(Y) was reported by Jonsson & Högdahl (2013) from Högfors. Additionally, the otherwise widespread REE phosphate monazite-(Ce) has been noted as a rare constituent of a banded magnetite-actinolite skarn associated with allanite-(Ce) from Bastnäs (Holtstam & Andersson 2007), and with other REE minerals in the banded iron formation at Högfors (Jonsson & Högdahl 2013).

A rare, tungsten-bearing mineral originally reported by Holtstam & Andersson (2007) has very recently been described as the new mineral delhuyarite-(Ce), occurring in association with e.g. percleveite-(Ce), cerite-(Ce), bastnäsite-(Ce), ferriallanite-(Ce), magnetite, and clinoamphibole (Holtstam et al. 2017a). Another new mineral named ferriperbøeite-(Ce), whose type locality has been stated as "Bastnäs mines" was also described recently (Bindi et al. 2017).

Skarpbergsgruvan/Öfra Bastnäs

The Skarpbergsgruvan mine, or Öfra Bastnäs ("Upper Bastnäs") is situated 100 m northeast of the Cerite mine (Fig. 50) and was reported to carry a hematite ore with disseminated sphalerite and pyrite (Tideström 1890, unpublished manuscript). An analysis of the iron ore by A. Tamm in 1874 mentions the presence of cerium oxide (as referred to by Tideström 1890). The suggestion of sphalerite seems questionable, and is also refuted by Geijer (1923), who believed this to be erroneous, either due to a mix-up of samples/labels, or misidentification of the brownish garnet occurring in this ore. But he did consider it to be fairly rich in barite, which might explain some of the problems encountered during beneficiation.

The Storgruvan mines (Bastnäs Storgruva)

Mining at Storgruvan (Bastnäs Storgruva), some 800 m northeast of Nya Bastnäs (Fig. 50) in the early 1900s exposed another REE mineralisation, comprising cerite associated with "allanite" and törnebohmite, of which approximately 5 tonnes of REE-mineralised material was separated and sold (e.g. Geijer 1923, 1961).

At Storgruvan, magnetite ore mixed with Mg-silicates (antophyllite, talc, biotite and cordierite) occurs. The abundant amphibole is often found as conspicuous, radiating crystal aggregates, up to 2 cm in size, and as more coarse-grained crystals dispersed in the ore (Källfallet ore type). Locally, antophyllite has been partly altered to talc. This ore type is typically banded with silicates separated from magnetite bands (Geijer 1923). The rock surrounding the ore may be described as a cordierite-antophyllite quartzite. Minor amounts of hematite, in the form of a banded iron formation associated with actinolite-bearing "quartzite" are also found here. However, a notable feature here is a body of "ophicalcitic" carbonate rock, as well as carbonates partly replaced by a tremolite-(chlorite) skarn with magnetite ore (Geijer 1961) (here, "ophicalcite" is a term denoting an often fine- to medium-grained carbonate rock, frequently dolomitic or calcitic, carrying abundant serpentine mineral pseudomorphs after olivine or humite-group minerals). Associated with this skarn is magnetite, traces of chalcopyrite and, to be noted, REE mineralisation. Apparently, the whole quantity of cerite-dominated REE-rich ore found here was separated and sent to the concentrating plant at Hultebo, so it is now seemingly impossible to find any remnants of REE-mineralised material at this locality. Geijer (1923) mentions "finger-thick" bands of heavily altered cerite occurring in association with törnebohmite, allanite ("orthite"), actinolite, magnetite and chalcopyrite. This REE mineralisation probably stems from the Storgruvan #4 claim. Analyses of magnetite-skarn samples from the dump, taken during the present project, yielded significant total REE contents of between 2000 and 10 000 ppm. Optical microscopy revealed this to be a pyrite-rich magnetite ore, in which the magnetite occurs as disseminations and as aggregates. Local concentrations of pyrite occur as well, and traces of hematite are seen within the magnetite. Coarse tremolite and anthophyllite make up the groundmass to the ore. As a likely REE carrier, brown anhedral grains of an unspecified allanite-like mineral up to 3 mm in size occur locally, and a colourless phase displaying marked relief occurs in association with this. This could potentially be cerite, since this has been noted and even extracted here (see above).

The Stora Högforsgruvan mine(s)

The Stora Högforsgruvan mine is located further to the northeast (Fig. 50) and features a hematite-dominated banded iron formation (BIF), with localised REE mineralisation (Högbom 1930, Geijer 1961, Jonsson & Högdahl 2013).

The mine dump material contains a well-banded, fine-grained hematite-quartz (meta-chert) ore, ranging to a strongly foliated and lineated magnetite-(hematite?)-anthophyllite-tremolite ore (Figs. 53, 54). No sulphides can be seen macroscopically. In polished thin section, hematite is seen as disseminations forming diffuse to semi-compact folded bands. A few small magnetite grains and hematite-altered magnetite grains are also visible. This is clearly a BIF-type ore, where locally tremolitic skarn together with quartz forms the groundmass to a semi-compact hematite ore.

Figure 53. Hematite-metachert-dominated banded iron ore (BIF) exhibiting chevron-style folding; dump sample at Stora Högforsgruvan (6636536/534256). Photo: Erik Jonsson.

Figure 54. Amphibole skarn-bearing magnetite-hematite banded iron ore from Stora Högforsgruvan (6636536/534256). Photo: Torbjörn Bergman.

REE mineralisation in turn occurs as sparse bands dominated by cerite-(Ce), the presumed Fe analogue of västmanlandite-(Ce), ferriallanite-(Ce) and gadolinite-(Ce), as well as additional minor minerals, which appear as fine-grained, recrystallised assemblages in folded bands or layers within the banded iron ore. These are locally cross-cut by later quartz veins carrying allanite-(Ce) (Jonsson & Högdahl 2013; Figs. 48, 49). In particular, the systematic appearance of a pale green tremolitic amphibole in association with REE enrichment in the banded iron ore suggests a link to the skarn-forming processes responsible for the main REE mineralisation at Nya Bastnäs.

Analyses of BIF samples from the dump, taken during the present project, showed total REE contents of between 1100 to 8500 ppm. In these samples, 0.10–0.15-mm-large grains of an unspecified allanite-like mineral are locally found together with tremolite, and possibly also törnebohmite or a gadolinite-like mineral in the form of an olive-green phase. An allanite-like mineral also occurs in close association with hematite bands, as intergrowths and larger inclusions. The concentrations of allanite occur as 0.5 to 1 mm veinlets that may be several millimetres long.

Besides the major occurrences, REE mineralisation has also been observed at Lerklockan, Stålklockan, Myrbacksfältet and several other localities in the Riddarhyttan area (Fig. 50). The occurrences where we have factual data on REE enrichment are described below, but a significant number of deposits/old mines are also known to carry disseminated allanites (*sensu lato*) or REE-bearing epidotes, in particular. This has been noted in the Hans Urbansson field, Persgruvan and other mines in the area (Geijer 1921b, 1923). In several of these occurrences, intermediate mixtures (not characterised using modern methods) between allanites and epidotes, previously referred to as "epidotortite", are widespread (cf. Geijer 1921b, 1923); no modern analyses have been performed on these occurrences or their minerals. The occurrence of allanite and REE-enriched epidotes is most likely also the main reason for the locally relatively high REE content found in several other iron oxide deposits in the area (see below).

Additional REE-mineralised zones at depth in the greater Bastnäs area were noted during exploratory drilling for gold and base metals from an exploratory underground drift driven northwards from the Bäckegruvan mine (Fig. 50). This prospecting campaign was run in 1982, and started at the 360 m level at Bäckegruvan, and ended within the Nya Bastnäs ore field; in total, eight cores were drilled here (Hålenius, 1987, unpublished report; Ihre & Sädbom, 1986, unpublished report). According to Hammergren (1988, unpublished report) and others, content of up to 8 wt% Ce and 5 wt% La were found in these cores. Analytical results of diamond drilling yielding anomalous REE contents (1–2% La, 2–4% Ce), were also recorded in the area between Lerklockan and Långgruvan; noteworthy elevated concentrations of La and Ce were also found during drilling east of Bjursjön (Fig. 50).

The Stålklockan mines

REE mineralisation at Stålklockan, north-northwest of the Bastnäs field (Fig. 50), was discovered in mine dump material during this project. A sampled compact amphibole skarn assemblage in contact with "ophicalcite" yielded significant REE enrichment as shown by XRF: (CeO_2 19%, La_2O_3 10%, Nd_2O_3 8% Pr_6O_{11} 2%, Sm_2O_3 1.4% Y_2O_3 0.9%). This material was subsequently characterised using a combination of optical microscopy, powder X-ray diffraction (XRD) and scanning electron microscopy with energy dispersive X-ray spectroscopy (EDS). As seen from optical microscopy, a network of a typical pleocroic (brown–green) allanite phase showing recrystallisation features and subgrain-formation coexists with a colourless heavily fractured epidote (dollaseite-like) mineral. Based on interpretations of the bulk sample XRD data, the fine-grained REE-rich assemblage predominantly comprises two minerals (disregarding ordinary skarn minerals), one related to the minerals of the epidote supergroup, i.e. allanite *sensu lato*, and one with an apatite-type structure. Scanning electron microscope study with EDS analyses yielded an empirical formula for the suggested apatite-structure phase, which is well comparable to fluorbritholite-(Ce); approximately $(Ce,La,Nd,Y,Ca)_5(SiO_4)_{3.3}F_{0.7}$. The epidote supergroup mineral is close in composition to an Fe-bearing dollaseite-(Ce), yet lacks fluorine, according to the analyses performed (Fig. 55). A dollaseite mineral is also probably an abundant phase, based on the XRD analyses. A related mineral, the proposed iron analogue of västmanlandite-(Ce), makes up the rest of the main REE silicate assemblage (Figs. 55, 56). Here too, a lack of reliable fluorine data hampered the chemical analyses, but the remaining element content and the resulting stoichiometries apparently suffice to identify the mineral as to its group. Associated minerals, besides abundant skarn silicates (primarily a clinoamphibole) and disseminated iron oxides (mainly magnetite), comprise fluorite, copper sulphides, anhedral grains of a partly molybdenum-substituted scheelite ("molybdoscheelite") and rare small grains of native bismuth. The magnetite locally carries exsolution lamellae of ilmenite.

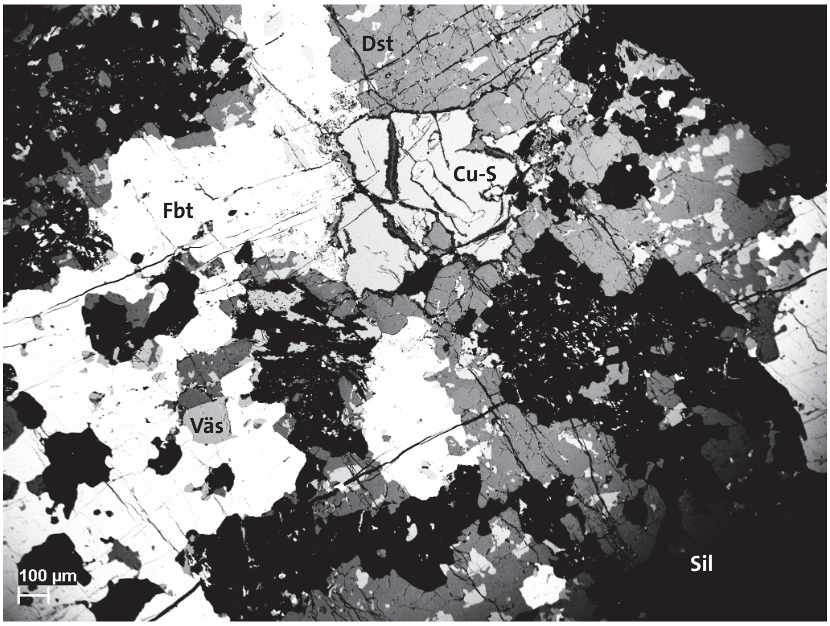

Figure 55. Back-scattered electron (BSE) image of the REE-rich mineralisation from Stålklockan: REE silicates predominate, mainly featuring white fluorbritholite-(Ce) (Fbt), minor medium grey västmanlandite-like mineral (Väs), and similarly medium grey dollaseite-like mineral (Dst), associated with copper sulphides (Cu-S) in skarn silicates (black; Sil), predominantly made up of amphibole. Photo: Erik Jonsson.

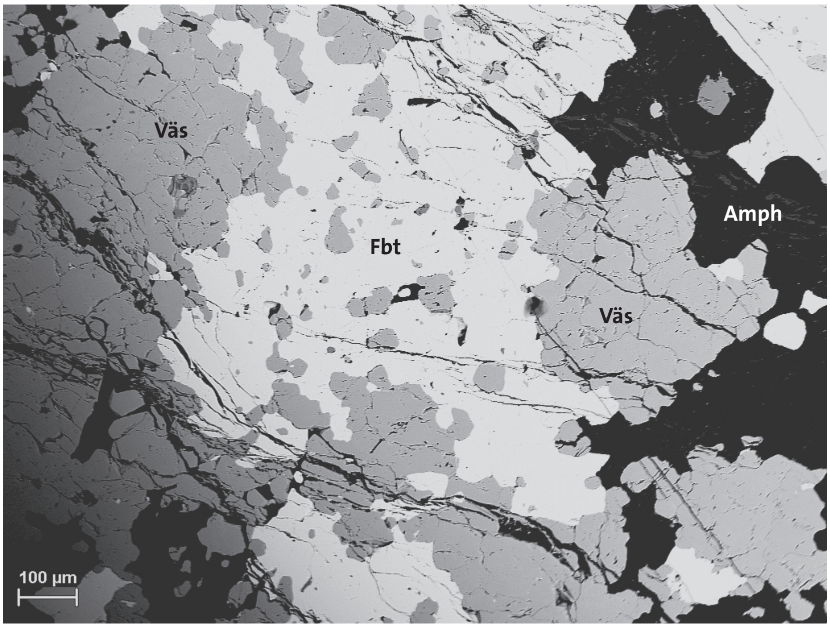

Figure 56. Back-scattered electron (BSE) image of the REE-rich mineralisation from Stålklockan, showing the predominant intergrowth of a BSE-white fluorbritholite-(Ce) (Fbt) with a västmanlandite-like mineral (Väs; medium grey), together with skarn amphibole (Amph; black). The fine-grained and recrystallised texture of the REE silicates is apparent. Photo: Erik Jonsson.

Lerklockan

The REE mineralisation at Lerklockan (Fig. 50) was described by Geijer (1961), as a railway cutting in an "ore quartzite carrying a network of orthite veinlets", with associated törnebohmite. A recent study of what is likely to be the cutting referred to by Geijer failed to locate visible REE mineralisation. Notably, the feature of allanite in later veinlets bears some similarity to the occurrence of later quartz veins (in that case, cross-cutting the "Bastnäs-type" mineralisation) with allanite-(Ce) at Högfors (Jonsson & Högdahl 2013).

REE enrichment in other iron oxide mineralisations in the (greater) Riddarhyttan district

During the course of this project, a suite of other iron mines in the Riddarhyttan district was sampled for whole-rock geochemical analyses, to test for "invisible" REE enrichment, and thus to potentially increase the area of known REE mineralisation. Some mines, like Storgruvan and Högfors, are also described above, and were sampled to assess whether seemingly ordinary ore and skarn assemblages would also exhibit markedly increased REE content. The sampled localities, here reported from south to north, that exhibit anomalous (>300) to high (>1000ppm) REE content are described below (Figs. 50, 58).

The Kanntalsgruvan mine

The Kanntal mine, or *Kanntalsgruvan*, is located in the Hans Urbansson mine field, southwest of the Bastnäs mines (Fig. 50), and is known for its locally rich cobalt mineralisation (e.g. Geijer 1923). A mine dump sample consisting of quartz-magnetite ore with chalcopyrite dissemination was taken and analysed in the present project and yielded a total REE content of 4800 ppm. The host rock is a fine-grained, felsic metavolcanic type, probably of rhyolitic composition. In thin section, semi-compact magnetite as anhedral to subhedral grains predominates, being euhedral towards chalcopyrite. The copper sulphide forms large grains intergrown with anhedral pyrite, which also occurs as small euhedral cubes. An accessory but important phase here is molybdenite, linking the sulphide inventory to the Bastnäs deposits. Magnetite displays even grain-boundaries and is relatively coarse-grained (0.2–0.3 mm). Pyrite is common along the grain boundaries between magnetite and silicates; the latter consist of greenish biotite, quartz, green chlorite oriented parallel to the foliation of the host rock. Minor calcite occurs as small pods scattered in the groundmass of the rock. As a potential REE carrier, an unspecified allanite-like mineral is relatively common, displaying brown to weakly green pleochroism. There is also an unknown colourless to weakly brown mineral with high relief in quartz. Parallel deformation zones transect the oxide matrix in broad bands.

Östergruvan/Mellangruvan mines

A sample from a dump between the mines Östergruvan and Mellangruvan in the Myrbacksfältet mine field, southwest of the Bastnäs area (Fig. 50), was taken and chemically analysed in the present project. It consists of rusty quartz-rich magnetite ore and contains 1700 ppm of total REEs.

Gamla Bastnäs

(Samples with thin sections and analyses, in profiles in the Gamla Bastnäs area, by M. Ripa; cf. chapter 7).

Bedrock mapping along a profile west of the Gamla Bastnäs ore field showed primarily metavolcanic siltstone. Microscopy of a thin section of this rock (sample CMR150054B, 6633973/ 532735) exhibits the presence of allanite and fluorite within a muscovite-biotite quartzite. Magnetite and traces of molybdenite also occur. It is notable that the allanite found here occurs in a rock seemingly devoid of skarn, and poor in iron oxides or sulphides.

A profile south of the Gamla Bastnäs ore field (sample and section CMR150055A, 6633789/ 532691) showed a volcanic siltstone in the western part, which is hematite-banded or hematite-spotted to the east. This sample was collected from a horizon that constitutes a weakly garnet-bearing banded iron formation. Hematite forms anhedral platy crystals in diffuse bands. The garnet is poikilitic with inclusions of hematite and quartz. The rich concentration of bluish-green tourmaline, showing zonation in bands, is noteworthy. Epidote occurs as pods, disseminations and bands. Biotite and chlorite are also found in this rock type. Minor amounts of a probable but unspecified allanite mineral have also been noted in this material.

The Sjögruvan mine

At the Sjögruvan mine, 2.5 km southwest of Nya Bastnäs (Figs. 50, 57a), a typical magnesium-rich skarn ore occurs, predominantly comprising anthophyllite and magnetite (Fig. 57b) and probably also talc. Mine dump samples were chemically analysed in the present project, and yielded a total REE contents

Figure 57. A. Overview of the mine dumps at Sjögruvan (6633505/530388). **B.** Massive magnetite ore with radial sprays of anthophyllite. Photos: Torbjörn Bergman.

of between 600 and 3200 ppm. No sulphides were observed. Locally semi-compact to compact magnetite forms anhedral to locally subhedral, 0.1–0.2-mm-large grains. Coarse, radial sprays of anthophyllite occur locally in a zone cutting the ore (Fig. 57b). Along contacts the magnetite exhibits subgrain formation and crack-fillings. Anthophyllite partly forms a parallel orientation. Talc and muscovite are probably present here as well. Anhedral, 0.1–0.2 mm large grains with brown to green pleochroism, forms overgrowths on the amphibole, and at the contact between amphibole and magnetite. This pleochroic phase is probably an unspecified allanite mineral or REE-enriched epidote, forming disseminations as well as local concentrations featuring aggregates up to 3 × 3 mm in size.

Kärrbo mine (Svavelgruvan)

The Kärrbo mine (*Kärrbo gruva* or *Svavelgruvan*), lies north of the main Riddarhyttan area, some 2.5 km northeast of the Stora Högfors mine (Fig. 58). It does not appear to be an iron oxide skarn deposit, but is included here because of its location and REE content. It is represented by a rather large water-filled mine opening (Fig. 59), with associated strongly rusted dump material, mainly consisting of compact pyrrhotite and minor pyrite and chalcopyrite. Pyrrhotite also forms disseminations within

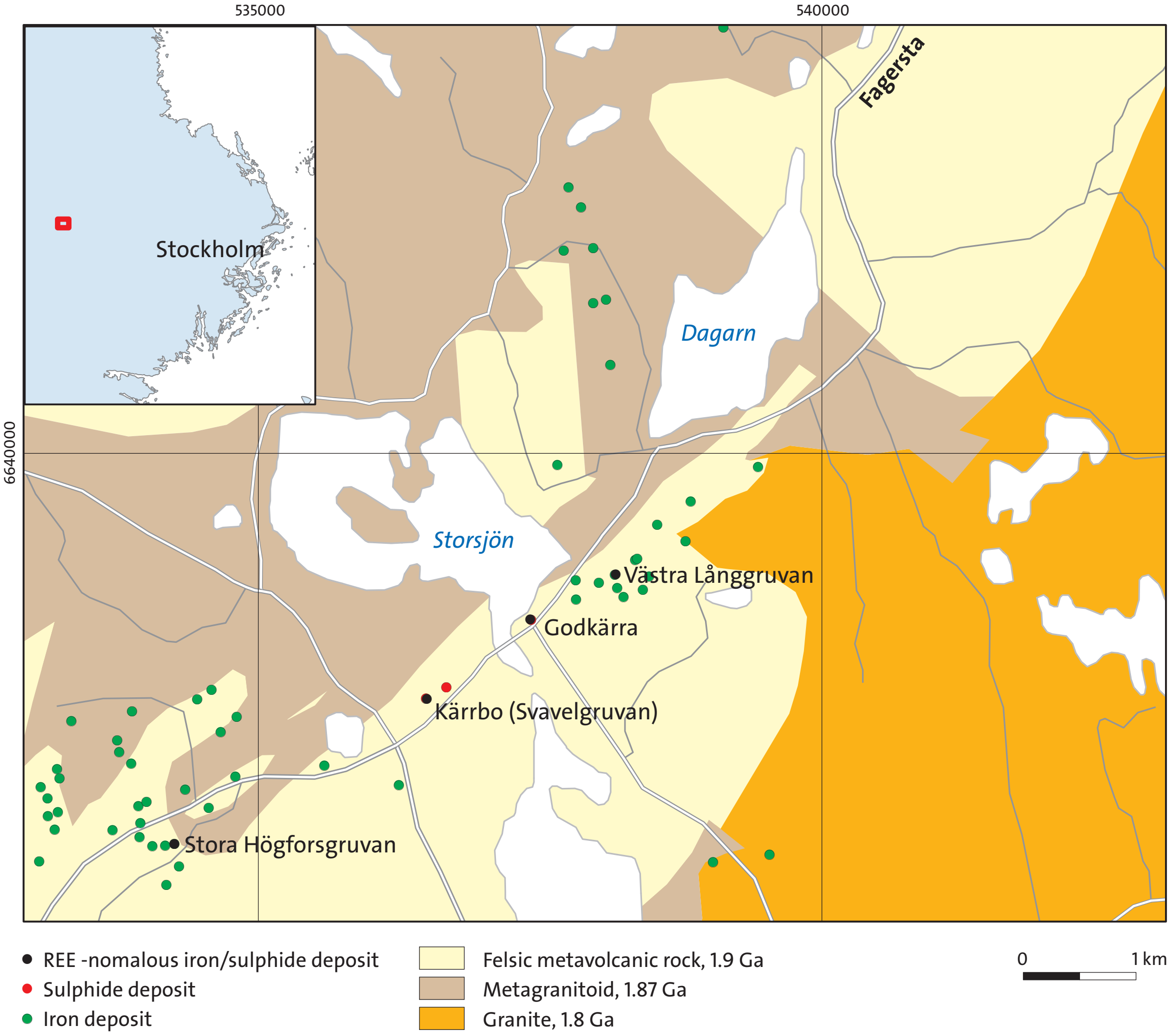

Figure 58. Simplified bedrock geology map showing the locations of mines in the area northeast of Bastnäs, Riddarhyttan area, in the central part of the REE line, highlighting those with REE enrichment.

the country rock. The sample investigated consists of compact iron sulphides with a 2 × 1-cm-large silicate inclusion. Pyrrhotite is the predominant sulphide, whereas pyrite and chalcopyrite form fairly large intergrowths. Locally, magnetite also occurs, in the form of subhedral crystals. The pyrrhotite shows modest alteration, especially along grain-boundaries. Large subhedral partly cracked pyrite crystals are apparent in the material. Goethite-veining occurs, transecting both sulphides and silicates. The latter consists of coarse tremolitic amphibole, with epidote and titanite as inclusions. A few grains of an unspecified allanite-like mineral have also been noted. Samples from this location were chemically analysed under the present project, and yielded total REE content of between 1700 and 3700 ppm.

Godkärra

During a drilling campaign, probably in the 1980s by SGAB, sample BBAC 525 from Godkärra northeast of the Bastnäs area (Fig. 58) was found to consist of a clinoamphibole skarn assemblage carrying chalcopyrite, pyrrhotite, bismuthinite, tellurobismuthite, native bismuth and gold, and featuring an anomalous REE content (Hålenius 1987, unpublished report).

Västra Långgruvan mine

The Västra Långgruvan mine is in turn located northeast of Godkärra (Fig. 58) Chemical analyses of dump samples from this mine yielded total REE contents of between 200 and 9500 ppm. These samples consist of actinolite-dominated magnetite skarn with relatively rich sulphide disseminations, mainly consisting of pyrite but also minor sphalerite. Polarised light microscopy revealed aggregates and disseminations of magnetite, locally as more compact ore, and large anhedral pyrite grains, traces of chalcopyrite, and later-formed goethite in fractures. The skarn groundmass consists of coarse, colourless clinopyroxene (diopsidic) and tremolitic amphibole. An unspecified, locally twinned allanite-like mineral (Fig. 60) occurs as up to 2 × 2-mm-large grains at the contact between diopside and magnetite. The allanite also forms aggregates of anhedral grains (0.3 mm) with magnetite inclusions.

Figure 59. The Kärrbo mine (Svavelgruvan) with partly visible mineralisation and associated rusty alteration (6637826/536489). Photo: Torbjörn Bergman.

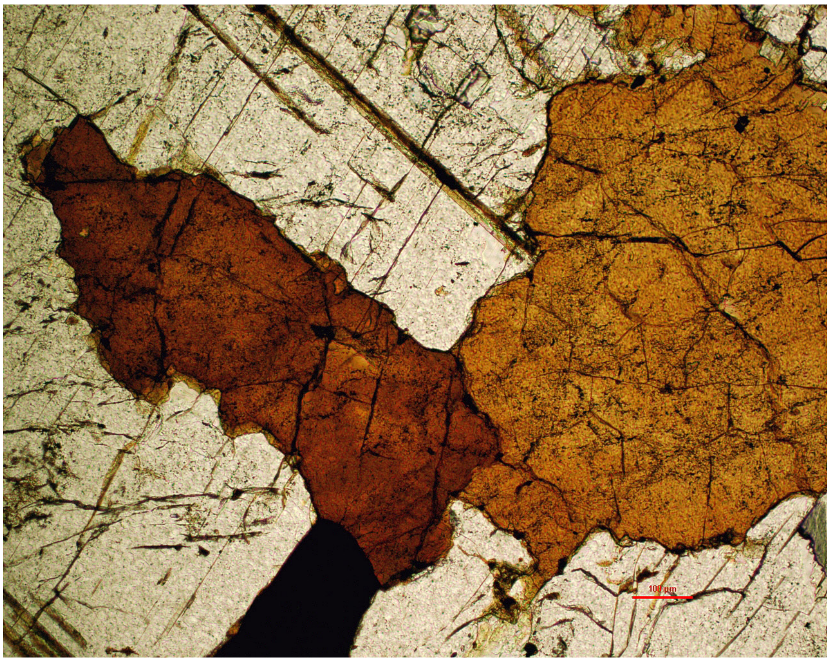

Figure 60. Brown-pleochroic, allanite-like mineral as subhedral to anhedral grains and aggregates in skarn from Stora Lång-gruvan. Photomicrograph in transmitted plane-polarised light. The scale bar equals 100 micrometres. Photo: Per Nysten.

The Nora district

Two "major" REE-enriched magnetite skarn occurrences are presently known from the Nora area: the Rödbergsgruvorna and Östra Gyttorp mines (Fig. 61). Several minor occurrences of unspecified allanites as well as other REE minerals have been noted in the greater Nora area, in addition to the deposits of the Bastnäs-type mentioned here. It is not known at present whether those minor occurrences might be related to the Bastnäs-type deposits, as is suggested in the Riddarhyttan and Norberg areas.

The Rödbergsgruvorna mines

The Rödbergsgruvorna mines (Fig. 61) were worked on a partly sulphide-bearing skarn iron ore, predominated consisting of dense to coarse-grained magnetite intergrown with quartz, among other things. Material collected at one of the dumps shows magnetite mineralisation locally rich in chalcopyrite in pods, and pyrite set in a matrix of even-grained, massive dark, calcic clinoamphibole (actinolite-edenite; Holtstam & Andersson 2007) skarn. The predominant REE assemblage at Rödbergsgruvorna consists of cerite-(Ce), allanite-Ce)-ferriallanite-(Ce), bastnäsite-(Ce), and a västmanlandite-like mineral, occurring as zoned veinlets in massive clinoamphibole skarn associated with magnetite and minor sulphides (Holtstam & Andersson 2007; Sahlström 2014; Fig. 62.) The grain size of this skarn varies from fine- to medium-grained. Polarised light microscopy of the sulphide-rich assemblages shows bismuthinite and possible bismuth sulphosalts. Magnetite devoid of sulphide occurs locally within actinolite, here somewhat lighter green in colour, and with centimetre(s)-thick veinlets consisting of coarser, black ferriallanite-(Ce) and "Fe-västmanlandite-(Ce)" as an outer rim surrounding finer-grained pink cerite-(Ce), often intermixed with bastnäsite-(Ce) and ferriallanite-(Ce) (Holtstam & Andersson 2007). These REE-rich veins may reach 5–10 cm in length, as observed in dump material. Locally, abundant white fluorite is also found here associated with magnetite, sulphides, and chlorite as well as minor molybdenite. The geochemical signature of Fe, Cu, Bi, Mo, F, and REE in the Rödbergsgruvorn skarn is markedly similar to that of the Nya Bastnäs field.

The REE-mineralised assemblages were only identified in dump material long after mining had ceased at Rödbergsgruvorna, so no information is available as to how, and specifically where, they occurred in the mine(s).

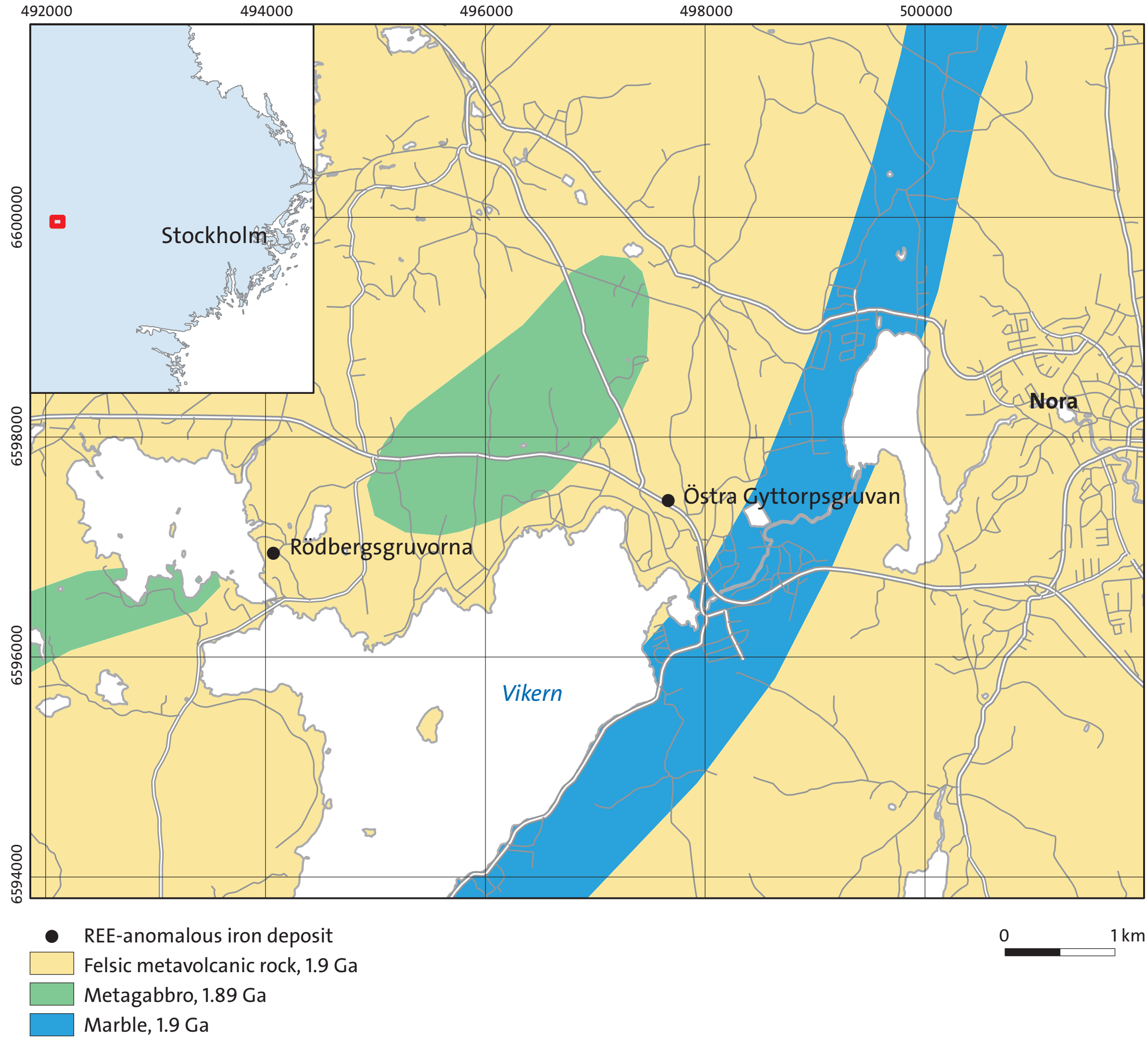

Figure 61. Simplified bedrock geology map showing locations of known REE mineralisations in the Nora area, in the southwestern part of the REE line.

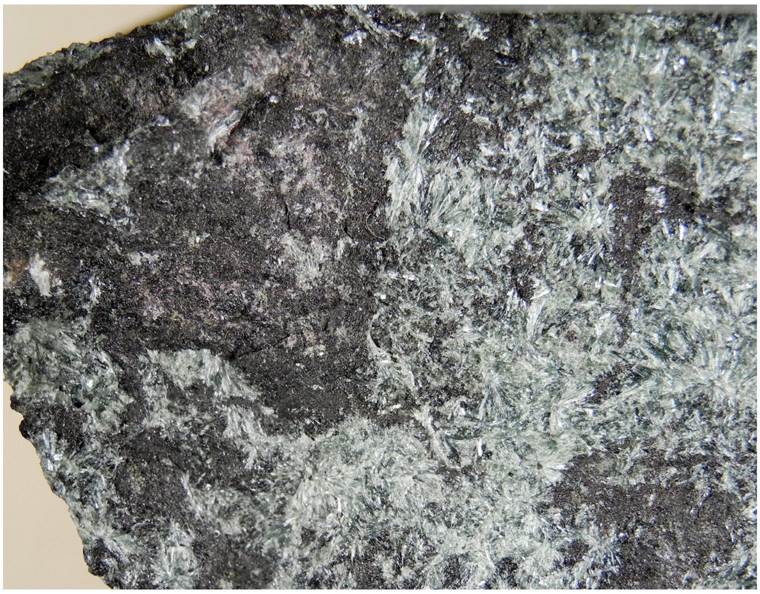

Figure 62. REE mineralisation at Rödbergsgruvorna: zoned veinlets of lighter, slightly pinkish-red cerite-(Ce) rimmed by black ferriallanite-(Ce), in a light green amphibole skarn. Photo: Per Nysten.

The Östra Gyttorp mine

Although neither Geijer (1921c) nor Holtstam et al. (2014) classifies it among the Bastnäs type deposits, the REE mineralisation at the Östra Gyttorp mine (Fig. 61) certainly shows both spatial and mineralogical/geological and geochemical relationships to those occurrences. REE mineralisation occurs here in the form of fine-grained allanite-(Ce)-dominated lenses associated with magnetite ore and modest amounts of skarn, hosted by felsic metavolcanic rocks (Sahlström et al. 2014, Sahlström 2014, Nordenström 1890).

The Östra Gyttorp deposit is a quartz-bearing magnetite ore associated with hornblende, actinolite and biotite. The surrounding metavolcanic host rock is variably altered into a mica-rich assemblage, in particular associated with the iron oxide ore and the allanite pods. Those pods also carry microscopic inclusions of additional REE minerals, including gadolinite-(Y)-hingganite-(Y) solid solution (Sahlström 2014). The REE content has been estimated at 2% in the mica-schist adjacent to the ore (Geijer & Magnusson 1944). The occurrence of molybdenite in the Östra Gyttorp mineralisation is also notable.

During mining in the late 1800s, approximately 100 tonnes of "allanite"-dominated rare earth ore were separated and sold, in addition to the iron ore (Tegengren 1924).

The Norberg district

The major occurrences of Bastnäs-type REE mineralisation in the area in and around the town of Norberg (Fig. 63) are the Östanmossa (Östanmossagruvan), Malmkärra (*Malmkärragruvan*), Johanna (*Johannagruvan*), Ås (Åsgruvan) and Södra Hackspik (*Södra Hackspikgruvan*) mines, all of which are magnetite-dominated skarn iron ore deposits. Since they are somewhat more enriched in HREE versus LREE than the deposits in the centre and southwest of the REE line, the Norberg deposits are classified as belonging to subtype 2 of the Bastnäs-type deposits (cf. above; Holtstam & Andersson 2007, Holtstam et al. 2014).

Silicates are the main hosts of REE in all these deposits, typically with the allanite-related minerals dollaseite-(Ce)–dissakisite-(Ce) as well as fluorbritholite-(Ce) as major phases. REE fluorocarbonates seem to occur in smaller total amounts. In contrast to the extensively polymetallic, sulphide-rich nature of the Nya Bastnäs mines in particular, featuring Bi, Co, Au, Mo etc., the REE-enriched mineralisations in the Norberg area are characteristically poor in those metals.

The relative abundance of fluorine in the Norberg area deposits is manifested by the common occurrence of humite-group minerals, including the eponymous norbergite [$Mg_3(SiO_4)(F,OH)_2$]. These minerals occur intimately with REE mineralisation, as at the type locality for norbergite, the Östanmossa mine (Geijer 1927, 1936), and at the Johanna mine. The (former) presence of humite-group minerals is also indicated by the common occurrence in these deposits of "ophicalcite"; an evenly fine-grained, often dolomitic carbonate rock containing pseudomorphs of humite-minerals, now mainly consisting of (dark) serpentine (*sensu lato*). A new mineral recently discovered in the Bastnäs-type deposits is gadolinite-(Nd) (Holtstam & Andersson 2007; Skoda et al. 2016, 2018), occurring mainly in the Norberg area (Malmkärra and Johanna mines), but also noted at Bastnäs. The optical appearance of the greenish gadolinite-(Nd) may have led to it being misidentified as törnebohmite-(Ce) in earlier studies.

Major REE minerals in the Norberg area

Dissakisite-(Ce) and dollaseite-(Ce) also belong to the allanite group (of the epidote supergroup) of minerals, and form a solid solution involving OH–F substitution. Exchange vectors involving Mg-Fe towards allanite *sensu stricto* also exist (Holtstam & Andersson 2007). Dollaseite-(Ce) is a major REE carrier in the Norberg area (cf. Johanna and Östanmossa mines, below), and was originally described from Östanmossa under the name "magnesium orthite" by Geijer (1927), and much later renamed

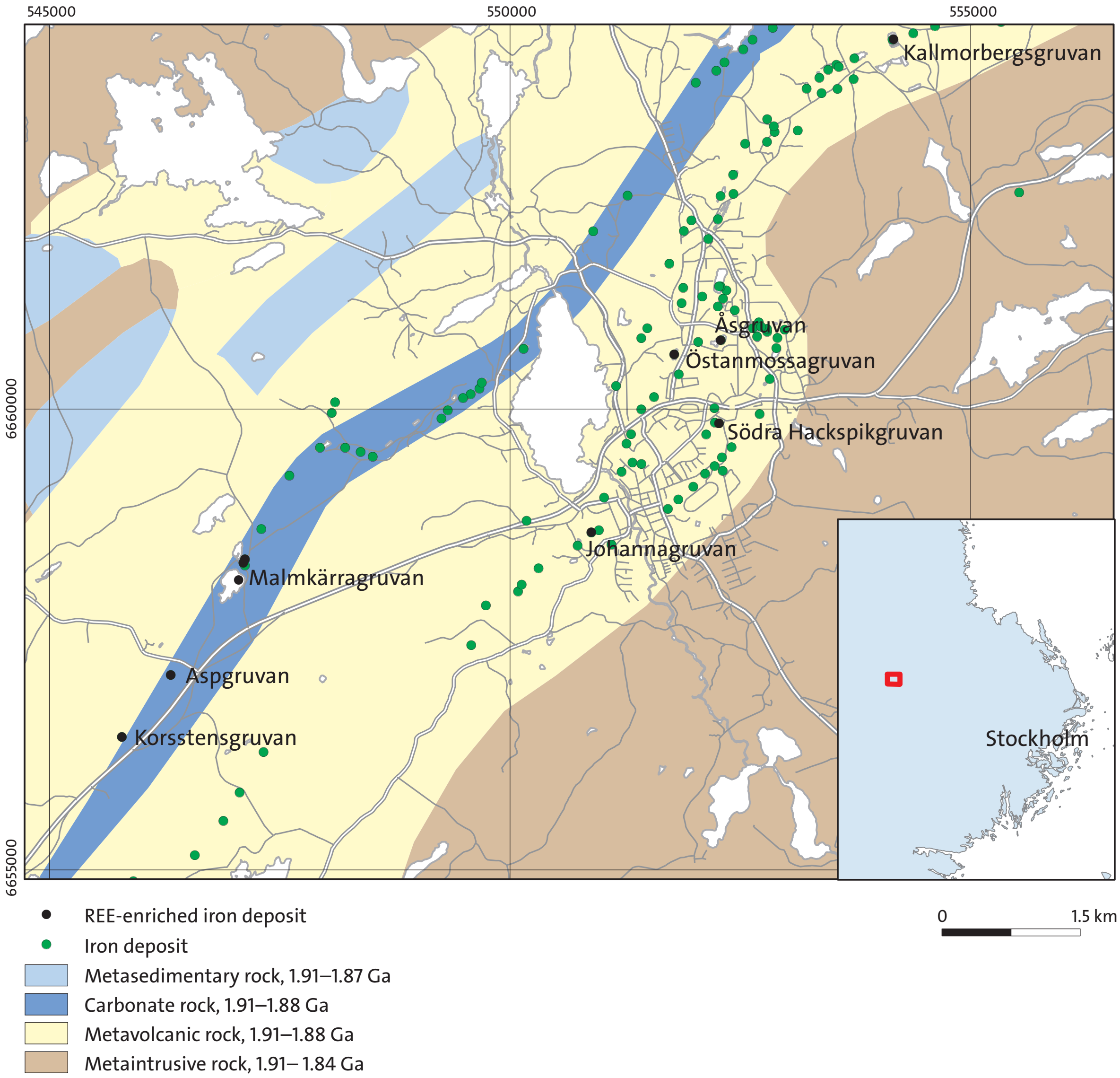

Figure 63. Simplified bedrock geology map showing locations of mines in the Norberg area, northeastern part of the REE line, highlighting those with known REE mineralisation.

"dollaseite" by Peacor & Dunn (1988). Typically, dollaseite (-dissakisite) occurs as relatively fine- to medium-grained masses, lumps and bands or schlieren, which may also be visibly deformed and folded (e.g. at Johanna; Fig 64), but it may also occur locally as radiating fans of twinned, elongated crystals, as well as stouter, larger, sometimes subhedral to euhedral crystals (to nearly 1 cm; e.g. at Östanmossa). The texture of the finer-grained bands and masses of dollaseite is typically recrystallised, presumably as a result of (Svecokarelian) regional metamorphism, as also indicated by the folding observed of the carbonate-Mg skarn-hosted bands or schlieren. Zoned dollaseite-dissakisite crystals occur at Östanmossa, while a mineral with a composition similar to dissakisite-(Ce) was also reported from the Södra Hackspiksgruvan mine, where it occurred as aggregates up to 4 mm in a rock composed of fluorite and fluorine-bearing phlogopite; accessory phases are magnetite and molybdenite (Holtstam & Andersson 2007).

Figure 64. Hand specimen image of a sawn and lightly polished slab showing deformed, partly folded and recrystallised bands of fine-grained REE silicate - fluorocarbonate mineralisation, dominated by dollaseite-(Ce), in a palest green amphibole-riddled (skarn-altered) dolomitic marble. Heavy black lines in the scale bar in the upper right part of the image are cm markings; fine lines represent millimetres. Johanna mine (6658660/550883), Norberg area. Photo: Per Nysten.

Fluorbritholite-(Ce) is locally important, particularly at Malmkärra, where it has been found in lumps weighing several kilograms, intimately associated with västmanlandite-(Ce), dollaseite-(Ce), gadolinite minerals, amphibole, dolomite, phlogopite, magnetite and pyrite (Holtstam & Andersson 2007). It has also been identified from the Södra Hackspik and Östanmossa mines; interestingly, fluorbritholite-(Y) has also been found in one sample from the latter deposit, where it occurs in a later skarn-dolomite vein cross-cutting a dollaseite-bearing amphibole skarn (Holtstam & Andersson 2007).

Gadolinite-group minerals are found in the Malmkärra, Johanna and Östanmossa mines. At the first-mentioned locality it may occur as fine-grained masses within an assemblage of fluorbritholite-(Ce), västmanlandite-(Ce) and dollaseite-(Ce), whereas in a tremolite-magnetite skarn carrying dissakisite-(Ce) and fluorbritholite-(Ce), gadolinite-(Nd) occurs as inclusions within dissakisite (Holtstam & Andersson 2007). The new mineral gadolinite-(Nd) has so far been identified in material from the Malmkärra and Johanna mines (Škoda et al. 2016, 2018; Holtstam & Andersson 2007). Gadolinite-(Y) is also found at the Östanmossa, Malmkärra and Johanna mines, often occurring as chemically zoned crystals with variable proportions of the predominant rare earth elements, Ce, Nd or Y (cf. Holtstam & Andersson 2007). It seems likely that the early observations of abundant törnebohmite at the Malmkärra mine (by Geijer 1936, which were not verified later (cf. Holtstam & Andersson 2007), might be due to a misidentification of what was in fact gadolinite-(Nd), which also exhibits a greenish colour in transmitted light.

Västmanlandite-(Ce) is found mainly in the Norberg area (subtype 2 of Holtstam & Andersson 2007), in which it occurs most abundantly at the type locality – the Malmkärra mine (Holtstam et al. 2005) –where it (at least locally) is one of the major REE hosts in the skarn. Here, the västmanlandite occurs as small, mostly anhedral grains associated with dollaseite-(Ce), fluorbritholite-(Ce), tremolite, dolomite and magnetite (Holtstam et al. 2005, Holtstam & Andersson 2007). Texturally, the relationships between fluorbritholite and västmanlandite seem to mimic the characteristic relationships between cerite and ferriallanite in Bastnäs, where the latter minerals rim and seem to replace the former (e.g. Holtstam & Andersson 2007). Västmanlandite-(Ce) could potentially also occur in the Knutsbo area, while its purported, fluorine-free iron analogue (as yet not fully characterised and hence unnamed) seems confined to localities of subtype 1 (see above; Holtstam & Andersson 2007, Jonsson & Högdahl 2013).

Cerite-(Ce) occurs only sparsely in the Norberg area, and it is likely that a number of early observations of "cerite" in these localities (e.g. Geijer 1927) were in fact of fluorbritholite-(Ce), hand specimens of which look rather similar. At the Johanna mine, cerite-(Ce) occurs in a texture similar to Nya Bastnäs, but with the cerite-(Ce) rimmed by mainly dollaseite-(Ce). Here, the cerite can also occur intergrown with bastnäsite-(La) (Holtstam & Andersson 2007).

In contrast to the deposits of subtype 1, and specifically the Nya Bastnäs field, bastnäsite-(Ce) (or –(La)) occurs only sparsely in the subtype 2 deposits of the Norberg area, except in the Södra Hackspik mine, where larger aggregates (up to approximately 2 cm) were found (Holtstam & Andersson 2007).

Magnesiorowlandite-(Y) was reported by Holtstam et al. (2007, 2014) from the Malmkärra mine.

The calcium-bearing REE fluorocarbonate parisite-(Ce) occurs together with a similar mineral with lower Ca and F content in the Östanmossa mine, where it partly replaces an yttrium-dominant fluorbritholite mineral, and is also disseminated in a magnetite-REE silicate-bearing carbonate aggregate (Holtstam & Andersson 2007). Törnebohmite-(Ce) was reported by Geijer (1936) to have occurred in significant amounts at the now inaccessible Södra Hackspik mine.

A chlorine-bearing REE silicate occurs at Malmkärra (Holtstam & Andersson 2007), and was recently described as the new mineral ulfanderssonite-(Ce) (Holtstam et al. 2017b). It occurs as relatively rich, fine-grained, granular aggregates associated with, among others, västmanlandite-(Ce), bastnäsite-(Ce), phlogopite and talc in the (type locality) Malmkärra mine dump material, but has also been identified previously in much smaller amounts in samples from Nya Bastnäs, in the central part of the REE line (Sahlström 2014, Holtstam et al. 2017b, R. Škoda, personal communication).

Malmkärra

The Malmkärra mines (Fig. 63) operated on magnetite skarn deposits occurring within a narrow layer of dolomitic marble, conformable with the surrounding metavolcanic rocks. The latter vary from moderately altered (in the west), to strongly altered to a cordierite-bearing schist in a zone next to the skarn-ore bodies (to the east). Local faulting has separated the ore into separate bodies. Between 1874 and 1936 a total of 145,000 tonnes of iron ore was mined at Malmkärra (Geijer & Magnusson 1944).

REE mineralisation, mainly in the form of fluorbritholite-(Ce), västmanlandite-(Ce) as well as REE fluorocarbonates and gadolinites (Holtstam & Andersson 2007, Andersson 2004), occurs in a skarn unit consisting mainly of clinoamphibole and humite minerals, in that marble at the contact towards cordierite schists. "Ophicalcite" with serpentine-altered chondrodite is common within the marble. Local concentrations of uranium (<1 wt%), as measured by hand-held XRF, also occur. This U-mineralisation is also associated with increased REE content (M. Leijd, personal communication). According to Geijer (1927), a rich band of REE silicates was found at the 205 m level in the Lill-gruve ore body, in a transitional zone from skarn ore to carbonate rock. Those REE silicates most likely correspond to the rich material found in more recent times on the old mine dumps and consist of several intergrown REE rich minerals, including fluorbritholite-(Ce) and västmanlandite-(Ce) (Holtstam & Andersson 2007).

Korsstensgruvan and Aspgruvan

The two small magnetite-actinolite skarn mines Aspgruvan and Korsstensgruvan are situated in the southwestern extension from the Malmkärra mines, between Fagersta and Norberg (Fig. 63). These skarn ores are hosted by marble in contact with felsic metavolcanic rock, partly displaying a volcaniclastic texture. The skarn consists mainly of actinolite and chondrodite (Geijer & Magnusson 1944). Polarised light microscopy of samples from Korsstensgruvan shows a poor to semi-compact magnetite ore in which magnetite forms aggregates cut by fractures. Magnetite also forms elongated grains, with the central parts carrying many inclusions of silicates in a lamellar orientation. Tremolitic amphibole and diopsidic pyroxene have also been noted. Diffuse aggregates of an unspecified allanite-type mineral occur at the contact between magnetite and amphibole. Additionally, such “allanite”, and to some extent also epidote, occur disseminated, locally rather abundantly, in the silicate groundmass. Chemical analyses of samples taken during the present project from the dumps at Korsstensgruvan yield total REE contents of 1000–5000 ppm, and from Aspgruvan 350–1600 ppm.

Johannagruvan

At the Johanna mine, situated near the southern outskirts of Norberg (Fig. 62), magnetite mineralisation in a dolomitic carbonate rock (marble) occurs associated with a pale greenish tremolitic skarn with local “ophicalcite” pods (Geijer 1936), and associated REE mineralisation, predominantly in the form of veins, bands or schlieren of dollaseite-(Ce) associated with sparse cerite-(Ce), REE carbonates and gadolinite-group minerals (Fig. 64). The REE minerals are typically fine-grained, show textures suggesting pervasive recrystallisation, and ductile deformation, including folding of the bands. Humite-group minerals, probably norbergite, also occur as coarse, subhedral crystals included in the bands or schlieren of REE silicates, predominantly comprising dollaseite-(Ce). In thin section the dollaseite is seen as pinkish-brown to greenish anhedral aggregates in the form of coarse-grained pods in tremolite skarn. Iron oxides are present as bands of platy hematite associated with large subhedral to euhedral magnetite. Bands rich in euhedral magnetite alternate with bands rich in platy hematite. Hematite with small remnants of magnetite suggests oxidation (martitisation).

The Östanmossa mine

The Östanmossa mine (Fig. 63) was worked on a magnetite-skarn mineralisation associated with carbonate rocks, similar to that at Åsgruvan (below), but featuring significantly more abundant REE mineralisation, mainly in the form of dollaseite-(dissakisite)-(Ce) and fluorbritholite-(Ce), characteristically associated with norbergite. The largest concentration of REE silicates (mainly dollaseite-(Ce)) was found in the drift “Grodorten” at the 47 m level, where it occurred with tremolite and dolomite in a zone up to 20 m wide (Geijer 1936). The skarn consists of garnet, diopside, actinolite, as well as tremolite, which are associated with phlogopite and humite minerals. The carbonate rocks consist of both a fine-grained dolomite and a more coarse-grained calcite marble. The former in particular exhibits “ophicalcite” texture, with altered humite-mineral spots.

The maximum depth of the mine was 115 m and a total production of 78,000 tonnes of Fe metal was obtained (Geijer & Magnusson 1944).

Åsgruvan (the **Ås mine**)

Åsgruvan (Fig. 63), is another marble-hosted magnetite skarn deposit, which in this case carries only sparse known REE mineralisation, mainly as “magnesiumortit” (of Geijer 1936; presumably dollaseite). As at Östanmossa, the carbonates occur both as dolomite and calcite marble. Dollaseite-like minerals were found at various places at the 130 m level in calcite marble and calcitic magnetite ore, in pods up to 20 cm in size. At one place the dollaseite-like mineral was associated with chondrodite, tremolite, and as microscopic grains, possibly fluorbritholite (Geijer 1936). That author also notes another association, in the form of an up to 15-cm-thick and 5-m-long, dark band, of probable dollaseite within calcite marble, which was associated with magnetite, tremolite, serpentine (*sensu lato*), and fluorite. Dollaseite-like minerals were also found as disseminated small grains within the actinolite skarn ore (Geijer 1936).

The Södra Hackspik mine

The Södra Hackspik mine (Fig. 63) is (was) also a skarn iron ore, within the Smörberget field, with magnetite associated with a very pale tremolite, fluorite, minor norbergite and REE minerals, described by Geijer (1936). The locality later disappeared, most likely during building projects. Specimens found at the dumps in former times consisted of biotite/phlogopite, deep violet fluorite, and rich mineralisation of molybdenite associated with at least one ten-centimetre-sized pod of törnebohmite, as well as relatively rich bastnäsite-(Ce). Overall, the Södra Hackspik mineralisation, with its fluorine-rich skarn and locally REE-rich assemblages with cerite-(Ce), törnebohmite-(Ce), dissakisite-(Ce), dollaseite-(Ce), bastnäsite-(Ce and La), and fluorbritholite-(Ce) (Holtstam & Andersson 2007; Geijer, 1936), appears to stand out significantly among the other occurrences in the Norberg area.

Additionally, local skarn assemblages of this type, chiefly bearing REE-enriched epidote, allanite and/or dollaseite/dissakisite-like minerals have also been encountered at several other mines in the Norberg area, such as Kallmorberg (e.g. Holmqvist 1975) and, as noted above, at the Stripåsen copper mines (Geijer 1936, 1961). As with the Riddarhyttan area, we find it likely that such minerals may also have escaped observation in other mineralisations, not least due to their often fine-grained and generally unobtrusive nature, and because REE were not included in analyses routinely performed during the mining and exploration heyday in these districts.

The Knutsbo district

The deposits in the neighbourhood of Knutsbo (Knutsbogruvorna, i.e. the Knutsbo mines) are likely to represent the northeasternmost continuation of the REE line (cf. also Geijer & Magnusson 1944), since they are REE-enriched, and predominantly (at least locally) consist of minerals similar to the skarns of Bastnäs type, while being located significantly further to the east, seemingly forming an offset part of this belt (Fig. 46). However, the Knutsbo area mineralisations are primarily interpreted to be hosted by mafic rocks (Fig. 65), which is in stark contrast to the ones of the REE line. Yet, observations in the mine dumps by Asklund (1946) and others indicate that the immediate host rock(s) at Knutsbogruvorna may be variably altered (grading into mica schists, similar to the Riddarhyttan area) felsic metavolcanic rocks.

The seemingly small iron mineralisations in the Knutsbo area were test-mined during the First World War (1914–1918), but according to Geijer & Magnusson (1944), no data are available on the quantities produced. Danielsgruvan and Haggruvan were noted for their REE content, with "magnesiumortit" (dollaseite-(Ce)?) and törnebohmite, for example, having been described from a talc-bearing amphibole skarn in the mine dumps (Geijer & Magnusson 1944, Asklund 1946, Geijer 1961). Recent sampling in the Knutsbo area during the present project, and subsequent studies, confirmed the occurrence of REE mineralisation at these localities. Major REE hosts here are dollaseite-allanite-like minerals.

It is notable that (unspecified) allanites have also been observed in several old (iron) mines to the north of the Knutsbo area. Among these are the Sjögruvan mine, located near the shore of lake Bäsingen, and an iron mine near the Bäsinge copper mine (e.g. Asklund 1946).

The Knutsbo mines

Three ore types were sampled from the mixed dumps at the Knutsbo mines proper, and of these, a dark amphibole skarn proved to contain abundant subhedral dollaseite-allanite. In thin section these are pale brown to colourless single crystals and aggregates of crystals locally showing twinning. Pyrite, chalcopyrite and magnetite occur in this skarn. Also observed was a uniaxial, optically positive, colourless mineral. This is probably either cerite-(Ce) or fluorbritholite-(Ce).

The Gruvhagen mines

Two minor skarn iron ore deposits are located at Gruvhagen, immediately southwest of Knutsbo (Fig. 65), and a porous/drusy calcite-bearing amphibole skarn was sampled here. This skarn is cut by a coarse vein, several mm thick, consisting of intergrown magnetite and dollaseite-like/allanite group mineral, together with minor amphibole. The REE silicates are brown to green pleochroic in thin section, and in part form radial aggregates. No REE-bearing minerals were observed outside this vein.

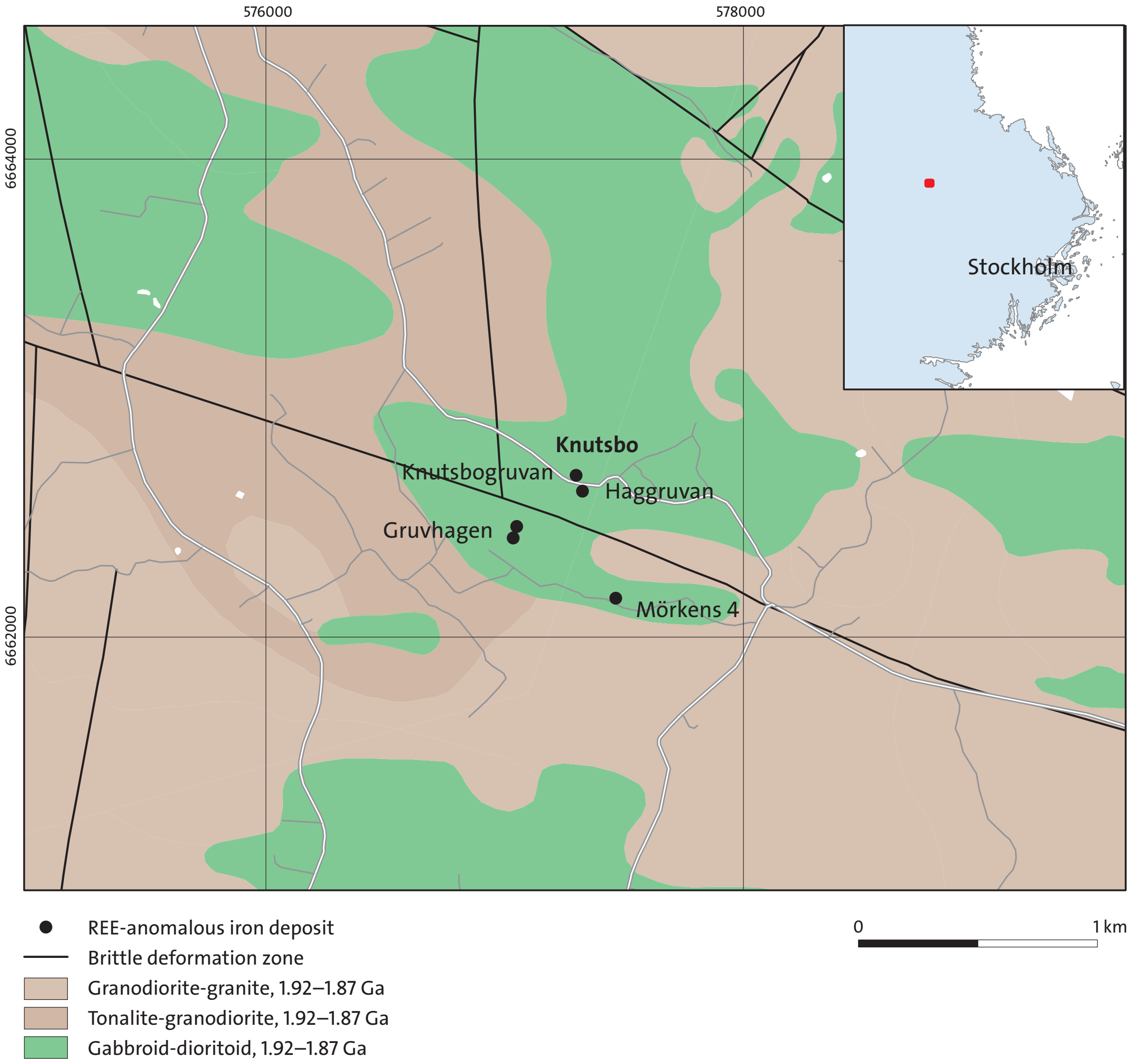

Figure 65. Simplified bedrock geology map showing locations of mines with REE mineralisation in the Knutsbo area, northeasternmost part of the REE line.

The drusy parts of the skarn contain euhedral amphibole as well as calcite crystals up to 5 mm in size. Local magnetite concentrations are found in association with calcite, although hematite is by far the commonest oxide present. No sulphides have been observed.

Mörkens # 4

This is a very small prospect for copper and to some extent also cobalt, within a tremolite-talc-quartz skarn. Since this deposit is located within a shear zone, the nature of the host rocks is somewhat uncertain. A granodioritic, in part strongly sheared rock, alternates with a fine-grained felsic meta-volcanic component. Mafic plutonic rocks are also present further away from the deposit. In a tremolitic skarn poor in oxides, a colourless to greyish-green, anhedral phase, possibly dollaseite or a similar allanite group mineral, is the predominant REE host. It is biaxial negative with a large 2V and exhibits low interference colours. It is locally intergrown with another dollaseite-like mineral, as well as minor amounts of a strongly pleochroic phase (displaying green to dark brown colours), likely to be allanite

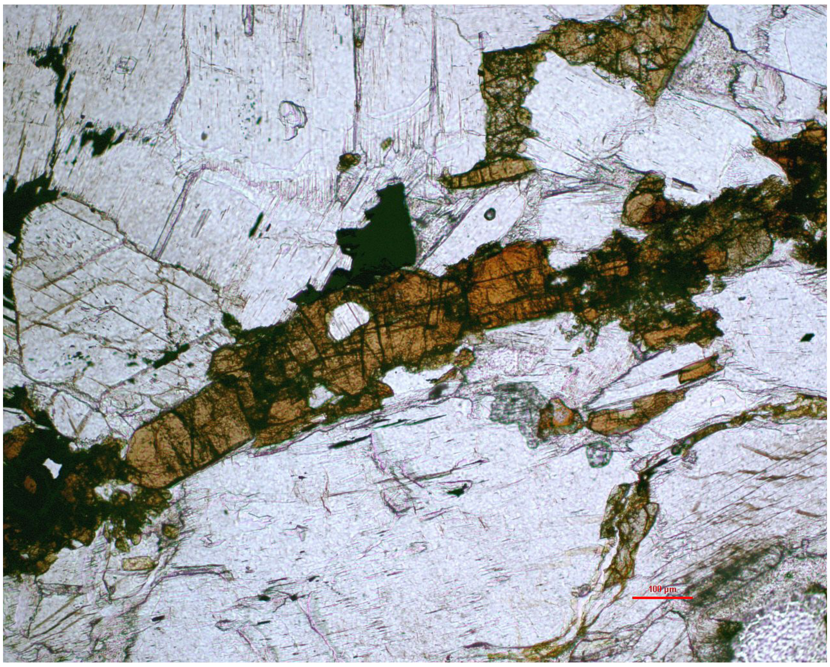

Figure 66. Brown, allanite-like mineral as subhedral crystals or fissure-fillings in skarn at Mörkens #4, Knutsbo area. Photomicrograph in transmitted plane-polarised light. The scale bar equals 100 micrometres. Photo: Per Nysten.

(or possibly västmanlandite). A network of REE minerals occurs in a more quartz-rich rock with disseminated chalcopyrite and altered pyrrhotite. EDS analyses performed by Mattsson (2016) suggest törnebohmite and västmanlandite compositions. Cataclastic zones are also present as well as cross-cutting veinlets with a wavy (folded?) appearance, filled by a dark brown allanite-like phase (Fig. 66). Minor amounts of brown REE minerals are also dispersed in the host rock to these veins.

In a coarse-grained tremolitic skarn with relatively rich disseminations of chalcopyrite and minor altered pyrrhotite, a colourless dollaseite-like mineral, forming partly twinned aggregates up to 5 mm in size occurs. Locally, a brown-pleochroic REE mineral is seen as rims around the colourless mineral, indicating overgrowth or replacement. This texture is clearly reminiscent of the characteristic relationship between ferriallanite and cerite at Nya Bastnäs. The latter mineral is also found forming crystals devoid of the colourless mineral. Mattsson (2016) suggests that these represent dollaseite-(Ce) and a västmanlandite-like mineral. Both REE phases occur intimately intergrown with chalcopyrite.

The REE line – concluding remarks

Despite the modest (where at all known) volumes and high proportions of the LREE in individual Bastnäs-type deposits, their locally (very) high grades and extended regional distribution along the 100 km+ REE line suggest some relevant exploration potential, not least when considered together with other potential ore metals (iron, cobalt, molybdenum, gold etc., which are in part typically associated with these REE-rich skarns, best exemplified at Nya Bastnäs). Several new observations of both "Bastnäs-like" (type) REE mineralisation, and REE enrichment without the presence of characteristic skarn assemblages, certainly point to a wider distribution of REE than earlier known or anticipated within the REE line, not least in the greater Riddarhyttan area, and mineralisations south and north of it.

A potential problem for the beneficiation of these deposits is their mineralogical complexity. But in most cases a few REE-rich silicate minerals (e.g., cerite-(Ce), dollaseite-(Ce), ferriallanite-(Ce), fluorbritholite-(Ce)) tend to predominate in any individual deposit, a feature that might make it easier to exploit them. In order to evaluate this, bulk sampling of megascopically visible REE-mineralised dump material from two contrasting deposits in the REE line was also undertaken under the EURARE project, at Nya Bastnäs (Riddarhyttan), and Johannagruvan (Norberg), for beneficiation tests.

REE mineralisation in other iron oxide deposits

We have only limited information on a number of iron oxide mineralisations showing enrichments in the REEs, not least as to their genesis and relationship with other types of deposits. They range from plainly unknown, via uranium-anomalous iron oxides and Bastnäs-type related mineralisations, to suspected apatite-iron oxide (Kiruna)-type deposits. The link between uranium enrichment and increased REE content is notable in several mines and mining areas in the Bergslagen ore province; we do not know much about the origin of these systems, however. Also, several additional localities such as Klacka–Lerberg and others are known to be significantly enriched in uranium, but nothing is currently known of their potential REE content, since this has not been studied previously, and was not within the scope of the present project.

Recent and earlier studies have also highlighted significantly increased REE content in some of the mined banded iron formations (BIFs), as well as other (non-apatite) iron ores in Bergslagen (Högdahl et al. 2015; Andersson 1972, unpublished report), and we find it likely that further investigation will yield additional discoveries.

It is hoped that future studies may resolve issues of origin and REE mineralogy, and provide new detailed information on some or all of the mineralisations described in this section.

REE-U-enrichment in the Skärhyttefältet iron mines, western Bergslagen

The Skärhyttefältet iron mines (also named "Blankagruvorna", or "Blankagruvan"; Hammergren 1988, unpublished report) near Blankafors, are located in western Bergslagen, 17 km west of Nora (Fig. 67; Blankagruvan). These iron oxide ores occur within mica-rich felsic (Svecofennian) metavolcanic rocks close to the contact of a K-feldspar porphyritic granite belonging to the Transscandinavian Igneous Belt (TIB) (Wiklander & Lundström, 1991; Högdahl et al. 2004).

Reviewing older analyses from the SGU uranium exploration period, Hammergren (1988, unpublished report) reported 4564 ppm of yttrium (associated with high U and marked Th and Zr) in a dump sample from "Blankagruvan"; another sample from nearby "Blankafall" reached 2808 ppm yttrium, also associated with high uranium and marked enrichment in thorium.

Later analytical data of Gustafsson (1991, unpublished report) confirmed that mine dump material consisting of magnetite and chlorite was enriched in Y, Mo, Th and Zr, and had high uranium content. No data were given for the other REEs. The yttrium content was reported as 0.3–0.5 wt%. More recently, dump material has also been found to contain local concentrations of grossular-andradite-actinolite skarn with accessory bismuthinite. It is not known at present whether such other skarn types may have elevated REE contents.

REE-U-enrichment in the Timansberg iron mines, southwestern Bergslagen

The Timansberg iron mines (Fig. 67) are located in southwestern Bergslagen, some 15 km northwest of Nora. The ore mined there was a felsic metavolcanic-hosted, quartz-skarn magnetite ore, characteristically exhibiting fracture network, breccia and other deformation textures (Swedish: "*knottermalm*"; Geijer & Magnusson 1944); the main associated minerals are actinolitic amphiboles and biotite, as well as quartz. Garnet and epidote generally occur more sparsely, while minor chlorite and talc have been observed in biotite-rich lithologies (*sköl* units). The latter typically occurred in the border zone between ore and the variably altered host rocks (Geijer & Magnusson 1944).

Some samples for bulk geochemical analysis, performed during the national uranium exploration programme in the 1970s, were also analysed for yttrium, and eight mine dump samples from Timansberg yielded between 1089 and 10105 (average 3433) ppm yttrium, and a uranium contents of between 100 and 28514 ppm (Hammergren 1988, unpublished report). Notably, no additional REEs were seemingly analysed, not much details can be had from the available report.

Gustafsson (1990, unpublished report) noted that Timansberg is likely to be the most uranium-rich

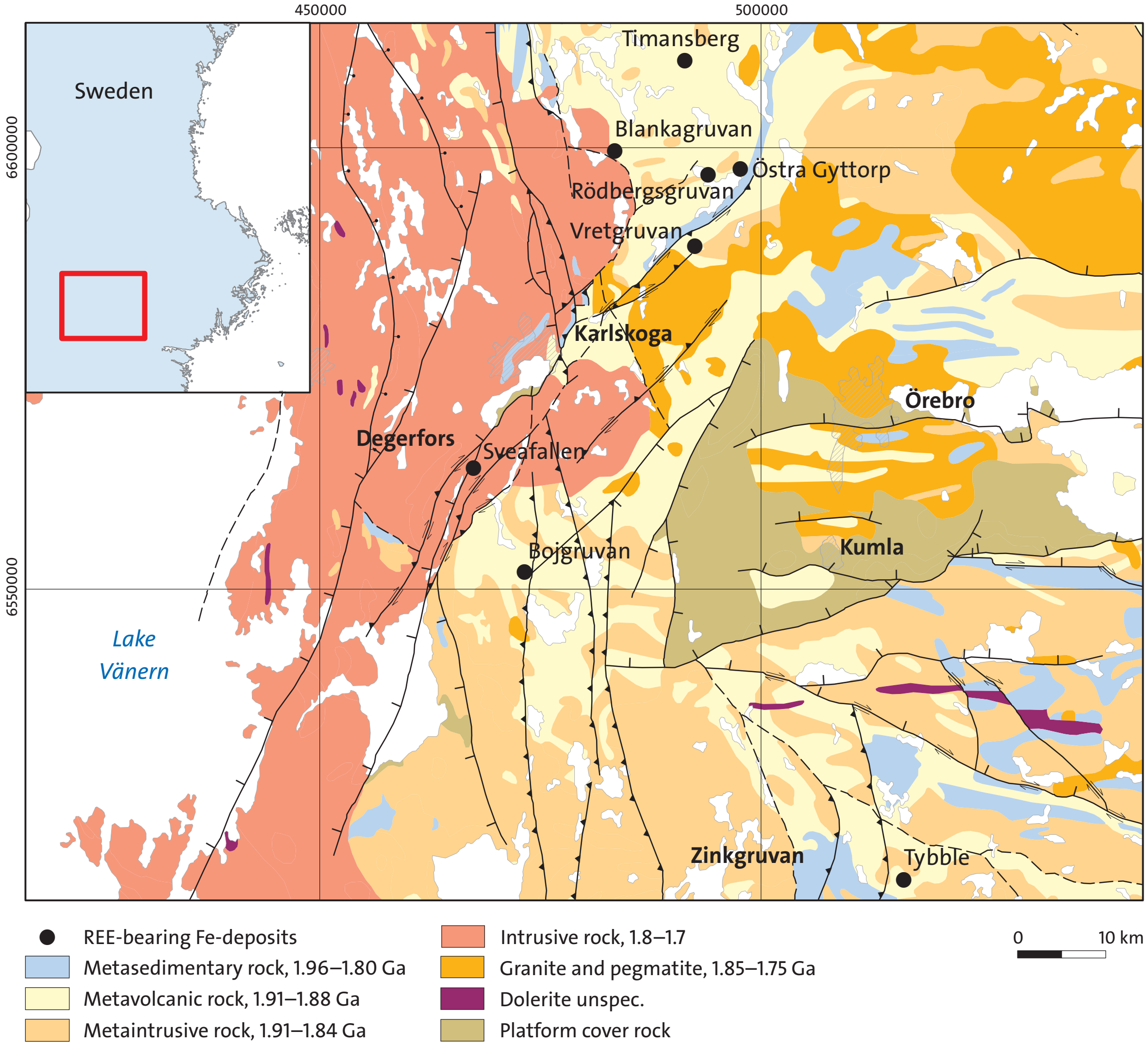

Figure 67. Simplified bedrock geology map showing locations of mines with REE mineralisation in the southwestern to southernmost part of the Bergslagen ore province, including the southwesternmost part of the REE line, and the Zinkgruvan mine for reference.

iron mine in Sweden, with uranium chiefly hosted by "pitchblende"/ uraninite in biotite-amphibole skarn). The secondary uranium mineral uranophane had also been recorded from Timansberg by Löfvendahl (1981). Interestingly, Gustafsson also mentioned briefly that the Timansberg skarn is enriched in beryllium (but without making any further reference to this). He also proposed more extensive sampling and study of the poorly known mineralisations between Timansberg and Blankafors.

The Sveafallen REE-(U-Th)-anomalous iron oxide mineralisation, southwest of Bergslagen

The mineralisation at Sveafallen is located immediately west of Bergslagen proper, southwest of Karlskoga, and close to the northeastern part of lake Vänern (Fig. 67). It consists of two small iron mines situated within a quartz monzonite to granite belonging to the c. 1.8 Ga Filipstad granite suite (Transscandinavian Igneous Belt; TIB; cf. Högdahl et al. 2004). Outcrops of an unaltered type of this rock occur 100 m to the east of the mines, where it is weakly porphyritic, greyish-red to reddish-grey and medium- to coarse-grained. At the actual mines, the granitic host rock appears to have been largely replaced by relatively compact magnetite; the appearance of (remnant?) K-feldspar megacrysts in the massive, fine-grained magnetite is conspicuous (Fig. 68). The water-filled mines are not accessible, but extensive dump material exists close to them. In hand specimen, magnetite and microcline are the predominant minerals.

The potential for REE mineralisation in the vicinity of Sveafallen was first highlighted by Hammergren (1988, unpublished report), due to a significant thorium anomaly. The area was subsequently visited by Gustafsson (1991, unpublished report), who sampled the old mine dumps (and noted that the consistently high radioactivity was due to elevated thorium content in the iron ore). He also found the iron oxide (magnetite) mineralisation to be anomalously high in REEs.

All material sampled during this project is weakly to moderately radioactive (0.1–0.3 mR/h), as measured with a scintillation detector, and gamma spectrometry measurements show high Th and U values (500–800 ppm).

Ore microscopy revealed that ilmenite occurs abundantly as exsolution lamellae in magnetite, while hematite occurs as irregular patches within that magnetite. Sulphides occur as 0.2 mm intergrowths of chalcopyrite and pyrite.

Scanning electron microscopy with EDS analysis shows that the main carrier of REE in this rather exotic mineralisation is a thorium-(uranium)-bearing monazite-(Ce), occurring as abundant, (sub-)rounded inclusions in the ilmenite-bearing massive magnetite ore, chiefly together with also widespread, mostly anhedral zircon (Fig. 69). In some cases, monazite-(Ce) and zircon occur as intergrowths or

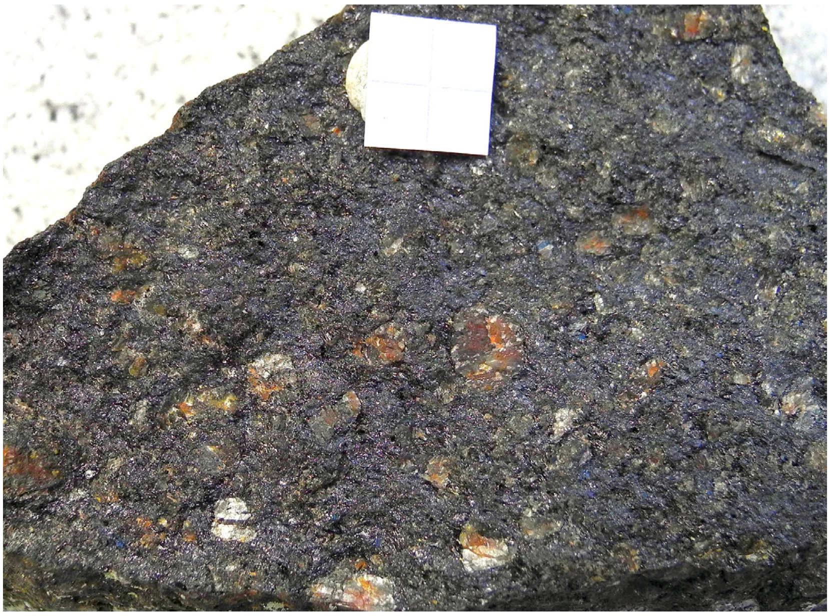

Figure 68. Hand specimen image of a fine-grained magnetite ore with abundant, subrounded feldspar clasts or crystals. The scale bar in the upper part of the image is 2 cm wide. Sveafallen (6563296/467479). Photo: Per Nysten.

composite grains in the magnetite (as can be seen in Fig. 69). As noted in the optical study, ilmenite is abundant, occurring as crystallographically oriented sets of exsolution lamellae within the magnetite, and shows modest manganese content (through pyrophanite solid solution). Subhedral, seemingly in part corroded grains/crystals of a mineral close to cerianite-(Ce) also occurs, which contain a U-Th-bearing monazite-(Ce), together with (a late-stage?) fluorapatite as minute grains or subhedral crystals.

The Sveafallen mineralisation does not correspond to any of the previously known types in the region and is clearly of some fundamental interest.

REE enrichment in the Bojgruvan mine, southwestern Bergslagen

Bojgruvan (the Boj mine) is located in the southern part of the Guldsmedsboda mine field near Svartå, southeast of Degerfors in the far southwest of Bergslagen (Fig. 67). The main hosts are felsic metavolcanic rocks. Little data are currently available on the exact nature of the Boj mine, but iron ores in this part of the Guldsmedsboda field consist of an intermix of magnetite and hematite; typically they are quartz and mica-rich, and carry lesser amounts of pyroxene, amphibole and epidote, and accessory tourmaline, allanite, apatite *sensu lato*, and zircon (Geijer & Magnusson 1944). Veins and dykes of pegmatite and aplite are common. According to Wikström & Karis (1997), the Kärrgruvan mine in the Guldsmedsboda ore field about 1 km south of Bojgruvan consists of mica and quartz-bearing *sköl* ore with minor epidote-clinopyroxene skarn. It is uncertain whether this is identical to Bojgruvan. This ore also contains remnants of cordierite-veined gneiss, as well as of the main host rock.

Within the present project, an iron ore sample from the Bojgruvan mine was subjected to bulk geochemical analysis, which yielded 563 ppm total REE. On the basis of this, polished thin sections were produced, and subjected to optical and scanning electron microscopy with energy-dispersive spectrometric analysis, in order to characterise the REE host minerals in the ore, and their textures. The sample material studied by scanning electron microscopy consists of fairly strongly foliated, magnetite-phyllosilicate rock ("*skölmalm*"), which carries anhedral to subhedral fluorapatite crystals, as well as other minerals (Fig. 70). Magnetite tends to occur in bands. Like many apatite-iron oxide deposits (see above, and Jonsson et al. 2016, and references therein), the apatites often carry variably-sized inclusions of REE phosphates, in the case of Bojgruvan, chiefly monazite-(Ce). The monazites

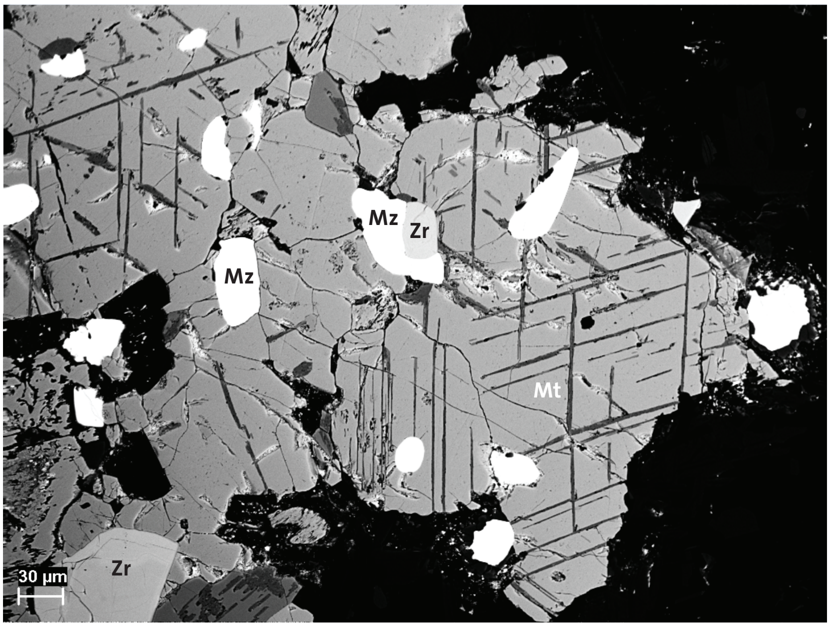

Figure 69. Back-scattered electron (BSE) image of magnetite aggregates (medium grey; Mt) with exsolution lamellae of ilmenite (black, crystallographically oriented) and abundant, subrounded inclusions of monazite-(Ce) (white; Mz) and zircon (light grey; Zr). Silicate minerals are dark grey to black. The scale bar equals 30 micrometres. Sveafallen (6563296/467479). Photo: Erik Jonsson.

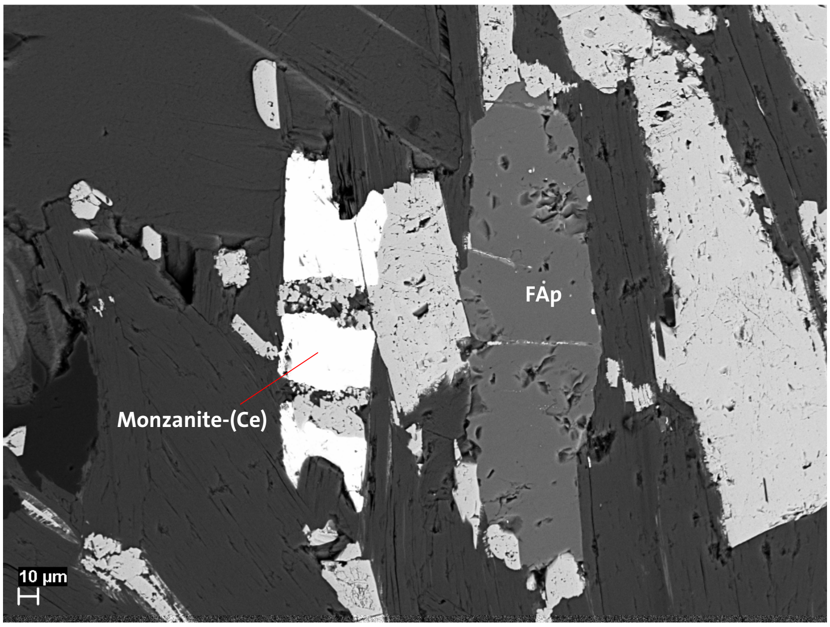

Figure 70. Back-scattered electron (BSE) image showing a silicate-bearing (darkest grey to black) magnetite (lightest grey) ore, with magnetite in part intergrown with blocky monazite-(Ce) (white), fluorapatite (REE-free; medium grey), locally hosting fine-grained fracture fillings and aggregates of REE-bearing phases). The scale bar equals 10 micrometres. Bojgruvan (6551501/473426). Photo: Erik Jonsson.

may in some cases carry small but detectable quantities of thorium. The REE-deficient (or at least below detection limits) fluorapatite, as well as monazite-(Ce) and the more sparsely occurring xenotime-(Y) tend to occur mostly in the silicates, rather than with, or directly associated with, the magnetite. Monazite may occur also as intergrowths, or intimately with magnetite, as can be seen in Fig. 70. Very small inclusions of BSE-white phases occurring as a "dusting" in fluorapatite may indicate fluid-mediated remobilisation of REE from the apatite into later-formed REE phosphates such as monazite and xenotime (cf. Jonsson et al. 2016, and references therein). Sparse barite, and complexly zoned zircons have also been observed. This REE mineralisation was discovered during the Eurare project.

REE enrichment in the U-anomalous Tybble iron mines, southernmost Bergslagen

The Tybble iron mines are located in the southernmost extension of the Bergslagen ore province proper (Fig. 67), approximately 11 km east-southeast of the active Zinkgruvan sulphide mine. This area features mostly relatively strongly metamorphosed and deformed Svecofennian metasupracrustal rocks, including felsic metavolcanic rocks, paragneisses and minor marble, and abundant older and younger granites, the latter belonging to the Transscandinavian Igneous Belt (TIB; Högdahl et al. 2004). The mines themselves occur within felsic metavolcanic rocks, near a marble interlayer, and the sequence is cut by both dioritic and pegmatitic dykes (Geijer & Magnusson 1944).

The magnetite-dominated ore may locally exhibit a diffuse banding, and contains variable amounts of quartz, apatite *sensu lato*, amphibole, micas, sulphides, tourmaline and allanite *sensu lato*; the latter two minerals also occur in the cross-cutting granitic pegmatites (Geijer & Magnusson 1944, Wikström & Karis 1991).

Hammergren (1988, unpublished report) mentioned the dumps at the Tybble iron mine(s) as being anomalously radioactive. Additionally, he noted that minor uranium mineralisations occur in the old "Blackfärdsfältet" mining area, 5.5 km northwest of Tybble, at Ilamgruvan. East of that area, felsic metavolcanic rocks also exhibited marked radioactivity. It was suggested that this is related to an approximately 100-m-long, north–south striking fracture zone. Anomalous radioactivity was also noted at Gruvmon, west of Godegård, and associated with a "uranium-anomalous" gneissic metavolcanic rock with pegmatitic parts between the lakes Skeppsjön and Bredsjön, some 6 km northwest of Tybble. It is not known whether all, or any, of these uranium-anomalous areas are also associated with increased REE content.

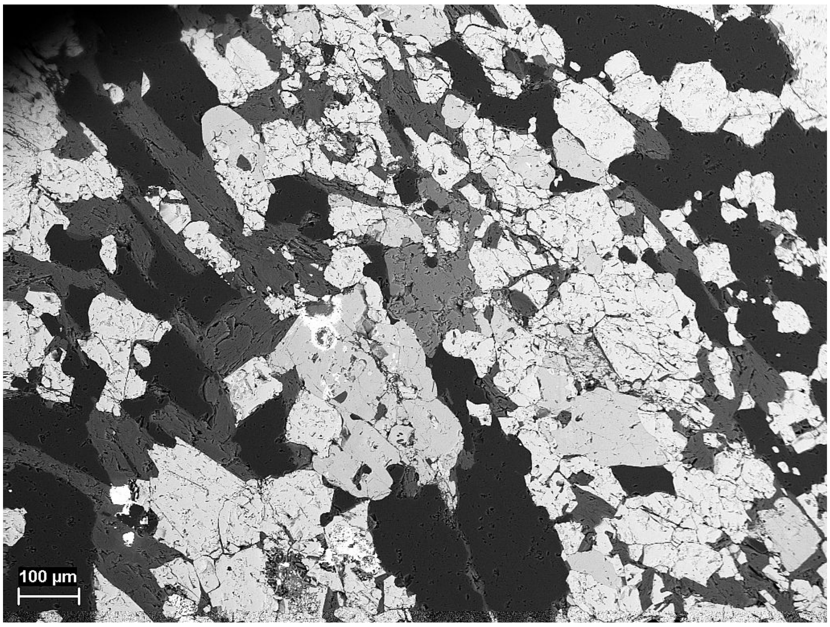

Figure 71. Back-scattered electron (BSE) image showing a silicate-bearing (darkest grey to black) magnetite (lightest grey) ore, with fluorapatite (REE-free; medium grey), locally hosting fine-grained fracture fillings and aggregates of Ca-REE compounds (white, e.g. in an atoll-type texture in the left-central part of the image), and minor allanite-(Ce). The scale bar equals 100 micrometres. Tybble iron mines (6517096/516016). Photo: Erik Jonsson.

Gustafsson (1991, unpublished report) subsequently reported that the iron oxide-mineralised, anomalously radioactive mine dump at Tybble was sampled and yielded increased REE, but that it was "too low to be of potential economic interest". Under the Eurare project, one iron ore sample from Tybble (SGUR10007) was subjected to bulk geochemical analysis, which yielded a very high 17 428 ppm total REE. On the basis of this, a polished thin section was produced, and subjected to optical and scanning electron microscopy with energy-dispersive spectrometric analysis (SEM-EDS), in order to characterise the REE host minerals in the ore. Based on this, rare earth element mineralisation at Tybble is hosted mainly by allanite-(Ce) to REE epidote, sparse monazite-(Ce), fine-grained REE fluorocarbonate(s), and unidentified (heterogeneous) oxidic U-Pb-REE phases, all associated with magnetite, and often REE-free (or at least below detection limits) fluorapatite (Fig. 71). If REE mineralisation and increased content of uranium and/or thorium are linked (as in the material studied from the Tybble mines), a larger area may be of interest for further study, as suggested by Hammergren (1988, above).

REE enrichment in the Gullebo iron mines, southeasternmost Bergslagen

The Gullebo iron mines are located near the southeasternmost extreme of the Bergslagen ore province proper (Fig. 72). Iron oxide mineralisation occurs here in the form of a quartz-biotite-bearing, fine-grained magnetite ore in what has been interpreted to be a fragment of fine-grained, reddish felsic metavolcanic rock, occurring as a mega-xenolith in a Filipstad-type TIB (Transscandinavian Igneous Belt; Högdahl et al. 2004) granite, which also cross-cuts both ore and the proposed metavolcanic rock (Geijer & Magnusson 1944). According to the latter authors, the magnetite ore contained some feldspar, epidote and titanite near the contacts to the cross-cutting dykes, and otherwise becomes sulphide-bearing at depth. Brun et al. (1995) also mentions the occurrence of garnet, coarse-grained hornblende and magnetite in associated amphibole skarn.

An iron ore sample from the Gullebo mines was subjected to bulk geochemical analysis, which yielded 932 ppm total REE. On the basis of this, polished thin sections were produced, and subjected to optical and scanning electron microscopy with energy-dispersive spectrometric (SEM-EDS) analysis, in order to characterise the REE host minerals in the ore, and their textures (Fig. 73). The notable titanium content observed was found to be hosted both by the magnetite and as separate minerals, chiefly ilmenite (in part showing Mn content, i.e. with a pyrophanite-type substitution) and titanite, as well as some

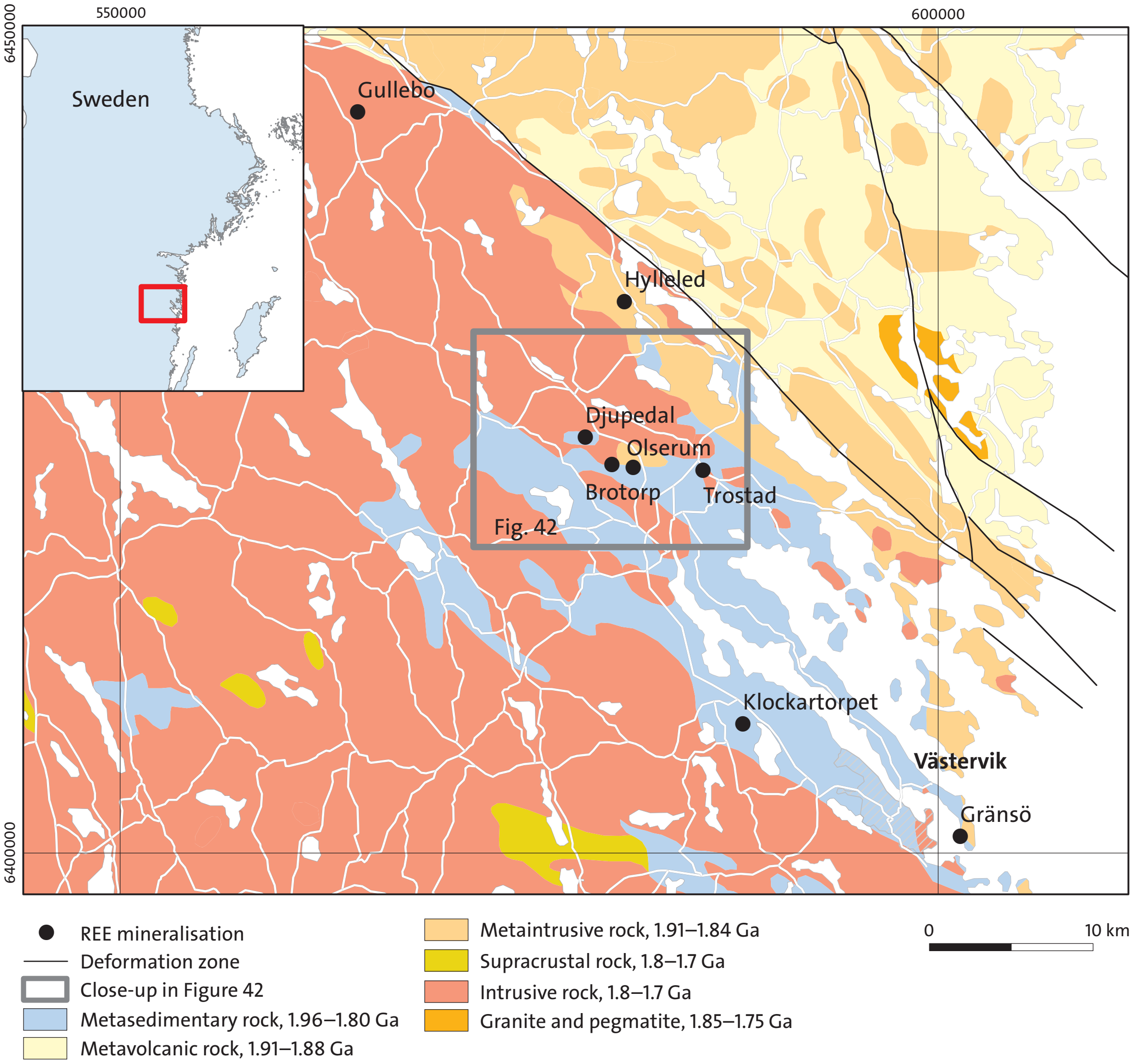

Figure 72. Simplified bedrock geology map showing the locations of the REE-mineralised iron oxide deposits at Gullebo and Hylleled, and their spatial relationship to the mineralisations in the Västervik area (inset rectangle corresponds to Fig. 42 in this chapter).

rutile or anatase. REEs seem to be mainly concentrated in (a?) relatively fine-grained, sometimes distinctly platy or sheaf-like mineral(s), giving the impression of alteration products or pseudomorphs after a primary phase. These are LREE-dominated, with some Y, Ca, F, variable Si, and locally, detectable Th content. Not uncommonly, lensoidal, rounded zircon crystals occur in the ore, among others as inclusions in magnetite. This REE mineralisation was discovered during the Eurare project.

REE enrichment in the Hylleled iron mines, southeasternmost Bergslagen

The Hylleled mines are located at Blidstena in the southeasternmost extension of the Bergslagen ore province proper (cf. Fig. 72). Iron oxide mineralisation occurs here as isolated magnetite-rich bodies associated with amphibolites, as what has been interpreted to be mega-xenoliths in the surrounding granite (Geijer & Magnusson 1944). This granite, the Loftahammar granite, has been variously ascribed to the Svecokarelian intrusions and those of the Transscandinavian Igneous Belt (TIB; Högdahl et al. 2004), with

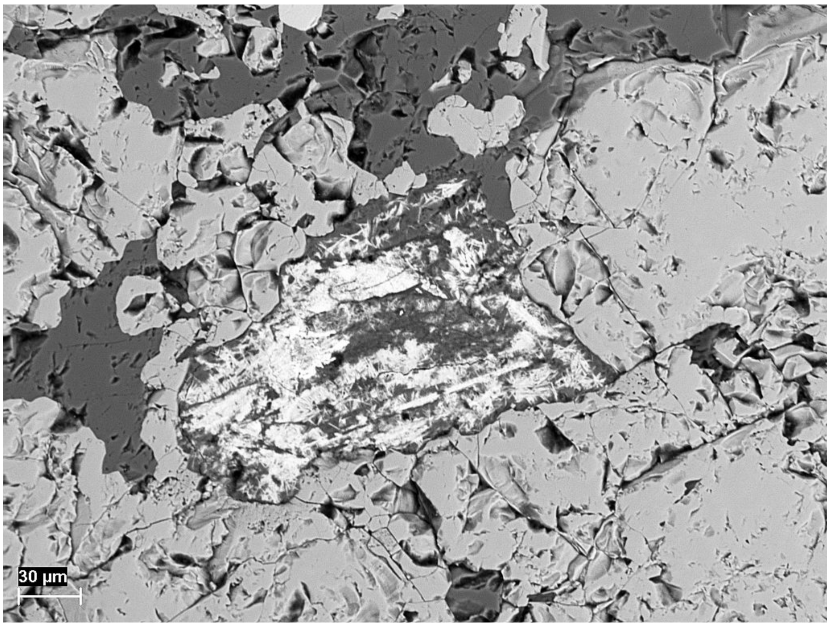

Figure 73. Back-scattered electron (BSE) image showing a heterogeneous aggregate of fine-grained, LREE-bearing silicate and probably fluorocarbonate (both white, centre of image) minerals, in a groundmass of medium grey magnetite and silicates (dark grey). The REE-rich minerals are most likely alteration products, representing a heterogeneous pseudomorph of an unknown primary phase. The scale bar equals 30 micrometres. Gullebo iron mines (6445227/564411). Photo: Erik Jonsson.

variable reported ages, from c. 1.86 to 1.80 Ga, based on U-Pb dating of zircon (cf. Wikström & Andersson 2004, and references therein).

The ore consists of anhedral to subhedral magnetite, mainly associated with quartz, biotitic mica, and amphibole, but locally, such as in the sample studied, also with variable amounts of (Cu-Fe) sulphides.

Within the present project an iron ore sample from Hylleled was subjected to bulk geochemical analysis (SGUR10232), which yielded 1999 ppm total REE. On the basis of this, polished thin sections were produced, and subjected to optical and scanning electron microscopy with energy-dispersive spectrometric analysis (SEM-EDS), in order to characterise the REE host minerals in the ore, and their textures.

Scanning electron microscopy with EDS analysis showed quite commonly occurring anhedral, sometimes slightly equant grains of fluorapatite (REE-free, as detected by this system, sometimes with measurable chlorine content), often at least partially enclosed in magnetite. These carry locally abundant, subhedral, often angular and platy crystals of xenotime-(Y) and monazite-(Ce) (Fig. 74). Texturally, the latter two phosphates seem to occur as epitaxially oriented exsolutions within the apatite. Monazite-(Ce) was also observed outside of apatite grains. Minor cassiterite and several anhedral grains of scheelite were also observed, as was an unidentified, probably oxidic U-Pb-Y-phase.

Based on both the overall mineralogy and textural relationships, this could well represent a previously unrecognised occurrence of an REE-rich apatite-iron oxide mineralisation (cf. Jonsson et al. 2016, and references therein), although this mineralisation differs from most such deposits studied, in that the predominant REE phosphate occurring in the fluorapatite is xenotime-(Y), with a marked content of ytterbium indicated by SEM–EDS. However, the proximity to the Olserum area (south of Hylleled; Fig. 72) may also indicate some link towards the type of REE mineralisation present there (which actually overlaps quite a few of the characteristics of apatite-iron oxide deposits). This REE mineralisation was discovered during the Eurare project.

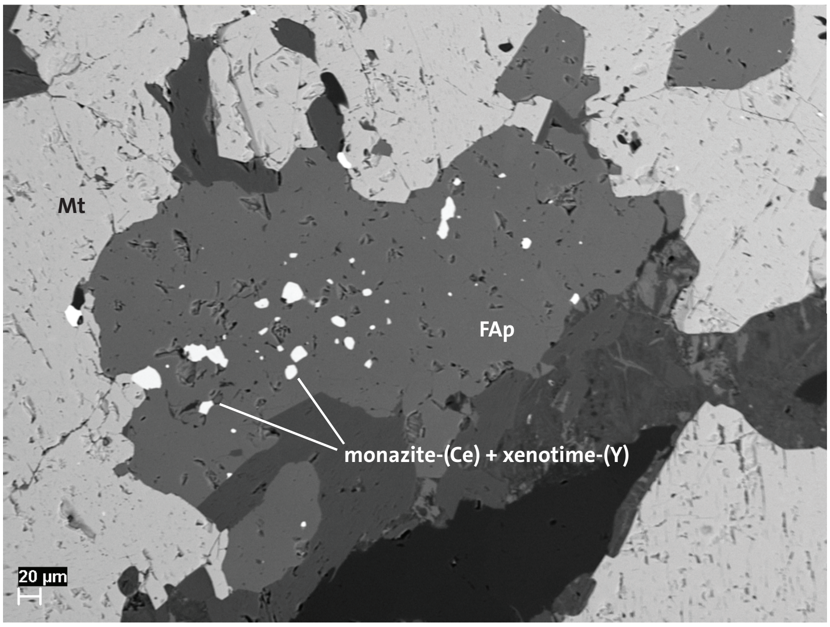

Figure 74. Back-scattered electron (BSE) image showing essentially anhedral fluorapatite (medium grey; FAp) associated with minor silicates (darker grey to black) intergrown in magnetite (lightest grey; Mt). This fluorapatite carries numerous subhedral inclusions of xenotime-(Y) and monazite-(Ce) (both white), texturally very similar to several REE-enriched apatite-iron oxide ores that have been studied. The scale bar equals 20 micrometres. Hylleled iron mines (6433571/580704). Photo: Erik Jonsson.

REE enrichment in the Bäckberg iron mines, northwestern Bergslagen

The Bäckberg iron mines (*Bäckbergsgruvorna*) are located west of Sunnansjö, in the Grangärde–Ludvika area of northwestern Bergslagen (northwest of Ludvika; Fig. 75). Overall, the iron oxide (magnetite) mineralisation is hosted by felsic metavolcanic rocks, but more immediately so by an extensive skarn (pyroxene-garnet-amphibole-epidote) unit, all cross-cut by numerous amphibolitic dykes (Geijer & Magnusson 1944). The ore is fine-grained and locally contains pyrite (Ripa et al. 2015).

An iron ore sample (SGUR10058) from the Bäckberg mines was subjected to bulk geochemical analysis, which yielded 2380 ppm total REE. On the basis of this, polished thin sections were produced, and subjected to optical and scanning electron microscopy with energy-dispersive spectrometric analysis (SEM-EDS), in order to characterise the REE host minerals in the ore, and their textures.

The main host for REE in the material studied is a somewhat low-REE_{tot} allanite-(Ce), chemically trending towards REE-rich epidote, as measured by EDS analysis. These occur as anhedral rounded grains, and more complexly zoned aggregates, sometimes with a radial habit. The chemical zoning, visible in back-scattered electron (BSE) image mode on the scanning electron microscope, is essentially related to variations in REE content (Fig. 76). The REE silicates occur both intergrown with magnetite and isolated in the silicate groundmass. Very small grains of an unidentified U-Pb-rich phase occur scattered in the material. Textural relationships suggest that the REE silicates are coeval with the formation of the bulk of the iron oxide-bearing skarn.

This REE mineralisation was discovered during the Eurare project.

The Bredåsen REE-mineralised polymetallic iron oxide mineralisation, northeastern Bergslagen

The Bredåsen area is situated about 45 km north of Uppsala in the northeastern part of the Bergslagen ore province (Fig. 77). A few minor mines and prospects for magnetite occur here in felsic, weakly banded metaryolite. The bands consist of mica or skarn. The host rock is also partly quartz or feldspar-porphyritic. The metavolcanic rocks are surrounded by granitoids (granite-tonalite). Magnetite associated with pyrite and chalcopyrite occurs in quartz-rich parts of this metavolcanic unit. As observed in available drill cores, the mica-rich parts consist of biotite and/or chlorite. Polarised light microscopy

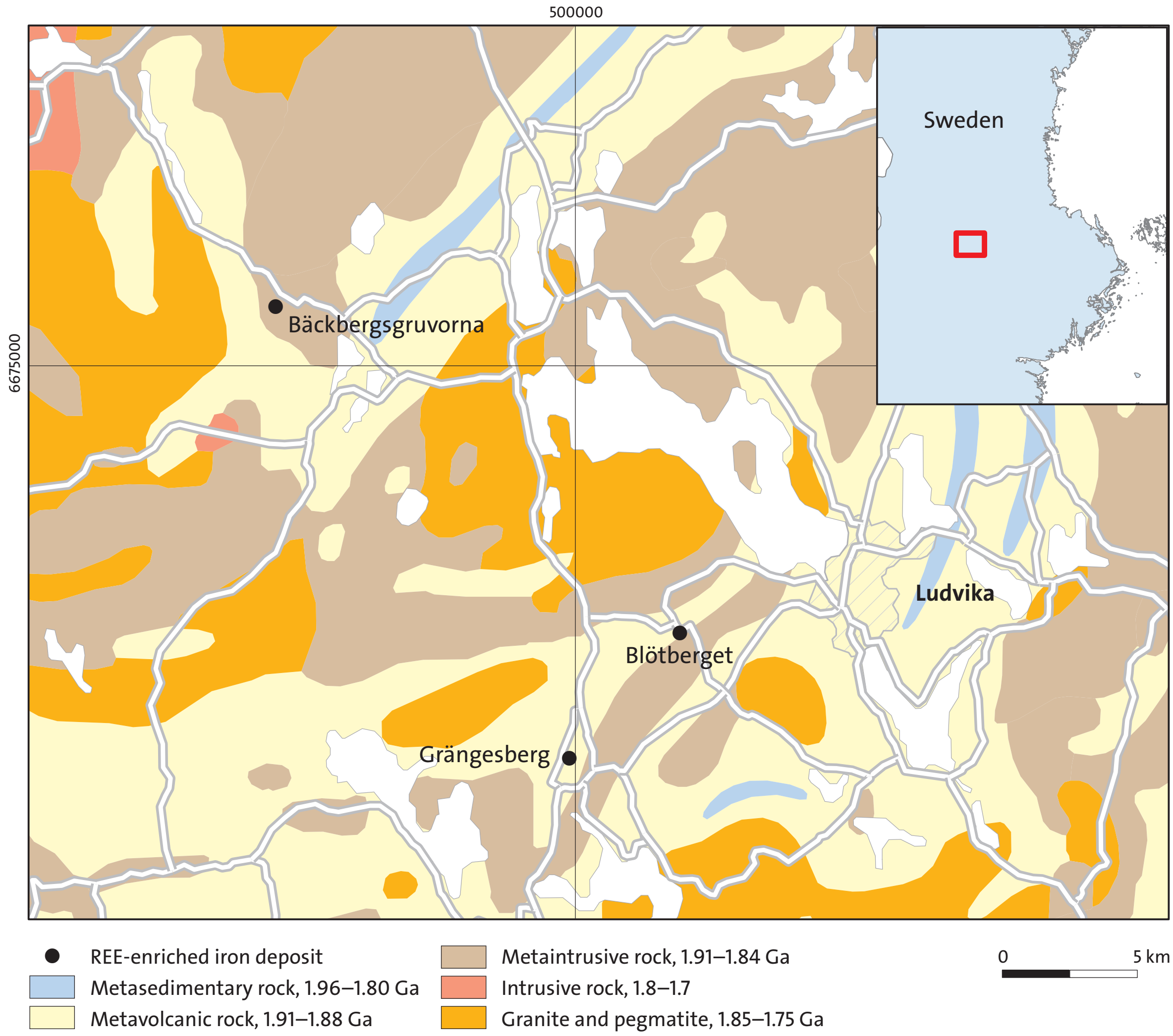

Figure 75. Simplified bedrock geology map showing the location of the REE-mineralised iron oxide mines Bäckbergs gruvorna, in the northwestern part of the Bergslagen province. The locations of the Blötberget and Grängesberg REE-enriched, major apatite-iron oxide deposits are also shown.

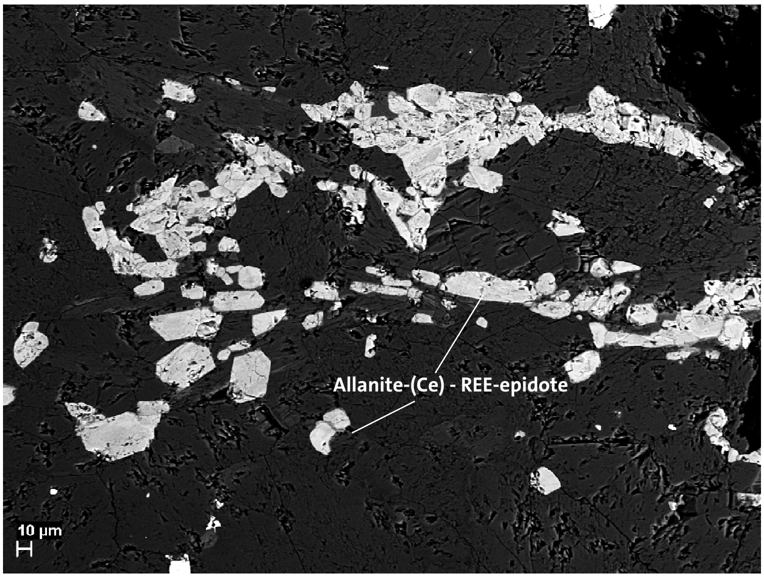

Figure 76. Back-scattered electron (BSE) image showing fine-grained crystals and aggregates of euhedral to subhedral REE epidote-allanite-(Ce) in a skarn silicate groundmass. The variable (mottled) grey scale of the crystals is primarily due to variations in REE content. The scale bar equals 10 micrometres. Bäckbergs-gruvorna. Photo: Erik Jonsson.

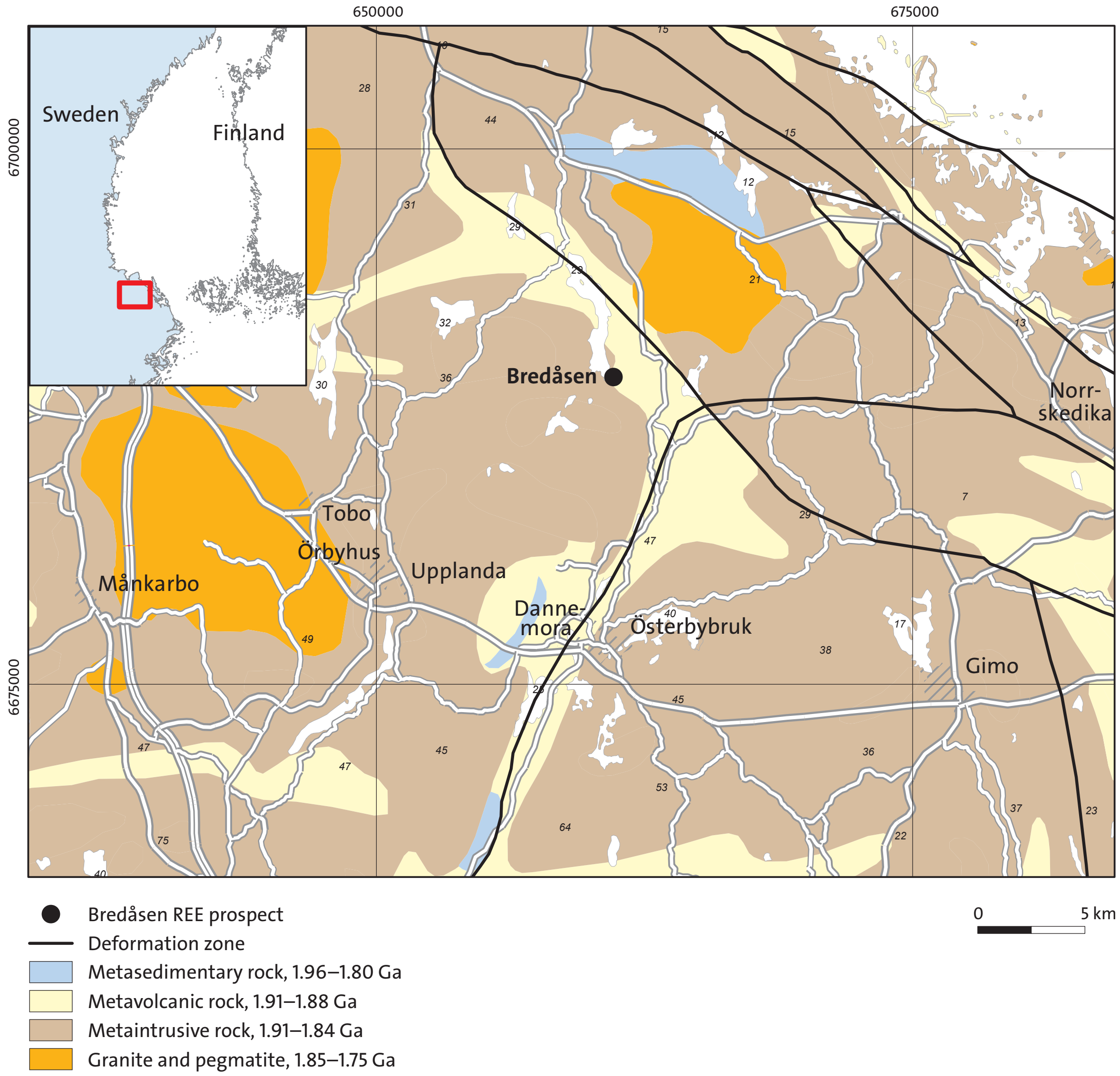

Figure 77. Simplified bedrock geology map showing the location of the Bredåsen mineralisation in northeastern Bergslagen.

revealed coarse chalcopyrite with minor pyrite, and more sulphide-rich samples also carry rare bismuthinite as inclusions in chalcopyrite. Locally, coarse aggregates of anhedral olive green allanite *sensu lato* occur, and these are often cut by secondary fractures filled by e.g. chlorite and additional phases, including REE minerals (see below). The matrix for these minerals consists of quartz and chloritised biotite.

Scanning electron microscopy (SEM) with energy-dispersive scanning analysis (EDS) confirmed that the main host of REE in the assemblage are minerals of the epidote supergroup, ranging from REE epidote, to (mostly) very close to allanite-(Ce) in composition. BSE-brighter zones may in part be Nd-dominant. The observed, fracture-hosted, later-stage REE minerals, partly associated with similarly late sulphides, comprise a modestly Y-enriched fluorite ("yttrofluorite"), Ca-bearing REE fluorocarbonates with compositions near synchysite-(Ce), and sparsely, a mineral with a composition very similar to gadolinite-(Y) (Figs. 78–80). A preliminary interpretation based on textures and mineralogy suggests that primary REE mineralisation was related to skarn formation, and that a later stage of brittle tectonism, coupled with fluid flow, remobilised part of the early components, forming the fracture-hosted, lower-temperature assemblages. No information concerning the REE mineralogy at Bredåsen was available before the present project.

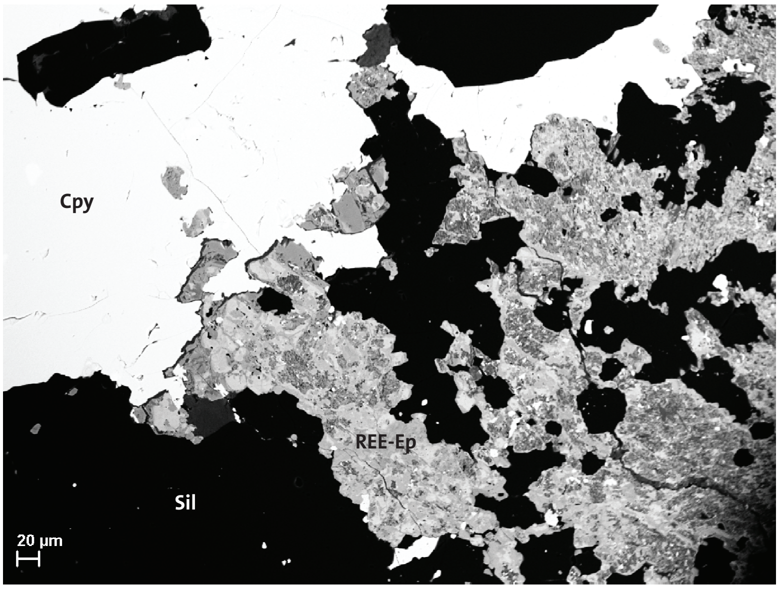

Figure 78. Back-scattered electron (BSE) image showing REE-enriched epidote to allanite-(Ce) (grey-mottled; REE-Ep) with abundant, small BSE-white inclusions which consist of an Y-Fe-silicate (gadolinite-group mineral?) intergrown with skarn silicates and quartz (black; Sil) and in contact with chalcopyrite (white; Cpy). The scale bar equals 20 micrometres. Bredåsen (6689355/ 661045). Photo: Erik Jonsson.

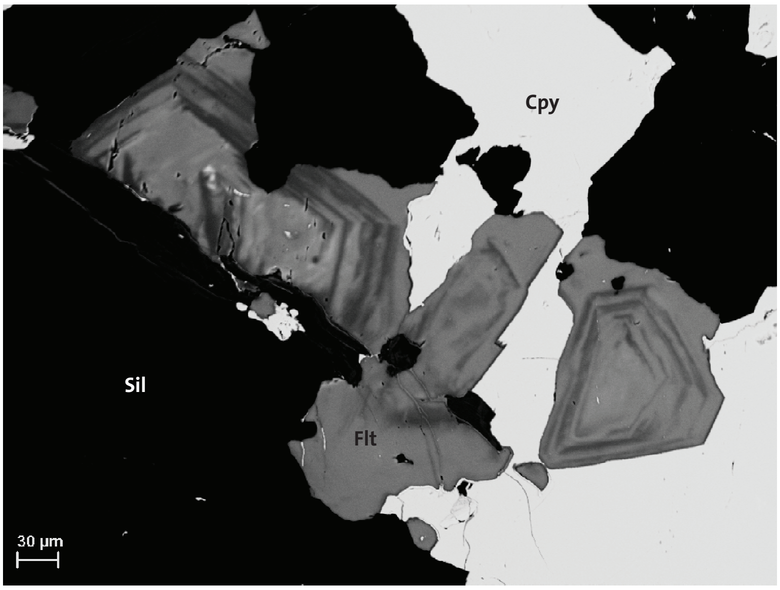

Figure 79. Back-scattered electron (BSE) image showing distinctly zoned subhedral crystals of REE-bearing fluorite (Flt; grey shades) in contact with a later-formed chalcopyrite infilling (Cpy; white) in a silicate groundmass (Sil; black). The scale bar equals 30 micrometres. Bredåsen (6689355/ 661045). Photo: Erik Jonsson.

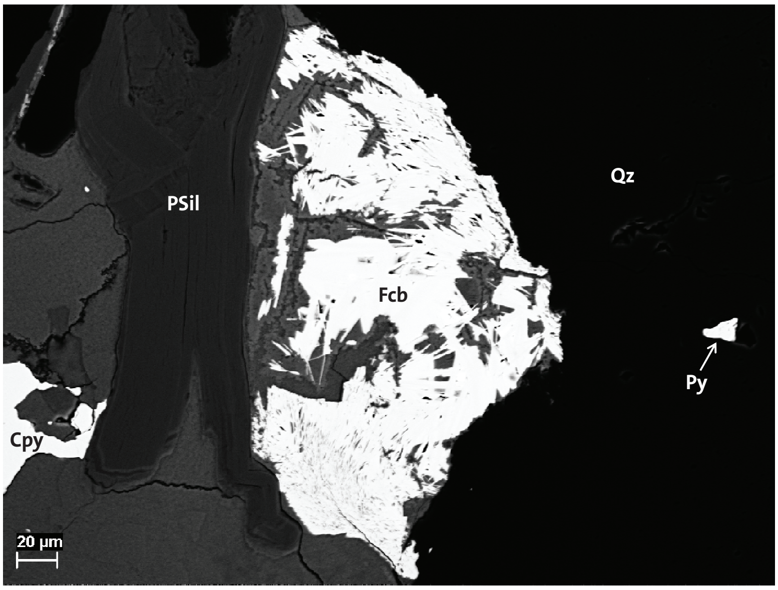

Figure 80. Back-scattered electron (BSE) image showing fracture-hosted, radial aggregates of an REE fluorocarbonate close to synchysite-(Y) (white; Fcb) associated with phyllosilicate minerals and quartz (dark grey to black; PSil and Qz) as well as minor sulphides (lightest grey to white; Cpy = chalcopyrite, Py = pyrite). The scale bar equals 20 micrometres. Bredåsen (6689355/ 661045). Photo: Erik Jonsson.

Secondary/sedimentary REE deposits

Secondary REE mineralisations form when enrichment develops through sedimentary processes such as erosion and fluvial transport leading to the accumulation of heavy minerals, as well as weathering and other supergene alteration, and soil development. Relatively few REE deposits or mineralisations in Sweden can be unequivocally classified as sedimentary in origin. Some occurrences are associated with geologically younger phosphorites in Sweden; the Tåsjö U-REE mineralisation in particular, located within the lower allochton units of the Caledonian front, is an example of this type of deposit. The REE-bearing iron oxide mineralisations within the Palaeoproterozoic Västervik formation metasedimentary rocks are examples of the "palaeoplacer" type of deposits, i.e. metamorphosed and recrystallised former placer deposits (fluvial heavy mineral accumulations).

Additionally, enrichment of U and LREEs has been noted in metasedimentary rocks at Pålänge, about 10 km southwest of Kalix (Fig. 24; Sundvall, 2003; Fagerberg & Sandgren 1970, unpublished report).

REE-(U)-anomalous iron oxide mineralisations in the Västervik formation, southeastern Sweden

The REE-bearing iron oxide mineralisation at Gränsö Södra is one of several purported palaeoplacer (metamorphosed heavy sand) deposits (e.g. Gustafsson 1990, 1991, unpublished reports) in the metasedimentary rocks of the Palaeoproterozoic Västervik formation (Fig. 81).

The rocks of the Västervik formation are variably deformed and recrystallised, but may exhibit well-preserved sedimentary features, such as primary bedding in many locations (Fig. 82). These were deposited between c. 1.88 and 1.85 Ga, possibly in a deltaic environment (Sultan et al. 2005), but also contain a small proportion of zircons that prove deposition as late as c. 1.80 Ga (Claesson & Sultan 2008). These rocks were affected by the extensive magmatic activity of the Transscandinavian Igneous Belt (TIB; Högdahl et al. 2004), and also underwent high temperature–low pressure metamorphism and deformation, whose effects include local migmatisation (Kleinhanns et al. 2012). Within this metasedimentary pile are also bedding-parallel, banded occurrences of heavy minerals, chiefly common iron (and titanium) oxides predominantly comprising magnetite, garnet, and zircon, but also including uranium and/or REE-bearing minerals such as uraninite, brannerite and davidite (Rydberg 1972, unpublished thesis; Gustafsson 1990, unpublished report), i.e. relatively clear-cut palaeoplacer mineralisations. These can be exemplified by that exposed at the old water tower in Västervik, originally drilled by the Johnson Company, which exhibits "heavy sands" in quartzite, including anatase, brannerite, davidite, rutile and zircon (Gustafsson 1990, unpublished report), or the outcropping, folded layers of heavy minerals at Klockartorpet, which exhibit marked content of e.g. Zr, Y, U, Th, and Fe, as measured in situ using a portable XRF (Fig. 83).

Later remobilisation, particularly of uranium, from these palaeoplacers led to precipitation of secondary minerals on fractures cross-cutting the stratification (e.g. Rydberg 1972, unpublished thesis; Löfvendahl 1981).

Less obvious interpretations can be made from some other REE-U-enriched mineralisations in the Västervik formation, such as at Södra Gränsö. Based on earlier work, Gustafsson (1990, unpublished report) referred to high yttrium content from Gränsö as a reason for further exploration, calling it a "heavy mineral accumulation", i.e. a palaeoplacer. A field visit, as well as observations made by means of an SEM study during the present project, suggest that this interpretation is somewhat problematic, at least as the *singular* process leading to the present mineralised system at Gränsö Södra in particular. The abundance of phyllosilicates directly associated with visible iron mineralisation in outcrop and dump material, as well as at microscale, suggests potential hydrothermal input, and there may be a genetic link to the genetically contentious mineralisations of the Olserum type (e.g. Andersson et al. 2016a,b; see that entry).

No information concerning the REE host mineralogy was available before this project.

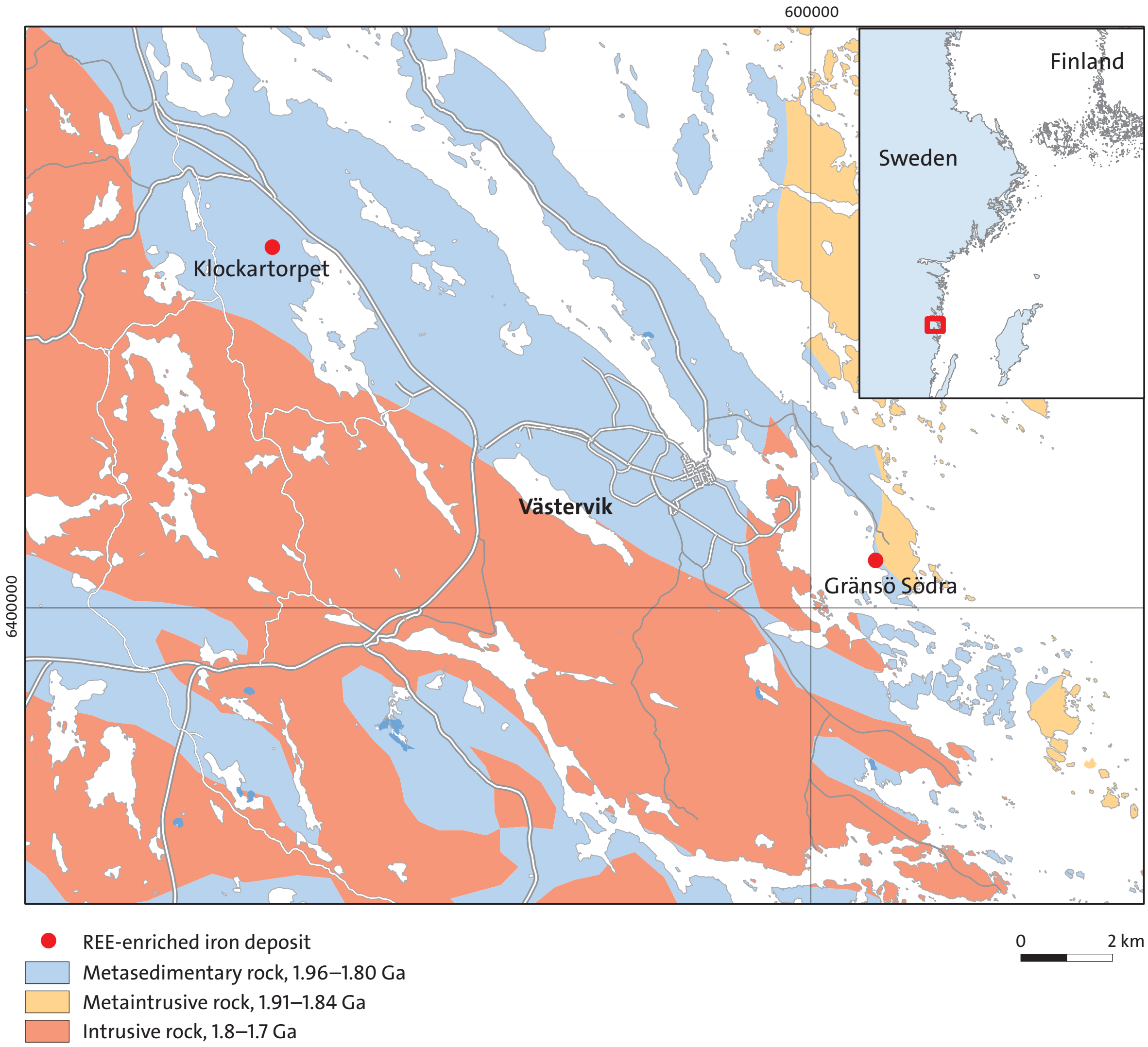

Figure 81. Simplified bedrock geology map showing the location of the Gränsö Södra and Klockartorpet mineralisations in the Västervik area.

Based on a scanning electron microscope study (with EDS analysis; cf. Figs. 84–86), the major host minerals for the REEs identified at Gränsö Södra are monazite-(Ce), xenotime-(Y), unidentified, partly altered REE-bearing oxidic uranium minerals (a U-Pb-Y-Dy-O-mineral, as well as partially altered wölsendorfite?), and a late-stage REE fluorocarbonate. Not least the occurrence of xenotime-(Y) in the material studied explains its yttrium-rich nature, as noted by Gustafsson (1990, unpublished report).

Figure 82. Primary bedding in the Västervik formation metasedimentary rocks at Berg, east of Gamlebyviken (6410970, 591620), between Västervik and Gamleby. Photo: Erik Jonsson.

Figure 83. Deformed primary bedding of bands of dark heavy minerals in Västervik formation metasedimentary rocks at Klockartorpet (6407832/ 588135). Photo: Erik Jonsson.

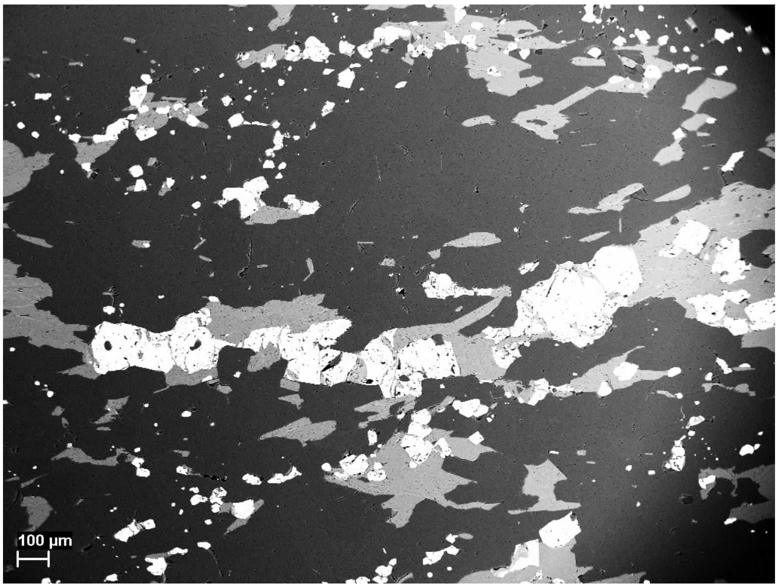

Figure 84. Back-scattered electron (BSE) image showing an overview of "heavy mineral bands" in a quartzitic rock from Gränsö Södra: the predominant white mineral is magnetite; smaller white(r) grains are monazite, xenotime and U-rich phases. The medium grey mineral directly associated with magnetite is a biotitic mica. The dark grey/black groundmass is quartz. Photo: Erik Jonsson.

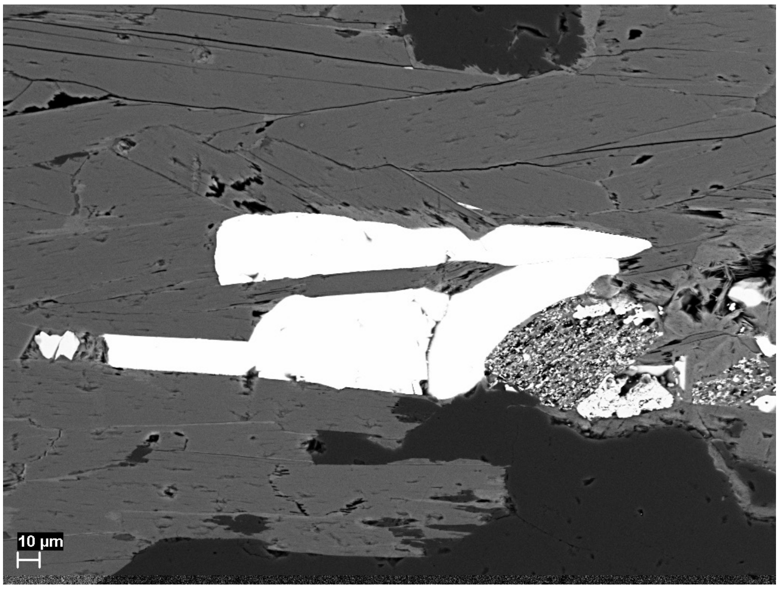

Figure 85. Back-scattered electron (BSE) image showing subhedral monazite-(Ce) crystals (white) intergrown in biotitic mica, with associated partly altered iron oxides to the right in the image. Photo: Erik Jonsson..

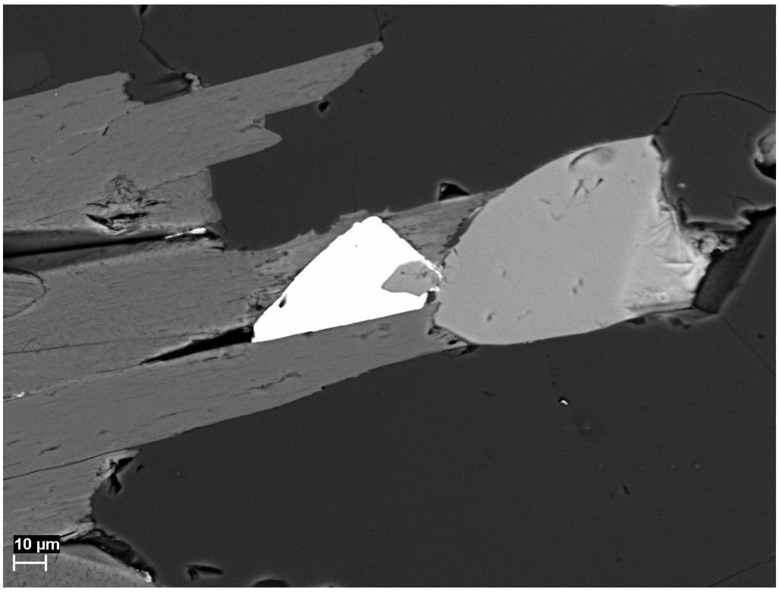

Figure 86. Back-scattered electron (BSE) image of REE mineralisation at Gränsö Södra: a subhedral crystal of xenotime-(Y) (white), enclosed in biotite (dark grey, platy), in contact with subhedral to anhedral fluorapatite (light grey) enclosed in quartz (darkest grey/black). Photo: Erik Jonsson.

The Tåsjö U-REE prospect

The Tåsjö U-REE prospect is situated in the Caledonides, approximately 45 km northwest of Dorotea in Västerbotten County, close to the border with Jämtland County (Fig. 87). It was discovered in 1957 by the Swedish Atomic Energy Company during uranium exploration. Since the discovery the Tåsjö area has been explored in several times, with nearly one hundred core drillings have been made over an area of approximately 500 km². The drilling programme was mainly funded by the Geological Survey of Sweden in the 1960s and 1970s (Gustafsson 1979). In addition, the Tåsjö area was claimed and further investigated by Mawson Resources Ltd between 2006 and 2010, with more drilling taking place. Mawson estimated the total tonnage of the area to be 75–150 million tonnes of ore at 0.03–0.07% uranium oxide and 0.11–0.24% total REE.

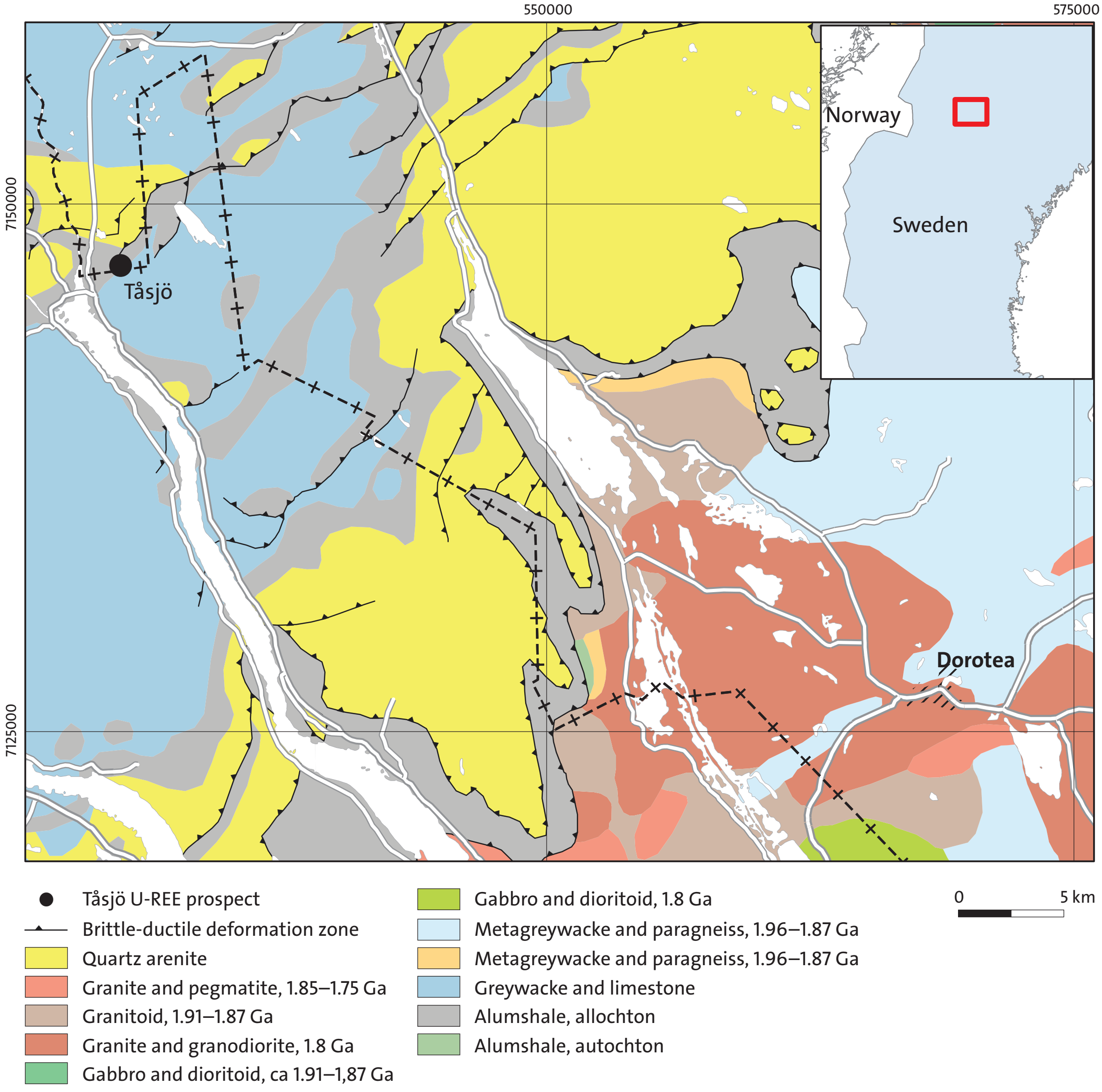

Figure 87. Simplified bedrock geology map showing the location of the Tåsjö U-REE prospect at the border between Västerbotten and Jämtland counties.

Geological setting and mineralogy

The U-REE mineralisation at Tåsjö is hosted by a phosphatic calcareous silt-sandstone (phosphorite) of Lower Ordovician age, stratigraphically overlying an alum shale (Asklund & Thorslund 1935; Andersson 1971; Gee 1972). The mineralisation is associated with apatite, which locally represents up to 20% of the rock (Gee 1972). The apatite-rich U-REE-bearing layer is generally 3 to 10 m thick. The mineralised unit is poorly exposed but has been studied in detail in drill cores (Andersson 1971). One of the best studied sites is 2.5 km northeast of Lake Tåsjön (Kronotorpet prospect), where the mineralised unit has been identified by drilling, from the surface to approximately 40 m vertical depth over an area of 0.3 km^2 (Hudson 2007). The total REE content in drilled sections at Krontorpet averages 0.09%, and the predominant REEs are Y, Ce, Nd, Eu and Yb.

A petrological study on the mineralised silt-sandstone unit shows that the major gangue minerals are glauconite, calcite, dolomite, siderite, carbonate-fluorapatite and quartz (Andersson 1971). The carbonate-fluorapatite is the main carrier of uranium and REE, and is generally associated with glauconite and carbonate minerals. The apatite appears as rounded or ellipsoidal grains varying in colour from light brown to black (Andersson 1971).

Notably, several additional names have been and are being used for prospects and projects in this mineralised sequence.

DISTRIBUTION OF RARE EARTH ELEMENTS IN SWEDISH SOILS AND ROCKS

Martiya Sadeghi

The Geological Survey of Sweden carried out a research project on the distribution of rare earth elements in soil, till and underlying bedrock across Sweden during 2012–2015 (Sadeghi & Andersson 2015). The main aims of the project were to collect available data on rare earth elements from the FOREGS database (subsoil and topsoil) (Salminen et al., 1998), GEMAS project (agriculture and grazing land soil) (Reimann et al. 2014a, b) and Geochemical Atlas of Sweden (till data) (Andersson et al. 2014), and to identify the variations in REE distribution in bedrock and REE mineralisations in Sweden. The first part of the study has been published by Sadeghi & Andersson (2015), where the following information is provided:

- Identification of the main changes in REE distribution related to geology and weathering
- Collection of basic information on REE in Sweden
- Construction of baseline level for REE in soil and bedrock (SGU lithogeochemical data) over Sweden
- Baseline maps for Sweden using the FOREGS and GEMAS databases.
- Description of anomalies and/or higher concentrations of REEs on maps related to geogenic phenomena.
- Summary statistics and application of statistical methods in interpretation of the data

The Geochemical Atlas of Sweden was published in 2014 (Andersson et al. 2014). It provides a harmonised, nationwide database with modern baseline geochemical data from the C horizon in till. The work was carried out between 2011 and 2014, and was based on till samples from the SGU archive as well as new sampling of till, conducted mainly in the mountainous areas of western Sweden. The Atlas includes a separate chapter on REE distribution in till in Sweden.

The FOREGS data (Salminen et al. 2005) have been investigated by Sadeghi et al. (2013a, focusing on REEs in different solid media (topsoil, subsoil and stream sediments) in order to identify REE background values (Sadeghi et al. 2013a). One of the main aims of this study was to compare the Swedish background values for REEs in different solid media with European levels. It was concluded by Sadeghi et al. (2013a) that lithology and bedrock geology are major factors controlling REE content in soil, so the main bedrock units in Sweden were introduced and a comprehensive introduction to Swedish bedrock geology was included. Another factor governing REE distribution in soil is mineralisation in underlying bedrock. This relationship has been presented as a map of REE mineralisation of various origins, the first of its kind published in Sweden (Sadeghi et al. 2013a).

Maps with interpolated REE concentrations have been produced, and anomalies or higher concentrations than the median value for each element are shown on each map and compared with European levels. Generally, both LREEs and HREEs show good internal correlation, whereas there is only a weak correlation between the groups. Principal component analysis (PCA) has been used, and the results of PC1 reveal two groups of association: one representing LREEs and the other HREEs. Colour composite maps derived from PCs also seem promising as a way of differentiating lithologies. Archaean rocks in northern Sweden, younger phases of the Svecokarelian orogeny, the greywackes of the Bothnian basin and young granites in the southwest stand out particularly in these plots (Fig. 88).

GEMAS is a joint project between the EGS and Eurometaux (Reimann et al. 2014a,b). Sadeghi et al. (2013b) investigated the GEMAS data with the emphasis on REEs in two solid media (top soil from agriculture (Ap) and grazing land (Gr) soil) to identify the background values of REEs in Sweden and in Europe. The Ap and Gr samples were partially leached in aqua regia and analysed using ICP-MS.

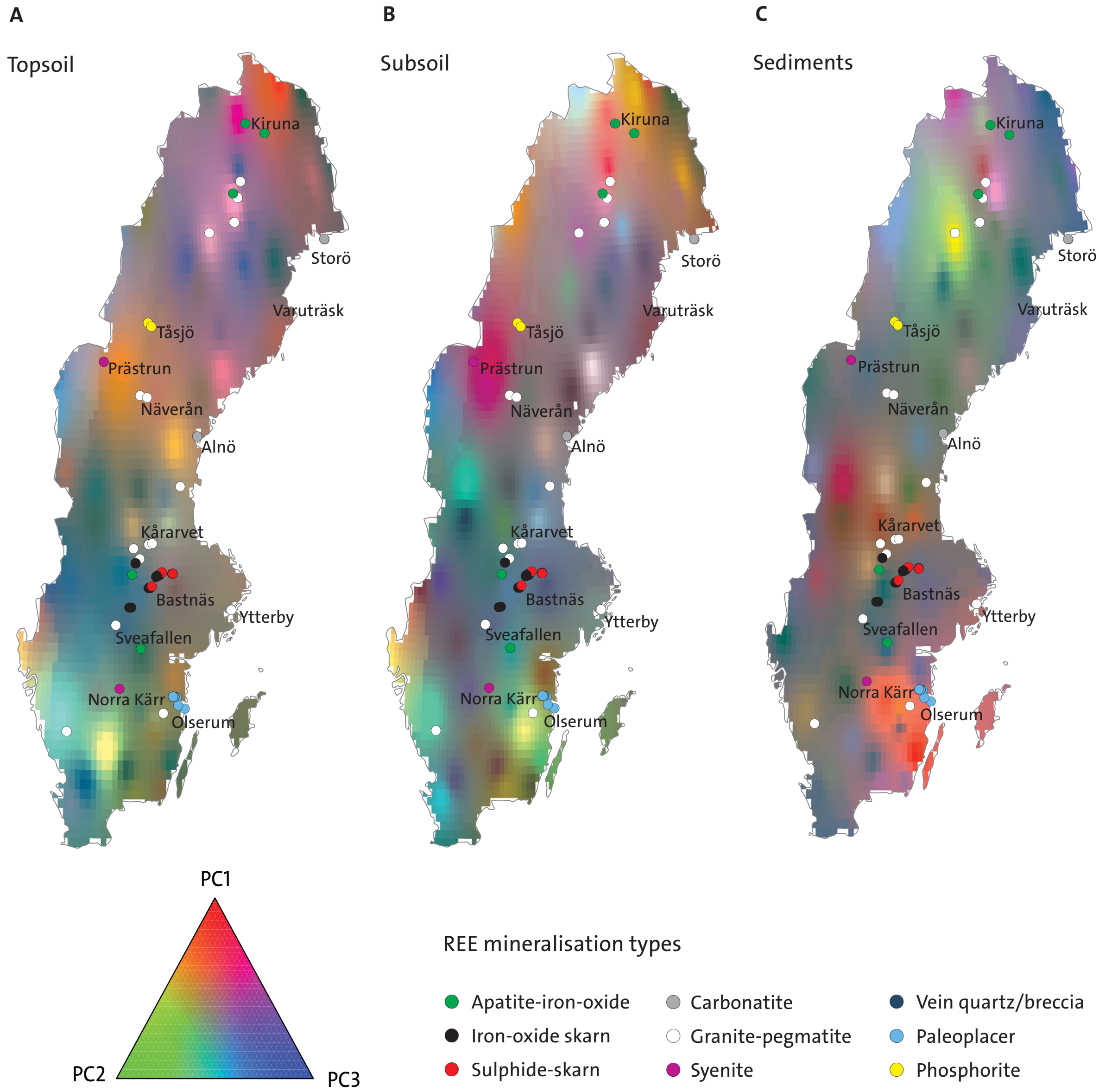

Figure 88. Colour composite images of PC1 (red), PC2 (green) and PC3 (blue) of individual Swedish FOREGS datasets: **A.** topsoils; **B.** subsoils; **C.** stream sediments.

Total REE concentrations were analysed using XRF. Sadeghi et al. 2013b discuss and compare Ce, La and Y concentrations based on analytical method and sample type. Raster maps for those three elements were produced for the whole of Europe. Interpolated maps using ArcView software and the Inverse Distance Weighting (IDW) method were generated and then classified using the concentration area (CA) fractal method (Cheng et al. 2011).

The REE and phosphate mineralisation/fertiliser map of Europe has been produced to show the correlation between REE concentration in soil and the presence of mineralisation. Sadeghi et al. (2013b) describe 40, 37, and 30 anomalies for Ce, La and Y, respectively. Of these, seven Ce, six La and five Y anomalies occur in Sweden. This study presented the ratio maps of Y/Ce and Y /La to show a correlation between REEs and the occurrences of ophiolites, alkaline and carbonate rocks.

An article by Petrosino et al. (2013) compares the FOREGS data on four sample media (topsoil, subsoil, and floodplain and stream sediment) between Italy and Sweden. Both countries show anomalous concentrations of REEs in arable soil, while having substantially different bedrock geology and soil cover developed under contrasting climate conditions. Basic statistical parameters for REE FOREGS data in four sample media are presented for the two countries and are accompanied by interpolated maps and anomaly description.

Principal component analysis has been used on FOREGS REE soil data in line with the approach by Sadeghi et al. (2013a). Based on PCA, several REE enrichment locations could be recognised in Sweden and explained by the presence of mineralisation; some REE enrichment in Italian soil more likely originates from the use of fertilisers.

Another source of REE enrichment is clay-rich soil, e.g. in eastern Sweden (Central Scandinavian clay belt) and alkaline volcanic and plutonic rocks in Italy. It has been concluded that the main factors controlling REE content in soil are: lithology, mineralisation, type of soil, weathering style and climate.

Sadeghi et al., (2015) discussed REE concentration in Swedish and Italian soils obtained from weak MMI® extraction and near total extraction. The results from MMI® extraction show that HREE enrichment in Swedish soil is comparable to the location of known REE mineralisation. In this study, the clr-transformation method has been used for principal component analysis.

Although all REEs have similar chemical properties and their spatial pattern tends to be similar, there are some differences in their distribution in soil. For example, using the near total extraction method, Ce concentration (LREE) shows elevated levels in central Sweden, which may relate to the presence of fine-grained (clay size) deposits. In the Bergslagen district, elevated Ce is possibly related to REE mineralisations, such as in the Bastnäs area, where Fe and Cu skarn mineralisations are also known. Soil samples collected in areas with granitic and pegmatitic bedrock in southern and western Sweden usually show a higher concentration of Ce. The highest concentration of Ce has been found in the sample from the tectonic window in the Caledonides, where the bedrock is composed of Proterozoic felsic igneous rocks, locally with Zn mineralisation (Sadeghi et al. 2015).

Near total extraction (SPF) shows two large regions with high yttrium concentrations. The first large Y anomaly extends from the northwestern part of the Swedish Caledonides in Norrbotten eastwards towards the Finnish border, where the soil developed from predominantly granitoid parent material and overlaps with some Th and U mineralisations. The second region with high Y concentrations occurs in central Sweden (Bergslagen); there, the large Y anomaly can be explained by clay-rich surficial deposits overlying felsic igneous rocks. This is an area with numerous Zn, Fe, Pb skarn mineralisations and local REE-enriched pegmatites (e.g. Ytterby).

The results from weak MMI® extraction show several single point anomalies that coincide generally with the granitic bedrock, U and Th mineralisations, and probably also pinpoint alkaline rock occurrences (e.g. carbonatite at Alnö) containing REE-bearing phosphate minerals (such as monazite, xenotime, apatite) (Fig. 89). The largest Y MMI® anomaly occurs in the Bergslagen district in conjunction with occurrences of granitoids, alkaline rocks, felsic volcanic rocks as well as mineralisations with

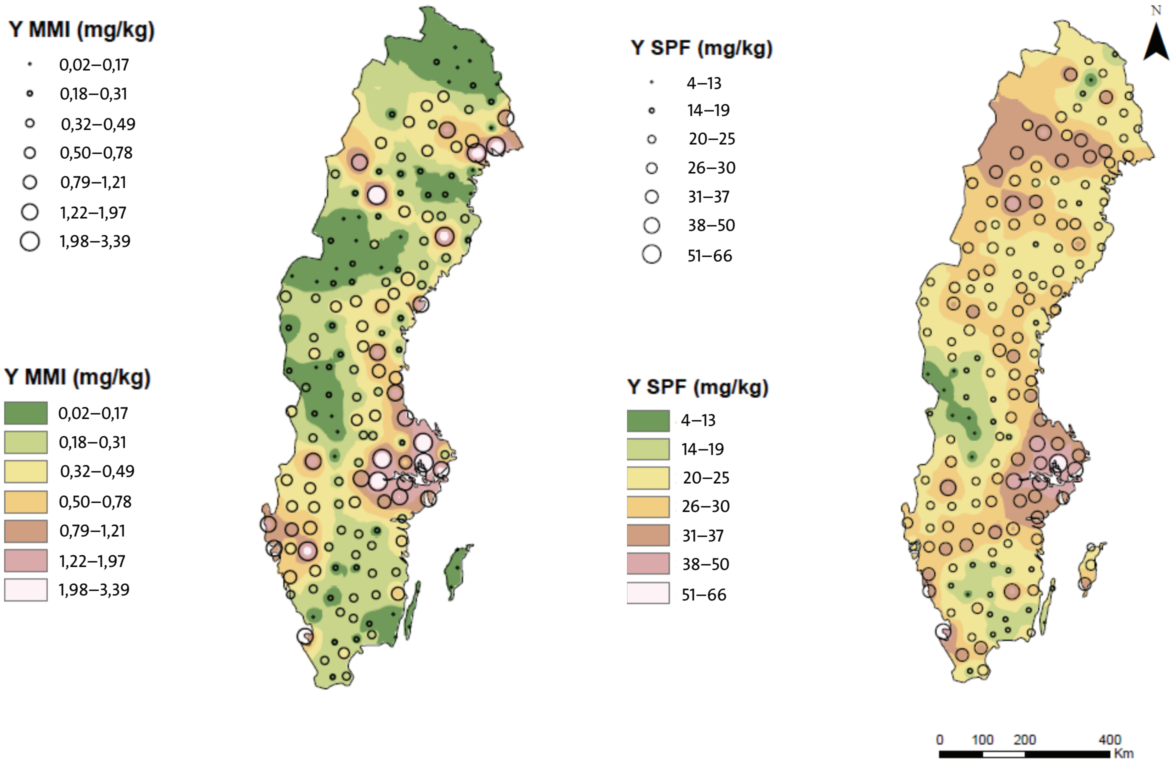

Figure 89. Colour map for Y in Ap soil in Sweden for MMI® extraction and sodium peroxide fusion technique (SPF)

REEs, Be, Cu, Ag, U and with Fe, Pb, Zn and Cu in skarns. Yttrium, with its strong tendency to bind to clay particles, is also enriched in areas with postglacial clay deposits and located below the highest coastline (Bothnian Bay coastal region, Bergslagen and near lake Vänern).

Lithogeochemistry and till data from the SGU database have been used to examine links between REE concentrations in bedrock and till with known REE mineralisation. This may provide a tool for future exploration and predictive mapping surveys. Generally, primary REEs are associated with magmatic (granite, pegmatite) and alkaline rocks. Rocks enriched in monazite and zircons often contain higher concentrations of rare earth elements. Sedimentary rocks, such as shale and greywacke, generally contain higher concentrations of rare earth elements than sandstone and limestone. During weathering rare earth elements are generally not very mobile, but this varies depending on the mineral in which they occur. Mobility is inhibited by adsorption onto iron oxides, phosphates and clay minerals. There are no obvious differences in the geochemical distribution patterns of elements in the LREE group (La, Ce, Pr, Nd and Sm) and the HREE group (Eu-Lu + Y) in till. However, their relative concentrations may differ in the anomalies of each element, probably due to the mineral composition of the till. For example, Europium is found in rock forming minerals such as plagioclase and in accessory minerals, mainly in allanite, bastnäsite, monazite, apatite, zircon and fluorite. Europium differs chemically from other rare earth elements, since the element can replace strontium and occurs in plagioclase and strontianite. High concentrations of Europium therefore occur in calcium-rich soils, for example in northernmost Sweden, where till has developed on bedrock composed of Svecokarelian gabbro-diorite and granite.

Our results show there to be a clear correlation between REE anomalies in surficial deposits and natural factors such as the lithology of the underlying bedrock, the presence of mineralisation, soil pH, climate and precipitation. A summary of the statistical parameters for REEs in different media is presented in Table 9, modified from Sadeghi & Andersson (2015).

Table 9. Summary of statistics on REEs in different media in Sweden. Q25: lower quartile (25% of population are below this value); Q75: upper quartile (75% of population are below this value).

Element	Database	Media	Fraction	Analyse	Metode	Number	Unit	Min.	Q25	Median	Q75	Max	max/ median	Std.Dev
Ce	SGU	Rock	grained	total	ICP-MS	5 761	mg/kg	0,4	24	57	89	900	16	61
Ce	GAOS	Till	<63 my	A.R.	ICP-MS	2 578	mg/kg	16	60	75	96	388	5	36
Ce	FOREGS	Subsoil	<2 mm	total	ICP-MS	51	mg/kg	23	43	49	67	101	2	19
Ce	FOREGS	Topsoil	<2 mm	total	ICP-MS	51	mg/kg	14	24	35	47	83	2	16
Ce	GEMAS	Ap	<2 mm	total	SPF	174	mg/kg	12	42	56	73	169	3	25
Ce	GEMAS	Ap	<2 mm	MMI®	ICP-MS	174	mg/kg	0,01	0,18	0,31	0,66	3	10	0,5
Ce	GEMAS	Ap	<2 mm	A.R.	ICP-MS	174	mg/kg	6	20	31	46	141	5	22
Ce	GEMAS	Gr	<2 mm	A.R.	ICP-MS	179	mg/kg	4	18	25	40	121	5	20
Dy	SGU	Rock	grained	total	ICP-MS	5 761	mg/kg	<	0,1	2,9	4,9	38	13	3,2
Dy	GAOS	Till	<63 my	A.R.	ICP-MS	2 578	mg/kg	0,9	2,9	3,5	4,3	23	6	1,4
Dy	FOREGS	Subsoil	<2 mm	total	ICP-MS	51	mg/kg	2,0	3,0	3,6	4,3	7	2	1,2
Dy	FOREGS	Topsoil	<2 mm	total	ICP-MS	51	mg/kg	1,5	2,3	2,9	3,4	6	2	0,9
Dy	GEMAS	Ap	<2 mm	total	SPF	174	mg/kg	0,6	3,6	4,3	5,2	11	3	1,5
Dy	GEMAS	Ap	<2 mm	MMI®	ICP-MS	174	mg/kg	0,004	0,042	0,071	0,133	0,479	7	0,10
Er	SGU	Rock	grained	total	ICP-MS	5 761	mg/kg	<	0,1	1,5	2,8	29	19	2,0
Er	GAOS	Till	<63 my	A.R.	ICP-MS	2 578	mg/kg	0,4	1,5	1,9	2,3	14	8	0,8
Er	FOREGS	Subsoil	<2 mm	total	ICP-MS	51	mg/kg	1,2	1,9	2,2	2,7	4,4	2	0,7
Er	FOREGS	Topsoil	<2 mm	total	ICP-MS	51	mg/kg	1,0	1,6	1,8	2,1	4,0	2	0,6
Er	GEMAS	Ap	<2 mm	total	SPF	174	mg/kg	0,3	2,1	2,6	3,1	5,6	2	0,8
Er	GEMAS	Ap	<2 mm	MMI®	ICP-MS	174	mg/kg	0,002	0,029	0,046	0,086	0,545	12	0,08
Eu	SGU	Rock	grained	tot	ICP-MS	5 761	mg/kg	0,03	0,4	0,9	1,5	39		1,2
Eu	GAOS	Till	<63 my	A.R.	ICP-MS	2 578	mg/kg	0,1	0,6	0,8	0,9	5,5	7	0,3
Eu	FOREGS	Subsoil	<2 mm	total	ICP-MS	51	mg/kg	0,4	0,7	0,8	1,0	1,6	2	0,3
Eu	FOREGS	Topsoil	<2 mm	total	ICP-MS	51	mg/kg	0,2	0,5	0,6	0,7	1,3	2	0,2
Eu	GEMAS	Ap	<2 mm	total	SPF	174	mg/kg	0,2	0,8	1,0	1,1	2,5	3	0,3
Eu	GEMAS	Ap	<2 mm	MMI®	ICP-MS	174	mg/kg	0,001	0,007	0,012	0,021	0,145	12	0,02

***Table 9.** Continuation.*

Element	Database	Media	Fraction	Analyse	Metode	Number	Unit	Min.	Q25	Median	Q75	Max	max/ median	Std.Dev
Gd	SGU	Rock	grained	total	ICP-MS	5 761	mg/kg	<	0,1	3,2	5,5	38	12	3,6
Gd	GAOS	Till	<63 my	A.R.	ICP-MS	2 578	mg/kg	1,1	3,6	4,4	5,4	22	5	1,7
Gd	FOREGS	Subsoil	<2 mm	total	ICP-MS	51	mg/kg	2,3	3,3	3,8	5,2	8	2	1,5
Gd	FOREGS	Topsoil	<2 mm	total	ICP-MS	51	mg/kg	1,2	2,4	2,9	3,6	6	2	1,1
Gd	GEMAS	Ap	<2 mm	total	SPF	174	mg/kg	0,8	3,6	4,7	5,7	13	3	1,8
Gd	GEMAS	Ap	<2 mm	MMI®	ICP-MS	174	mg/kg	0,003	0,035	0,069	0,119	0,657	10	0,10
Ho	SGU	Rock	grained	total	ICP-MS	5 761	mg/kg	<	<	0,5	1,0	20		0,7
Ho	GAOS	Till	<63 my	A.R.	ICP-MS	2 578	mg/kg	0,1	0,6	0,7	0,9	4,8	7	0,3
Ho	FOREGS	Subsoil	<2 mm	total	ICP-MS	51	mg/kg	0,4	0,6	0,8	0,9	1,5	2	0,2
Ho	FOREGS	Topsoil	<2 mm	total	ICP-MS	51	mg/kg	0,3	0,5	0,6	0,7	1,3	2	0,2
Ho	GEMAS	Ap	<2 mm	total	SPF	174	mg/kg	0,1	0,7	0,9	1,0	2,1	2	0,3
La	SGU	Rock	grained	total	ICP-MS	5 761	mg/kg	0	18	31	47	875	28	32
La	GAOS	Till	<63 my	A.R.	ICP-MS	2 578	mg/kg	8	26	32	40	199	6	14
La	FOREGS	Subsoil	<2 mm	total	ICP-MS	51	mg/kg	12	18	21	31	47	2	9
La	FOREGS	Topsoil	<2 mm	total	ICP-MS	51	mg/kg	7	12	17	22	34	2	7
La	GEMAS	Ap	<2 mm	total	SPF	174	mg/kg	6	20	27	37	97	4	14
La	GEMAS	Ap	<2 mm	MMI®	ICP-MS	174	mg/kg	0,003	0,07	0,14	0,29	3,3	24	0,3
La	GEMAS	Ap	<2 mm	A.R.	ICP-MS	174	mg/kg	3	10	16	23	85	5	12
La	GEMAS	Gr	<2 mm	A.R.	ICP-MS	179	mg/kg	3	9	13	22	230	18	21
Lu	SGU	Rock	grained	total	ICP-MS	5 761	mg/kg	<	0,1	0,30	0,50	9,7		0,37
Lu	GAOS	Till	<63 my	A.R.	ICP-MS	2 578	mg/kg	<0,1	0,19	0,24	0,30	2,6	11	0,1
Lu	FOREGS	Subsoil	<2 mm	total	ICP-MS	51	mg/kg	0,18	0,30	0,35	0,44	0,59	2	0,10
Lu	FOREGS	Topsoil	<2 mm	total	ICP-MS	51	mg/kg	0,17	0,26	0,30	0,34	0,58	2	0,08
Lu	GEMAS	Ap	<2 mm	total	SPF	174	mg/kg	0,03	0,35	0,40	0,46	0,83	2	0,12

Table 9. *Continuation.*

Element	Database	Media	Fraction	Analyse	Metode	Number	Unit	Min.	Q25	Median	Q75	Max	max/ median	Std.Dev
Nd	SGU	Rock	grained	total	ICP-MS	5 761	mg/kg	0,1	10	24	39	400	16	26
Nd	GAOS	Till	<63 my	A.R.	ICP-MS	2 578	mg/kg	7	23	28	35	129	5	11
Nd	FOREGS	Subsoil	<2 mm	total	ICP-MS	51	mg/kg	12	16	19	26	41	2	7
Nd	FOREGS	Topsoil	<2 mm	total	ICP-MS	51	mg/kg	7	10	15	19	32	2	6
Nd	GEMAS	Ap	<2 mm	total	SPF	174	mg/kg	5	19	25	33	77	3	11
Nd	GEMAS	Ap	<2 mm	MMI®	ICP-MS	174	mg/kg	0,008	0,13	0,23	0,50	4,67	21	0,47
Pr	SGU	Rock	grained	total	ICP-MS	5 761	mg/kg	<	0,1	4,3	8,9	76	18	6,6
Pr	GAOS	Till	<63 my	A.R.	ICP-MS	2 578	mg/kg	1,9	6,3	7,7	9,4	38	5	3,1
Pr	FOREGS	Subsoil	<2 mm	total	ICP-MS	51	mg/kg	2,9	4,4	5,4	7,3	11	2	2,0
Pr	FOREGS	Topsoil	<2 mm	total	ICP-MS	51	mg/kg	1,6	2,7	3,9	5,1	8	2	1,6
Pr	GEMAS	Ap	<2 mm	total	SPF	174	mg/kg	1,5	5,2	6,9	9,1	22	3	3,2
Pr	GEMAS	Ap	<2 mm	MMI®	ICP-MS	174	mg/kg	0,001	0,028	0,048	0,110	1,1	23	0,11
Sm	SGU	Rock	grained	total	ICP-MS	5 761	mg/kg	0,1	2,4	4,8	7,2	45	9	4,3
Sm	GAOS	Till	<63 my	A.R.	ICP-MS	2 578	mg/kg	1,4	4,4	5,4	6,7	24	4	2,1
Sm	FOREGS	Subsoil	<2 mm	total	ICP-MS	51	mg/kg	2,3	3,3725	3,8	5,3	8	2	1,5
Sm	FOREGS	Topsoil	<2 mm	total	ICP-MS	51	mg/kg	1,4	2,125	2,8	3,725	6	2	1,1
Sm	GEMAS	Ap	<2 mm	total	SPF	174	mg/kg	0,9	3,8	5,0	6,3	12	2	2,1
Sm	GEMAS	Ap	<2 mm	MMI®	ICP-MS	174	mg/kg	0,002	0,031	0,061	0,113	0,86	14	0,10
Tb	SGU	Rock	grained	total	ICP-MS	5 761	mg/kg	<	0,2	0,6	1,0	97		1,67
Tb	GAOS	Till	<63 my	A.R.	ICP-MS	2 578	mg/kg	0,2	0,52	0,64	0,78	3,6	6	0,2
Tb	FOREGS	Subsoil	<2 mm	total	ICP-MS	51	mg/kg	0,36	0,535	0,61	0,8	1,2	2	0,21
Tb	FOREGS	Topsoil	<2 mm	total	ICP-MS	51	mg/kg	0,22	0,375	0,47	0,57	1,1	2	0,18
Tb	GEMAS	Ap	<2 mm	total	SPF	174	mg/kg	0,1	0,6	0,7	0,9	1,9	3	0,26
Tb	GEMAS	Ap	<2 mm	MMI®	ICP-MS	174	mg/kg	0,001	0,006	0,011	0,020	0,08	7	0,01

Table 9. *Continuation.*

Element	Database	Media	Fraction	Analyse	Metode	Number	Unit	Min.	Q25	Median	Q75	Max	max/ median	Std.Dev
Tm	SGU	Rock	grained	total	ICP-MS	5 761	mg/kg	<	<	0,2	0,4	46		0,69
Tm	GAOS	Till	<63 my	A.R.	ICP-MS	2 578	mg/kg	0,05	0,21	0,26	0,32	2,0	8	0,12
Tm	FOREGS	Subsoil	<2 mm	total	ICP-MS	51	mg/kg	0,17	0,28	0,36	0,44	0,7	2	0,11
Tm	FOREGS	Topsoil	<2 mm	total	ICP-MS	51	mg/kg	0,13	0,24	0,28	0,32	0,6	2	0,08
Tm	GEMAS	Ap	<2 mm	total	SPF	174	mg/kg	0,03	0,34	0,41	0,47	0,9	2	0,13
Y	SGU	Rock	grained	total	ICP-MS	5 761	mg/kg	0,2	13	22	33	296	13	19
Y	GAOS	Till	<63 my	A.R.	ICP-MS	2 578	mg/kg	4	15	18	23	163	9	8
Y	FOREGS	Subsoil	<2 mm	total	XRF	51	mg/kg	13	19	23	27	47	2	76
Y	FOREGS	Topsoil	<2 mm	total	XRF	51	mg/kg	9	16	18	21	41	2	6
Y	GEMAS	Ap	<2 mm	total	SPF	174	mg/kg	4	21	25	30	66	3	8
Y	GEMAS	Ap	<2 mm	MMI®	ICP-MS	174	mg/kg	0,02	0,23	0,39	0,70	3,4	9	0,62
Y	GEMAS	Ap	<2 mm	A.R.	ICP-MS	174	mg/kg	1	4	6	11	38	6	6
Y	GEMAS	Gr	<2 mm	A.R.	ICP-MS	179	mg/kg	1	4	5	9	71	13	9
Yb	SGU	Rock	grained	total	ICP-MS	5 761	mg/kg	0,1	1,3	2,2	3,5	78	35	2,5
Yb	GAOS	Till	<63 my	A.R.	ICP-MS	2 578	mg/kg	0,3	1,35	1,69	2,13	15	9	0,8
Yb	FOREGS	Subsoil	<2 mm	total	ICP-MS	51	mg/kg	1,3	1,9	2,4	3,0	4,4	2	0,7
Yb	FOREGS	Topsoil	<2 mm	total	ICP-MS	51	mg/kg	1,1	1,7	2,0	2,2	4,2	2	0,6
Yb	GEMAS	Ap	<2 mm	total	SPF	174	mg/kg	0,3	2,2	2,6	3,1	5,6	2	0,8
Yb	GEMAS	Ap	<2 mm	MMI®	ICP-MS	174	mg/kg	0,002	0,026	0,042	0,082	0,741	18	0,09

GEOCHEMISTRY OF REE MINERALISATIONS

Martiya Sadeghi

REE deposits may be divided into regolith, basinal, metamorphic and magmatic associations based on a mineral system approach ("mineral system association"; Fig. 90). An essential element of the magmatic association is the emplacement of an REE-enriched melt. Various deposit types result either directly from crystallisation of the melt and/or fluids predominantly derived from the melt. The magmatic association deposit may essentially be divided into orthomagmatic and hydrothermal types. In the orthomagmatic type, the REE-bearing mineral(s) form from crystallisation in a magma or from a hydrothermal fluid exsolved from that magma. In the hydrothermal type, the REE-bearing mineral(s) form from a fluid apparently not chemically related to orthomagmatic processes.

Deposit types of the basinal association can be formed from mechanical (e.g. placer) and chemical (e.g. phosphorite) sedimentary processes and from diagenetic fluids generated in sedimentary basins. Deposit types of the regolith association require an REE-bearing source rock to form economic-grade concentrations of REE. REE deposits are formed either due to enrichment of REE in the residual material and/or from local remobilisation of REE.

Deposit types of the metamorphic association are generated during regional and/or contact metamorphism and involve metamorphic-derived fluids.

Hydrothermal REE mineralisations

Evaluation of the REE geochemistry of hydrothermal mineral deposits, and the processes by which they are concentrated, is a complex task (Samson & Wood 2005). However, these mineralisations can be grouped on the basis of their geochemical and mineralogical characteristics. The degree of REE enrichment in a deposit is a function of the concentration of REE in the fluid, the water-rock ratio, the efficiency of the precipitation process and the nature and amount of co-precipitated phases (Samson & Wood, 2005).

Oreskes & Einaudi (1990) suggested that the high abundance of fluorocarbonates and the lack of Ca minerals in REE deposits (e.g. Olympic Dam) indicated that the fluids behind hydrothermal REE mineralisations may have been F- and CO_2-rich and that the REEs were transported as Cl and/or F complexes. Lottermoser (1995) suggested that the association of REE with U minerals indicated that U and REE were complexed by the same ligands and inferred that those were CO_3, F or SO_4.

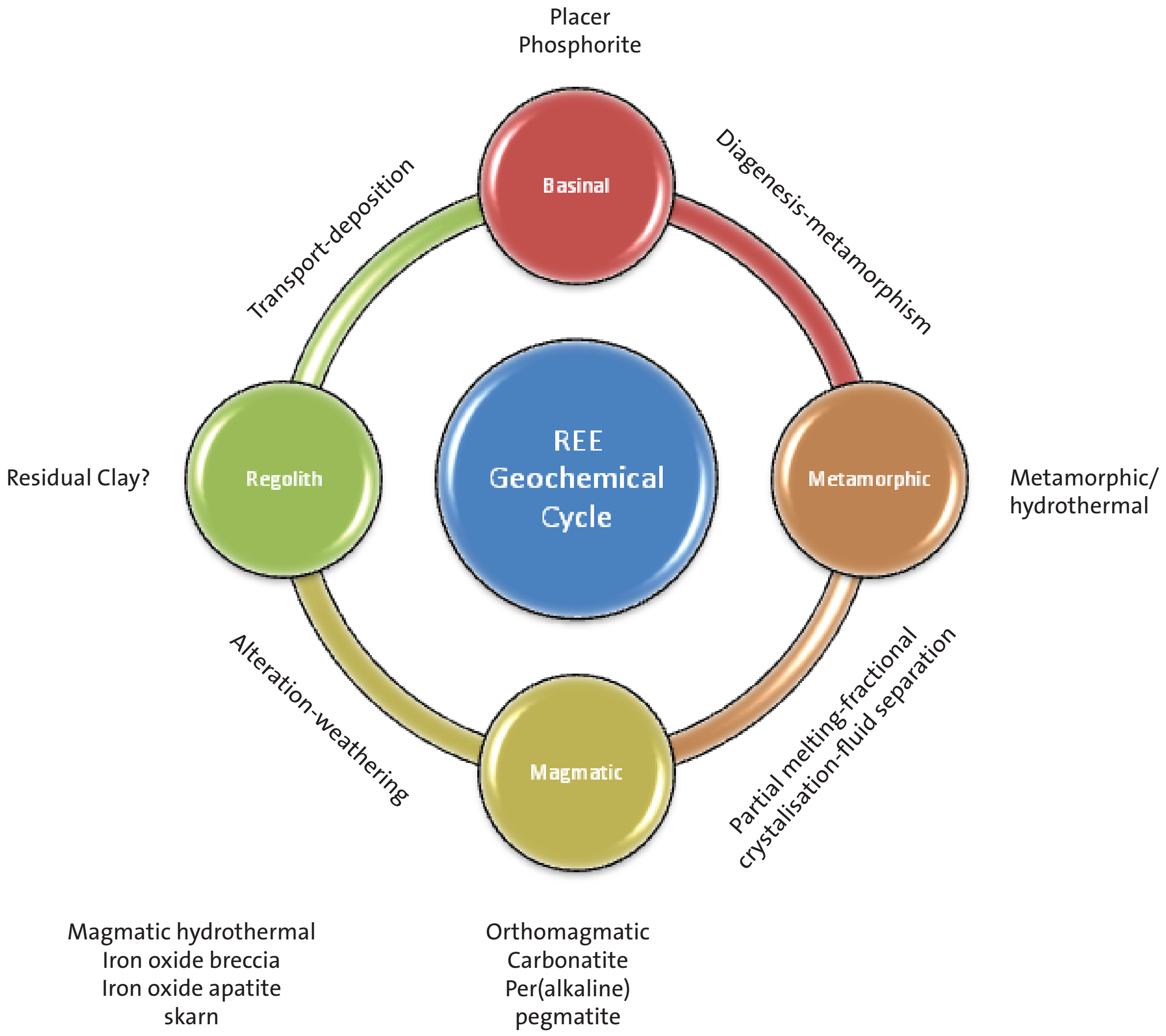

Figure 90. Geochemical cycle for rare earth elements (only REE mineralisations in Sweden have been considered here; modified from Hoatson et al. 2011). Alkaline and carbonatitic melts, produced by the partial melting of mantle, transport rare earth elements from the mantle into the crust. Granites that are produced from the partial melting of crustal material are also enriched in rare earth elements (less enriched than alkaline and carbonatitic melts).

Orthomagmatic REE mineralisations

In some cases, carbonatites represent orthomagmatic-type REE mineralisations that tend to be variably enriched in a elements including REEs, Sr, Ba, U, Th, Nb, Ta, P, and F. Although the overall REE content of carbonatites may vary, their shape on the chondrite-normalised plots almost invariably displays high LREE content and no negative Eu anomalies (Verplanck et al. 2016). REE-bearing mineral phases have the highest REE content, but major carbonate minerals, including calcite and dolomite, may also contain substantial concentrations of REEs (Mariano 1989). Barium and strontium are generally abundant, whereas uranium, thorium, niobium and phosphorus are variably abundant in the mineralised carbonatite.

Chemically, Potassic lamprophyre dykes are normally characterised by relatively low SiO_2, TiO_2 and high MgO, K_2O concentrations. In addition, they show high content of other large-ion lithophile elements (e.g. Rb, Sr, Ba) and LREE, but low content of high-field-strength elements (e.g. Nb, Ta, Zr, Hf, and Ti) (Chai et al., 2006).

Several REE deposits associated with peralkaline complexes (syenitic rocks) have a number of geochemical characteristics in common; e.g., they are mostly enriched in U and Th and have a relatively high HREE content but low LREE content compared with carbonatites (Dostal 2016). In general, sövitic carbonatitic melts show the highest levels of REE enrichment. They also show significant enrichment in LREE (LREE/HREE ratio of ~40, compared with ~7 for alkaline and felsic melts).

Partial melting of crustal material also produces felsic melts that are enriched in REE, but the enrichment factors are relatively smaller (by an order of magnitude). Elements in pegmatites that may be enriched to minable (ore) grades include Li, Cs, Be, Sn, Nb, Ta, U, Y, Zr, and REE. This long and diverse list of elements, to which significant high content of B, P, F, Rb, Bi, Hf, etc. could be added, makes fractionated pegmatites among the most mineralogically complex deposit types on Earth. Pegmatitic facies associated with syenite-alkaline granite complexes constitute important deposits of REE, U, Nb and Zr, and less commonly, Be and P (London 2016).

Jolliff et al. (1992) observed appreciable heterogeneity in the modal compositions of border zone samples of individual pegmatites, and statistically a poor correlation between Rb and Cs content in muscovite and the known internal zonation of the bodies. However, they did recognise a trend in K/Rb ratios versus Cs content that correlated in a general sense with the overall chemical fractionation of the body (Jolliff et al. 1992).

Placer and phosphorite REE mineralisations

Trace elements associated with heavy mineral placers primarily include Ti, Hf, the REEs and Y, Th, and U. These elements may be used for the analyses of stream sediments to evaluate the presence of heavy mineral sands on a regional scale (Grosz 1993). These pathfinder (exploration) elements reflect the composition of the potentially economic heavy minerals of this deposit type, including ilmenite ($FeTiO_3$), rutile (TiO_2), zircon (Zr, Hf, U) SiO_4), monazite (La, Ce, Th, U) PO_4), and xenotime (YPO_4). Monazite is preferentially enriched in LREEs relative to HREEs. Variation in chemistry at deposit scale most likely indicates variations in heavy mineral content rather than geochemical gradients due to hypogene, hydrothermal or supergene processes. Hydrothermal alteration and other forms of geochemical diffusion that are typical of most ore deposits are not associated with heavy mineral sands.

Phosphorite is a marine sedimentary rock in which phosphate minerals are the main constituents (more than ~18 % P_2O_5; Cathcart 1980b). "Francolite" is essentially the only phosphate-bearing mineral present in phosphorites unaltered by metamorphism or weathering. This structurally and chemically complex mineral is a carbonate-fluorapatite with >1% F and believed to contain appreciable amounts of CO_2 (Jarvis et al. 1994). The major element geochemistry of unaltered

francolite is relatively uniform and includes approximately 32 to 40% P_20_5, 50% CaO, 5% CO_2, 4% F, 3% SO_4 and 1% Na (Jarvis et al. 1994, Piper 2001). The apatite structure allows numerous trace element substitutions, including of the REEs. Rare earth element enrichment in francolite, whereby REE is substituted for Ca in the mineral lattice (Jarvis et al. 1994, Piper 1999), was documented more than a century ago (Jarvis et al. 1994).

REE chemistry in Sweden

During the EURARE field campaign approximately 200 samples were taken for petrography and mineralogy studies and for geochemical analysis. The location of the samples and type of mineralisation are shown in Fig. 91, and the results of samples analysed are given in Appendix. 1.

The geochemical analyses of the samples collected during the EURARE project show that 68 samples have a total REE content above 1000 ppm and of those 28 have more than 1% total REE.

The samples with more than 1% REEs represent mineralisations classified in this project as: iron

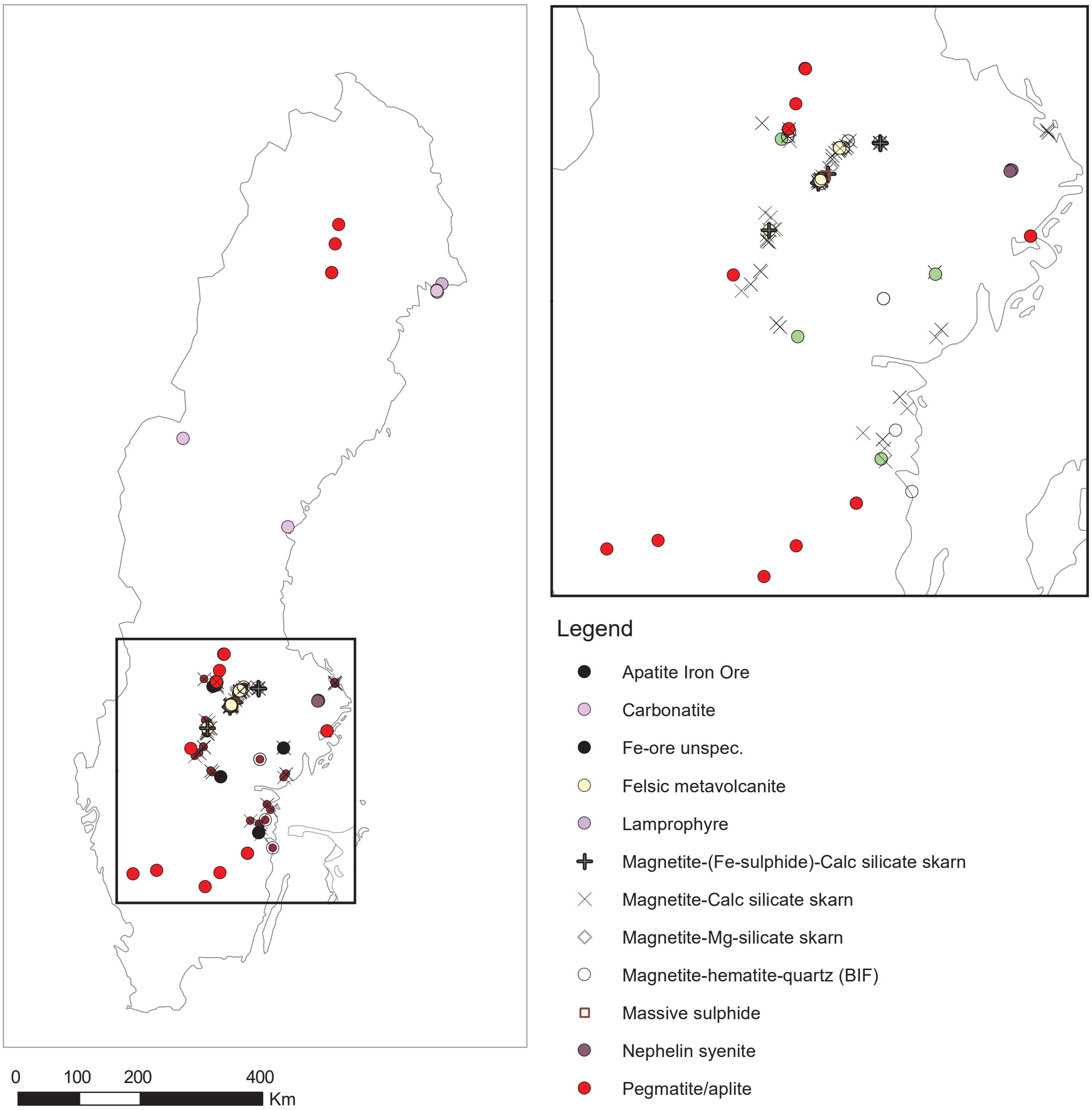

Figure 91. Simplified location map of samples in the EURARE project.

oxide apatite (4 samples), magnetite-calc-silicate skarn (11 samples), magnetite-hematite-quartz (BIF; 2 samples) and granitic pegmatite (11 samples). These resulted are summarised in Table 10.

A bivariate plot of La vs La/Yb (Fig. 92) shows a weak but overall positive correlation between the two variables, except in some samples, which show higher HREE concentrations. This suggests that those samples with a high LREE content also have relatively high LREE/HREE ratios. They mostly represent REE mineralisations associated with granitic pegmatites. Some samples from iron oxide-apatite deposits contain REE-bearing minerals such as xenotime and monazite, and show higher concentrations of HREE (Fig. 92).

Thorium and uranium content and their ratio are useful for recognising geochemical facies and also the content of radioactive elements in different types of mineralisation. In some samples from REE mineralisations the total content of REEs shows a positive correlation, with elevated U and Th concentrations (Figs. 93a-b). Fig. 93a shows Th concentration versus total REEs. In general, skarn and

Table 10. Summary of samples analysed with a total REE (TotREE) content above 1% (10,000 ppm). N and E are SwerefTM coordinates.

Name	N	E	Type	TotREE	LREE	HREE
Stålklockan	6635349	532852	Magnetite-Calc silicate skarn	45511	34001	11510
Tåresåive Mo-REE	7421196	709317	Pegmatite/aplite	42651	33055	9595
Bastnäs	6634470	532926	Magnetite-Calc silicate skarn	38078	33149	4929
Bastnäs	6634470	532926	Magnetite-Calc silicate skarn	38078	33149	4929
Bastnäs	6634425	533003	Magnetite-Calc silicate skarn	37907	33134	4773
Gyttorp	6597427	497660	Magnetite-Calc silicate skarn	37069	33233	3835
Mörkens 4	6662160	577465	Magnetite-(Fe-sulphide)-Calc silicate skarn	36921	33224	3696
Djupedalsgruvan	6425442	578440	Magnetite-Calc silicate skarn	34643	22745	11897
Ytterby	6592332	690226	Pegmatite/aplite	30624	13624	17000
Rödbergsgruvan A	6597194	494237	Magnetite-Calc silicate skarn	30536	29378	1157
Östanmossa	6660543	551764	Magnetite-Calc silicate skarn	30318	28849	1469
Djupedalsgruvan	6425442	578440	Magnetite-Calc silicate skarn	29990	16625	13364
Holmtjärn	6691407	514383	Pegmatite/aplite	29550	12550	17000
Ytterby	6592332	690226	Pegmatite/aplite	26418	10238	16180
Djupedalsgruvan	6425442	578440	Magnetite-Calc silicate skarn	25903	11132	14771
Mörkens 4	6662160	577465	Magnetite-(Fe-sulphide)-Calc silicate skarn	24970	21635	3335
Gruvhagen SV om Knutsbo gruvor	6662377	577026	Magnetite-Calc silicate skarn	24574	23618	955
Ytterby	6592332	690226	Pegmatite/aplite	18695	3801	14894
Reunavaare	7342033	697981	Pegmatite/aplite	18206	13158	5048
Tybble gruva	6517096	516016	Apatite Iron Ore	17427	17273	153
Flakaberget	7389427	703658	Pegmatite/aplite	15555	1627	13928
Johanna	6658660	550883	Magnetite-Calc silicate skarn	14007	12965	1042
SVEAFALLEN	6563279	467518	Pegmatite/aplite	13220	12579	641
SVEAFALLEN	6563279	467518	Pegmatite/aplite	13220	12579	641
Mörkens 4	6662160	577465	Magnetite-Calc silicate skarn	11077	9203	1874

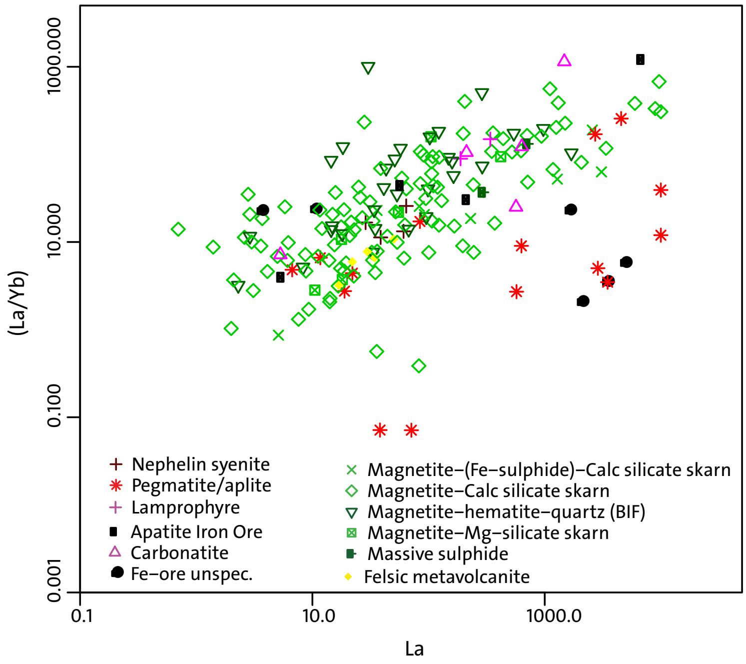

Figure 92. Bivariate plot of La versus La/Yb for the samples analysed.

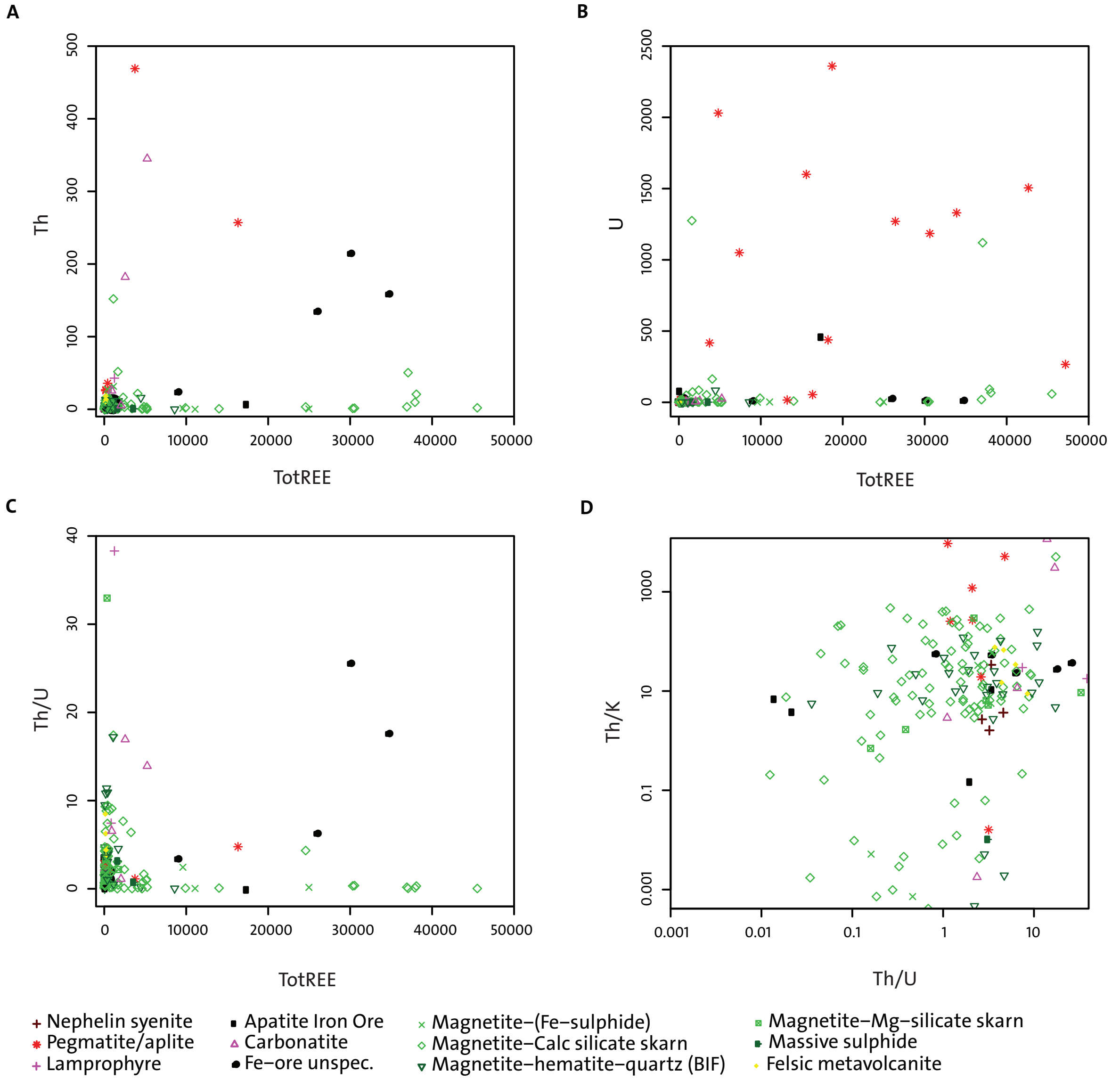

Figure 93. Bivariate plots of **A.** Th vs total REE; **B.** U vs total REE; **C.** Th/U vs total REE; and **D.** log Th/K ratio vs log Th/U ratio for the samples analysed. Symbols as in Fig. 92.

iron oxide-apatite mineralisations with higher concentrations of total REEs show a positive correlation with low concentrations of Th. A few samples from iron oxide-apatite mineralisations show higher concentration of Th up to 200 ppm and total REE concentrations of up to 3.5%. Granitic pegmatites and lamprophyres show higher concentrations of Th, whereas those of total REEs are low, which means that the concentration of Th in those samples is not related to REE-bearing minerals, and Th and U concentrations are probably related to rock-forming minerals such as feldspar and plagioclase.

The U/total REE ratios (Fig. 93b) of the samples analysed show that those with higher concentrations of U belong to REE mineralisation in granitic pegmatites. A few samples from skarn-type deposits show higher concentrations of U, >1000 ppm. Of those, one also shows a higher content of total REE, which may reflect the concentration of U in the REE-bearings minerals.

A plot of Th/U ratio versus the concentration of total REE (Fig. 93c) shows that lamprophyres with low concentrations of total REE have higher Th than U concentrations. The Th/U ratio is generally low in the samples from skarn and iron oxide-apatite REE mineralisations. Two samples of iron oxide-apatite REE mineralisation from the Djupedalsgruvan show high concentrations of both Th and REE. Those two samples contain xenotime and allanite minerals (Fig. 93c). Two samples come from other iron oxide-apatite REE mineralisations, and show higher concentrations of total REE and Th. The plot of Th/K versus Th/U shows a positive correlation between U and K in the skarn type but less so in REE mineralisations associated with granitic pegmatites (Fig. 93d).

Fig. 94 shows positive correlations between some trace and rare earth elements and total concentration of REE. In general, Ce and La show a linear correlation with total REE, but several samples belonging to the granitic pegmatite mineralisations contain higher total REE, whereas Ce and La concentrations are not very high. This means that some of those samples have relative enrichment of HREE.

There is no correlation between Y and total REE in the samples analysed. Those with higher concentrations of Y and total REE are related to samples with obvious REE mineralisation.

Sr is an element that can be used to distinguish lamprophyres and carbonatites from other types of REE mineralisation. High Rb content was observed in a few samples. Most REE mineralisations associated with iron oxides without apatite contain higher content of both Rb and total REE. Higher Zr content is only observed in REE mineralisations associated with granitic pegmatites.

Unmineralised or less REE-mineralised iron-oxide apatite and skarn samples show a range in Fe oxide concentrations. whereas REE mineralised ones only show lower Fe concentrations. This characteristic may be related to the presence of silica and actinolite. This means that no iron oxide-apatite and skarn type samples with more than 40% Fe_2O_3 show high concentrations of REE.

Chondrite-normalised (McDonough & Sun 1995) REE diagrams for carbonatites display enrichment in LREE and no Eu depletions (Fig. 95a). The samples with REE mineralisation differ from non-mineralised ones based on LREE enrichment factors. One carbonatite sample shows higher concentrations of HREE than the other (Fig. 95a). Similar patterns are displayed by the lamprophyre samples (Fig. 95b).

Chondrite-normalised REE patterns (McDonough and Sun 1995) for samples with TREE above 1% represent iron skarn-type mineralisations. They show enrichment in LREE, a flat HREE segment and pronounced Eu depletion in most cases (Fig. 95c).

Iron oxide-apatite samples with some sulphide mineralisation show REE patterns similar to those of the iron oxide skarn samples, with enrichment in LREE and negative Eu anomalies, whereas the segment of HREE generally decreases from Tb to Lu (Fig. 95d). The samples of magnetite-hematite-quartz (BIF) display similar trends (Fig. 95e).

The chondrite-normalised (McDonough & Sun 1995) REE patterns for pegmatite samples show distinct depletion of Eu and enrichment of LREE as well as HREE in some cases. Mineralised and non-mineralised pegmatite samples are differentiated in this diagram (Fig. 95f). Nepheline syenite samples show similar trends to those for the carbonatites and lamprophyres with no Eu depletion and decreasing content from LREE to HREE (Fig. 95g).

There are several iron oxide samples that cannot be classified (more mineralogical and petrological investigations are needed). However, their REE patterns suggest they constitute two groups. One group shows a similar trend to the iron oxide-apatite- and skarn-type REE samples, with a negative Eu anomaly, although they have overall higher concentrations of HREE. The other group shows weak positive Eu anomalies and decreasing trends from LREE to HREE (Fig. 95h). They may have an alkaline or peralkaline origin, but this also needs investigation and research (Fig. 95h).

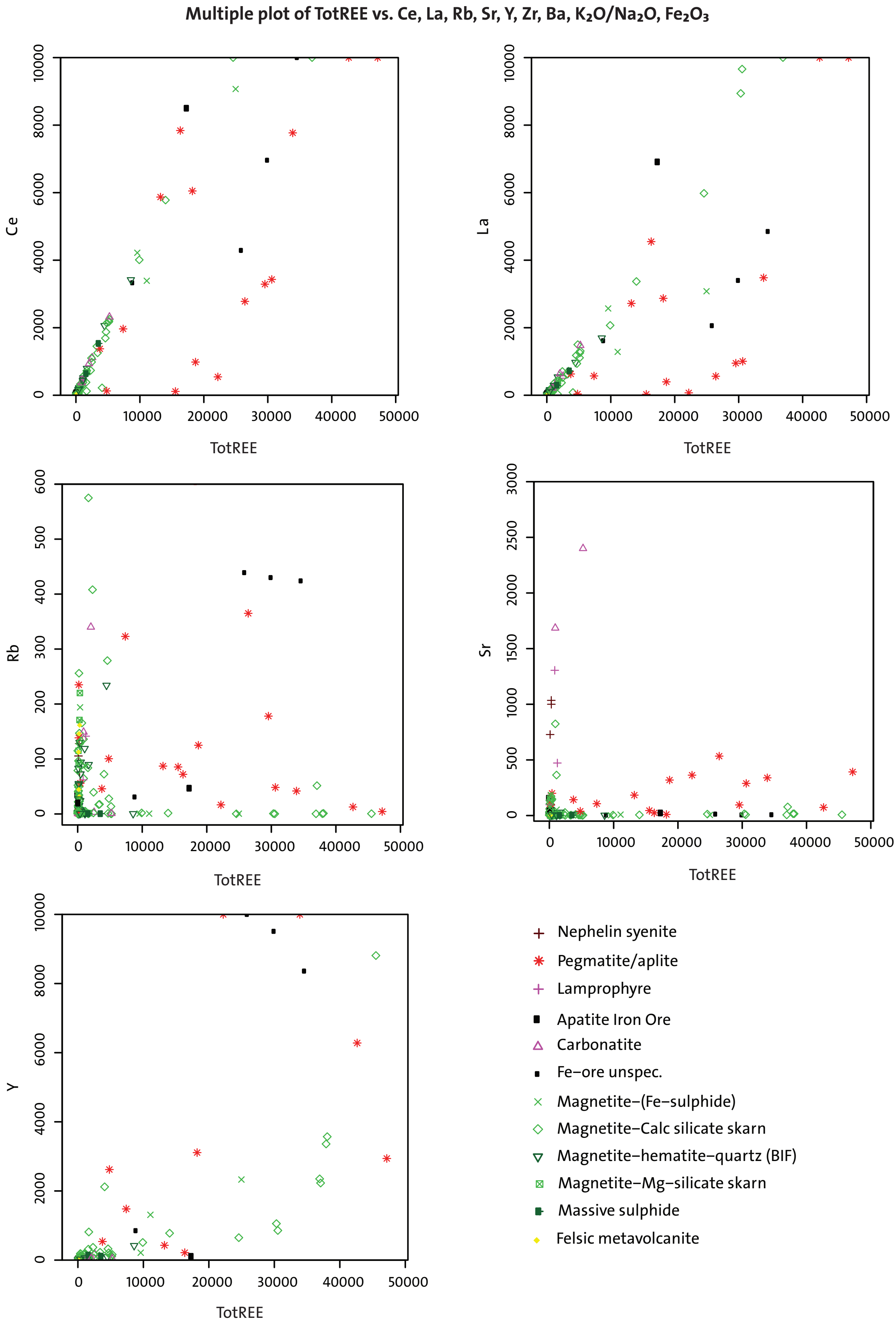

Figure 94. Plots of some elements versus total REE in the samples analysed. The figure continues on the next page.

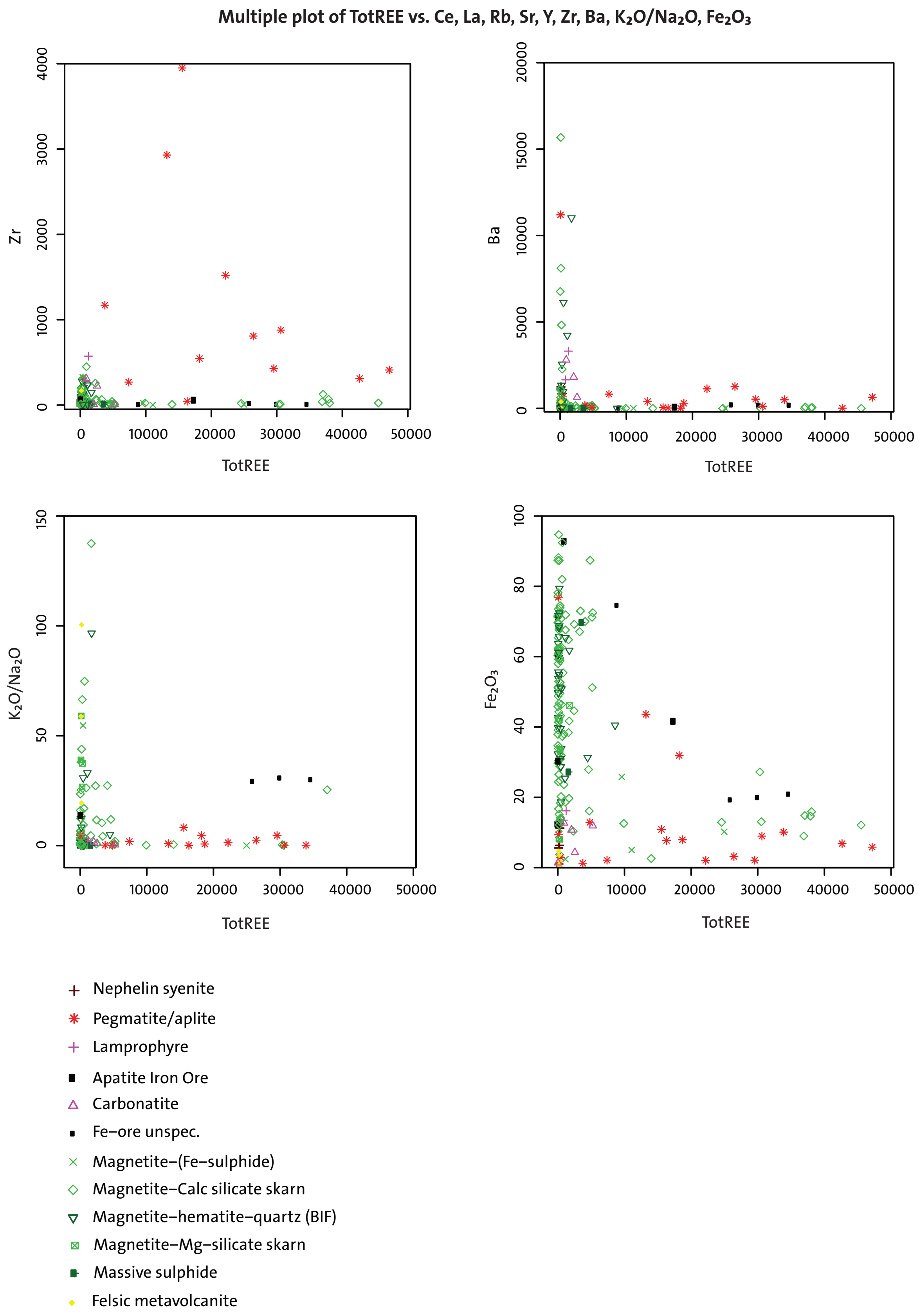

Figure 94. Plots of some elements versus total REE in the samples analysed. Continuation from the previous page.

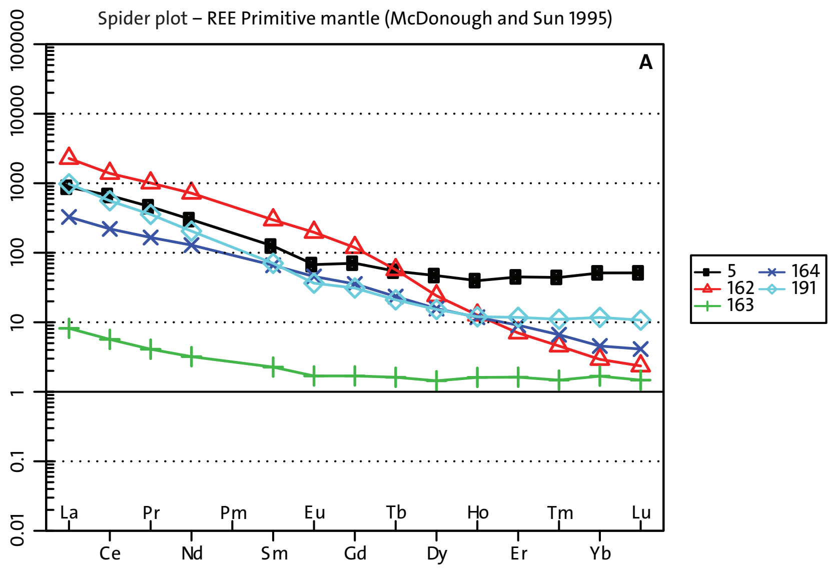

Carbonatite

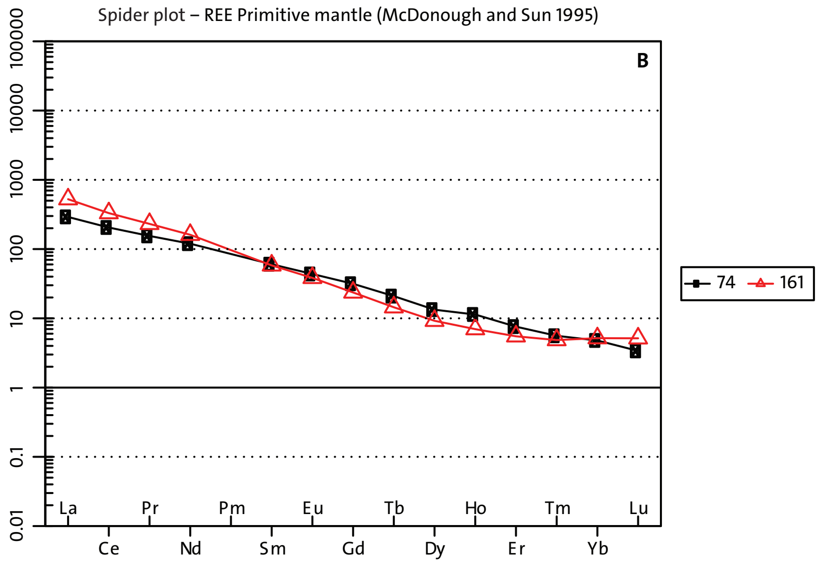

Lamprophyre

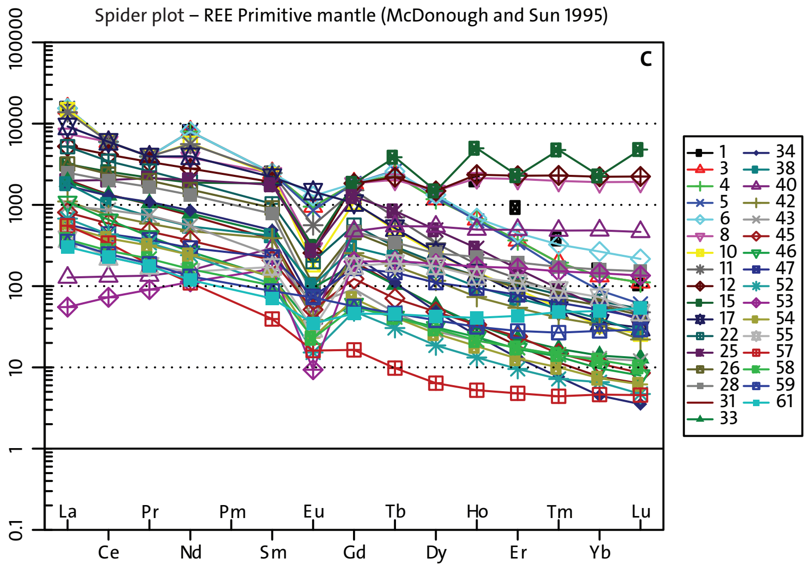

Magnetite – Calc silicate skarn

Figur 95. Chondrite-normalised (McDonough & Sun 1995) REE patterns of **A.** carbonatites; **B.** lamprophyres; **C.** iron skarn; **D.** iron oxide (sulphide) skarn; **E.** magnetite hematite quartz (BIF); **F.** granitic pegmatites; **G.** nepheline syenite; and **H.** other oxides. The figure continues on the next page.

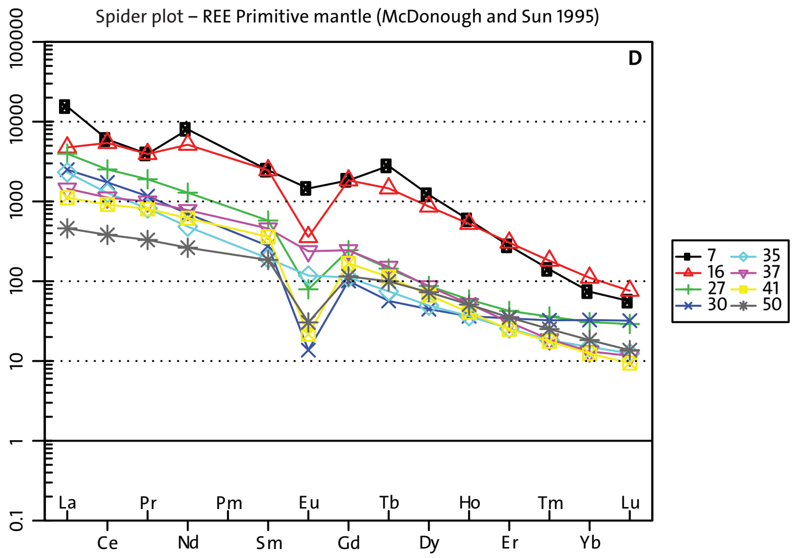

Magnetite – (Fe – sulphide) – Calc silicate skarn

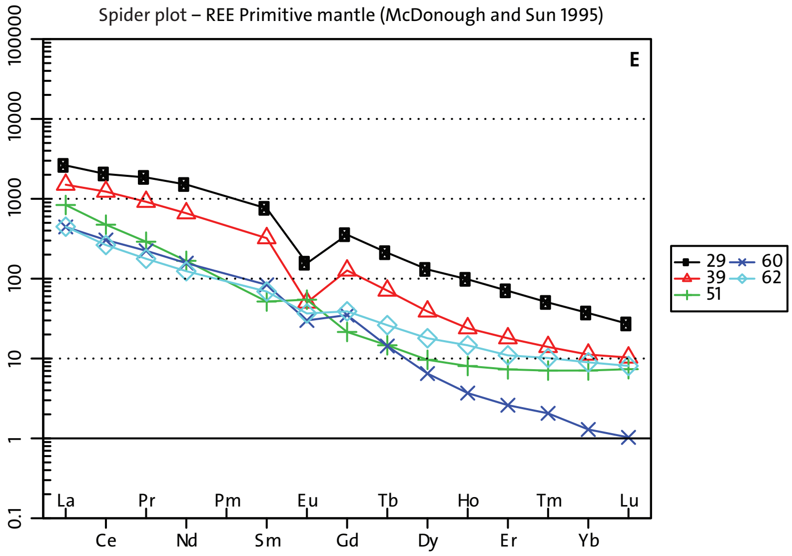

Magnetite – hematite – quartz (BIF)

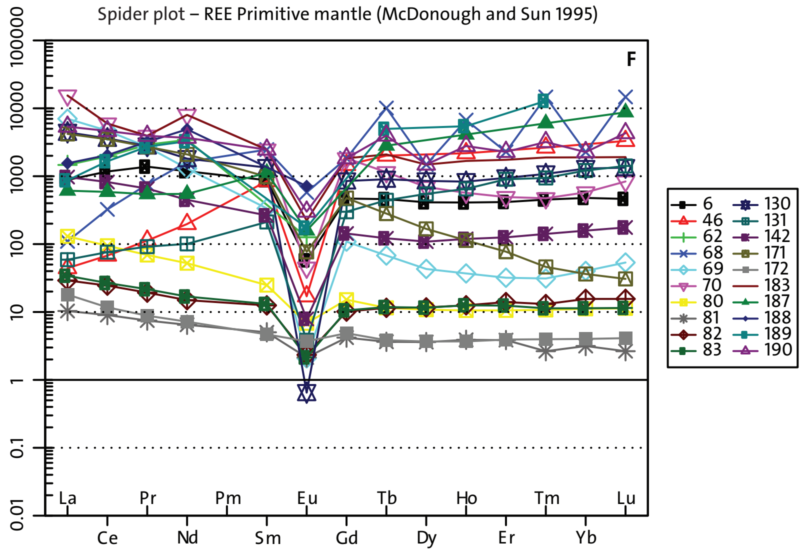

Pegmatite/aplite

Figur 95. Chondrite-normalised (McDonough & Sun 1995) REE patterns of **A.** carbonatites; **B.** lamprophyres; **C.** iron skarn; **D.** iron oxide (sulphide) skarn; **E.** magnetite hematite quartz (BIF); **F.** granitic pegmatites; **G.** nepheline syenite; and **H.** other oxides. The figure continues on the next page.

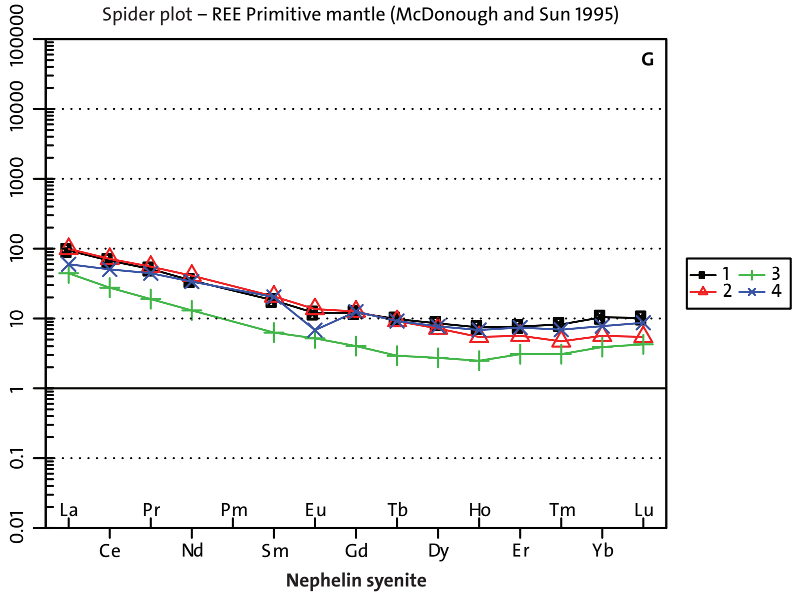

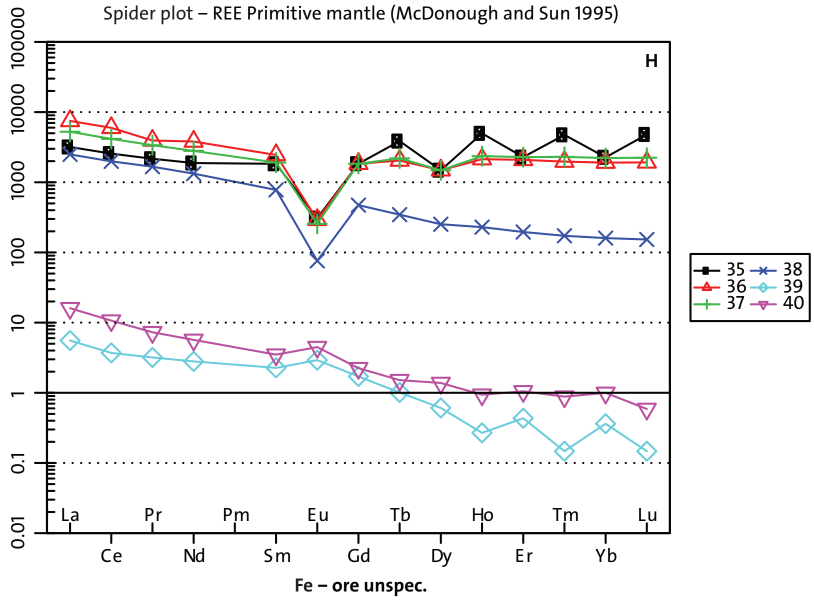

Figur 95. Chondrite-normalised (McDonough & Sun 1995) REE patterns of **A.** carbonatites; **B.** lamprophyres; **C.** iron skarn; **D.** iron oxide (sulphide) skarn; **E.** magnetite hematite quartz (BIF); **F.** granitic pegmatites; **G.** nepheline syenite; and **H.** other oxides. Continuation from the previous pages.

Principal component analysis

Principal component (PC) analysis is a conventional multivariate technique that is often is used for studying geochemical data (Carranza 2008, Grunsky 2010, Sadeghi et al. 2013a). PC analysis reduces a large number of variables to a smaller number, allowing the user to determine the components (groups of variables) that account for variation in multivariate data (Güller et al. 2002). PC analysis has often been used to process and interpret geochemical and other types of spatial data (e.g., Harris et al. 1997, Carranza 2008, Cheng et al. 2011, Sadeghi et al. 2013 a, b). PC analysis is founded on the correlation (covariance) matrix, which measures the interrelationships among multiple variables. The first PC (PC1) explains most of the variance within the original data, and each subsequent PC (PC2–n) explains progressively less of the variance. A multivariate dataset can usually be reduced to two or three PCs that account for the majority of the variance within the dataset.

PC analysis was performed on average values of the different mineralisation types as discussed above. Thirty-seven elements were chosen for PC analysis based on correlation coefficients. The results are reported in Table 11, and show that PC1 and PC2 explain 32% and 13%, respectively, of the total variance among the REE-mineralised samples. It implies that in PC1 there is an association of CaO, Cr_2O_3 and Fe_2O_3, which probably represent iron-oxide apatite and skarn samples, while there is an association of Na_2O-BaO-Hf-Sr, representing REE mineralisations associated with felsic rocks and pegmatite.

The PC2 shows an association of Al_2O_3-Na_2O-LOI-C-Nb-Sr-Ta-Th, which probably represents granite-pegmatite associated with polymetallic mineralisation (Table 12).

Table 11. Principal component loading, eigenvalues, % variance explained and cumulative % variance for PC1 to PC5.

	Eigenvalues of correlation matrix, and related statistics			
Value number	**Eigenvalue**	**% Total**	**Cumulative % eigenvalue**	**Cumulative % variance**
PC1	12	32	12	32
PC2	5	13	17	45
PC3	3	10	21	56
PC4	3	8	24	64
PC5	2	5	26	70

Table 12. Explanation of the five principal components for elements analysed, accounting for 74% of the total variance.

		Log normal transformed data	
Component	**% of variance explained**	**Association**	**Interpretation**
PC1	32	(i) Cao-Cr_2O_3-Fe_2O_3 (ii) Na_2O-BaO-C-Hf-Sr	(i) Iron skarn vs (ii) Felsic rock
PC2	13	(i) Al_2O_3-Na_2O-TiO_2-SrO-LOI-C-Nb-Sr-Ta-Th (ii) MgO-MnO-Er-Ho-Lu-Tm-Yb	(i) Lamprophyre and peralkaline rock (ii) REE enrichment in Mafic rock
PC3	10	(i) CaO-MnO-Dy-Ta-Tb-Th (ii) Na_2O	REE enrichment related to plagioclase content in rock
PC4	8	(i) SiO_2-K_2O-Gd-Nb (ii) MgO-TiO_2-S-Dy-Rb-Tb	(i) Granite pegmatite bearing critical metals (ii) Mg skarn with sulphide mineralisation
PC5	5	(i) Fe_2O_3-Na_2O-P_2O_5-Ce-Er-Ho-La-Tm-Y (ii) SrO-C-Gd-Sm	(i) IOA mineralisation (ii) Carbonatite?

Plots of pairs of PCs have been produced and show that it is possible to distinguish between different types of REE mineralisation or to distinguish between samples with higher concentration of REEs and those with less (Fig. 96). For example, in the plot of PC1 versus PC2 (Fig. 96a) there are several clusters representing an association of REE, iron oxide and rocks associated with Ta-Nb mineralisation. A plot of PC2 versus PC4 distinguishes between REE mineralisation associated with Mg-skarn, Fe-skarn, Ta-Nb-bearing granite-pegmatite and lamprophyre (Fig. 96b). Summarised explanations of the PC plots are given in Table 13.

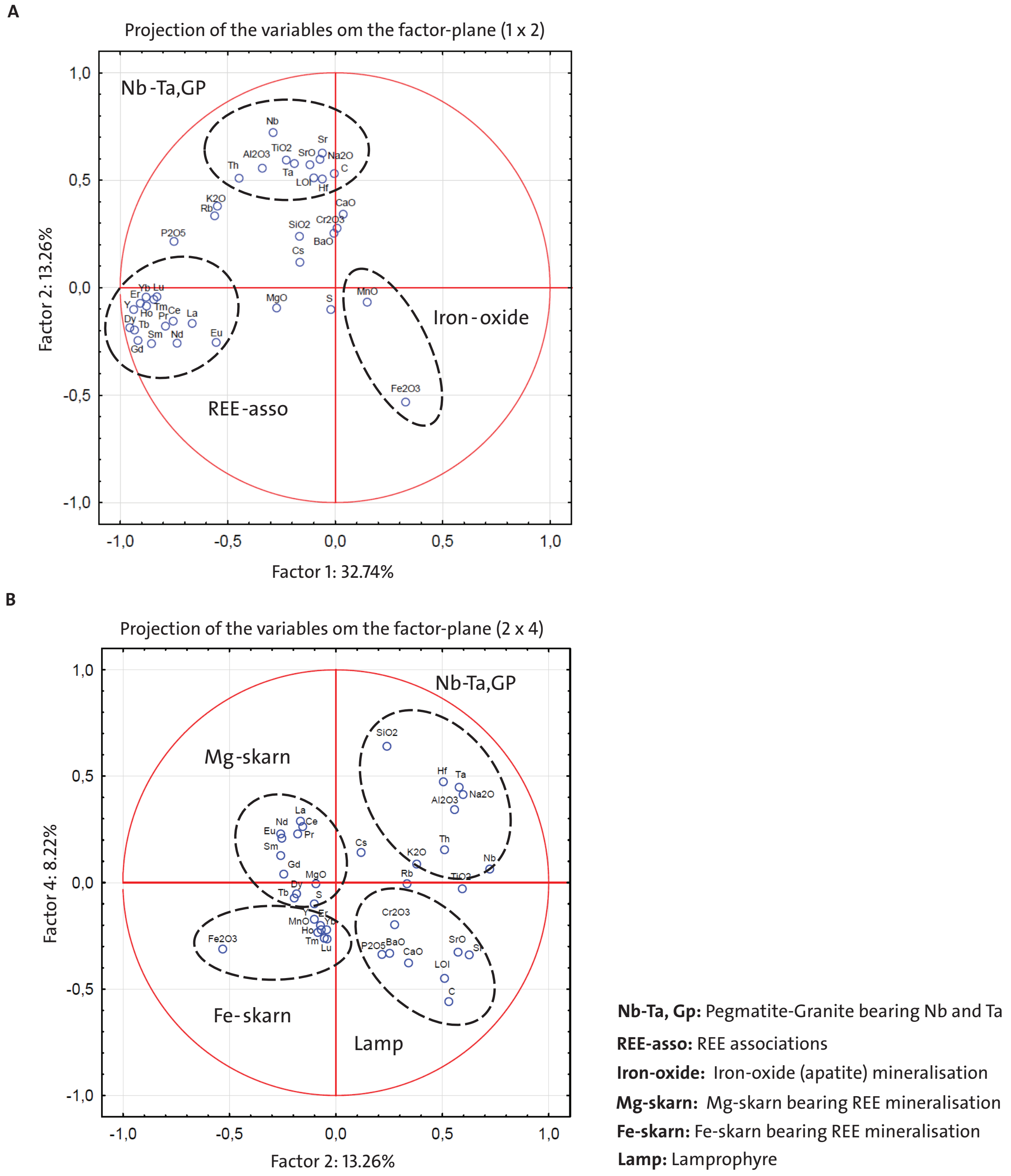

Nb-Ta, Gp: Pegmatite-Granite bearing Nb and Ta

REE-asso: REE associations

Iron-oxide: Iron-oxide (apatite) mineralisation

Mg-skarn: Mg-skarn bearing REE mineralisation

Fe-skarn: Fe-skarn bearing REE mineralisation

Lamp: Lamprophyre

Figure 96. Plots of **A.** PC1 vs PC2; and **B.** PC2 vs PC4.

Table 13. Summary of bivariate plot pairs and eventual interpretation.

Biplots	**Interpretation – distinguish group**
PC1 vs PC2	Lamprophyre-REEs- pegmatite/aplite bearing Nb, Ta
PC1 vs PC3	REE-related apatite ore
PC1 vs PC4	REE-related apatite ore-lamprophyre-Pegmatite/aplite bearing Ta
PC1 vs PC5	REE-related apatite ore
PC2 vs PC3	Granite bearing Nb and Ta-Mg-skarn REE mineralisation
PC2 vs PC4	Lamprophyre-Mg-skarn bearing REE – granite/volcanic bearing Ta and Nb
PC2 vs PC5	Mg-skarn bearing REE – granite/volcanic bearing Ta and Nb
PC3 vs PC4	Iron oxide-apatite mineralisation – non-mineralised lamprophyre
PC3 vs PC5	Non-mineralised granite – REE-related apatite-mineralised lamprophyres
PC4 vs PC5	Non-mineralised granite – mineralised granite enriched in Ta-Nb

CONCEPTUAL MODELS FOR RARE EARTH ELEMENT EXPLORATION IN SWEDEN

Martiya Sadeghi & Magnus Ripa

This section presents a synthesis of major prospecting and exploration methods. Different key criteria for prospecting based on the mineral system framework have been used to form a general conceptual model for each type of REE mineralisation. The models may be used to suggest which method should be used and where to look for new targets. They may also be used to map mineral system factors and in prospectivity analysis methods.

Mineral deposits can be grouped or classified into different types, depending on their characteristics. Each class (which may include considerable variation) can be represented by an idealised mineral deposit, known as a mineral deposit model (Bonham-Carter 1994). Mineral deposits models are conceptual models, usually described in words and diagrams.

Because the deposit model usually focuses on the general characteristics of the geological environment at or near the deposits themselves, the conceptual model for favourability mapping is closer to the "exploration" model (Sadeghi 2008). The deposit exploration model comprises all the deposit model components that provide criteria for exploration and recognition of deposit indicators from data derived from geological, geophysical and geochemical surveys.

A more detailed example of a conceptual model and prospectivity mapping on Bastnäs type REE mineralisation is given at the end of this chapter.

Key exploration criteria

Key exploration criteria for carbonatites

- Identifying and evaluating provinces with alkaline igneous rocks and known carbonatites is a starting point. Carbonatites are primarily found in rift settings but also occur in orogenic belts, such as those within the Qinling orogenic belt of central China.
- Potential geochemical indicators include fenitised wall rock and enrichment in LILE (particularly Ba). Some elements anomalously enriched in carbonatites (P, Nb, REEs, Ti, U, and Th) may reside in relatively resistant minerals, and regional heavy mineral stream-sediment surveys could help to locate targets.
- Geophysical surveys may be useful to identify buried or concealed targets, and a variety of methods (radiometric, magnetic, and gravimetric) can be used to find carbonatite systems. Slight to moderate

enrichment in U and Th relative to host rocks are general characteristics of many carbonatite systems and may be identified by ground or airborne radiometric surveys. Carbonatites may contain radioactive minerals including monazite and pyrochlore, and thus give a positive radiometric signal.

- Mineralisation in carbonatite complexes is often hosted by plugs, cone sheets, flows, dykes, and sills instead of large homogeneous plutons. This feature requires more detailed local-scale exploration methods, such as detailed airborne gravity, magnetic, electromagnetic, and geochemical surveys.
- Since the predominant carbonate minerals (calcite, dolomite) in some cases have greater densities than quartz and feldspar, carbonatites may generate positive gravity anomalies. However, this will largely depend on the densities of the country rocks.
- Geochemical methods (soil, whole-rock, water, overbank sediments) can be used to identify (per) alkaline rock anomalous in indicator elements, such as LREE, Rb, Sr, Ba, U, Th, and F.
- Mapping of alteration zones can be a very efficient method for local-scale targeting.
- Heavy-mineral indicator surveys. REE-bearing minerals, such as monazite, are commonly resistant to weathering. Other heavy minerals, such as pyrochlore, perovskite, zirconolite, and apatite, are associated with carbonatites.
- In general, the best tools for discovering carbonatites may be a combination of aeromagnetic measurements followed by closer-spaced magnetic studies, drilling and geochemical analysis of the REE-enriched zone. An example of this approach is the targeting of carbonatite in Australia (Dentith et al. 1994)

Key exploration criteria for REE deposits in alkaline/peralkaline rocks

- Tectonic environment: The deposits and their peralkaline host complexes typically occur in continental anorogenic tectonic settings and are associated with zones of rifting and/or faulting.
- Mineralogy: Peralkaline complexes, particularly those that are mineralised, may contain relatively rare but colourful indicator minerals. According to Richardson & Birkett (1996), these potentially useful minerals include eudialyte (pink/red), sodalite (dark blue), aegirine (dark green), riebeckite/arfvedsonite (dark bluish-green), and fluorite (purple).
- Geochemistry: Peralkaline rocks associated with REE mineralisation have anomalously high concentrations of REE, Zr, Hf, Nb, Ta, Th, U, and F compared with most granitic rocks (Bowden 1985, Linnen & Cuney 2005). The elevated abundances of these elements typically contrast with regional background concentrations (Richardson & Birkett 1996), and are useful reconnaissance indicators of the mineralisation during geochemical surveys of stream sediments, residual soils, and rocks (Richardson & Birkett 1996, Verplanck et al. 2014). Regional lake water surveys revealed that F, U, and Pb can be useful pathfinders for REE mineralisation (Richardson & Birkett 1996).
- Geophysics: Ground and airborne geophysical exploration methods are excellent exploration tools for these deposits. The REE deposits are enriched in U and Th, and their inherent radioactivity makes gamma-ray (radiometric) survey an effective exploration tool. In fact, many known REE deposits/advanced exploration projects (e.g., in Greenland) were discovered during the search for uranium deposits (Verplanck et al. 2014). Magnetic and gravity surveys can be used to locate peralkaline intrusions; their anomalies do not reflect REE mineralisation but are typically produced by the magnetic and density characteristics of intrusions. Distinct magnetic and gravity anomalies can delineate igneous bodies or tectonic lineaments. Detailed geophysical exploration techniques (magnetic, radiometric, gravity, and aeromagnetic) can locate density, magnetic, and conductivity contrasts generated by fluid flow.
- Mapping of alteration zones can be effective for local-scale targeting.

Key exploration criteria for REE mineralisation in granitic pegmatite

Exploration for rare-element pegmatites has been conducted successfully based on current models for pegmatite zonation and the signatures of chemical alteration around pegmatite bodies (London 2016). A summary of key criteria for REE exploration in pegmatite are:

- Regional zonation of pegmatite compositions (of the LCT family) with distance from source.
- Chemistry of border zones: An explanation for the compositions of the border zones, which are far from the bulk composition of the pegmatite-forming melt, yet commonly saturated in beryl, apatite, tourmaline, garnet, and columbite, was presented as the "subsolidus isothermal fractional crystallisation" concept by London (2014a, 2014b).
- The compositions of pegmatitic micas and K-feldspar have been similarly used to assess the extent of chemical fractionation in a pegmatitic body. Smeds (1992) augmented the existing databases on trace-element content of pegmatitic muscovite by studying unmineralised (common) pegmatites as well as those proved to be rich in Li, Be, and Sn.
- Exogenic chemical halos: Galeschuk & Vanstone (2005) suggested that a geochemical survey of soil horizons may be a useful tool. They defined "combination anomalies," i.e. positive concentration anomalies directly above the body of the mineralised pegmatitic granite and on its flanks. Two of the most geochemically mobile elements, Rb and Cs, form combination anomalies, along with two of the most immobile elements, Re and Ti.
- REE-bearing NYF-type pegmatites are subaluminous to metaluminous (rarely subalkaline). The major element geochemistry of pegmatites can distinguish pegmatites as indicators of prospective REE deposits.
- Most REE-bearing pegmatites are characterised by anomalous concentrations of uranium and thorium and thus create positive radiometric anomalies, both when the pegmatites crop out and when they are buried under a shallow cover. Fertile pegmatites are enriched in LREE, Nb, Ta, F, P, Zr, and Li.
- Geochemical surveys (soil, overbank, bedrock, stream sediments and water, and ground water) can be an effective way of mapping prospective areas.

Key exploration criteria for REE mineralisations in skarn

- Geophysical techniques (magnetic, gravity) which can map regional-scale and lower-order faults that may have acted as fluid conduits.
- Radiometric survey to map positive anomalies caused by anomalous concentrations of uranium and thorium in these deposits.
- Most skarn deposits are enriched in iron oxides (magnetite and hematite) and commonly have positive magnetic and gravity anomalies.
- Geochemical survey (bedrock, soil, and water) to map halo of dispersed elements (REE, P, F, U, Th).

Key exploration criteria for iron-oxide breccia complexes

- Major deposits of this type are controlled by large regional-scale structures and lineaments, which can be mapped using geophysical techniques (gravity, magnetic, seismic, magnetotelluric).
- Most Olympic Dam-style deposits of this type are associated with A-type uranium-rich melts. Major and minor element geochemistry of felsic rocks can identify prospective intrusive-volcanic complexes.
- The presence of iron-rich (meta-) sedimentary rocks are a common feature of many mineralised districts. Mapping of such rocks using geophysical techniques (magnetic and gravity) can delineate regional-scale prospective targets.
- Mineral deposits of this type are known to have coincident, but offset gravity and magnetic anomalies.

- Hydrothermal-mineralised systems associated with deposits are known to form extensive alteration haloes.
- Since deposits of this type are often enriched in uranium and thorium, they form positive radiometric anomalies.
- Relatively large hydrothermal systems create haloes of dispersed elements around these deposits. The haloes can be mapped by geochemical (bedrock, soil, stream sediments, stream, and ground water) surveys.

Conceptual model for rare earth element exploration in Bergslagen

A conceptual model on REE mineralisation in Bergslagen is described in this section. Understanding structures and relationship of different types of host rock and REE mineralisation is a key issue, so a summary on detailed mapping carried out during the EURARE project of a few deposits in Bergslagen focusing on REE mineralisation is presented.

Detailed bedrock mapping with focus of REE mineralisations in Bergslagen

In September 2015 three weeks were spent mapping the bedrock at and around some documented occurrences of REE-bearing minerals along the "REE line" (Jonsson & Högdahl 2013) in Bergslagen, Sweden (Fig. 97). From southwest to northeast along this line, these are predominantly iron mineralisations at the Stora Rödbergsgruvan, Bastnäsfältet, Stora Malmkärragruvan, Johannagruvan and Östanmossagruvan deposits. Sampling at the Kuså Cu-Ni deposit was also performed during this period.

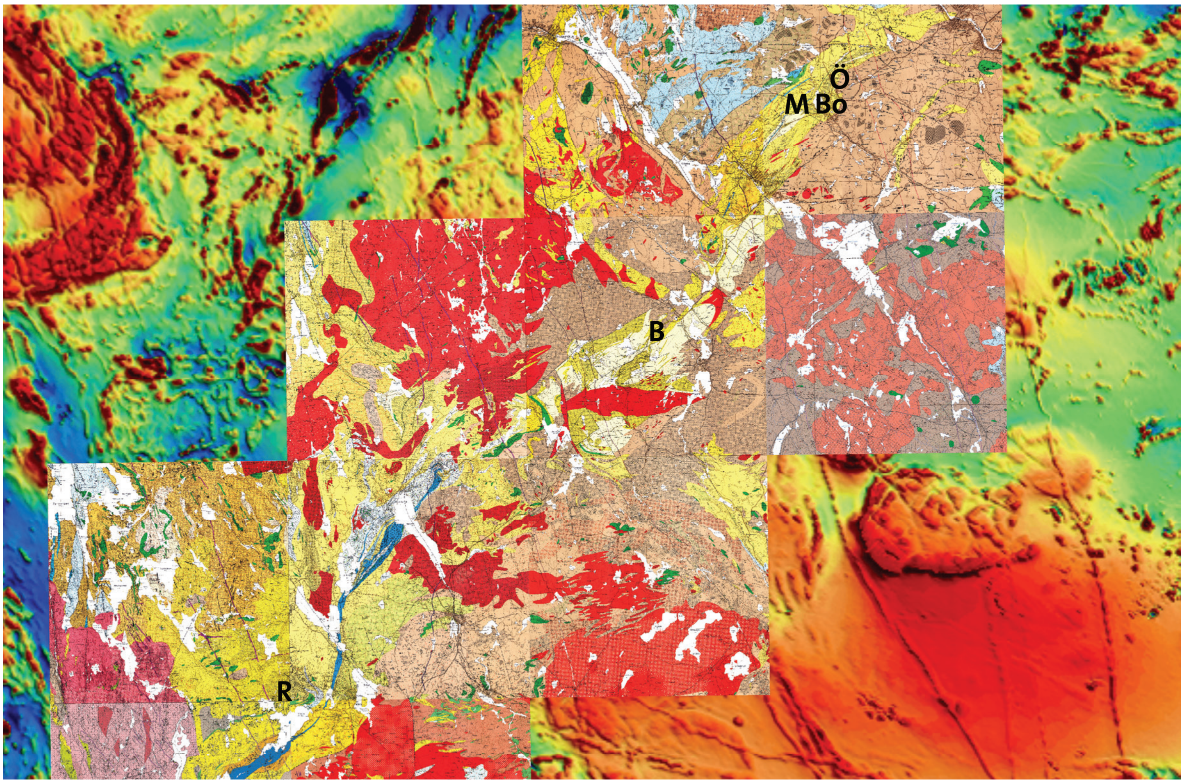

Figure 97. The approximate extent of the REE line on bedrock maps (scale 1:50 000) published by the Geological Survey of Sweden and a background of the aeromagnetic anomaly map. The extent of each bedrock map is 25 x 25 kilometres, north is up. R denotes Rödbergsgruvan, B – Bastnäs, M – Malmkärra, Bo – Bojmossfältet and Ö – Östanmossa.

Geology

The geology of the area at **Stora Rödbergsgruvan** is shown in Figure 98. The background in this illustration is the bedrock map by Stephens (1998). The bedrock of the area predominantly comprises intensely hydrothermally altered, mica-rich felsic metavolcanic rocks. In places, they carry cordierite and anthophyllite. The precursors locally seem to have been heterogeneous at cm scale. On better preserved outcrop surfaces, it may be seen that the heterogeneity may be due to both a volcanic breccia origin and boudinage of bedding.

Outcrops along the southeast shore of lake Fogdhyttetjärnen consist of a red, fine-grained, isotropic granite to quartz monzonite. Metabasic rocks, probably dykes, as shown on the map by Stephens (1998), occur in the area.

The predominant mesoscale structure is a moderately to shallowly plunging lineation trending east-northeast. Locally, the lineation is an F2 axis along which an S1 foliation is folded or crenulated at cm scale. Outcrops showing a crenulated foliation are presumably situated in F2 fold hinges, whereas outcrops showing just one foliation occur in the limbs where the strikes of S0, S1 and S2 are largely parallel. The F2 axial surfaces and S2 are apparently vertical. The S1 foliation is mica-dominated and shows that hydrothermal alteration was pre- or syn-D1.

The present interpretation of the map scale structure of the area depicted in Figure 98 is a D2-folded F1 syn- or anticline with its approximate centre line indicated by a broken blue line on the map. The areal distribution of slightly more well-preserved rocks suggests that the structure is most likely a syncline.

Pegmatite veins are parallel to the S1 foliation.

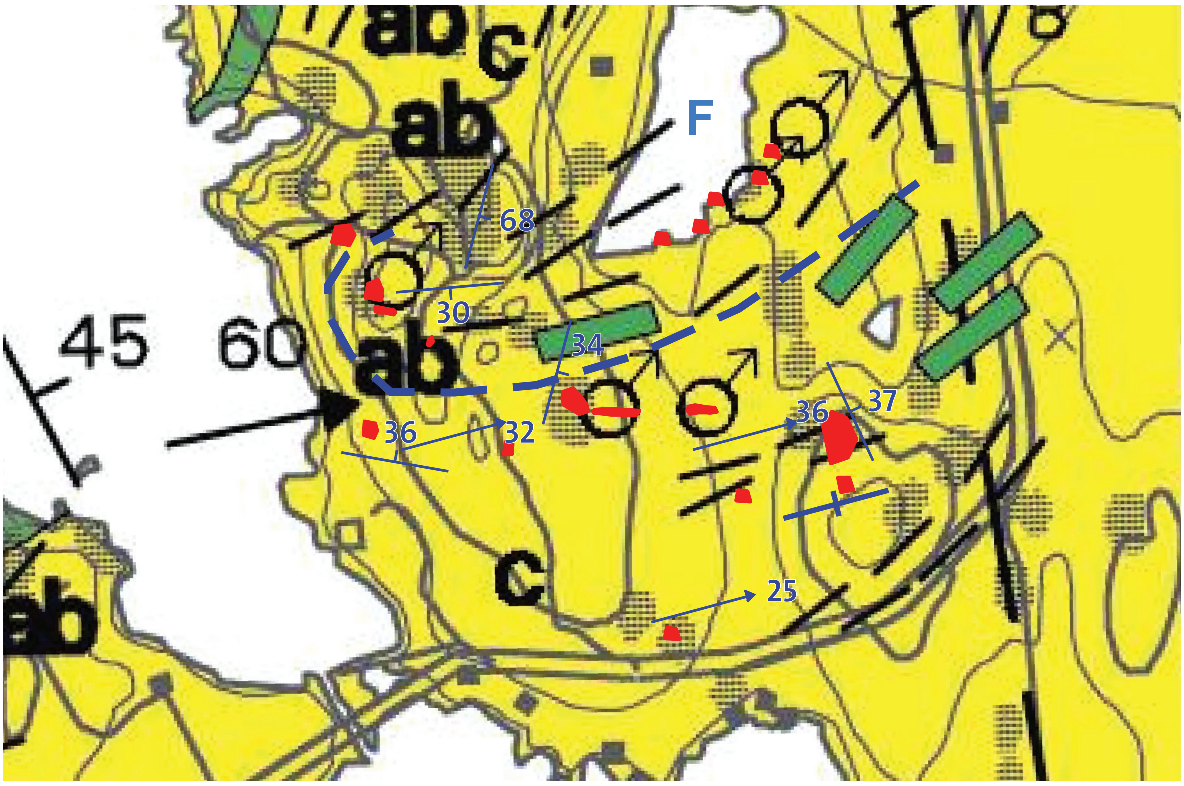

Figure 98. The area around Stora Rödbergsgruvan. F denotes lake Fogdhyttetjärnen. The background bedrock map is by Stephens (1998). The width of view is approximately 1.5 km, N is up. Red dots are observed outcrops and pits in this study. The blue structural symbols and broken line are measurements and interpretation by this study.

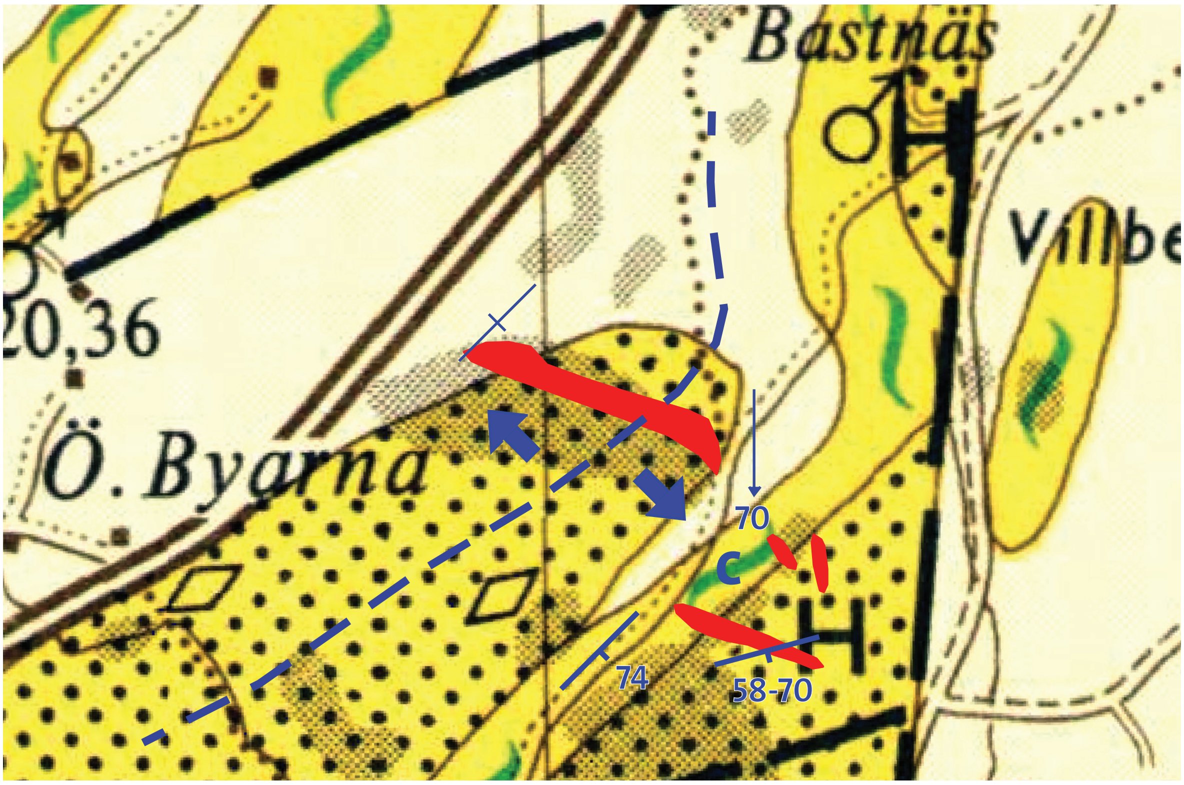

Figure 99. The geology of the Bastnäs area. The background is the bedrock map by Ambros (1983). Red areas are mapped outcrops and blue symbols are additional structural data from this study. C denotes cordierite-bearing. The view is approximately 1.5 km wide. N is up.

The geology at **Bastnäs** is shown in Figure 99, which is based on the map by Ambros (1983). The rocks of the area predominantly comprise volcanic breccias that grade into volcanic siltstone. The latter is variably hematite- and skarn-banded. The volcanic breccias are of two types, and appear to form an anticline west of the mineralised strata at Bastnäs. In the centre of the inferred anticline the breccia is a lithic clast-bearing volcanic sandstone. The clasts are scarce, cm-sized and consist mainly of volcanic sand- to siltstone. Pumice-looking clasts, about 10 cm in diameter, occur in a few places. Overlying this unit is another breccia of volcanic siltstone with abundant, pumice-looking clasts, about 10 cm in diameter. The breccias are slightly to moderately mica-altered. The overlying volcanic siltstone formation is locally cordierite-bearing in the lower parts, but grades upwards into the above-mentioned hematite- and skarn-bearing varieties. The cordierite porphyroblasts appear to occur in D2-folded bands in some places, but in others seem to be largely syn-D2. They may originally have been pre-D2 but then recrystallised during that phase.

The mineralised parts are approximately 200 m thick, south of and at the Gamla Bastnäsfältet mines and grade from hematite-banded volcanic rock to skarn-banded hematite, in both cases the banding is from mm to cm scale. No signs of original carbonate rocks can be seen in this part of the ore field.

As mentioned above, the predominant map scale structure is a north-dipping anticline (approximate position marked by a broken line in Fig. 99). Mesoscale structures are steeply and predominantly south-plunging lineations and northeast to north-northeast-striking bedding in the siltstone facies.

The geology at the Stora **Malmkärra** and Plåtängsgruvan mines is shown in Figure 100. The background is the bedrock map by Ambros (1988). The rocks to the east of a mineralised (carbonate?) horizon (blue in Fig. 100) are intensely and pervasively mica-altered and have a presumed volcanic origin. Locally, they are cordierite-bearing. The mineralised horizon is green amphibole- and magnetite-altered and hosted by skarn-bedded volcanic siltstone and, at Plåtängsgruvan, skarn-altered quartz-phyric metarhyolite.

A reworked, volcanogenic breccia to conglomerate occurs west of the approximately 10-m-wide,

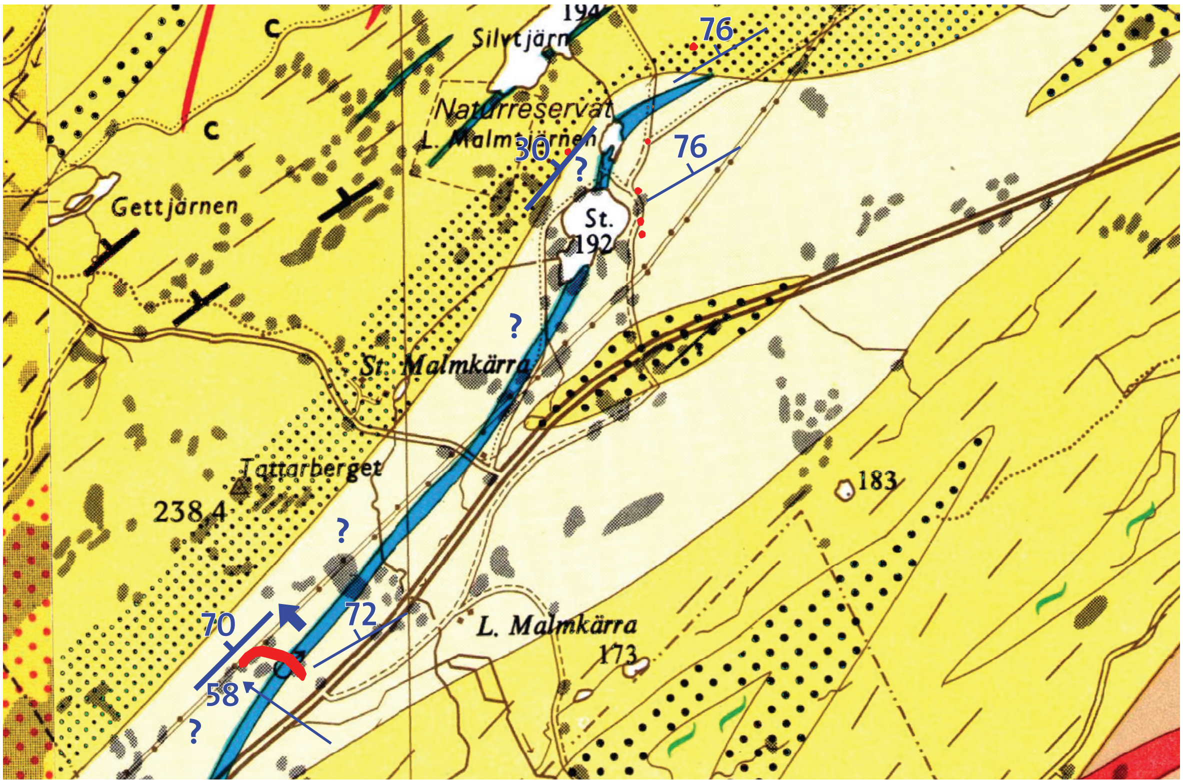

Figure 100. The geology of the Malmtjärnen-Plåtängsgruvan area. The background is the bedrock map by Ambros (1988). Red dots and lines (except those in the uppermost part of the map) denote outcrops investigated in this study. The arrow denotes interpreted younging direction. Additional structural measurements in blue. Question marks west of carbonate rock horizon (in blue) denote our interpretation that the rocks here are generally less mica-altered than those east of it. The view is approximately 4.2 km wide. N is up.

mineralised horizon at Plåtängsgruvan mine. It is heterogeneously (slightly to moderately) mica-altered and only locally altered to the same extent as the strata east of the mineralised horizon. In addition, it is sparsely but penetratively magnetite-altered. The alteration pattern and possible grading in the beds suggest that stratigraphic up is to the west. The rocks west of the mineralised horizon at Malmkärra are harder to interpret, but volcanic siltstone, quartz-phyric metarhyolite and volcanic breccia all occur. Some blasted outcrops, probably related to prospecting, are found west of lake Lilla Malmtjärnen (Fig. 100).

The predominant tectonic structure is an S2 foliation, which is the axial plane in a tightly to isoclinally folded mica foliation. This shows that mica alteration was syn-D1 at the latest.

The **Johannagruvan** mine, the Bojmossfältet ore field and the Östanmossagruvan mine are among deposits occurring in and around the village of Norberg (Fig. 101). However, none of the pits at the Johannagruvan or Östamossa mines is readily accessible, and no outcrops are accessible either, so this investigation concentrated on their surroundings instead.

Southwest of the Johannagruvan mine lies the Bojmossfältet ore field (by "Karlberg" in Fig. 101). Here the rocks are equigranular to sparsely quartz-phyric and biotite-altered felsic metavolcanic rock and volcanic siltstone. The former rock may represent a volcanic sandstone facies (or a largely aphyric coherent facies). The volcanic siltstone has banding of locally magnetite-bearing hematite. These bands have been mined in places. According to Geijer (1936), the mineralisation at the Johannagruvan mine was hosted by skarn.

The Östamossagruvan mine is situated west of the word "Åsgruvan" in Figure 101. Similar hematite-bearing (with some magnetite) volcanic siltstones as in the Bojmossfältet ore field occur west of the mine, although here they are also skarn-bearing in places. According to Geijer (1936), the Östanmossagruvan mineralisation is hosted by skarn. Orange, medium-grained calcitic marble and fine-grained, magnetite-

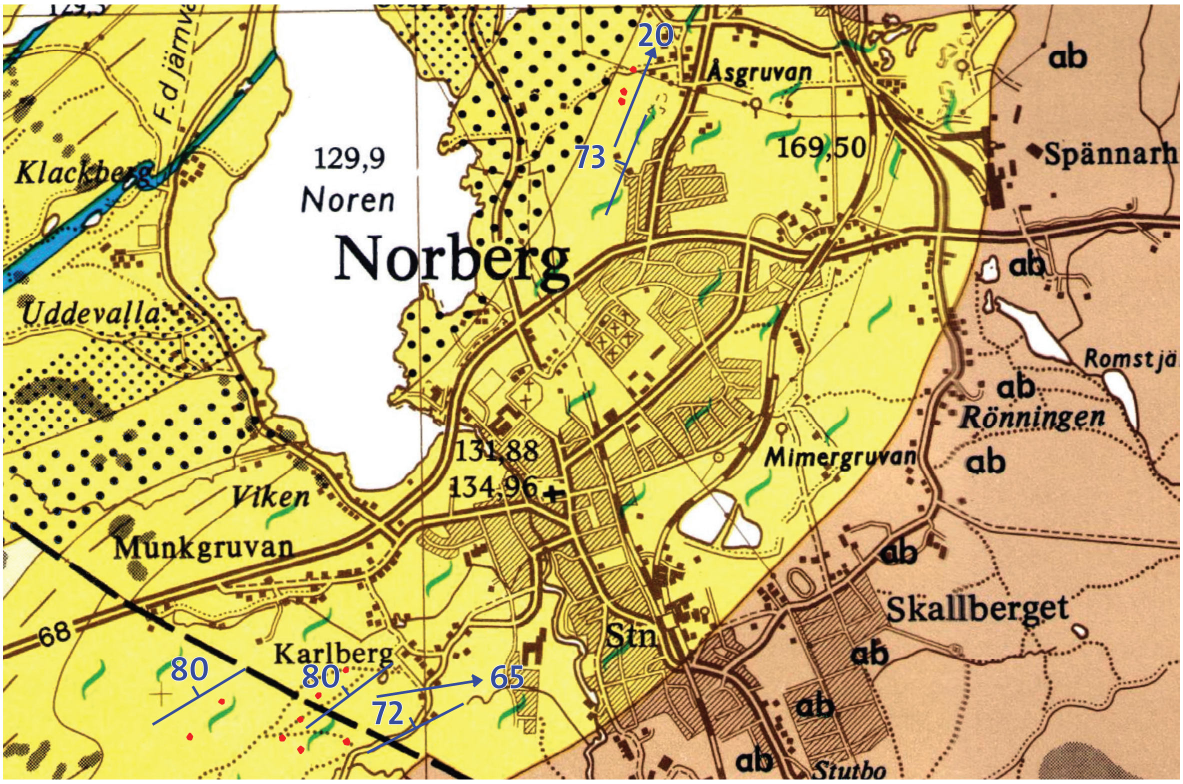

Figure 101. Geology of the Norberg area. The background is the bedrock map by Ambros (1988). Small, red dots denote outcrops investigated in this study. Additional structural measurements in blue. The view is approximately 4.5 km wide. N is up.

bearing skarn occur in dumps by the remains of the old railway track just west of the mine. Fold axes in this area dip shallowly towards the north, and some of the repetition of mm- to 10-cm-wide mineralised beds is due to tight folding along these axes. The northernmost outcrop visited shown in Figure 101 has contact between volcanic siltstone and a red, quartz-phyric metavolcanic rock.

Aeromagnetic data

The aeromagnetic anomaly map of the REE line area of Bergslagen is shown in Figure 102. The most conspicuous feature on this map is the band of highly magnetic rocks that stretches from southwest to northeast. It represents some of the variably magnetite-bearing mineralisations of the area. The white circles in Figure 102 show the positions of the Rödbergsgruvan mine, the Bastnäs ore field and the deposits in Norberg as described above from southwest to northeast.

According to Stephens et al. (2009), the southwest–northeast trend shown by the magnetic data (Fig. 102) is the general trend of S2 foliation in this part of Bergslagen. The magnetic anomaly pattern is openly s-folded, suggestive of sinistral shearing in relation to the D2 deformational event. Some of the known REE-bearing deposits appear to be localised at specific portions of these s-shaped kinks, namely close to where the pattern turns more northerly going from southwest to northeast.

Some west-northwest–east-southeast-trending lineaments (marked by white broken lines) may be interpreted from the magnetic anomaly map (Fig. 102). The Knutsbo deposit (marked K) lies along the northernmost of these lineaments. The Knutsbo deposit is REE-bearing. The country rocks at Knutsbo are intensely foliated to mylonitic with a trend parallel to that of the lineaments, which suggests that the lineaments represent ductile shear zones.

In addition to their locations at kinks of the general S2-trend, the REE deposits at Bastnäs and Norberg are situated close to a west-northwest–east-southeast-trending lineament.

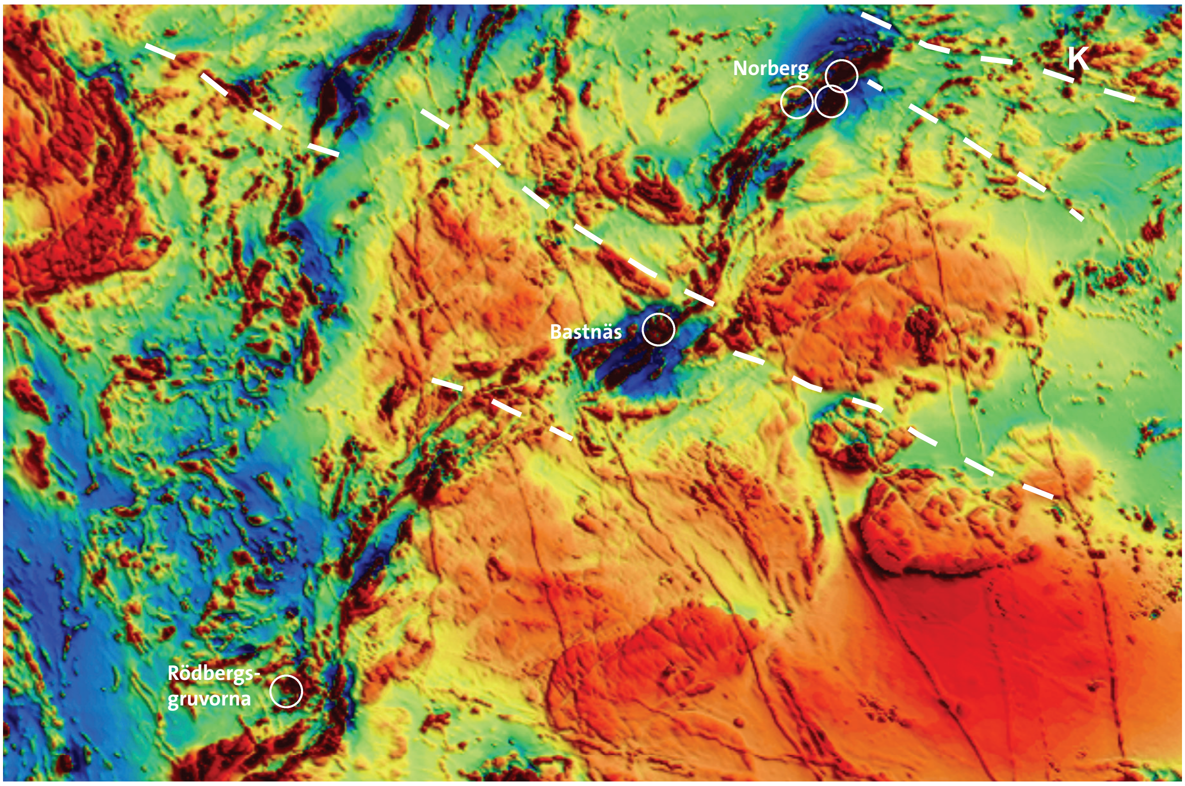

Figure 102. Aeromagnetic anomaly map of the REE line area. White circles mark locations of known REE mineralisations. Broken white lines mark interpreted lineaments. K marks the location of the Knutsbo REE deposit.

Interpretation

It is evident from the descriptions by Geijer & Magnusson (1944) of the REE-bearing mineralisations mentioned above that almost all occur in close proximity to original banded iron formations (BIFs). The BIFs were largely overprinted by hydrothermal processes that, to a varying extent, formed skarn and reduced some of the original hematite to magnetite. However, some of the deposits are also associated with skarn-altered carbonate rocks, and no BIF is evident in the Malmkärra-Plåtänggruvan area. The country rocks of the REE line area were also intensely altered on a semi-regional scale.

Field observations suggest that the above hydrothermal alteration occurred before, or least synchronously with, D1-deformation and the formation of S1. On the other hand, the spatial distribution of the REE mineralisations in relation to structures revealed by the aeromagnetic data suggest that their formation was somehow related to the phase of D2-deformation, or to processes coeval with it, and was thus probably later than the phase of intense and semi-regional hydrothermal alteration.

However, since most REE mineralisations of this type in Bergslagen are found in this area, and less so elsewhere, it seems likely that 1) the presence of BIFs and carbonate-skarn strata, 2) the phase of intense and widespread hydrothermal alteration, and 3) processes at the time of D2 together were somehow crucial to the formation of these REE mineralisations. The BIFs, with local skarns and carbonate rocks, may have served as trap rocks during any phase of alteration since their formation. The phase of hydrothermal alteration may locally have led to initial LREE enrichment of the country rocks as described elsewhere (e.g. MacLean 1988). Metamorphic to metasomatic processes during M2/D2 may have formed fluids that released the REEs from the country rocks and then precipitated them in trap rocks at certain structurally favourable sites.

Prospectivity mapping for REE mineralisation in Bergslagen

One of the major strengths of a GIS is the ability to integrate and combine multiple layers of geoscience data. Once the data have been properly prepared, the GIS can be used in combination with other statistical and geostatistical methods to manipulate and visualise them. One obvious geological application for GIS is to produce mineral potential maps showing favourable areas for mineral exploration (Carranza & Sadeghi 2010). There are two approaches to predictive prospectivity mapping: the "mechanistic modelling approach" and the "empirical modelling approach".

- **Mechanistic approach:** The mechanistic approach, also known as the "theoretical approach", is basically sub-divided into two kinds, namely deterministic and stochastic mechanistic modelling. Both models use a mathematical approach, which in a mineral prospectivity mapping context would show relationships and controls on ore-forming processes. A significant difference between the two types of mechanistic approach is that the deterministic model does not consider randomness when working out the distribution of predictor variables in the target variables, whereas the stochastic model does. In terms of results, the stochastic model produces a probability distribution for the target variables, whereas the deterministic model produces a single estimate for them (Caranza 2008).
- **Empirical approach:** An empirical model characterises or quantifies empirical relationships between the target variables and a number of predictor variables. This model is particularly useful for mapping prospectivity where the controls on the ore-forming processes are poorly or indirectly known. There are two types of empirical model, namely quantitative and qualitative empirical, and selecting the one to use to map mineral potential depends entirely on the amount of data available. The quantitative empirical model is also known as a data-driven model. This is because it requires ample data on both target and predictor variables to estimate their relationships accurately. On the other hand, the qualitative empirical model, also termed a knowledge-driven model, is most suitable when data are insufficient or lacking and where the relationships between the target and predictor variables are generally determined on the basis of expert opinion (Carranza, 2008; Carranza & Sadeghi 2010).

Key exploration criteria for REE mineralisations in Bergslagen

Bastnäs-type rare earth element deposits are magnetite skarn-hosted silicate mineralisations that variably also contain Fe oxide-REE-Cu-(Co-Au-Bi-Mo). This mineralisation type occurs within an approximately 100-km-long, discontinuous belt of mostly strongly altered, c. 1.90–1.87 Ga felsic metavolcanic and meta-sedimentary rocks in the Nora–Riddarhyttan–Norberg area. The belt was called the "REE-line" by Jonsson et al. (2013). The REE silicate-bearing mineralisations generally occur as seemingly epigenetic, massive to disseminated magnetite-skarn replacements in dolomitic marbles (Holtstam 2004). Based on slight local differences in the chemistry and mineralogy of the deposits, Holtstam & Andersson (2007) suggested a subdivision of the Bastnäs-type deposits into two subtypes: those mainly enriched in LREE and Fe-rich silicates, and those enriched in LREE and HREE+Y together with Mg, Ca and F (Holtstam & Andersson 2007).

Apatite-iron oxide deposits are another type of REE-bearing mineralisation in the Bergslagen region. They have been classified as being of the Kiruna-type, since they show similarities to the type locality at Kirunavaara in northern Sweden, in their geological features, host rock relationships, mineralogy, geochemistry and geometry. The host rocks are mainly intermediate to felsic metavolcanic and meta-subvolcanic rocks. Iron oxide-apatite mineralisations only occur in the west of Bergslagen, along an approximately 40-km-long, southwest–northeast-trending zone from Grängesberg through Blötberget to Idkerberget (Fig. 103).

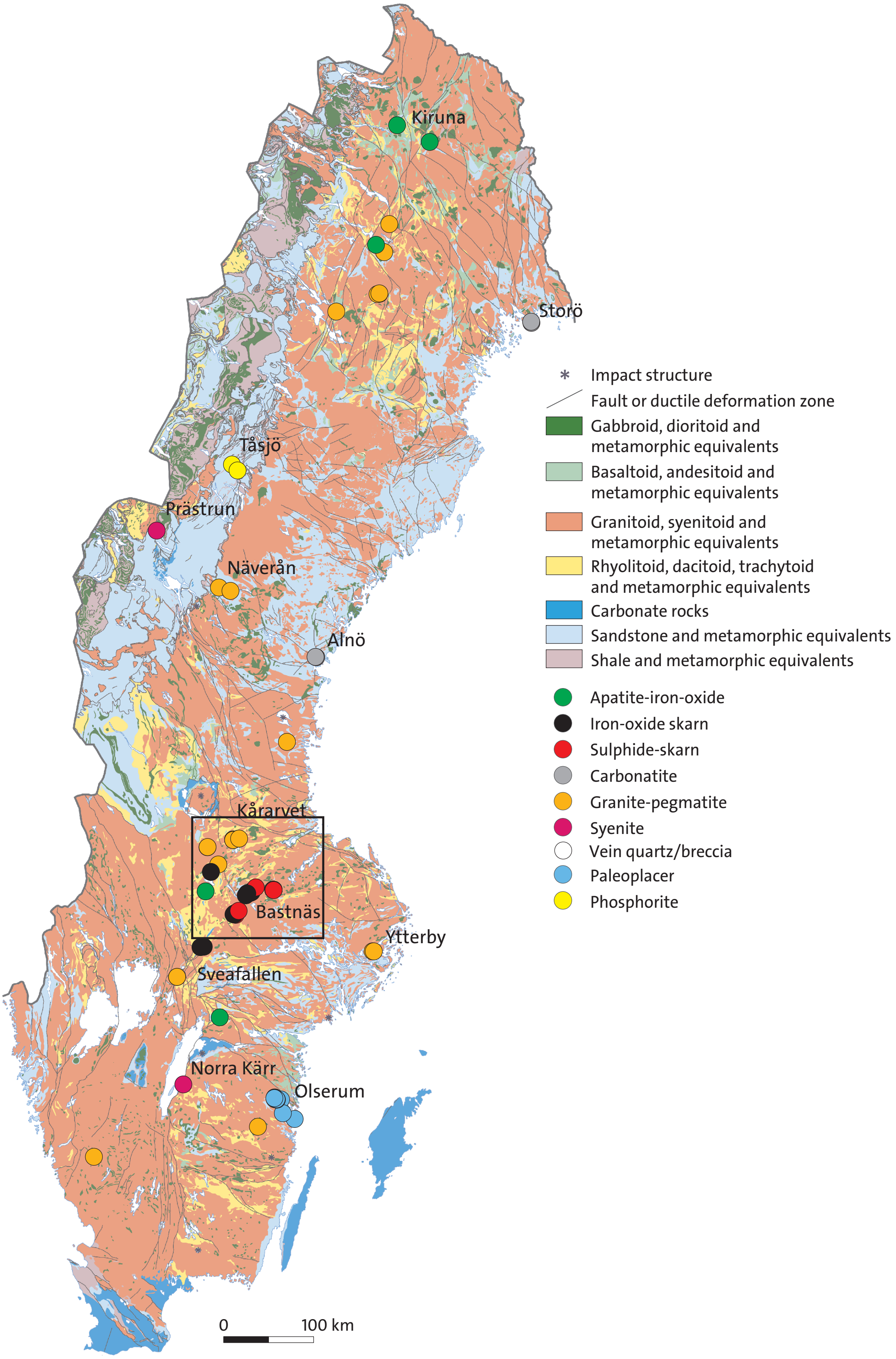

Figure 103. Simplified geological map and classified REE mineralisations in Sweden. The study area is marked by the black rectangle. (Source: SGU, Mineral resources database)

Methodology and Results

The present investigation demonstrates a technique to define favourable areas for REE mineralisation associated with skarn in the Bergslagen region. Here, a weighted overlay technique has been used, and favourable layers have been chosen based on a conceptual model focusing on a mineral system approach using geological (including structures and alteration patterns), geochemical and geophysical factors (Sadeghi et al. 2017b, Sadeghi 2017). A conceptual model for skarn-type REE mineralisation in Bergslagen may be:

- **Lithostratigraphic factor:** Spatial association with felsic metavolcanic or subvolcanic rocks with calc-alkaline affinity (1.9–1.87 Ga). The analysis shows that volcanic rocks with a skarn or limestone contact and close proximity to banded iron formations should be expected to be favourable areas (trap rocks) for REE mineralisation.
- **Geochemical factor:** Positive spatial association with higher concentrations of Fe, Mg and Y and spatial association with P may be related to REE mineralisation.
- **Geophysical factor:** A one-dimensional scatter plot of geophysical values shows a positive spatial association with high total magnetic intensity. The aeromagnetic anomaly map of the REE line part of Bergslagen shows a band of highly magnetic rocks stretching from southwest to northeast. This band represents some of the variably magnetite-bearing mineralisations of the area.
- **Alteration factor:** Mineralisations occur in rocks showing K, Na and/or Mg alteration. Calculated alteration index (AI) or chlorite-pyrite-plagioclase index (CCPI) are therefore good tools for detecting regional alteration possibly related to mineralisation in the area. Rocks are either enriched or depleted in K, Na and Mg. At the regional scale, mineralisations are generally associated with BIFs and skarn-altered carbonate rocks.
- **Heat source factor:** Synvolcanic or intrusive rocks with ages of both c. 1.9–1.87 and c. 1.8 Ga may act as engines driving hydrothermal fluids.
- **Structural factors:** According to Stephens et al. (2009), southwest–northeast is the general trend of S2 foliation in this part of Bergslagen. The magnetic anomaly pattern is openly s-folded, suggesting sinistral shearing in relation to the D2 deformational event. Some of the known REE-bearing deposits appear to be located at specific points along these s-shaped kinks, namely close to where the pattern turns more northerly going from southwest to northeast. On the other hand, the spatial distribution of the REE mineralisations in relation to structures revealed by the aeromagnetic data suggests that their formation was somehow related to the phase of D2-deformation, or to processes coeval with it, and was thus probably later than the phase of intense and semi-regional hydrothermal alteration.

A predictive target map for REE mineralisation based on the conceptual model and available data may provide useful spatial information for exploration of skarn-hosted REE in the Bergslagen district and is shown in Figure 104.

In summary, since most skarn-related REE mineralisations in Bergslagen are found in this area, and less so elsewhere, it seems likely that: 1) the presence of BIFs, skarn and limestone, 2) the phase of intense and wide-spread hydrothermal alteration, and 3) processes at the time of D2 together were somehow crucial to the formation of REE mineralisations. The BIFs, with local skarns and carbonate rocks, may have served as trap rocks during any phase of alteration since their formation. The phase of hydrothermal alteration may locally have led to initial LREE enrichment of the country rocks as described elsewhere (e.g. MacLean 1988). Metamorphic to metasomatic processes during M2/D2 may have formed fluids that released the REEs from the country rocks and then precipitated them in trap rocks at certain structurally favourable sites.

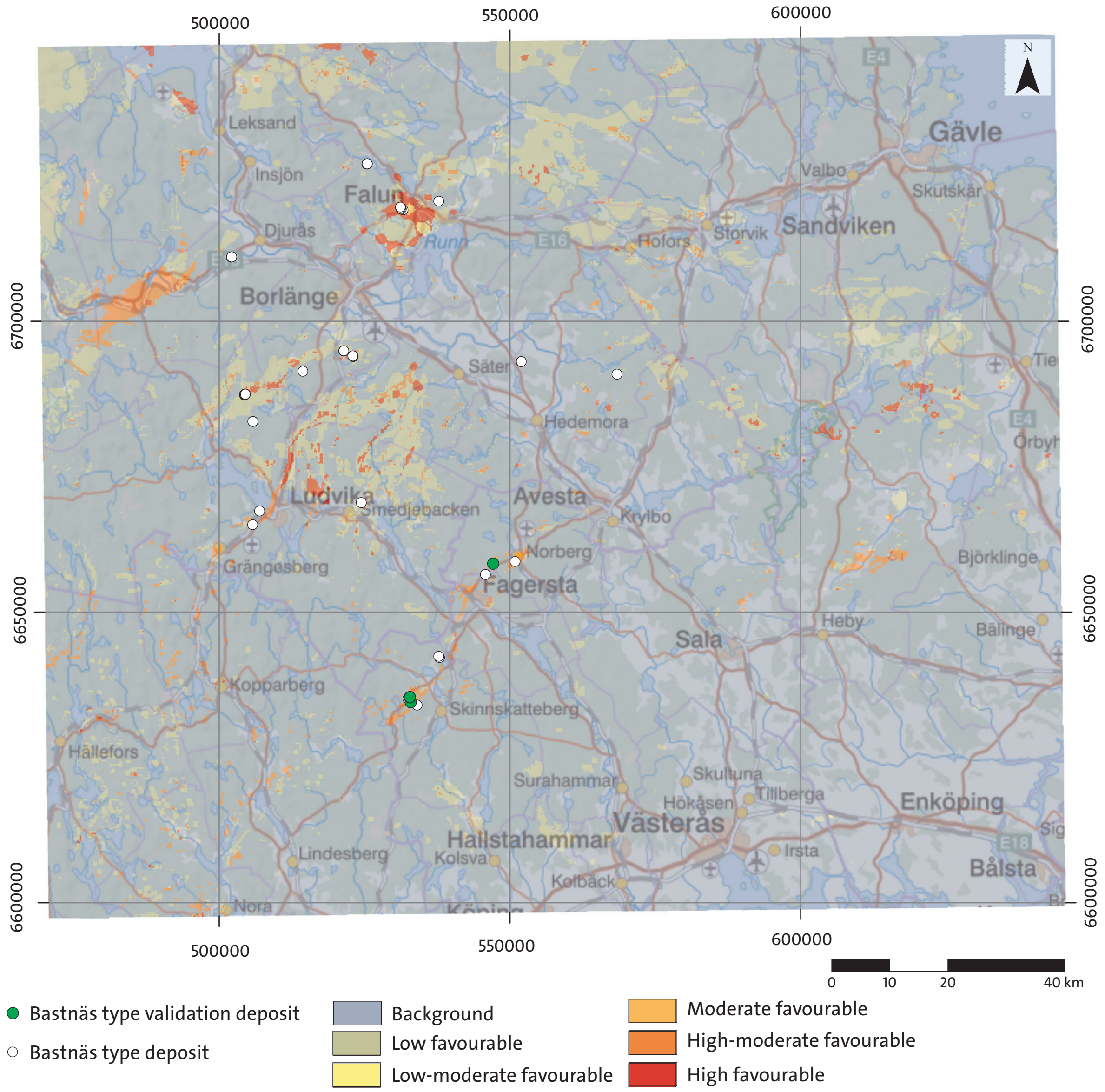

Figure 104. Relative degree of prospectivity for skarn-hosted REE mineralisation in Bergslagen.

A conceptual model for Kiruna-type REE mineralisation in Bergslagen may be:

- **Lithology:** Dacite to rhyolite, and andesite are the known primary host rocks for the apatite-iron ores. Intermediate-felsic metavolcanic rocks (1.90–1.87 Ga) are indicative of REE mineralisation.
- **Mineralisation:** Mainly hosted by magnetite-bearing ores (80%) and a minor component by hematite-bearing ores (20%). Fluorapatite is known to be the most important mineral for the high REE content in apatite-rich ores. The apatite-rich ore samples are those that have the highest ΣREE contents in this study.
- **Geophysics:** Positive gravimetrical anomaly, magnetic anomaly.
- **Geochemistry:** Positive spatial association with Cu and Zn anomalies.
- **Alteration:** Enriched in Th, U, La, Ce, Nd, P, Fe, Sm, Tb, Y, Tm, and Yb and depleted in K, Ba, Sr, Zr and Ti. Negative Eu anomalies and flat HREE patterns.
- **Heat source:** Magmatic and hydrothermal fluids. Subvolcanic rocks of an age similar to that of the volcanic country rocks are probably the heat source.

SUMMARY AND CONCLUSIONS

Martiya Sadeghi, Erik Jonsson & Nikolaos Arvanitidis

Elevated concentrations of REEs are generally found in association with alkaline igneous rocks, iron oxide-apatite ores, iron oxide breccias, iron skarn rocks, granitic pegmatites and granitoids, phosphorites and carbonatites. REE mineralisations in Sweden are associated with igneous, sedimentary, metamorphic and metasomatic rocks in a wide range of geological environments.

Alkaline to peralkaline syenitic rocks and carbonatites are most commonly found in extensional and rift settings. Within these igneous systems, REEs can be concentrated into mineralisations through magmatic differentiation processes and/or by hydrothermal as well as metamorphic activity during and after emplacement of the intrusive rocks. In suitable climates, weathering of surficially exposed rocks of these types may also lead to economically viable deposits. Even though such deposits may once have formed here, they are unlikely to have been preserved in the extensively glaciated terrains of the Fennoscandian Shield.

Although the overall most significant primary types of REE enrichment are associated with alkaline igneous rocks and carbonatites, REE enrichment can be also found in association with hydrothermal veins, breccias and carbonate replacement zones in a variety of sedimentary and metamorphic environments. These range from well-known, to uncertain origin and conditions of formation. In the case of the "Kiruna-type" iron ores, it is clear that while the origin of the deposits as such is still debated, and the actual REE host minerals and their evolution is being actively studied, these iron oxide-apatite deposits may be utilised as a future source of both phosphorus and REEs as by-products, at least in Sweden.

The genesis of the Bastnäs iron skarn-type deposits has been debated over the years, and these deposits are now generally interpreted as resulting from skarn-forming reactions between pre-existing carbonate or volcanic rocks and medium to high-temperature, metal-rich hydrothermal fluids of a magmatic nature. The source(s) of the REE and the reason for the high concentrations in the skarn mineralisations in this specific linear belt of metavolcanic rocks remain open questions for future investigation and research. Even though known very REE-rich deposits of this type (e.g. Nya Bastnäs) seem to have limited tonnages, this general type of skarn-hosted deposit occurs along a more than 100-km-long, narrow belt, known as "the REE line". This suggests mineralising processes on a regional scale, which also indicates potential for new discoveries.

Several REE mineralisations were discovered during the project, and these may be relevant for future study, at least from a scientific perspective, but also in developing ore-genetic models and concepts to be applied elsewhere in the Bergslagen and other similar REE-metallogenetic settings. These REE-enriched mineralisations are the Bredåsen polymetallic iron oxide mineralisation, the Sveafallen oxide mineralisation, the Tybble iron deposits, the Hylleled iron deposits, the Bäckberg iron deposits, and the Gullebo iron deposits. Other poorly investigated iron oxide deposits and area s are also suggested for further study.

The Gävle graben area seems to have potential for future exploration after what could be a relevant apatite-REE-mineralised carbonatite occurrence. The topographically low, flat and wet terrain makes both bedrock mapping and exploration work problematic; but this also makes it more credible that an occurrence of an exotic rock such as carbonatite could have escaped attention.

In summary, it is evident that although Sweden currently has no active mining of REE, it does have a number of regions with suitable geology and past geological processes, featuring recognised REE resources. Several of these deposits are currently listed among the more advanced REE projects globally. The Norra Kärr deposit has high proportions of HREE, is well situated and contains (very) low grades of radioactive elements that are otherwise typically associated with such deposits (http://tasmanmetals.se/projekt/). Another potential REE exploration target is the iron oxide-associated REE phosphate mineralisations of the Olserum area in southeastern Sweden. According to a previous survey, the Olserum REE deposit covers only part of a broader mineralised area, and is open at depth. For this limited part of the mineralised area, indicated resources have been estimated at 4.5 Mt at 0.6% TREO and 33.9% HREO (Reed 2013, unpublished report).

Considering the diverse and favourable geological and metallogenetic settings of Sweden, there is good potential for discovering new REE deposits. This will naturally require more comprehensive and advanced mineral exploration, including the development of conceptual models for deeper-seated REE mineral systems. Applied geophysical and geochemical methods should also be integrated in a multidisciplinary way, to improve understanding of ore genesis and related geo-modelling. This holistic approach, also including ore geochemistry and mineralogy, will provide a well-documented REE mineral knowledge base and intelligence. There is a need for further joint research and innovation actions in the fundamental understanding of the formation of REE mineralisations, geological modelling of the mineral deposits, ore-forming systems and exploration geochemistry, as well as in developing new REE extraction and processing technologies.

Each ore body is 'unique', posing different geological, geochemical, mineralogical and metallurgical challenges. The chain from exploration and discovery of a REE deposit to mining and production is a challenging process, requiring new innovative technologies and expensive commitments. The REE value chain is demanding, particularly as regards processing and metallurgical methods for REE recovery and separation efficiency, along with related environmental issues.

ACKNOWLEDGEMENTS

The EURARE project was funded by the European Community Seventh Framework Programme (FP7/2007-2013) under grant agreement no. 309373. The project, number 35242, was co-funded by the Geological Survey of Sweden (Sveriges geologiska undersökning). The editor thanks go to Magnus Ripa, Anna Ladenberger, Erik Jonsson, Nikolaos Arvanitidis for their constructive comments on an earlier draft of this report. Ildikó Antal Lundin is thanked for her support during the preparation and publication of this manuscript.

We also wish to thank Thomas Eliasson and Ulf Bergström (SGU/Gothenburg) for supplying unpublished data on granitoid intrusives in southwestern Sweden, as well as for images of the RA granite; Dick Claeson (SGU/Uppsala) for supplying data on Tåresåive occurrence; Jörgen Langhof, Swedish Museum of Natural History (Stockholm) for help in locating and photographing the sample of the Främlingshem carbonatite; Mark Saxon and Magnus Leijd, Tasman Metals, for supplying data and geological information on Norra Kärr, Olserum and Näverån. Helge Reginiussen (SGU/Uppsala) is thanked for supplying hyperspectral infrared imaging data. We are grateful to Gary Wife, Milos Bartol and Michael Streng, Uppsala University, for their helpful assistance during SEM-EDS work.

We also thank Daniel Larsson (SGU/Malå) for assistance in the fieldwork from the Alnö and Kalix area. Language control of the entire manuscript was done by Maxwell Arding. Lina Rönnåsen is thanked for editorial work.

REFERENCES

Adamson, O. J., 1944: The Petrology of the Norra Kärr District — An occurrence of alkaline rocks in southern Sweden. *Geologiska Föreningens i Stockholm Förhandlingar 66*, 113–255.

Allen, R.L., Weihed, P., Svenson, S.-Å., 1996a: Setting of Zn-Cu-Au-Ag massive sulfide deposits in the evolution and facies architecture of a 1.9 Ga marine volcanic arc, Skellefte district, Sweden. *Economic Geology 91*, 1022–1053.

Allen, R.L., Lundström, I., Ripa, M., Simeonov, A., Christofferson, H., 1996b: Facies analysis of a 1.9 Ga, contintental margin, back-arc, felsic caldera province with diverse Zn-Pb-Ag-(Cu Au) sulfide and Fe-oxide deposits, Bergslagen region, Sweden. *Economic Geology 91*, 979–1008.

Ambros, M., 1983: Beskrivning till berggrundskartan 11F Lindesberg NO. *Sveriges Geologiska Undersökning Af 141*, 75 pp.

Ambros, M., 1988: Berggrundskartan 12G Avesta SV, 1:50 000. *Sveriges geologiska undersökning Af 153*.

Andersen, T., 1996: Sr, Nd and Pb isotopic data of the Alnö carbonatite complex. *Abstract volume, 22nd Nordic Geological Winter Meeting*, p. 11.

Andersson, A., 1971: Petrographic and chemical study of the Lower Ordovician uranium-bearing sedimentary unit at Tåsjö lake. *Geologiska föreningens i Stockholm Förhandlingar (GFF), Vol. 93*, 117–135.

Andersson, M., Carlsson, M., Ladenberger, A., Morris, G., Sadeghi, M., Uhlbäck, J., 2014: *Geochemical Atlas of Sweden* (Geokemisk atlas över Sverige). Sveriges geologiska undersökning, ISBN 978-91-7403-258-1, p. 210.

Andersson, S. S., Wagner, T., Jonsson, E., Leijd, M., Berg, J., 2016a: REE mineralisation in the Olserum area, SE Sweden. *Bulletin of the Geological Society of Finland, Special volume,* 113.

Andersson, S. S., Wagner, T., Jonsson, E., 2016b: Mineralogy and mineral chemistry of the Olserum-Djupedal REE deposits, southeastern Sweden. *Proceedings of the 2nd European Mineralogical Conference.* Rimini, Italy, 11–15 September 2016, 508.

Andersson, S. S., Wagner, T., Jonsson, E. & Michallik, R. M. 2018a: Mineralogy, paragenesis, and mineral chemistry of REEs in the Olserum-Djupedal REE-phosphate mineralization, SE Sweden. *American Mineralogist 103*, 125–142.

Andersson, S. S., Wagner, T., Jonsson, E., Fusswinkel, T., Leijd, M. & Berg, J. 2018b: Origin of the high-temperature Olserum-Djupedal REE-phosphate mineralisation, SE Sweden: a unique contact metamorphic-hydrothermal system. *Ore Geology Reviews 101*, 740–764.

Andersson, U. B., 2001: An overview of the geochemical evolution in the Mesoproterozoic (1.58–1.50 Ga) anorogenic complexes of central Sweden. *Zeitschrift für Geologische Wissenschaften 29*, 455–470.

Andersson, U. B. (ed.), 2004: The Bastnäs-type REE mineralisations in north-western Bergslagen, Sweden. Sveriges geologiska undersökning. *Rapporter and Meddelanden 119*, 34 pp.

Andersson, U.B., Wikström, A., 2004: The Småland-Värmland Belt: Overview. In: K. Högdahl, U.B. Andersson, O. Eklund, (eds.) 2004. The Transscandinavian Igneous Belt (TIB) in Sweden: a review of its character and evolution. *Geological Survey of Finland Special paper 37,* 15–20.

Andersson, U.B., Begg, G.C., Griffin, W.L., Högdahl, K., 2011: Ancient and juvenile components in the continental crust and mantle: Hf isotopes in zircon from Svecofennian magmatic rocks and rapakivi granites in Sweden. *Lithosphere 3*, 409–419.

Andersson, U. B., Holtstam, D., Broman, C., 2013: Additional data on the age and origin of the Bastnäs-type REE deposits, Sweden. In E. Jonsson et al. (eds.) Mineral deposit research for a high-tech world, *Proceedings of the 12th biennial SGA meeting*, Uppsala, Sweden, 12–15 August, 1639–1642.

Andersson, U. B., Zack, T., Aupers, K., Blomgren, H., Hogmalm, J., Schulz, B., Krause, J., 2016: Ages of hydrothermal overprints in the Kiruna iron oxide-apatite ores as recorded in secondary monazite and xenotime. *International Geological Congress,* Cape Town, South Africa, 2016-09-02, Abstracts.

Andréasson, P.-G. & Rodhe, A., 1990: Geology of the Protogine Zone south of Lake Vättern, southern Sweden: A reinterpretation. *Geologiska Föreningens i Stockholm Förhandlingar 112,* 107–125.

Armands, G., 1970: A uranium-bearing layer from the Lower Ordovician, Sweden. *Geologiska Föreningen i Stockholm Förhandlingar (GFF),* Vol. 92, 481–490.

Asklund, B., & Thorslund, P., 1935: Fjällkedjerandens bergbyggnad i norra Jämtland och Ångermanland. *Sveriges geologiska undersökning Ser. C 382*.

Asklund, B., 1946: Beskrivning till kartbladet Möklinta. *Sveriges geologiska undersökning Aa 186*, 101 pp.

Atencio, D., Andrade, M. B., Christy, A. G., Gieré, R., Kartashov, P. M., 2010: The pyrochlore supergroup of minerals: nomenclature. *Canadian Mineralogist 48*, 673–698.

Austin Hegardt, E., Cornell, D. H., Hellström, F. A., Lundqvist, I., 2007: Emplacement ages of the mid-Proterozoic Kungsbacka Bimodal Suite, SW Sweden. *GFF 129*, 227–234.

BABEL Working Group, 1990: Evidence for Early Proterozoic plate tectonics from seismic reflection profiles in the Baltic Shield. *Nature 348*, 34–38.

BABEL Working Group, 1993: Integrated seismic studies of the Baltic Shield using data in the Gulf of Bothnia region. *Geophysical Journal International 112,* 305–324.

Bačík, P., Uher, P., Ertl, A., Jonsson, E., Nysten, P., Kanický, V., Vaculovič, T., 2012: Zoned REE-enriched dravite from a granitic pegmatite in Forshammar, Bergslagen province, Sweden: an EMPA, XRD and LA-ICP-MS study. *Canadian Mineralogist 50*, 825–841.

Back, F., 1991: *Grängesbergs malmfält.* Slutrapport Grängesbergs Gruvor AB. 10 p. + appendices.

Balashov, Y.A., Pozharitskaya, L.K., 1968: Factors governing the behavior of rare earth elements in the carbonatite process. *Geochemistry International 5*, 271–288.

Bárdossy, G., 1982: *Karst Bauxites (Bauxite deposits on carbonate rocks*). Budapest, Hungary.

Bark, G. & Weihed, P., 2012: Geodynamic settings for Paleoproterozoic gold mineralization in the Svecofennian domain: a tectonic model for the Fäboliden orogenic gold deposit, northern Sweden. *Ore Geology Reviews 48*, 403–412.

Barton, M.D., & Johnson, D.A., 1996: Evaporitic source model for igneous-related Fe oxide-(REE-Cu-Au-U) mineralization: *Geology, v. 24*, p. 259–262.

Bauer, T., Skyttä, P., Allen, R., Weihed, P., 2013: Fault-controlled sedimentation in a progressively opening extensional basin: the Palaeoproterozoic Vargfors basin, Skellefte mining district, Sweden. *International Journal of Earth Sciences 102*, 385–400.

Bejgarn, T., Söderlund, U., Weihed, P., Årebäck, H., Ernst, R.E., 2013: Palaeoproterozoic porphyry Cu-Au, intrusion-hosted Au and ultramafic Cu-Ni deposits in the Fennoscandian Shield: temporal constraints using U-Pb geochronology. *Lithos, Volume 174*, 1 August 2013, Pages 236–254

Berg, L., Nordström, T., Sjögren, A., Lundbohm, H., 1890: Underdånig berättelse jemte betänkanden afgifna af den för undersökning af apatittillgångar i Norrbotten enligt nådigt beslut den 14 juni tillsatta kommission. *Sveriges geologiska undersökning C 111*, 1–16 + appendices.

Bergman Weihed, J., Bergström, U., Billström, K., Weihed, P., 1996: Geology and tectonic evolution of the Paleoproterozoic Boliden Au-Cu-As deposit, Skellefte district, northern Sweden. *Economic Geology 91*, 1073–1097.

Bergman, S., Billström, K., Persson, P.-O., Skiöld, T., Evins, P., 2006: U-Pb age evidence for repeated Palaeoproterozoic metamorphism and deformation near the Pajala shear zone in the northern Fennoscandian shield. *GFF 128*, 7–20.

Bergman, S., Högdahl, K., Nironen, M., Ogenhall, E., Sjöström, H., Lundqvist, L., Lahtinen, R., 2008: Timing of Palaeoproterozoic intra-orogenic sedimentation in the central Fennoscandian Shield; evidence from detrital zircon in metasandstone. *Tectonophysics 161*, 231–249.

Bergman, S., Kübler, L., Martinsson, O., 2001: Description of regional geological and geophysical maps of northern Norrbotten county (east of the Caledonian orogen). *Sveriges geologiska undersökning Ba 56*, 110 pp.

Bergman, S., Persson, P.-O., Kübler, L., 2002: U-Pb titanite and zircon ages of the Lina granite at the type locality NW of Gällivare, northern Sweden. In: S. Bergman (ed.), Radiometric dating results 5. *Sveriges geologiska undersökning C 834*, 12–17.

Bergman, S., Sjöström, H., Högdahl, K., 2006b: Transpressive shear related to arc magmatism: The Paleoproterozoic Storsjön–Edsbyn Deformation Zone, central Sweden. Tectonics 25 TC1004, doi:10.1029/2005TC001815.

Berthelsen, A., & Marker, M., 1986: 1.9–1.8 Ga old strike-slip megashears in the Baltic shield, and their plate tectonic implications. *Tectonophysics 128*, 163–181.

Berthelsen, A., 1980: Towards a palinspastic tectonic analysis of the Baltic shield. In J. Cogne & M. Slansky (eds.): *Geology of Europe from Precambrian to Post-Hercynian sedimentary basins*. International Geological Congress Colloquium C6 Paris, 5–21.

Berzelius, J., 1815: Undersökning af en ny gadolinit-art från Kårarfvet i grannskapet af Fahlun. *Afhandlingar i Fysik, Kemi och Mineralogi 4*, 388–396.

Berzelius, J., 1825a: Flusspatssyradt och kolsyradt cerium. Årsberättelser om vetenskapernas framsteg, 201–202.

Berzelius, J., 1825b: Kohlensaures Ceroxydul. *Zeitschrift für Mineralogie 2*, 209.

Beunk, F.F. & Kuipers, G., 2012: The Bergslagen ore province, Sweden: rewiev and update of an accreted orocline, 1.9–1.8 Ga BP. *Precambrian Research 216–219*, 95–119.

Beunk, F.F., & Page, L.M., 2001: Structural evolution of the accretional continental margin of the Paleoproterozoic Svecofennian orogen in southern Sweden. *Tectonophysics 339*, 67–92.

Bevins, R. E., Rowbotham, G., Stephens, F. S., Turgoose, S., Williams, P. A., 1985: Lanthanite-(Ce), $(Ce,La,Nd)_2(CO_3)_3 \cdot 8H_2O$, a new mineral from Wales, UK. *American Mineralogist 70*, 411–413.

Bindi, L., Holtstam, D., Fantappiè, G., Andersson, U. B. & Bonazzi, P. 2017: IMA No. 2017-037, Ferriperbøeite-(Ce). In: Hålenius, U., Hatert, F., Pasero, M. & Mills, S. J. (eds.), IMA Commission on New Minerals, Nomenclature and Classification (CNMNC) Newsletter 38. *Mineralogical Magazine 81*, 1037–1038.

Bingen, B., Andersson, J., Söderlund, U., Möller, C., 2008: The Mesoproterozoic in the Nordic countries. *Episodes 31*, 29–34.

Boldyrev, A., 1930: Apatites de la mine Lebiajinsky et du mont Vyssokaya dans l´Oural (French summary of text in Russian). *Matériaux pour la géologie générale et appliqué, livraison 142*, Leningrad.

Bonham-Carter, G.F., 1994: *Geographic Information Systems for Geoscientists: Modelling with GIS*, Pergamon, Oxford.

Brotzen, O., 1959: Mineral association in granitic pegmatites. A statistical study. *Geologiska Föreningens i Stockholm Förhandlingar 81*, 231–296.

Brown, M., 2009: Metamorphic patterns in orogenic systems and the geological record. In P.A. Cawood & A. Kroner (eds.): Earth accretionary systems in space and time. *Geological Society London Special Publications 318*, 37–74.

Browne, A., 2008: Report on current resource estimates for Kläppibäcken and Duobblon uranium properties, and review of Tåsjö uranium project, Northern Sweden. Prepared for Mawson Resources limited. Report number 080204.

Brueckner H. K., & Rex D. C., 1980: K-Ar and Rb-Sr geochronology and Sr isotopic study of the Alnö alkaline complex, northeastern Sweden. *Lithos 13*, 111–119.

Brun, Å., Nilsson, C.-A., Sundberg, A., Wik, N.-G., Wikström, A., XXXX: Malmer, industriella mineral och bergarter i Östergötlands län. *Sveriges geologiska undersökning, Rapporter och meddelanden 80*, 340 pp.

Bylund, G., Patchett, P. J., 1977: Palaeomagnetic and Rb-Sr isotope evidence for the age of the Särna alkaline complex, western central Sweden. *Lithos 10*, 73–79.

Carlborg, H., 1923: Riddarhytte malmfält i Skinnskattebergs socken, Västmanlands län. Teknisk-ekonomisk beskrivning. Kungliga Kommerskollegium och Sveriges Geologiska Undersökning, *Beskrivningar över mineralfyndigheter 1*, 139–343.

Carranza, E.J.M., 2008: Geochemical Anomaly and Mineral Prospectivity Mapping in GIS. *Handbook of Exploration and Environmental Geochemistry, vol. 11*. Elsevier, Amsterdam.

Carranza, E.J.M., Sadeghi, M., 2010: Predictive mapping of prospectivity and quantitative estimation of undiscovered VMS deposits in Skellefte district (Sweden). *Ore Geology Reviews, 38(2010)*, 219–241.

Castor, S.B., & Hedrick, J.B., 2006: Rare earth elements. In: Kogel, J.E., Trivedi, N.C., Barker, J.M., Krukowski, S.T. (eds.), *Industrial Minerals and Rocks*. Society for Mining, Metallurgy and Exploration, pp. 769–791.

Cathcart, J.B., 1980a: The phosphate industry of the United States. In Khasawneh, F.E., (ed.), *The role of phosphorus in agriculture: Madison, Wisconsin*. American Society of Agronomy, p. 19–42.

Cathcart, J.B., 1980b: World phosphate reserves and resources: The role of phosphorus in agriculture: Madison, Wisconsin. American Society of Agronomy, p. 1–18.

Cawood, P.A., Kroner, A., Collins, W.J., Kusky, T.M., Mooney, W.D., Windley, B.F., 2009: Accretionary orogens through Earth history. In P.A. Cawood & A. Kroner (eds.): Earth accretionary systems in space and time. *Geological Society London Special Publications 318*, 1–36.

Čečys, A., 2004: *Tectonic implications of the ca.1.45 Ga granitoid magmatism at the southwestern margin of the East European Craton*. Ph.D. thesis, University of Lund, Lund. 29 pp.

Černý, P., 1991: Rare-element granitic pegmatites. Part 1: Anatomy and internal evolution of pegmatite deposits. Part 2: Regional to global environments and petrogenesis. *Geoscience Canada 18*, 49–81.

Černý, P., Ercit, T.S., 2005: The Classification of Granitic Pegmatites revisited. The Canadian Mineralogist 43, 2005–2026.

Chai, F., Zhang, Z., Mao, J., Parat, A., Wang, L., Dong, L., Ye, H., Chen, l., Zheng, R., 2006: Lamprophyre or Lamproite Dyke in the SW Tarim Block? —Discussion on the Petrogenesis of These Rocks and Their Source Region, *Journal of China University of Geosciences*, Volume 17, Issue 1, 2006, Pages 13–24.

Cheng, Q., Bonham-Carter, G.F., Wang, W., Zhang, S., Li, W., Xia, Q., 2011: A spatially weighted principal component analysis for multi-element geochemical data for mapping locations of felsic intrusions in the Gejiu mineral district of Yunnan, China. *Computers & Geosciences 5*, 662–669.

Claeson, D., Antal Lundin, I., Persson, P.-O. & Morris, G., 2018: U-Pb zircon age of the host granite of the REE and Mo (U, Th, Nb, Ta) mineralisation at Tåresåive, map sheet 27J Porjus SV, Norrbotten County. In D. Claeson & Antal Lundin (red.): U-Pb zircon geochronology of rocks from the mid and southwestern part of Norrbotten County, Sweden. *SGU-rapport 2018:22*, Sveriges geologiska undersökning, 96–105.

Claeson, D., Antal Lundin, I., 2019: Beskrivning till berggrundskartan 27J Porjus SV. Sveriges geologiska undersökning K 627, 46–50.

Claesson, S. & Sultan, L., 2008: Constraints on Svecofennian evolution from detrital zircon ages – the Palaeoproterozoic Västervik quartzites. *33rd IGC*, Oslo, 6–14 August 2008. CD-ROM.

Cronstedt, A.F., 1751: Rön och försök giorde med trenne järnmalms arter. *Kungliga Vetenskapsakademiens Handlingar*, 226–232.

Daly, J.S., Balagansky, V.V., Timmerman, M.J., Whitehouse, M.J., 2006: The Lapaland Kola orogen: Palaeoproterozoic collision and accretion of the northern fennoscndian lithosphere. In D.G. Gee & R.A. Stephenson (eds.): European lithosphere dynamics. *Geological Society London Memoirs 32*, 579–598.

Deady, E. A., Mouchos, E., Goodenough, K. M., Williamson, B. J., Wall, F., 2016: A review of the potential for rare-earth element resources from European red muds: examples from Seydisehir, Turkey and Parnassus-Giona, Greece. *Mineralogical Magazine 80*, 43–61.

Deady, E., Mouchos, E., Goodenough, K.M., Williamson, B., Wall, F., 2014: Rare earth elements in karst-bauxites: a novel untapped European resource? *ERES2014: 1st Conference on European Rare Earth Resources*, Milos, Greece

Delin, H. & Bastani, M., 2009: Berggrundskartan 11I Uppsala NO, scale 1:50 000. *Sveriges geologiska undersökning K 145*.

Dentith, M.C., Frankcombe, K.F., Ho, S.E., Shepherd, J.M., Groves, D.I. and Trench, A. (editors), 1994: Geophysical Signatures of Western Australian Mineral Deposits. Geology & Geophysics Department (Key Centre) and UWA Extension Publication No.26, *Australian Society of Exploration Geophysicists Special Publication 7*, 454 pp.

Dostal, J., 2016: Rare metal deposits associated with alkaline/peralkaline igneous rocks: *Reviews in Economic Geology, v. 18*, p. 33–54.

Eby, G.N., 1975: Abundance and distribution of the rare earth elements and yttriumin the rocks and minerals of the Oka carbonatite complex, Quebec. *Geochimica et Cosmochimica Acta 39*, 597–620.

Eckermann, H. V., 1960: Contributions to the knowledge of the alkaline dikes of the Alnö region. III. Radioactive beforsitic carbonatite dike. *Arkiv för Mineralogi och Geologi 2*, 546–550.

Eckermann, V., 1948: The alkaline district of Alnö island. *Sveriges Geologiska Undersökning ser Ca* 36, p. 176.

Eilu, P. & Weihed, P., 2005: Fennoscandian Shield – orogenic gold deposits. *Ore Geology Reviews 27*, 326–327.

Eliasson, T. & Schöberg, H., 1991: U-Pb dating of the post-kinematic Sveconorwegian (Grenvillian) Bohus granite, SW Sweden: evidence of restitic zircon. *Precambrian Research 51*, 337–350.

Eliasson, T., 1987: Trace element fractionation in the late Proterozoic Bohus granite, SW Sweden. Proceedings, International Symposium on Granites and Associated Mineralizations, Salvador, Brazil, 211–214.

Ensterö, B., 2003: *En mineralogisk studie av sulfidparageneser i Nya Bastnäsfältets lantanidmalmer*. MSc thesis, Department of Geology and Geochemistry, Stockholm University, 51 pp.

Fedele, L., Plant, J.A., De Vivo, B., Lima, A., 2008: The rare element distribution map over Europe: geogenic and anthropogenic sources. *Geochemistry: Exploration, Environment, Analysis 8*, 3–18.

Flink, G., 1910: Bidrag till Sveriges mineralogi II. *Arkiv för Kemi, Mineralogi och Geologi 3*, 35, 1–166.

Friese, N., Vollbrecht, A., Tanner, D.C., Fahlbusch, W., Weidemann, M., 2012: Multistage emplacement of the Götemar Pluton, SE Sweden: new evidence inferred from field observations and microfabric analysis, including cathodoluminescence microscopy. *International Journal of Earth Sciences 101*, 1149–1167.

Frietsch, R., 1972: A late-metasomatic iron mineralization in the Narken area and its occurrence as glacial boulders at Kihlanki, both in northern Sweden. *Sveriges geologiska undersökning C 672*, 44 pp.

Frietsch, R., 1978: On the magmatic origin of iron ores of the Kiruna type. *Economic Geology 73*, 478–485.

Frietsch, R. & Perdahl, J.-A., 1995: Rare earth elements in apatite and magnetite in Kiruna-type iron ores and some other iron ore types. *Ore Geology Reviews 9*, 489–510.

Frietsch, R., Tuisku, P., Martinsson, O., Perdahl, J.-A., 1997: Early Proterozoic Cu-(Au) and Fe ore deposits associated with regional Na–Cl metasomatism in northern Fennoscandia. *Ore Geology Reviews 12*, 1–34.

Frondel, C., 1958: Systematic mineralogy of uranium and thorium. *USGS Bulletin 1064*, 326–333.

Gaal, G., 1982: Proterozoic tectonic evolution and late Svecokarelian plate deformation of the Central Baltic Shield. *Geologische Rundschau 71*, 158–170.

Gaal, G., Gorbatschev, R., 1987: An outline of the Precambrian evolution of the Baltic Shield. *Precambrian Research 35*, 15–52.

Gadolin, J., 1794: Undersökning af en svart tung stenart ifrån Ytterby stenbrott i Roslagen. *Kongliga Vetenskaps Academiens Nya Handlingar 15*, 137–155.

Gahn, J. G. & Berzelius, J., 1815: Undersökning af några i grannskapet af Fahlun funna fossilier. *Afhandlingar i Fysik, Kemi och Mineralogi 4*, 148–216.

Gahn, J. G., Berzelius, J., Wallman, C., Eggertz, H. P., 1818: Undersökning af några i grannskapet af Fahlun funna fossilier, och af deras lagerställen. *Afhandlingar i Fysik, Kemi och Mineralogi 5*, 1–93.

Galeschuk, C.R & Vanstone, P.J., 2005: Exploration for buried rare-element pegmatites in the Bernic Lake area of southeastern Manitoba: Geological Association of Canada Short Course Notes, v. 17, p. 159–173.

Gates, P., Horlacher, C. F. & Reed, G. C., 2013: Amended and Restated Preliminary Economic Assessment NI 43-101 Technical Report for the Norra Kärr (REE-Y-Zr) Deposit, Gränna, Sweden. Vancouver, Tasman Metals.

Gee, D. G., 1972: The regional context of the Tåsjö uranium project, Caledonian Front, Central Sweden. *Sveriges geologiska undersökning, Ser. C 671*. 36 pp

Geijer, P., 1917: Falutraktens berggrund och malmfyndigheter. *Sveriges geologiska undersökning C 275*, 319 pp.

Geijer, P., 1921a: On fluocerite and tysonite. *Geologiska Föreningens i Stockholm Förhandlingar 43*, 19–23.

Geijer, P., 1921b: Epidotorthit als die Ursache von Färbung in Flusspat. *Geologiska Föreningens i Stockholm Förhandlingar 43*, 386–388.

Geijer, P., 1921c: The cerium minerals of Bastnäs at Riddarhyttan. *Sveriges geologiska undersökning Serie C 304*, 24 pp.

Geijer, P., 1923: Riddarhytte malmfält i Skinnskattebergs socken, Västmanlands län. Geologisk beskrivning. Kungliga Kommerskollegium och Sveriges geologiska undersökning, *Beskrivningar över mineralfyndigheter 1*, 1–138.

Geijer, P., 1927: Some mineral associations from the Norberg district. *Sveriges geologiska undersökning C 343*, 1–32.

Geijer, P., 1931: The iron ores of the Kiruna type: geographical distribution, geological characters, and origin. *Sveriges geologiska undersökning C 367*, 39 pp.

Geijer, P., 1936: Norbergs berggrund och malmfyndigheter. *Sveriges geologiska undersökning Ca 24*, 162 p.

Geijer, P. & Magnusson, N. H., 1944: De mellansvenska järnmalmernas geologi. *Sveriges Geologiska Undersökning Ca 35*, 654 pp.

Geijer, P., 1950: The Rektorn ore body at Kiruna. *Sveriges geologiska undersökning C 514*, 18 pp.

Geijer P., 1961: The geological significance of the cerium mineral occurrences of the Bastnäs type in central Sweden. *Arkiv för Mineralogi och Geologi 3*, 99–105

Goodenough, K. M., Schilling, J., Jonsson, E., Kalvig, P., Charles, N., Tuduri, J., Deady, E. A., Sadeghi, M., Schiellerup, H., Müller, A., Bertrand, G., Arvanitidis, N., Eliopolous, D. G., Shaw, R. A., Thrane, K., Keulen, N., 2016: Europe´s rare earth element resource potential: an overview of metallogenetic provinces and their geodynamic setting. *Ore Geology Reviews 72*, 838–856.

Gorbatschev, R., 1960: On the alkali rocks of Almunge. A preliminary report on a new survey. *Bulletin of the Geological Institute of Uppsala XXXIX 5,* 69 pp.

Gorbatschev, R., 1970: K-Ar age of biotite from the Almunge alkaline intrusion. *Geologiska Föreningens i Stockholm förhandlingar 92,* 501–502.

Grip, E. & Frietsch, R., 1973: *Malm i Sverige 2, norra Sverige.* Almqvist & Wiksell, 295 pp.

Grunsky, E.C., 2010: The interpretation of geochemical survey data. *Geochemistry: Exploration, Environment, Analysis 10*, 27–74.

Gustafsson, B., 1979: Uranuppslag inom Norrbotten och Västerbotten 1979. *Sveriges geologiska undersökning, BRAP 79056.*

Güller, C., Thyne, G., McGray, J.E., Turner, A.K., 2002: Evaluation of graphical and multivariate statistical methods for classification of water chemistry data. *Hydrogeology Journal 10*, 455–474.

Hallberg, A., 1994: The Enåsen gold deposit, central Sweden. 1. A Paleoproterozoic high sulphidation epithermal gold mineralization. *Mineralium Deposita 29*, 150–162.

Hallberg, A., Albrecht, L., Jonsson, E., Olsson, A., 2006: The Grängesberg apatite-iron deposit — biggest in Bergslagen, Sweden. *Bulletin of the Geological Society of Finland, Special issue 1*, 45.

Hallberg, A., 2012: S011 Riddarhyttan REE-Fe. In: Eilu, P. (ed.), *Geological Survey of Finland, Special Paper 53*, 162–163.

Harlov, D.E., Andersson, U. B., Förster, H.-J., Nyström, J. O., Dulski, P., Broman, C., 2002a: Apatite-monazite relations in the Kiirunavaara magnetite-apatite ore, northern Sweden. *Chemical Geology 191*, 47–72.

Harlov, D.E., Förster, H.J., Nijland, T.G., 2002b: Fluid-induced nucleation of REE-phosphate minerals in apatite: Nature and experiment. Part I. Chlorapatite. *American Mineralogist 87*, 245–261.

Harlov, D.E., Wirth, R., Förster, H.J., 2005: An experimental study of dissolution- reprecipitation in fluorapatite: fluid infiltration and the formation of monazite. *Contributions to Mineralogy and Petrology 150*, 268–286.

Harris, J.R., Grunsky, E.C., Wilkinson, L., 1997: Developments in the effective use of lithogeochemistry in regional exploration programs: application of GIS technology. In: Gubins, A.G. (Ed.), *Proceedings of the Exploration'97, Fourth Decennial International Conference on Mineral Exploration*, pp. 285–292.

Haxel, G.B., Hedrick, J.B., Orris, G.J., 2002: Rare Earth Elements — Critical Resources for High Technology. *Fact Sheet 087–02*. US Geological Survey.

Hedenberg, L., 1806: Undersökning af en krumbladig fältspats-art från Finbo i Dalarna. *Afhandlingar i Fysik, Kemi och Mineralogi 1*, 118–124.

Hedrick, J.B., 1997: Rare-earth metal prices in the USA ca. 1960 to 1994. *Journal of Alloys and Compounds 250*, 471–481.

Hedström, P., Simeonov, A., Malmström, L., 1989: The Zinkgruvan ore deposit, southcentral Sweden: A Proterozoic, proximal Zn-Pb-Ag deposit in distal volcanic facies. *Economic Geology 84*, 1235–1261.

Hermansson, T., Stephens, M.B., Corfu, F., Page, L.M., Andersson, J., 2008a: Migratory tectonic switching, western Svecofennian orogen, central Sweden: Constraints from U/Pb zircon and titanite geochronology. *Precambrian Research 161*, 250–278.

Hermansson, T., Stephens, M.B., Page, L.M., 2008b: 40Ar/39Ar hornblende geochronology from the Forsmark area in central Sweden: Constraints on late Svecofennian cooling, ductile deformation and exhumation. *Precambrian Research 167*, 303–315.

Hietanen, A., 1975: Generation of potassium poor magmas in the northern Sierra Nevada and the Svecofennian of Finland. *U.S. Geological Survey Journal of Research 3*, 631–645.

Hisinger, W. & Berzelius, J., 1804: *Cerium, en ny metall, funnen i Bastnäs Tungsten, från Riddarhyttan i Westmanland.* Henrik A. Nordström förlag, Stockholm 1–24.

Hisinger, W. & Berzelius, J., 1806: Undersökning af pyrophysalith, ett nytt stenslag från Finbo i Dalarna. *Afhandlingar i Fysik, Kemi och Mineralogi 1,* 111–118.

Hisinger, W., 1826: *Versuch einer mineralogischen Geographie von Schweden. Ubersetz von der Handschrift von F. Wöhler*, Leipzig, 250 pp.

Hisinger, W., 1838: Analyser av några svenska mineralier – Basiskt fluor-cerium från Bastnäs. Kungliga Vetenskaps Akademiens Handlingar, 1–9.

Hitzman, M.W., 2000: Iron oxide–Cu–Au deposits: What, where, when, and why. In T.M. Porter (ed.): *Hydrothermal iron oxide copper–gold and related deposits: a global perspective.* Australian Mineral Foundation, Adelaide, 9–25.

Hitzman, M.W., Oreskes, N. Einaudi, M.T., 1992: Geologic characteristics and tectonic setting of Proterozoic iron oxide (Cu-U-Au-REE) deposits. *Precambrian Research 58*, p. 241–287.

Hjelmqvist, S., 1966: Beskrivning till berggrundskarta över Kopparbergs län. Summary: Description to map of the Kopparberg County, Central Sweden. With map to the scale 1:200000. *Sveriges geologiska undersökning Ca 40*, 217 p.

Hode Vuorinen J., Hålenius U., Whitehouse M.J., Mansfeld J. and Skelton A.D.L., 2005: Compositional variations (major and trace elements) of clinopyroxene and Ti-andradite from pyroxenite, ijolite and nepheline syenite, Alnö Island, Sweden. *Lithos 81*, 55–77.

Hode Vuorinen, J. & Hålenius, U., 2005: Nb-, Zr- and LREE-rich titanite from the Alnöalkaline complex: crystal chemistry and its importance as a petrogenetic indicator. *Lithos 83*, 128–142.

Hode Vuorinen, J., 2005: *The Alnö alkaline and carbonatitic complex, east central Sweden – a petrogenetic study.* Doctoral thesis. Stockholm University. 130 pp.

Holmqvist, A., 1989: Be-F-Nb-REE-Sn-Ta-Th-U-Zr-mineraliserad granit i Västsverige. Sveriges Geologiska AB, Division Prospektering, *PRAP-rapport 89026*, 14 pp. + appendices.

Holmqvist, A.,1975: Low-2V allanite and Mg-bearing allanite from the Kallmorberg mine, Norberg, Sweden. *Geologiska Föreningens i Stockholm Förhandlingar 97*, 162–166.

Holtstam, D. & Ensterö, B., 2002: Does the Bastnäs REE deposit in central Sweden belong to the Fe oxide-Cu-U-Au-REE class of ores? *Abstract volume, 25th Nordic Geological Winter Meeting*, Reykjavík, Iceland, 83.

Holtstam, D. Andersson, U. B., Norrestam, R., 2003a: Percleveite-(Ce) – a new lanthanide disilicate mineral from Bastnäs, Skinnskatteberg, Sweden. *European Journal of Mineralogy 15*, 725–731.

Holtstam, D., Andersson, U. B., Mansfeld, J., 2003b: Ferriallanite-(Ce) from the Bastnäs deposit, Västmanland, Sweden. *Canadian Mineralogist 41*, 1233–1240.

Holtstam, D., Grins, J., Nysten, P., 2004: Håleniusite-(La) from the Bastnäs deposit, Västmanland, Sweden: a new REE oxyfluoride mineral species. *Canadian Mineralogist 42*, 1097–1103.

Holtstam, D., Kolitsch, U., Andersson, U. B., 2005: Västmanlandite-(Ce) – a new lanthanide- and F-bearing sorosilicate mineral from Västmanland, Sweden: description, crystal structure, and relation to gatelite-(Ce). *European Journal of Mineralogy 17*, 129–141.

Holtstam, D. & Andersson, U. B., 2007: The REE minerals of the Bastnäs-type deposits, south-central Sweden. *Canadian Mineralogist 45*, 1073–1114.

Holtstam, D., Andersson, U. B., Broman, K., Mansfeld, J., 2014: Origin of REE mineralisation in the Bastnäs-type Fe-REE-(Cu-Mo-Bi-Au) deposits, Bergslagen, Sweden. *Mineralium Deposita 49*, 933–966.

Holtstam, D., Bindi, L., Hålenius, U., Kolitsch, U., Andersson, U. B., 2017a: Delhuyarite-(Ce) – Ce4MgFe3+2W)£(Si2O7)2O6(OH)2 – a new mineral of the chevkinite group, from the Nya Bastnäs Fe-Cu-REE deposit, Sweden. *European Journal of Mineralogy 29*, 1–9.

Holtstam, D., Bindi, L., Hålenius, U., Kolitsch, U., Mansfeld, J., 2017b: Ulfanderssonite-(Ce), a new Cl-bearing REE silicate mineral species from the Malmkärra mine, Norberg, Sweden. *European Journal of Mineralogy*, PrePub DOI: 10.1127/ejm/2017/0029-2670

Hoppe, F., 1884: Praktiskt geologiska undersökning inom norra delen af Kalmar län. *Sveriges geologiska undersökning C 64*, 118 pp.

Hornig-Kjarsgaard, I. 1998: Rare earth elements in sövitic carbonatites and their mineral phases. *Journal of Petrology 39*, 2105–2121.

Howells, M.F., Reedman, A.J., Campbell, S.D.G., 1991: *Ordovician (Caradoc) marginal basin volcanism in Snowdonia (north-west Wales)*. London HMSO, British Geological Survey, 191 pp.

Hudson, M., 2007: Drilling expands near-surface Uranium at Tåsjö, Sweden. Mawson Resources Ltd, News Release June 11 2007

Högbom, A., 1930: Beskrivning till kartbladet Malingsbo. *Sveriges geologiska undersökning Aa 168*, 181 pp.

Högdahl, K., Sjöström, H., 2001: Evidence for 1.82 Ga transpressive shearing in a 1.85 Ga granitoid in central Sweden: implications for the regional evolution. *Precambrian Research 105*, 37–56.

Högdahl, K., Andersson, U. B., Eklund, O., (eds.) 2004: The Transscandinavian Igneous Belt (TIB) in Sweden: a review of its character and evolution. *Geological Survey of Finland Special Paper 37*. 125 pp.

Högdahl, K., Sjöström, H., Bergman, S., 2009: Ductile shear zones related to crustral shortening and domain boundary evolution in the central Fennoscandian Shield. *Tectonics 28* (TC1003, doi:10.1029/2008TC002277), 18 pp.

Högdahl, K., Troll, V.R., Nilsson, K.P., Jonsson, E., 2013: Structural evolution of the apatite-iron oxide deposit at Grängesberg, Bergslagen, Sweden. In: E. Jonsson et al. (eds.), *Mineral Deposit Research for a High-Tech World*, Society for Geology Applied to Mineral Deposits, 1650–1653.

Högdahl, K., Jonsson, E., Kritikos, A., Sahlström, F., 2015: Turning yesterday´s waste into tomorrow´s treasure: searching for base and critical metals in central Sweden´s ancient mine dumps. In: André-Meyer, A.-S. et al. (eds.), *Mineral Resources in a Sustainable World,* 757–760.

Hölttä, P., Balagansky, V., Garde, A.A., Mertanen, S., Peltonen, P., Slabunov, A., Sorjonen- Ward, P., Whitehouse, M., 2008: Archaean of Greenland and Fennoscandia. *Episodes 31*, 13–19.

Jansson, N., Allen, R., 2011a: The origin of skarn beds, Ryllshyttan Zn-Pb-Ag+magnetite deposit, Bergslagen, Sweden. *Mineralogy and Petrology 103,* 49–78.

Jansson, N., Allen, R., 2011b: Timing of volcanism, hydrothermal alteration and ore formation at Garpenberg, Bergslagen, Sweden. *GFF 133*, 3–18.

Jansson, N., Allen, R., 2013: Timing and setting of skarn and iron oxide formation at the Smältarmossen calcic iron skarn deposit, Bergslagen, Sweden. *Mineralium Deposita 48*, 313–339.

Jiao, J., 2011: *Petrography and geochemistry of a section through the Blötberget apatite-iron oxide deposit, Bergslagen south central Sweden*. MSc thesis, Uppsala University, 72 pp.

Jiao, J., Jonsson, E., Barker, A., Troll, V. R., 2012: Petrography and geochemistry of REE-bearing apatite-iron oxide ores and host rocks at Blötberget, Bergslagen, Sweden. In: T. Saemundsson & I. Ö. Benediktsson (eds.), *30th Nordic Geological Winter Meeting, programme and abstracts*, 175–176.

Johansson, A., Bogdanova, S., Čečys, A., 2006: A revised geochronology for the Blekinge Province, southern Sweden. *GFF 128*, 287–302.

Johansson, H., 1910: Die eisenerzführende Formation in der Gegend von Grängesberg. *Geologiska Föreningens i Stockholm Förhandlingar 32*, 239–410.

Jonsson, E., 2001: Vårt närmaste alkalina massiv: Almungeintrusionen i Uppland. *Stockholm Amatörgeologiska Sällskap Berg & Mineral 11*, 8–15.

Jonsson, E. & Stephens, M.B., 2004: Investigation of alkaline rocks in the Prästrun and Åkersjön areas, Jämtland. *SGU report 08/1129/2004*.

Jonsson, E. & Stephens, M.B., 2006: Metamorphosed U-Nb-Ta-REE-bearing alkaline rocks from the Swedish Caledonides in Jämtland. *Bulletin of the Geological Society of Finland, Special issue 1*, 63.

Jonsson, E., 2008: Epigenetic REE-U-Th-anomalous Fe oxide mineralisation in the Narken area, NE Sweden. *33rd International Geological Congress, Oslo, Norway, Abstracts, MRD-11.*

Jonsson, E., Persson Nilsson, K., Hallberg, A., Högdahl, K., 2010a: The Palaeoproterozoic apatite-iron oxide deposits of the Grängesberg area: Kiruna-type deposits in central Sweden. In Nakrem, H. A., Harstad, A. O. & Haukdal, G. (eds.), *29th Nordic Geological Winter Meeting, Oslo, NGF abstracts and proceedings vol. 88–89.*

Jonsson, E., Persson Nilsson, K., Högdahl, K., Troll, V. R., Hallberg, A., 2010b: REE distribution and mineralogy in a Palaeoproterozoic apatite-iron oxide deposit: Grängesberg, Bergslagen, Sweden. *Acta Mineralogica-Petrographica abstract series 6*, 234.

Jonsson, E., Persson Nilsson, K., Hallberg, A., Högdahl, K., Troll, V. R., Weis, F., Harris, C., 2011: Oxygen isotopes and geochemistry of Palaeoproterozoic Kiruna-type deposits in the Bergslagen province, Sweden. In: Aguilera, F. et al. (eds.) *Let´s Talk Ore Deposits*, UCN, Antofagasta, Chile, 494–496.

Jonsson, E. (ed.) 2013: The Norra Kärr REE-Zr project and the birthplace of the light REEs. *Society for Geology Applied to Mineral Deposits (SGA) Excursion guidebook SWE3, SWE6 & SWE7*, 36–51.

Jonsson, E. & Högdahl, K., 2013: New evidence for the timing of formation of Bastnäs-type REE mineralisation in Bergslagen, Sweden. In E. Jonsson et al. (eds.) *Mineral deposit research for a high-tech world*, 1724–1727.

Jonsson, E. & Kero, L., 2013: Beskrivning till berggrundskartorna 27M Korpilombolo NV, NO, SV, SO och 27N Svanstein NV, SV. *Sveriges Geologiska Undersökning K 391–394*, 20 pp.

Jonsson, E., Troll, V. R., Högdahl, K., Harris, C., Weis, F., Nilsson, K. P., Skelton, A., 2013: Magmatic origin of giant central Swedish ”Kiruna-type” apatite-iron oxide ores. Scientific Reports 3: 1644, 1–8. DOI: 10.1038/srep01644

Jonsson, E., Högdahl, K., Sahlström, F., Nysten, P., Sadeghi, M., 2014: The Palaeoproterozoic skarn-hosted REE mineralisations of Bastnäs-type: overview and mineralogical-geological character. In: *ERES2014: 1st European Rare Earth Resources Conference*, Milos, 382–390.

Jonsson, E., Högdahl, K., Persson Nilsson, K., Hellström, F., 2015: Apatite-iron oxide-hosted REE mineralisation at Kopslahyttan, NW Bergslagen, Sweden. In: André-Meyer, A.-S. et al. (eds.) *Mineral Resources in a Sustainable World, Strategic Metals: their sources, and ore-forming processes,* 781–784.

Jonsson, E., Harlov, D., Majka, J., Högdahl, K., Persson-Nilsson K., 2016: Fluorapatite-monazite-allanite relations in the Grängesberg apatite-iron oxide ore district, Bergslagen, Sweden. *American Mineralogist 101*, 1769–1782.

Kapustin, Y.L., 1966: Geochemistry of rare earth elements in carbonatites. *Geochemistry International 3*, 1054–1064.

Kathol, B., Weihed, P. (eds.), 2005: Description of regional geological and geophysical maps of the Skellefte District and surrounding areas. *Sveriges geologiska undersökning Ba 57*, 197 pp.

Kjarsgaard, B.A. & Hamilton, D.L., 1989: The genesis of carbonatites by immiscibility. In: Bell, K. (Ed.), *Carbonatites: Genesis and Evolution*. Chapman & Hall, London, pp. 388–404.

Kjarsgaard, B.A., 1998: Phase relations of a carbonated high-CaO nephelinite at 0.2 and 0.5 GPa. *Journal of Petrology 39*, 2061–2075.

Kjellman, J., Cerny, P., Smeds, S.-A., 1999: Diversified NYF pegmatite populations of the Swedish Proterozoic: outline of a comparative study. The Eugene E. Foord Memorial Symposium on NYF-type Pegmatites, Denver, Colorado, Program and abstracts. *Canadian Mineralogist 37*, 832–833.

Kleinhanns, I. C., Fischer-Gödde, M., Hansen, B. T., 2012: Sr-Nd isotope and geochemical characterisation of the Paleoproterozoic Västervik formation (Baltic Shield, SE-Sweden): a southerly exposure of Svecofennian metasiliciclastic sediments. *International Journal of Earth Science (Geologische Rundschau) 101*, 39–55.

Koistinen, T., Stephens, M.B., Bogatchev, V., Nordgulen, O., Wennerström, M., Korhonen, J., 2001: Geological map of the Fennoscandian Shield, scale 1:2 000 000. Geological Surveys of Finland, Norway and Sweden and the North-West Department of Natural Resources of Russia.

Korja, A. , Heikkinen, P., 2005: The accretionary Svecofennian orogen – insight from the BABEL profiles. *Precambrian Research 136*, 241–268.

Korja, A., Heikkinen, P.J., 2008: Seismic images of Paleoproterozoic microplate boundaries in the Fennoscandian Shield. In K.C. Condie & V. Pease (eds.): When did plate tectonics begin on planet Earth? *Geological Society of America Special Paper 440*, 220–248.

Kresten, P., 1976: A magnetometric survey of the Alnö complex. *Geologiska Föreningens i Stockholm Förhandlingar 98,* 364–365.

Kresten, P. & Chyssler, J., 1976: The Götemar massif in south-eastern Sweden: A reconnaissance survey. *Geologiska Föreningens i Stockholm Förhandlingar 98,* 155–161.

Kresten P., Printzlau I., Rex D.C., Vartiainen H., Woolley A.R., 1977: New ages of carbonatitic and alkaline ultramafic rocks from Sweden and Finland. *Geologiska Föreningens i Stockholm Förhandlingar 99*, 62–65.

Kresten, P., 1979: The Alnö complex: discussion of the main features, bibliography and excursion guide. *Nordic carbonatite symposium*, pp 67.

Kresten, P., 1990: The Alnö area (Alnöområdet) in: Lundqvist T., Gee D., Kumpulainen R., Karis L. and Kresten P. (eds), 1990. Beskrivning till berggrundskartan över Västernorrlands län. *Sveriges geologiska undersökning ser Ba nr 31*, 238–278.

Kresten, P., Rex, D.C., Guise, P.G. 1997: 40Ar-39Ar ages of ultramafic lamprophyres from the Kalix area, northern Sweden. In Lundqvist, T.(ed.): *Radiometric dating results 3. SGU C830.*

Kresten, P., Åhman, E., Brunfelt, A.O., 1981: Alkaline ultramafic lamprophyres and associated carbonatite dykes from the Kalix area, northern Sweden. *Geologische Rundschau 70*, 3, 1215–1231.

Kärki, A., Laajoki, K., Luukas, J., 1993: Major Palaeoproterozoic shear zones of the central Fennoscandian Shield. *Precambrian Research 64*, 207–223.

Lahtinen, R., Korja, A., Nironen, M., 2005: Paleoproterozoic tectonic evolution. In M. Lehtinen, P.A. Nurmi, O.T. Ramo (eds.): *Precambrian geology of Finland – key to the evolution of the Fennoscandian Shield*. Elsevier B.V., Amsterdam, 481–532.

Lahtinen, R., Garde, A.A., Melezhik, V.A., 2008: Paleoproterozoic evolution of Fennoscandia and Greenland. *Episodes 31*, 20–28.

Landergren, S., 1936: En orienterande undersökning över elementfördelningen i några svenska järnmalmstyper. *Jernkontorets Annaler*, 12.

Landergren, S., 1948: On the geochemistry of Swedish iron ores and associated rocks. A study of iron-ore formation. *Sveriges geologiska undersökning C 496,* 182 pp.

Langhof, J., 1991: *REE-mineralogi i Mo-förande granitpegmatiter i Vetlandatrakten, Småland*. Examensarbete vid Institutionen för geologi och geokemi, Stockholms universitet, 37 pp. + appendices.

Langhof, J., 1996: Thortveitite from granitic NYF pegmatites in Sweden. *GFF 118 Jubilee Issue, A54.*

Larson, S.A. & Berglund, J., 1992: A chronological subdivision of the Transscandinavian Igneous Belt – three magmatic episodes? *Geologiska Föreningens i Stockholm Förhandlingar 114*, 459–461.

Larsson W., 1943: Zur Kenntnis der alkalinen ultrabasischen Ganggesteine des Kalixgebiets, Nord-Schweden. *Sveriges geologiska undersökning ser C nr 456.*

Le Maitre, R.W., 2002: *Igneous Rocks: A Classification and Glossary of Terms. International Union of Geological Sciences. Subcommission on the Systematics of Igneous Rocks.* Cambridge University Press, Cambridge. 236 pp.

Lindblom, S., Broman, C., Martinsson, O., 1996: Magmatic–hydrothermal fluids in the Pahtohavare Cu–Au deposit in greenstone at Kiruna, Sweden. *Mineralium Deposita 31*, 307–318.

Linders, W. 2016: *U-Pb geochronology and geochemistry of host rocks to the Bastnäs-type REE mineralization in the Riddarhyttan area, west central Bergslagen, Sweden*. MSc thesis, Lund University, 466, 60 p. + appendices.

Lindström, M., Lundqvist, J., Lundqvist, T., 2000: *Sveriges geologi från urtid till nutid*, 2:a upplagan. Studentlitteratur, Lund, 491 pp.

London, D., 2008: Pegmatites. *Mineralogical Association of Canada Special Publication 10*, 347 pp.

London, D., 2014a: A petrologic assessment of internal zonation in granitic pegmatites: *Lithos, v. 184–187,* p. 74–104.

London, D., 2014b: Subsolidus isothermal fractional crystallization: *American Mineralogist, v. 99*, p. 543–546.

London, D., 2016: Rare-element granitic pegmatites: *Reviews in Economic Geology, v. 18*, p. 165–193.

Looström, R.,1929: Likheter mellan Lapplands- och Grängesbergsmalmerna. *Geologiska Föreningens i Stockholm Förhandlingar 51*, 303–308.

Lottermoser, B. G., 1995: Rare earth elements in Australian uranium deposits. in Uranium – past and future challenges. *Proceeding of the 7th international conference on Uranium mining and hydrogeology*. Merkel B.J. and Arab, A. (eds.). p 25–30.

Lumpkin, G. R. & Ewing, R. C., 1992: Geochemical alteration of pyrochlore group minerals: microlite subgroup. *American Mineralogist 77,* 179–188.

Lundegårdh, P. H., 1971: *Nyttosten i Sverige*. Almqvist & Wiksell, Stockholm. 271 pp.

Lundqvist, L., Karis, L. & Lundin, I., 2003: Berggrundskartan 19F Häggenås SV, *Sveriges geologiska undersökning Ai 193*.

Löfroth, B. & Pettersson, B., 1982: Detailed prospecting at the Prästrun and Valle concession areas.

Löfvendahl, R., 1981: Secondary uranium minerals in Sweden. *Sveriges geologiska undersökning C 779*, 31 pp.

MacLean, W.H., 1988: Rare earth element mobility at constant inter-REE ratios in the alteration zone at the Phelps Dodge massive sulphide deposit, Matagami, Quebec. *Mineralium Deposita 23*, 231–238.

Magnusson, N. H. 1923: The alkaline rocks of Siksjöberget and Ekorråsen in Särna. *Geologiska Föreningens i Stockholm Förhandlingar 45*, 295–334.

Majka, J., Jonsson, E., Högdahl, K., Troll, V. R., Harlov, D., Nilsson, K. P., 2013: Textural relations and mineral chemistry of REE in the Grängesberg apatite-iron oxide deposit, Sweden: the role of fluids. In: E. Jonsson et al. (eds.) *Mineral deposit research for a high-tech world*, 1728–1731.

Martinsson, O., 1997: *Tectonic setting and metallogeny of the Kiruna greenstones*. PhD Thesis, Luleå University of Technology, Luleå, Sweden.

Martinsson, O., 2001: Diversity and character of apatite iron ores and their relation to epigenetic Cu–Au deposits in the Norrbotten Fe–Cu–Au province, northern Sweden. GSA Annual Meeting, Special session: ironoxide (–copper–gold) systems – deposit studies to global context, Boston 4 November 2001. *GSA Website Abstracts with Programs 33*. http://gsa.confex.com/gsa/2001AM/finalprogram/ abstract_26785.htm.

Mattson, K., 2016: *Mineralogical characterisation of REE-bearing mineralisations in Knutsbo, Bergslagen*. Självständigt arbete, Department of Geological sciences, Stockholm University, 20 pp.

Meert, J.G., Walderhaug, H.J., Torsvik, T.H., Hendriks, B.W.H., 2007: Age and paleomagnetic signature of the Alnö carbonatite complex (NE Sweden): Additional controversy for the Neoproterozoic paleoposition of Baltica. *Precambrian Research 154*, 159–174.

Mellqvist, C., Öhlander, B., Skiöld, T., Wikström, A., 1999: The Archaean–Proterozoic Palaeoboundary in the Luleå area, northern Sweden: field and isotope geochemical evidence for a sharp terrane boundary. *Precambrian Research 96*, 225–243.

Mercier-Langevin. P., McNicoll, V., Allen, R.L., Blight, J.H.S., Dube, B., 2013: The Boliden gold-rich volcanogenic massive sulfide deposit, Skellefte district, Sweden: new U–Pb age constraints and implications at deposit and district scale. *Mineralium Deposita 48,* 485–504.

Moffett, S., Palmer, 2012: China's rare earth monopoly challenged. *Financial Post*, March 13. Collected from: http://business.financialpost.com/2012/03/13/chinas-rare-earth-monopoly-challenged/ (last accessed 140111).

Mordberg, L., 1993: Patterns of distribution and behaviour of trace elements in bauxites. *Chemical Geology, 107(3),* 241–244.

Möller, P., Morteani, G., Schley, F., 1980: Discussion of REE distribution patterns of carbonatites and alkali rocks. *Lithos 13*, 171–179.

Möller, P., 1986: Rare earth mineral deposits and their industrial importance. In: Möller, P., Cerney, P., Saupe, F. (eds.), *Lanthanides, Tantalium and Niobium.* Proceeding of a workshop in Berlin, November 1986. Spring-Verlag.

Niiranen, T., Poutiainen, M., Manttari, I., 2007: Geochemistry, alteration, fluid inclusion characteristics, and U-Pb age data on the iron oxide-Cu-Au deposits in the Kolari region, northern Finland. *Ore Geology Reviews 30*, 75–105.

Nilsson, K. P., Högdahl, K., Jonsson, E., Troll, V. R., Weis, F., Persson, L., Majka, J., Skelton, A., 2013: The Grängesberg apatite-iron oxide deposit. *Geological Survey of Sweden (SGU) report, projects 35189 and 60-1629/2008*. 45 pp.

Nironen, M., 1997: The Svecofennian Orogen: a tectonic model. *Precambrian Research 86*, 21–44.

Nordenskiöld, A.E., 1873: Om ceritens kristallform. *Öfversigt af Kongliga Vetenskaps-Akademiens Förhandlingar, 7.* 13–16.

Nordenström, G., 1890: Fynd av allanit (cerin) vid Gyttorp i Nora Bergslag. *Geologiska Föreningens i Stockholm Förhandlingar 12*, 540–544.

Nyström, J. O., Svensson, N.-B., Åberg, G., 1985: An occurrence of apatite-rich rocks of carbonatitic affinity near the Jotnian graben structure in Gävle, central Sweden. *Geologiska Föreningens i Stockholm Förhandlingar 107*, 185–195.

Nyström, J. O. & Henriquez, F., 1994: Magmatic features of iron ores of the Kiruna type in Chile and Sweden: ore textures and magnetite geochemistry. *Economic Geology 89*, 820–839.

Nyström, J.-O., 1982: Post-Svecokarelian Andinotype evolution in central Sweden. *Geologische Rundschau 71*, 141–157.

Nyström, J.-O., 2004: Dala volcanism, sedimentation and structural setting. In K. Högdahl, U.B. Andersson & O. Eklund (eds.): The Transscandinavian Igneous Belt (TIB) in Sweden: a review of its character and evolution. *Geological Survey of Finland Special Paper 37*, 58–70.

Oberti, R., Cámara, F., Hawthorne, F.C., Ball, N.A., 2009: Fluoro-aluminoleakeite, NaNa2(Mg2Al2Li) Si8O22F2, a new mineral of the amphibole group from Norra Kärr, Sweden: description and crystal structure. *Mineralogical Magazine 73*, 817–824.

Orbe, R. 2016: *Karakterisering av REE-förande mineral från Flintgruvan: en sydlig utlöpare av Falufältet i norra Bergslagen?* Självständigt arbete vid Institutionen för Geovetenskaper, Uppsala universitet, 2016:33, 36 pp.

Oreskes, N. & Einaudi, M.T., 1990: Origin of rare earth element-enriched hematite breccias at the Olympic Dam Cu-U-Au-Ag deposit, Roxby Downs, South Australia, *Economic Geology, vol. 85, no. 1*, pp. 1–28, 1990

Orris, G.J. & Grauch, R.I., 2002: Rare Earth Element mines, Deposits, and Occurrences. U.S. Geological Survey Open-File Report 02-189. U.S. Geological Survey, Tucson, AZ

Pan, Y. & Fleet, M. E., 2002: Composition of the fluorapatite-group minerals: substitution mechanisms and controlling factors. *Reviews in Mineralogy and Geochemistry 48*, 13–49.

Parák, T., 1973: Rare earths in the apatite iron ores of Lappland together with some data about the Sr, Th and U content of these ores. *Economic Geology 68*, 210–221.

Parák, T., 1975: Kiruna iron ores are not "intrusive-magmatic ores of the Kiruna type". *Economic Geology 70*, 1242–1258.

Park, A.F., 1985: Accretion tectonism in the Proterozoic Svecokarelides of the Baltic Shield. *Geology 13*, 725–729.

Patchett, P.J., Gorbatschev, R., Todt, W., 1987: Origin of continental crust of 1.9–1.7 Ga age. Nd isotopes in the Svecofennian orogenic terrains of Sweden. *Precambrian Research 35*, 145–160.

Peacor, D. R., Simmons, W. B., Essene, E. J., Heinrich, E. W., 1982: New data on and discreditation of "texasite", "albrittonite", "cuproartinite", "cuprohydromagnesite", and "yttromicrolite", with corrected data on nickelbischofite, rowlandite, and yttrocrasite. *American Mineralogist 67*, 156–169.

Peacor, D.R. & Dunn, P. 1988. Dollaseite-(Ce) (magnesium orthite redefined): structure refinement and implications for F - M2+ substitutions in the epidote-group minerals. *American Mineralogist 73*. 838–842.

Pell, J., 1996: *Mineral deposits associated with carbonatites and related alkaline igneous rocks. Undersaturated Alkaline Rocks: mineralogy, petrogenesis and economic potential*, Mineralogical Association of Canada, Short Course Series, Winnipeg, Manitoba, pp. 271–310.

Petrosino, P., Sadeghi, M., Albanese, S., Andersson, M., Lima, A., De Vivo, B., 2013: REE contents in solid media and stream waters from different geological contexts: comparison between Italy and Sweden. *Journal of geochemical exploration, volume 133*, 176–201

Prego, R., Caetano, M., Vale, G., Marmolejo-Rodríguez, J., 2009: Rare earth elements in sediments of the Vigo Ria, NW Iberian Peninsula. *Continental Shelf Research 29*, 896–902.

Pålsson, B. I. & Fredriksson, A., 2012: Beneficiation of REE containing minerals. *Conference in Mineral Processing, Luleå, Sweden, Proceedings*, 1–20.

Pålsson, B. I., Martinsson, O., Wanhainen, C., Fredriksson, A., 2014: Unlocking rare earth elements from European apatite-iron ores. *ERES2014, 1st European Rare Earth Resources Conference, Milos, Greece, Proceedings*, 211–220.

Quensel, P.D., 1914: The alkaline rocks of Almunge. *Bulletin of the Geological Institute of Uppsala 12*, 129–200.

Quensel, P., 1956: The paragenesis of the Varuträsk pegmatite including a review of its mineral assemblage. *Arkiv för Mineralogi och Geologi 2*, 9–126.

Reimann, C., Birke, M., Demetriades, A., Filzmoser, P., O'Connor, P. (eds.), 2014a: Chemistry of Europe's Agricultural Soils – Part A: Methodology and Interpretation of the GEMAS Dataset. *Geologisches Jahrbuch (Reihe B).* Schweizerbarth, Stuttgart, p. 528.

Reimann, C., Birke, M., Demetriades, A., Filzmoser, P., O'Connor, P. (eds.), 2014b: Chemistry of Europe's Agricultural Soils – Part B: General Background Information and Further Analysis of the GEMAS Dataset. *Geologisches Jahrbuch (Reihe B).* Schweizerbarth, Stuttgart, p. 352.

Richardson, D.G., Birkett, T.C., 1996: Peralkaline rock-associated rare metals. Geology of Canadian Mineral Deposits, Geological Association of Canada, *Geology of Canada No.8*, pp. 523–540.

Ripa, M., 1988: Geochemistry of wall-rock alteration and of mixed volcanic-exhalative facies at the Proterozoic Stollberg Fe-Pb-Zn-Mn(-Ag) deposit, Bergslagen, Sweden. *Geologie en Mijnbouw 67*, 443–457.

Ripa, M., 1994: The mineral chemistry of hydrothermally altered and metamorphosed wall-rocks at the Stollberg Fe-Pb-Zn-Mn(-Ag) deposit, Bergslagen, Sweden. *Mineralium Deposita 29(2)*: 180–188. June 1994.

Ripa, M., 2012: Metal zonation in alteration assemblages at the volcanogenic Stollberg Fe-Pb-Zn-Mn(-Ag) skarn deposit, Bergslagen, Sweden. *GFF 134*, 317–330.

Ripa, M., Sundberg, A., Wik, N-G., Bergman, T., Claeson, D., Hallberg, A., Kübler, L., Nysten, P., 2015: Malmer, industriella mineral och bergarter i Dalarnas län. *Sveriges geologiska undersökning Rapporter och meddelanden 139:2*, 317–632.

Romer, R.L. & Smeds, S.-A., 1994: Implications of U-Pb ages of columbite-tantalites from granitic pegmatites for the Palaeoproterozoic accretion of 1.90–1.85 Ga magmatic arcs to the Baltic Shield. *Precambrian Research 67*, 141–158.

Romer, R. L. & Smeds, S.-A., 1996: U-Pb columbite ages of pegmatites from Sveconorwegian terranes in southwestern Sweden. *Precambrian Research 76*, 15–30.

Romer, R.L. & Smeds, S.-A., 1997: U-Pb columbite chronology of post-kinematic Palaeoproterozoic pegmatites in Sweden. Precambrian *Research 82*, 85–99.

Sadeghi, M., 2008: Application of GIS to integration of SGU data base: predictive prospectivity mapping of volcanic massive sulphide potential in the Skellefte District. *Sveriges geologiska undersökning, Rapport 2008:30.* 122 pp.

Sadeghi, M., Morris, G.A, Carranza, E.J.M., Ladenberger, A., Andersson, M., 2013a: Rare earth element distribution and mineralisation in Sweden: An application of principal component analysis to FOREGS soil geochemistry. *Journal of geochemical exploration. Volume 133*, 160–175

Sadeghi, M., Petrosino, P., Ladenberger, A., Albanese, S., Andersson, M., Morris, G., Lima, A., De Vivo, B., 2013b: Ce, La and Y concentration in agricultural and grazing land soils of Europe – an exercise for mapping and exploration. *Journal of geochemical exploration. Volume 133*, 202–213

Sadeghi, M. & Andersson, M., 2015: Sällsynta jordartsmetaller i Sverige, förekomst och utbredning i berg och jord "The rare earth element distribution over Sweden" (in Swedish and English). *Geological survey of Sweden. Report no 2015-21*, 98 pp.

Sadeghi, M., Albanese, S., Morris, G. Ladenberger, A., Andersson, M., Cannatelli, C., Lima, A., De Vivo, B., 2015: REE concentrations in agricultural soil in Sweden and Italy: Comparison of weak MMI® extraction with near total extraction data. *Applied Geochemistry 63*. 22–36.

Sadeghi, M. 2017: Regional-scale prospectivity mapping on REE mineralization in Bergslagen district, Sweden. Mineral Prospectivity, current approaches and future innovations. *Orléans, France, 24–26 October 2017–book of extended abstract.* 61–63

Sadeghi, M., Jonsson, E., Arvanitidis, N., Bergman, T., 2017a: Critical minerals and metals in Sweden: A Review. *2th European Rare Earth Resources 2017, Santorini, Greece, Proceedings*. p 71–72.

Sadeghi, M., Ripa, M., Agbonifo, E.-O., Berman, T., 2017b: Regional scale targeting for REE mineralisation: A preliminary result on Bastnäs (Skarn)- type REE mineralisation in Bergslagen, Sweden. *2th European Rare Earth Resources 2017, Santorini, Greece, Proceedings.* p 50–51

Sahlström, F., 2012: *Ore petrography and geochemistry of some REE-bearing Fe-oxide assemblages from the Idkerberget deposit, Bergslagen, Sweden*. BSc thesis, Uppsala University, 38 pp.

Sahlström, F., 2014: *Stable isotope systematics of skarn-hosted REE-silicates-magnetite mineralisations in central Bergslagen, Sweden.* MSc thesis, Department of Earth Sciences, Uppsala university, 279, 82 pp.

Sahlström, F., Jonsson, E., Högdahl, K., Harris, C., 2014: Magnetite oxygen isotope constraints on the genesis of Bastnäs-type REE mineralisation in Bergslagen, Sweden. In M. D. Johnson (ed.) *31st Nordic Geological Winter Meeting, abstract volume*, 60.

Sahlström, F., Jonsson, E., Högdahl, K., Harris, C., Troll, V. R., Jolis, E. M. 2015: O and C isotope study of Bastnäs-type rare earth element mineralisation, Bergslagen, Sweden. *PacRim 2015*, 439–443.

Saintilan, N.J., Schneider, J., Stephens, M.B., Chiaradia, M., Kouzmanov, K., Wälle, M., Fontbote, L., 2015: A Middle Ordovician age for the Laisvall sandstone-hosted Pb-Zn deposit, Sweden: a response to Early Caledonian orogenic activity. *Economic Geology 110*, 1779–1801.

Saintot, A., Stephens, M.B., Viola, G., Nordgulen, O., 2011: Brittle tectonic evolution and paleostress field reconstruction in the southwestern part of the Fennoscandian Shield, Forsmark, Sweden. *Tectonics 30*, TC4002, doi:10.1029/2010TC002781.

Salminen, R., Batista, M.J., Bidovec, M., Demetriades, A., De Vivo, B., De Vos, W., Duris, M., Gilucis, A., Gregorauskiene, V., Halamic, J., Heitzmann, P., Lima, A., Jordan, G., Klaver, G., Klein, P., Lis, J., Locutura, J., Marsina, K., Mazreku, A., O'Connor, P.J.,Olsson, S.A., Ottesen, R.T., Petersell, V., Plant, J.A., Reeder, S., Salpeteur, I.,Sandström, H., Siewers, U., Steenfelt, A., Tarvainen, T. (Eds.), 2005: *FOREGS Geochemical Atlas of Europe*, Part 1: Background Information, Methodology and Maps. Geological Survey of Finland, Espoo.

Samson, I.M. & Wood, S.A., 2004: Fluid inclusion characteristics and genesis of the fluorite-parisite mineralization in the Snowbird deposit, Montana. *Economic Geology 99*, 1727–1744.

Samson, I.M. & Wood, S.A., 2005: The rare earth elements: behavior in hydrothermal fluids and concentration in hydrothermal mineral deposits, exclusive of alkaline setting: in Linnen, R.I. and Samson, I.M., edt., Rare elements Geochemistry and Mineral Deposits, *Geological Association of Canada short course Notes, v.17*, p 269–297.

Sandström, Å. & Fredriksson, A., 2012: Hydrometallurgical extraction of REE from apatite. *Conference in Mineral Processing, Luleå, Sweden, Proceedings*, 1–9.

Sanematsu, K., & Watanabe, Y., 2016: Characteristics and genesis of ionadsorption-type rare earth element deposits: *Reviews in Economic Geology, v. 18,* p. 55–79.

Saxon, M., Leijd, M., Forrester, K., Berg, J., 2015: Geology, mineralogy, and metallurgical processing. Symposium on critical and strategic materials. *British Columbia Geological Survey Paper 2015-*3 of the Norra Kärr heavy REE deposit, Sweden

Sengupta, D., and Van Gosen, B.S., 2016: Placer-type rare earth element deposits: *Reviews in Economic Geology, v. 18*, p. 81–100.

Short, M., Apelt, T., Moseley, G., Mounde, M. & La Touche, G. D., 2015: Amended and restated prefeasibility study – NI 43-101 – Technical report for the Norra Kärr rare earth element deposit. GBM Consultants Ltd.

Sjöberg, J., 2004: *Ultramafic diatremes in middle Sweden*. Undergraduate Thesis, Department of Earth Sciences, Uppsala University, 39 pp. + appendices.

Sjöqvist, A. S. L., 2015: *Agpaitic rocks of the Norra Kärr alkaline complex. Chemistry, origin and age of eudialyte-hosted zirconium and rare-earth element ore.* University of Gothenburg, Department of Earth Sciences, Licentiate thesis A157, 41 pp.

Sjöqvist, A. S. L., Cornell, D. H., Andersen, T., Erambert, M., Ek, M., Leijd, M., 2013a: Three compositional varieties of rare-earth element ore: eudialyte-group minerals from the Norra Kärr alkaline complex, southern Sweden. *Minerals 3*, 94–120.

Sjöqvist, A. S. L., Leijd, M., Jonsson, E., Andersson, U. B., 2013b: The Norra Kärr REE-Zr project. In: E. Jonsson (ed.), *The Norra Kärr REE-Zr project and the birthplace of light REEs, SGA Excursion Guidebook SWE3, SWE6, SWE7*, 36–48.

Škoda, R., Plášil, J., Jonsson, E., Čopjakova, R., Langhof, J., Vasinova Galiova, M., 2015: Redefinition of thalénite-(Y) and discreditation of fluorthalénite-(Y): a re-investigation of type material from the Österby pegmatite, Dalarna, Sweden, and from additional localities. *Mineralogical Magazine 79*, 965–983.

Škoda, R., Plášil, J., Čopjaková, R., Novák, M., Jonsson, E., Vašinová Galiová, M. & Holtstam, D., 2016: Gadolinite-(Nd), a new member of the gadolinite supergroup from Fe-REE deposits of Bastnäs-type, Sweden. *Mineralogical Magazine 82 (S1)*, 133–145.

Skyttä, P., Bauer, T.E., Tavakoli, S., Hermansson, T., Andersson, J., Weihed, P., 2012: Pre-1.87 Ga development of crustal domains overprinted by 1.87 Ga transpression in the Palaeoproterozoic Skellefte district, Sweden. *Precambrian Research 206–207*, 109–136.

Smeds, S.-A., 1990: Regional trends in mineral assemblages of Swedish Proterozoic granitic pegmatites and their geological significance. *Geologiska Föreningens i Stockholm Förhandlingar 112*, 227–242.

Smeds, S.-A., 1994: Geochemical fractionation and zoning of some granitic rare-element pegmatite fields in Sweden. *Acta Universitatis Upsaliensis, Comprehensive summaries of Uppsala dissertations from the Faculty of Science and Technology 56*, 19 pp.

Smith, M., Coppard, J., Herrington, R., Stein, H., 2007: The geology of the Rakkurijärvi Cu-(Au) prospect, Norrbotten: a new iron oxide-copper-gold (IOCG) deposit in Northern Sweden. *Economic Geology 102*, 393–414.

Smith, M. P., Storey, C. D., Jeffries, T. E., Ryan, C., 2009: In situ U-Pb and trace element analysis of accessory minerals in the Kiruna district, Norrbotten, Sweden: new constraints on the timing and origin of mineralization. *Journal of Petrology 50*, 11, 2063–2094.

Sohlenius, G., Bastani,M., Persson, L., Lax, K., 2009: On the recognition of areas with problematic sulphidic sediments usingmulti-disciplinary data. *Environmental Geology 56*, 973–984.

Stephens, M.B. (ed.), 1986: Stratabound sulphide deposits in the central Scandinavian Caledonides. 7th IAGOD symposium, excursion guide 2. *Sveriges geologiska undersökning Ca 60*, 68 p.

Stephens, M.B., 1988: The Scandinavian Caledonides: a complexity of collisions. *Geology Today 4*, 20–26.

Stephens, M.B., Wahlgren, C.-H., Weihed, P., 1997: Sweden. In E.M. Moores, R.W. Fairbridge (eds.): *Encyclopedia of European and Asian regional geology*. Encyclopedia of Earth Sciences Series, Chapman, Hall, 690–704.

Stephens, M.B., 1998: Berggrundskartan 10E Karlskoga NO, skala 1:50 000. *Sveriges geologiska undersökning Af 184.*

Stephens, M.B. & Karis, L., 2005a: Bedrock map 20E Hotagen NV, scale 1:50 000. *Sveriges geologiska undersökning, Ai 178.*

Stephens, M.B. & Karis, L., 2005b: Bedrock map 20E Hotagen SV, scale 1:50 000. *Sveriges geologiska undersökning, Ai 180.*

Stephens, M. B., Ripa, M., Lundström, I., Persson, L., Bergman, T., Ahl, M., Wahlgren, C.-H., Persson, P.-O- & Wickström, L., 2009: Synthesis of the bedrock geology in the Bergslagen region, Fennoscandian Shield, south-central Sweden. *Sveriges geologiska undersökning Ba 58*, 259 pp.

Stephens, M.B. & Weihed, P., 2013: Tectonic evolution and mineral resources in the Fennoscandian Shield, Sweden. *12th Biennial SGA Meeting, Uppsala, Sweden, excursion guide books SWE 1–7.*

Strömberg, A., 1988: Berggrundskartan 12 F Ludvika SV, *SGU Ser Af nr 158.*

Strömberg, A. & Sukotjo, S., 1988: Strukturgeologiska kartan 12F Ludvika SV, *SGU Ser. Af nr 158.*

Sultan, L., Claesson, S., Plink-Björklund, P., 2005: Proterozoic and Archaean ages of detrital zircon from the Palaeoproterozoic Västervik basin, SE Sweden: implications for provenance and timing of deposition. *GFF 127*, 17–24.

Sundberg, A. 2000: Stora Åstjärnen, det första bekräftade "kimberlit"-diatremet i Sverige. *SGU Report 2000:10 (BRAP200006)*, 8 p. + appendix.

Sundius, N., 1952: Kvarts, fältspat och glimmer samt förekomster där av i Sverige. *Sveriges geologiska undersökning C 520*, 231 pp.

Sundvall, R., 2003: *En petrologisk studie av de ultramafiska lamprofyrerna i Kalix, Norrbotten*. MSc. thesis. Stockholm University. 65 pp.

Söderlund, U., Isachsen, C., Bylund, G., Heaman, L., Patchett, P.J., Vervoort. J.D., Andersson, U.B., 2005: U-Pb baddeleyite ages and Hf, Nd isotope chemistry constraining repeated mafic magmatism in the Fennoscandian Shield from 1.6 to 0.9 Ga. *Contributions to Mineralogy and Petrology 150*, 174–194.

Tarvainen, T., Reeder, S., Albanese, S., 2005: Database management and map production. In: Salminen, R., Batista, M.J., Bidovec, M., Demetriades, A., De Vivo, B., De Vos, W., Duris, M., Gilucis, A., Gregorauskiene, V., Halamic, J., Heitzmann, P., Lima, A., Jordan, G., Klaver, G., Klein, P., Lis, J., Locutura, J., Marsina, K., Mazreku, A., O'Connor, P.J., Olsson, S.A., Ottesen, R.T., Petersell, V., Plant, J.A., Reeder, S., Salpeteur, I., Sandström, H., Siewers, U., Steenfelt, A., Tarvainen, T. (Eds.), *FOREGS Geochemical Atlas of Europe, Part 1: Background Information, Methodology and Maps.* Geological Survey of Finland, Espoo, pp. 95–108.

Tasmet Metal AB, 2013: Amended and restated technical report for Olserum REE deposit, southern Sweden. Prepared for Tasman metal limited by Reed Leyton consulting. https://finance.yahoo.com/news/tasman-submits-mining-lease-application-124500119.html

Taylor, S.R. & McLennan, S.M., 1985: *The Continental Crust: Its Composition and Evolution*. Blackwell, Oxford.

Tegengren, F., 1924: Sveriges ädlare malmer och bergverk. *Sveriges geologiska undersökning Ca 17*, 1–406.

Tenow, O., 1902: Über einen mineralführenden Albitpegmatit von Stripåsen in Westmanland. *Bulletin of the Geological Institution of the University of Upsala 5,* 267–270.

Törnebohm, A. E., 1906: Katapleiit-syenit, en nyupptäckt varietet af nefelinsyenit i Sverige. *Sveriges geologiska undersökning C 199*, 54 pp.

Törnebohm, A.E. 1883: Om den s.k. Fonoliten från Elfdalen, dess klyftort och förekomstsätt. *Geologiska Föreningens i Stockholm Förhandlingar.*

Walderhaug H.J., Torsvik T.H., Eide E.A., Meert J.G. 2003: Magnetic properties and age of the Alnö Complex, Sweden. *EUG-EGS-AGU 2003 Meeting. Geophysical Research Abstracts EAE03-A,* 10358.

Valeton, L.,1972: Bauxites: Elsevier, Amsterdam-London- New York, p. 226.

Walters, A., Lusty, P., Chetwyn, C., Hill, A., 2011: Rare Earth Elements. British Geological Survey Report. 45 pp.

Wanhainen, C., Broman, C., Martinsson, O., 2003: The Aitik Cu–Au–Ag deposit in northern Sweden: A product of high salinity fluids. *Mineralium Deposita 38*, 715–726.

Weihed, P., 2001: A review of Palaeoproterozoic intrusive hosted Cu-Au-Fe-oxide deposits in northern Sweden. *Sveriges geologiska undersökning C 833*, 4–32.

Weihed, P., Bergman Weihed, J., Sorjonen-Ward, P., 2003: Structural evolution of the Björkdal gold deposit, Skellefte district, northern Sweden: Implications for early Proterozoic mesothermal gold in the late stage of the Svecofennian orogen. *Economic Geology 98,* 1291–1309.

Weihed, P., Arndt, N., Billström, K., Duchesne, J.-C., Eilu, P., Martinsson, O., Papunen, H., Lahtinen, R., 2005: Precambrian geodynamics and ore formation: the Fennoscandian Shield. *Ore Geology Reviews 27*, 273–322.

Welin, E., 1966: Uranium mineralizations and age relationships in the Precambrian bedrock of central and southeastern Sweden. *Geologiska Föreningens i Stockholm Förhandlingar 88*, 34–67.

Verplanck, P.L., Van Gosen, B.S., Seal, R.R, and McCafferty, A.E., 2014: A deposit model for carbonatite and peralkaline intrusion-related rare earth element deposits: *U.S. Geological Survey Scientific Investigations Report 2010-5070J*, 58 p.

Verplanck, P.L., Mariano, A.N., and Mariano, A., Jr., 2016: Rare earth element ore geology of carbonatites: *Reviews in Economic Geology, v. 18*, p. 5–32.

Wiens, K. 2012: A Visit to the Only American Mine for Rare Earth Metals. *The Atlantic*, February 21. Collected from: http://www.theatlantic.com/technology/archive/2012/02/a-visit-to-the-only-american-mine-for-rare-earthmetals/ 253372/ (last accessed 140111).

Wik, N.-G., Stephens, M. B., Sundberg, A., 2004: Malmer, industriella mineral och bergarter i Stockholms län. *Sveriges geologiska undersökning Rapporter och meddelanden 117*, 144 pp.

Wiklander, U. & Lundström, I., 1991: Berggrundskartan 11E Filipstad SO. *Sveriges geologiska undersökning Af 177.*

Wikström, A. & Karis L., 1991: Beskrivning till berggrundskartorna Finspång NO, SO, NV och SV. *Sveriges geologiska undersökning Af 162–165.*

Wikström, A. & Karis, L., 1997: Beskrivning till berggrundskartan Karlskoga SO. *Sveriges geologiska undersökning Af 183*, 111 pp.

Wikström, A. & Andersson, U. B., 2004: Geological features of the Småland-Värmland belt along the Svecofennian margin, part I: from the Loftahammar to the Tiveden-Askersund areas. In: Högdahl, K., Andersson, U, B. & Eklund, O. (eds.), The Transscandinavian Igneous Belt (TIB) in Sweden: a review of its character and evolution, *Geological Survey of Finland, Special Paper 37*, 22–39.

Viladkar, S.G., Pawaskar, P.B., 1989: Rare earth element abundances in carbonatites and fenites of the Newania complex, Rajasthan India. *Bulletin of the Geological Survey of Finland 61*, 113–122.

Williams, P. J., Barton, M. D., Johnson, D. A., Fontboté, L., de Haller, A., Mark, G., Oliver, N. H. S., Marschik, R., 2005: Iron oxide copper-gold deposits: geology, space-time distribution, and possible modes of origin. *Economic Geology 100th Anniversary Volume*, 371–405.

Viola, G., Venvik Ganerød, G., Wahlgren, C.-H., 2009: Unraveling 1.5 Ga of brittle deformation history in the Laxemar–Simpevarp area, southeast Sweden: A contribution to the Swedish site investigation study for the disposal of highly radioactive nuclear waste. *Tectonics 28*, TC 5007, DOI:10.1029/2009TC002461.

Von Eckermann, H., 1928: Hamrongite, a new Swedish alkaline mica lamprophyre. *Fennia 50, 13*, 1–21.

Von Haidinger, W.K., 1845: *Handbuch der bestimmenden Mineralogie, enthalden Die Terminologie, Systematik, Nomenklatur, und Characteristik der Naturgeschichte des Mineralreiches*. Vienna, Braumuller und Seidel, 630 pp.

Von Maravic, H., Morteani, G., 1980: Petrology and geochemistry of the carbonatite and syenite complex of Lueshe (NE Zaire). *Lithos 13*, 159–170.

Åhäll, K.-I., Connelly, J., Brewer, T.S., 2000: Episodic rapakivi magmatism due to distal orogenesis? Correlation of 1.69–1.50 Ga orogenic and inboard “anorogenic” events in the Baltic Shield. *Geology 28*, 823–826.

Öhlander, B., Ingri, J., Ponter, C., 1991: Geochemistry of till weathering in the Kalix River Watershed, northern Sweden. In: Rosen, K. (Ed.), *Chemical Weathering under Field Conditions Report 63*, Reports in Forest Ecology and Forest Soils, pp. 1–18.

Öhlander, B., Skiöld, T., Elming S.A., BABEL Working Group, Claesson, S., Nisca, D.H., 1993: Delineation and character of the Archaean–Proterozoic boundary in northern Sweden. *Precambrian Research 64*, 67–84.

Öhlander, B., Land, M., Ingri, J., Widerlund, J., 1996: Mobility of rare earth elements during weathering of till in northern Sweden. *Applied Geochemistry 11*, 93–99.

Öhman, L., Nysten, P., Langhof, J., 2004: The Bastnäs mines. *Mineralogical Record 35*, 187–200.

List of unpublished references

Andersson, L.-G. 1972: Sällsynta jordartsmetaller i svenska järnmalmer. STU-rapport 69-704/U 550 och 70-794/U 653, unpublished report, 40 p.

Andersson, L.-G., 1974: Sällsynta jordartsmetaller (REM) i Grängesberg. Unpublished report.

Dagbo, E. & Martinsson, O., 1981: Ruoutevarepegmatiten, Jokkmokk, en mineralogisk-geologisk undersökning. Unpublished thesis, Luleå Tekniska Högskola, 1981:081E, 61 pp.

Fagerberg, B., Sandgren, P-M., 1970: Undersökning av uran-haltig malm från Pålänge. LKAB Malmberget. Unpublished report. 16 pp.

Gustafsson, B., 1990: Sällsynta jordartsmetaller i Sverige. Sveriges geologiska AB, Division Prospektering, Prospekteringsrapport PRAP 90024 (Unpublished exploration report, in Swedish), 36 p.

Gustafsson, B., 1991: Sällsynta jordartsmetaller. Regional fältkontroll 1991 av arkivuppslag. Sveriges Geologiska AB, Division Prospektering, Prospekteringsrapport PRAP 91047 (unpublished exploration report, in Swedish), 65 p.

Hammergren, P., 1988: Sällsynta jordartsmetaller i Sverige – förstudie. Sveriges Geologiska AB, Division Prospektering, Prospekteringsrapport PRAP 88509 (unpublished exploration report, in Swedish), 71 p.

Holmqvist, A., 1989: Prästrun. Ett nytt alkalint bergartsområde. Unpublished SGAB report PRAP 89 019.

Hålenius, U., 1987: Au-mineralogi Riddarhyttefältet. Sveriges Geologiska AB Unpublished prospecting report, Division prospektering PRAP 87018, 10 pp.

Hålenius, U., 1990: Holmslättmyren mineralogi. Unpublished SGAB report PRAP 90 010.

Ihre, P., Sädbom, S., 1986: Riddarhytte malmfält. Prospekteringsarbeten 1986. Sveriges Geologiska AB, Unpublished prospecting report, Division prospektering PRAP 86541, 261 pp.

Pettersson, B., 1980a: Results from drilling and till spectrometry at Näverån, Stugun area. Sveriges geologiska undersökning. BRAP 80049, unpublished exploration report. 9 pp

Pettersson, B., 1980b: Results from mineralogical investigations and chemical analyses of some boulder occurrences in the Stugun area. Sveriges geologiska undersökning. BRAP 80064, unpublished exploration report. 23 pp

Reed, G. C., 2013: Technical report for Olserum REE deposit. Unpublished report, Tasman Metals Ltd., Reed Leyton consulting, Australia. 84 pp.

Rydberg, S. 1972: Uranmineraliseringar i trakten av Västervik. Trebetygsarbete, Lunds Universitet (unpublished thesis), 11 p. + appendices.

Sundberg, A. 2005: Fältbesöksprotokoll, Mineraljakten 2005. 3 poäng. Kbl 17HNO. SGU, unpublished report, 1 p.

Svensson, U. 1972: Sällsynta jordartsmetaller på Alnön. Boliden Mineral AB, Årsrapport 1971, bilaga 36, 5 p. + appendix (unpublished report).

Tideström, C.J., 1890: Anteckningar och utdrag rörande Riddarhytte bruks hemmansegare och bergshandtering. Unpublished manuscript.

APPENDIX 1

Table 1. Results of the chemical analysis performed during the EURARE project, and type of mineralisation. Rare earth metals have been analyzed at ALS Scandinavia AB and are derived from a lithium borate fusion followed by either ICP-AES or ICP-MS.

Locality	Sample	x	y	Type	Beskrivning	TotREE	LREE	HREE	Ce	Dy	Er	Eu	Gd	Ho	La	Lu	Nd	Pr	Sm	Tb	Tm	Y	Yb	Sc
Tybble gruva	SGUR10006	6517096	516016	Apatite Iron Ore	Kvartsrik	176.73	162.21	14.52	76.5	1.5	1.03	0.41	2.18	0.33	58.3	0.24	14.1	5.65	2.17	0.25	0.15	9.7	1.32	2.9
Tybble gruva	SGUR10007	6517096	516016	Apatite Iron Ore	Kvartsrik	17427.63	17273.85	153.78	8500	22.6	7.9	11.55	44.7	3.57	6910	0.88	1145	579	80.8	5.21	0.91	107	5.71	2.8
Blötberget	SGUR10030	6664986	503759	Apatite Iron Ore	Apatitmalm	1069.94	940.59	129.35	432	16.75	8.48	4.69	24	3.44	217	1.11	183	48.5	30.9	3.01	1.22	88.2	7.14	0.5
Blötberget	SGUR10032	6664986	503759	Apatite Iron Ore	Apatitmalm	58.18	37.03	21.15	10.8	2.33	1.45	0.84	2.22	0.57	5.5	0.24	7.4	1.45	1.82	0.34	0.23	14.6	1.39	7
Storön S om Kalix	JSM150001C	7310740	870343	Carbonatite	Skitig karbonatit el silikosövit	5240.26	5169.4	70.86	2320	16.2	3.07	30.3	64.6	1.89	1475	0.16	899	256	120.5	5.64	0.31	42.3	1.29	4
Storön S om Kalix	JSM150003B	7313636	869907	Carbonatite	Karbonatit	33.06	22.34	10.72	9.5	0.97	0.71	0.26	0.92	0.24	5.3	0.1	4	1.04	0.92	0.16	0.1	7.7	0.74	0.4
Storön S om Kalix	JSM150004B	7312505	869766	Carbonatite	Skitig karbonatit el silikosövit	914.75	850.16	64.59	369	10.6	3.97	7.01	19.35	1.76	212	0.28	161	42.1	26.8	2.32	0.45	43.2	2.01	12.9
ALNÖ140001	Alnö, Smedsgården (ca.-koord.)	6926012	625783	Carbonatite		2552.82	2279.7	273.12	1115	31.6	19.65	10.4	38.4	5.91	566	3.49	374	116.5	50.6	5.37	3	181.5	22.6	8.8
ÅKER140001	Åkersjön	7071134	454780	Carbonatite		2045.8	1969.72	76.08	936	10.3	5.15	5.62	16.9	1.79	635	0.73	256	90.4	28.6	2.08	0.75	50.1	5.18	1.2
SO Rödbergsgruvan, Fogdhyttan	cmr150049a	6596800	494682	Felsic metavolcanite	Glimmerskiffer	249.12	176.18	72.94	74	7.97	5.35	0.94	9.06	1.86	34.3	0.81	38.7	9.22	8.96	1.31	0.75	49.7	5.19	1
V Gamla Bastnäsfältet	cmr150054a	6634035	532725	Felsic metavolcanite	Vulkanisk breccia	133.18	92.03	41.15	40.1	3.26	3.04	0.59	2.63	0.99	22.1	0.6	18.1	4.73	2.98	0.4	0.53	28.6	3.73	0.8
V Gamla Bastnäsfältet	cmr150054b	6633973	532735	Felsic metavolcanite	Pimpstensförande siltsten	211.59	144.57	67.02	64.1	5.21	3.74	0.83	4.4	1.37	29.7	0.6	31.6	7.89	5.25	0.73	0.54	51	3.83	0.8
Stora Malmkärra gruvan	cmr150058a	6658165	547147	Felsic metavolcanite	Glimmerskiffer	175.61	100.05	75.56	43.2	7.46	5.54	0.27	5.42	1.88	16.9	0.82	22.7	5.4	4.56	0.99	0.8	52.8	5.27	1.6
N Stora Malmkärragruvan	cmr150059a	6658433	546862	Felsic metavolcanite	Vulkanisk breccia, sprängsten	298.91	229.76	69.15	99.7	7.76	4.94	1.07	8.18	1.86	50.2	0.74	47.9	12.25	9.16	1.31	0.69	47.2	4.65	1.3
Elgsjögruvan	SGUR10090	6563796	619137	Fe-ore unspec.	Gnejs	21.23	18.01	3.22	6.2	0.41	0.19	0.45	0.93	0.04	3.6	0.01	3.5	0.81	0.92	0.1	0.01	2.3	0.16	1.6
Elgsjögruvan	SGUR10092	6563796	619137	Fe-ore unspec.	Gnejs	48	41.18	6.82	17.9	0.93	0.46	0.69	1.22	0.14	10.4	0.04	7.1	1.85	1.42	0.15	0.06	4.6	0.44	0.6
PNY160099A	Hästbäck	6651729	560048	Magnetite-(Fe-sulphide)-Calcsilicate skarn	Sufidförande skarn	6099.52	5865.11	234.41	2900	30.1	15	2.11	54.8	5.43	1620	2.18	877	296	112.5	5.6	2.2	159.5	14.4	2.7
Storön S om Kalix	JSM150001B	7310740	870343	Lamprophyre	Karbonatrik lamprofyr?	1243.91	1204.36	39.55	554	6.21	2.41	5.91	12.85	1.04	340	0.35	201	58.7	23.6	1.43	0.33	25.5	2.28	8.3
Karlsborg, Kalix	JSM150002B	7323930	877941	Lamprophyre	Karbonatrik lamprofyr?	841.95	784.77	57.18	343	8.98	3.32	6.72	17.15	1.69	188.5	0.23	149.5	39.3	24.5	2.07	0.38	38.4	2.11	16.1
Kanntalsgruvan	TOB150043B	6632354	530860	Magnetite-(Fe-sulphide)-Calcsilicate skarn	Magnetitskarn med sulfider	4838.57	4611.45	227.12	2140	33.4	11.2	18.15	60.6	5.43	1500	0.85	604	208	78.6	7.39	1.24	161	6.61	2.1
Stora Långgruvan	TOB150058A	6638935	538148	Magnetite-(Fe-sulphide)-Calcsilicate skarn	Magnetitskarn med sulfidimpregnation	216.31	90.62	125.69	19.3	19.3	8.05	1	20.3	3.42	5.1	0.72	26.4	4.27	14.15	3.52	0.98	83.8	5.9	0.1
Stora Långgruvan	TOB150058B	6638935	538148	Magnetite-(Fe-sulphide)-Calcsilicate skarn	Magnetitskarn med sulfidimpregnation	9593.7	9261.3	332.4	4220	58.8	18.6	12.2	133	8.77	2570	1.98	1610	482	234	14.25	2.45	214	13.55	0.1

***Table 1.** Continuation.*

Locality	Sample	x	y	Type	Beskrivning	TotREE	LREE	HREE	Ce	Dy	Er	Eu	Gd	Ho	La	Lu	Nd	Pr	Sm	Tb	Tm	Y	Yb	Sc
Knutsbo gruvor	KNUT3	6662595	577230	Magnetite-(Fe-sulphide)-Calcsilicate skarn	Aktinolit-magnetit-skarn med pyrit	4706.77	4393.5	313.27	1875	58.2	13.45	36.6	133	7.74	937	0.79	972	253	186	15	1.27	211	5.82	0.9
Mörkens 4	MÖRK2	6662160	577465	Magnetite-(Fe-sulphide)-Calcsilicate skarn	Cu-förande kvartsigt skölskarn	36921.29	33224.5	3696.79	10000	816	121.5	224	1000	87.3	10000	3.82	10000	1000	1000	276	9.57	2350	32.6	0.5
Mörkens 4	MÖRK3	6662160	577465	Magnetite-(Fe-sulphide)-Calcsilicate skarn	Cu-förande amfibols-karn	24970.97	21635.6	3335.37	9070	583	133.5	55.2	1000	78.1	3080	5.17	6430	1000	1000	144.5	12.3	2330	48.8	0.4
Mörkens 4	MÖRK4	6662160	577465	Magnetite-(Fe-sulphide)-Calcsilicate skarn	Kloritskölig felsisk vulkanit	228.74	199.46	29.28	86.1	3.59	1.71	1.49	6.09	0.7	36	0.24	42.4	10.5	8.78	0.72	0.25	20.5	1.57	8.1
Stora Rödbergs gruvan, Fogdhyttan	cmr150052a	6596978	494083	Magnetite-(Fe-sulphide)-Calcsilicate skarn	Bio-amf-klo-grt-skarn, varp	374.47	322.21	52.26	139	5.12	3.84	1.78	6.99	1.17	92	0.69	53.7	15.1	8.64	0.87	0.6	35.5	4.47	5
Kanntalsgruvan	TOB150043C	6632354	530860	Magnetite-Calc silicate skarn	Aktinolit-magnetit-skarn	224.28	134.9	89.38	55.9	9.5	5.95	1.47	7.2	2.12	33.2	0.61	23.8	6.28	5.75	1.5	0.75	64.6	4.35	1.3
Höjdgruvan	TOB150044A	6632327	531317	Magnetite-Calc silicate skarn	Magnetit-px-amf-granatskarn	408.77	252.12	156.65	103.5	16.75	10.4	1.47	15.2	3.67	61.5	1.48	46.8	11.85	11.7	2.97	1.48	110.5	9.4	0.1
Höjdgruvan	TO-B150044B	6632327	531317	Magnetite-Calc silicate skarn	Magnetit-px-amf-granatskarn	209.08	152.69	56.39	65.4	5.55	4.29	2.16	4.46	1.44	32.5	0.76	29.1	8.05	5.62	0.82	0.67	38.6	4.26	5.4
Sjögruvan	TOB150045A	6633544	530412	Magnetite-Calc silicate skarn	Magnetit-antofyllit-skarn	636.96	603.78	33.18	262	3.84	1.58	1.98	12.4	0.69	106	0.21	156.5	38.6	25.3	1.05	0.22	24.3	1.29	1
Sjögruvan	TOB150045B	6633544	530412	Magnetite-Calc silicate skarn	Magnetit-antofyllit-skarn	3270.66	3111.94	158.72	1450	18.7	7.67	9.14	50.2	3.17	626	0.82	690	188	97	4.7	0.96	117	5.7	1.6
Thalengruvan	TOB150046A	6633644	532703	Magnetite-Calc silicate skarn	Magnetit-kvarts-(aktinolit)malm	68.05	38.02	30.03	14.7	3.66	1.78	1.62	2.49	0.7	8.7	0.22	6.5	1.82	1.79	0.55	0.21	21.7	1.21	0.4
Thalengruvan	TO-B150046B	6633644	532703	Magnetite-Calc silicate skarn	Magnetit-kvarts-(aktinolit)malm	306.4	268.07	38.33	114	6.04	1.92	5.1	9.82	0.98	58.9	0.15	53.3	13.8	12.65	1.34	0.2	26.6	1.1	0.5
Stora Kvickstens-gruvan	TOB150050A	6634619	532977	Magnetite-Calc silicate skarn	Magnetit-aktinolit-skarn	384.96	330.2	54.76	168.5	5.11	3.4	1.63	6.35	1.14	94.7	0.46	39.3	12.75	6.37	0.94	0.49	40.2	3.02	0.6
Stora Kvickstens-gruvan	TOB150050B	6634619	532977	Magnetite-Calc silicate skarn	Magnetit-aktinolit-skarn	479.91	375.66	104.25	140.5	10.85	4.87	3.21	15.3	2.08	129.5	0.66	58	15.95	12.7	2.12	0.7	78.6	4.37	0.5
Storgruvan nr 4	TOB150051A	6635124	533269	Magnetite-Calc silicate skarn	Magnetit-aktinolit-skarn	2305.29	1769.45	535.84	736	74.4	34.2	11.55	89.9	14.05	371	2.78	368	94.5	92.7	14.55	4.26	369	22.6	5.8
Storgruvan nr 4	TOB150051B	6635124	533269	Magnetite-Calc silicate skarn	Magnetit-aktinolit-skarn	9908.08	9153.6	754.48	4010	120.5	41.9	16.2	249	20.1	2070	2.98	1930	505	373	28.7	4.8	510	25.5	0.4
Granåsgruvan nr 1	TOB150056A	6637353	533770	Magnetite-Calc silicate skarn	Magnetit-aktinolit-skarn	171.45	62.71	108.74	22.9	9.8	6.66	0.69	6.42	2.35	14.2	0.97	11.2	2.86	3.54	1.41	1	80.3	6.25	0.9
Granåsgruvan nr 1	TOB150056B	6637353	533770	Magnetite-Calc silicate skarn	Magnetit-aktinolit-skarn	209.72	128.58	81.14	40	7.89	4.79	0.51	7.46	1.72	33	0.79	29.3	7.69	7.02	1.26	0.77	58.6	5.32	3.6
Billsjöfältet (sydost-ligaste gruvhålet)	TOB150060A	6643786	539113	Magnetite-Calc silicate skarn	Magnetit-aktinolit-skarn	123.14	97.18	25.96	32.8	3.34	1.57	1.33	3.96	0.62	15.5	0.26	19.5	4.53	4.06	0.57	0.23	17.7	1.67	15.5
Billsjöfältet (sydost-ligaste gruvhålet)	TO-B150060B	6643786	539113	Magnetite-Calc silicate skarn	Magnetit-px-epidot-kvarts-kalcitskarn	1116.67	838.44	278.23	384	28.6	18.85	5.34	25	6.07	197	3.68	148.5	45	28.6	4.48	3.25	191.5	21.8	5
Saragruvan	TOB150061A	6650139	541488	Magnetite-Calc silicate skarn	Magnetit-aktinolit-skarn	580.21	500.66	79.55	232	10.55	4	4.41	17.7	1.7	110	0.32	90.9	26.1	18.45	2.19	0.48	57.8	2.51	1.1
Saragruvan	TOB150061B	6650139	541488	Magnetite-Calc silicate skarn	Magnetit-aktinolit-skarn	356.36	310.82	45.54	139.5	5.14	2.45	1.94	8.01	1.05	85	0.27	51.8	13.85	9.62	0.97	0.33	33.5	1.83	1.1

Table 1. *Continuation.*

Locality	Sample	x	y	Type	Beskrivning	TotREE	LREE	HREE	Ce	Dy	Er	Eu	Gd	Ho	La	Lu	Nd	Pr	Sm	Tb	Tm	Y	Yb	Sc
Långgruvan	TOB150062A	6652724	541461	Magnetite-Calc silicate skarn	Magnetit-aktinolit-hornblände-biotitskarn	326.1	267.35	58.75	117	7.75	4.24	2.18	7.97	1.5	62.5	0.61	51.5	14.35	9.65	1.3	0.66	38.7	3.99	2.2
Långgruvan	TOB150062B	6652724	541461	Magnetite-Calc silicate skarn	Magnetit-aktinolit-hornblände-biotitskarn	654.88	546.82	108.06	242	13.95	7.89	4.32	16.4	2.82	123	1.13	108.5	29	20.8	2.55	1.22	70.6	7.9	2.8
Dammsjögruvan	TOB150063A	6654922	543467	Magnetite-Calc silicate skarn	Magnetit-aktinolitskarn	152.93	92.81	60.12	37	5.74	3.89	1.63	6.08	1.31	17.5	0.54	17.9	4.7	4.8	1.03	0.61	43.5	3.5	3.2
Dammsjögruvan	TOB150063B	6654922	543467	Magnetite-Calc silicate skarn	Magnetit-aktinolitskarn	153.97	98.02	55.95	39.9	5.77	3.49	1.43	5.95	1.19	19.5	0.52	19.1	5.04	5	0.97	0.53	40.1	3.38	2.1
Korsstensgruvan	TOB150064A	6656438	545791	Magnetite-Calc silicate skarn	Magnetit-aktinolitskarn	5168	4987.55	180.45	2190	38.2	9.76	14.75	101	4.99	1255	0.88	979	266	181.5	10.3	1.15	109	6.17	0.3
Korsstensgruvan	TOB150064B	6656438	545791	Magnetite-Calc silicate skarn	Magnetit-aktinolitskarn	1147.16	1033.51	113.65	458	20.1	7.59	3.51	30.2	3.19	243	0.69	202	55.2	41.4	4.1	0.98	71.6	5.4	0.2
Aspgruvan	TOB150065A	6657116	546319	Magnetite-Calc silicate skarn	Magnetit-aktinolitskarn	336.78	280.07	56.71	111.5	10.05	3.53	1.12	15.15	1.6	52.1	0.3	66.8	15.6	17	2.03	0.44	36.4	2.36	0.8
Aspgruvan	TOB150065B	6657116	546319	Magnetite-Calc silicate skarn	Magnetit-aktinolitskarn	1699.49	1623.35	76.14	726	12.55	4.19	2.35	26.6	1.97	439	0.32	300	86.2	42.9	3.02	0.49	50.7	2.9	0.3
Svartbergsgruvan	TOB150068A	6664138	554608	Magnetite-Calc silicate skarn	Magnetit-aktinolitskarn	416.4	174.93	241.47	64	28.9	13.7	5.96	19	5.71	34.8	0.91	30.7	8.07	12.1	4.36	1.6	178.5	7.79	0.3
Svartbergsgruvan	TOB150068B	6664138	554608	Magnetite-Calc silicate skarn	Magnetit-aktinolitskarn	255.67	171.72	83.95	72.2	7.65	5.05	2.97	8.41	1.71	36.1	0.72	33.8	9.01	8.33	1.34	0.68	62.2	4.6	0.9
Gruvhagen SV om Knutsbo gruvor	GRUVHAG1	6662377	577026	Magnetite-Calc silicate skarn	Fintrådigt aktinolitskarn	24574.11	23618.2	955.91	10000	177	35.8	224	573	21.7	5980	2.1	4950	1000	891	51.2	3.46	649	15.65	0.2
Gruvhagen SV om Knutsbo gruvor	GRUVHAG2	6662377	577026	Magnetite-Calc silicate skarn	Fintrådigt aktinolitskarn	788.86	728.43	60.43	326	8.26	2.36	8.23	16	1.22	199	0.19	121.5	36.4	20	1.78	0.17	45.3	1.15	1.3
Knutsbo gruvor	KNUT1	6662595	577230	Magnetite-Calc silicate skarn	Tremolitskarn	1135.13	939.75	195.38	417	25.6	12.3	11.15	30.7	4.7	230	1.98	165	47.9	35.3	4.58	1.82	132	12.4	2.7
Knutsbo gruvor	KNUT4	6662595	577230	Magnetite-Calc silicate skarn	kvarts och amfibolbandad magnetit	238.61	184.04	54.57	78.8	6.67	2.42	3.24	6.8	1.08	53.5	0.2	26.9	8.05	6.35	1.15	0.23	41.3	1.52	0.4
Mörkens 4	MÖRK1	6662160	577465	Magnetite-Calc silicate skarn	Tremolitskarn	11077.36	9203.4	1873.96	3390	332	71.4	42.2	688	43.7	1285	2.62	2540	541	717	83.3	6.34	1310	24.6	0.2
Stora Malmkärra gruvan	cmr150058b	6658282	547136	Magnetite-Calc silicate skarn	Amfibolskarn. varp	908.73	670.23	238.5	258	38.9	17.05	4.93	42.6	7.38	166.5	1.45	128	31.2	35.6	6.67	2.1	154	10.95	3.4
Djupedalsgruvan	JSM150006A	6425442	578440	Magnetite-Calc silicate skarn	Xenotim xx i biotit	25903.8	11132.8	14771	4290	1000	1000	47.4	1000	741	2060	326	2350	549	744	382	322	10000	1000	92.4
Djupedalsgruvan	JSM150007A	6425442	578440	Magnetite-Calc silicate skarn	Allanit och xenotim i biotit	34643	22745.5	11897.5	10000	1000	913	44.9	1000	318	4850	130.5	4760	1000	995	202	134	8360	840	95.6
Djupedalsgruvan	JSM150008A	6425442	578440	Magnetite-Calc silicate skarn	Monazit i biotit	29990	16625.5	13364.5	6960	1000	1000	39.4	1000	351	3400	152	3500	858	776	217	156.5	9510	978	92.1
Djupedalsgruvan	JSM150009A	6425442	578440	Magnetite-Calc silicate skarn	Magnetitmalm	8908.65	7640.9	1267.75	3330	170	85.6	11.7	257	34.2	1615	10.4	1660	423	316	34.2	11.75	851	70.6	28.2
Skyttebo	SGUR10005	6566793	487280	Magnetite-Calc silicate skarn	Skarn	30.15	21.81	8.34	8.8	0.79	0.45	0.61	1.05	0.14	3	0.03	5	1.32	0.93	0.11	0.02	6.5	0.3	1.1
Åmme gruva	SGUR10012	6527343	499480	Magnetite-Calc silicate skarn	Kvartsrik	102.78	96.1	6.68	41.1	1.28	0.32	1.55	2.97	0.14	28	0.01	14.4	4.33	3.45	0.29	0.02	4.5	0.12	0.3
Åmme gruva	SGUR10014	6527343	499480	Magnetite-Calc silicate skarn	Kvartsrik	171.73	85.83	85.9	34	9.98	5.65	1.36	7.8	2.09	22.7	0.74	11.3	3.41	4.46	1.36	0.83	59.7	5.55	0.8
Mogruvan	SGUR10017	6565880	488166	Magnetite-Calc silicate skarn	Skarn	30.22	18.78	11.44	7.3	1.24	0.68	0.16	1.07	0.22	4.1	0.16	3.9	0.92	1.03	0.14	0.11	8	0.89	0.3

Table 1. *Continuation.*

Locality	Sample	x	y	Type	Beskrivning	TotREE	LREE	HREE	Ce	Dy	Er	Eu	Gd	Ho	La	Lu	Nd	Pr	Sm	Tb	Tm	Y	Yb	Sc
Nyhyttegruvan	SGUR10019	6524545	502183	Magnetite-Calc silicate skarn	Kvartsrik	98.17	78.57	19.6	33.1	2.17	1.33	0.5	2.45	0.44	21.6	0.18	13.1	3.68	2.54	0.33	0.17	13.7	1.28	1.6
Nyhyttegruvan	SGUR10020	6524545	502183	Magnetite-Calc silicate skarn	Kvartsrik	112.95	87.77	25.18	36.1	2.69	1.54	2.13	2.84	0.58	22.9	0.24	15.4	3.92	2.88	0.42	0.25	17.8	1.66	1.6
Hemgruvorna	SGUR10026	6556375	480421	Magnetite-Calc silicate skarn	Skarn	12.27	8.69	3.58	3.2	0.35	0.24	0.06	0.44	0.07	2.6	0.03	1.5	0.34	0.35	0.05	0.01	2.6	0.23	0.2
Hemgruvorna	SGUR10029	6556375	480421	Magnetite-Calc silicate skarn	Skarn	260.63	206.58	54.05	85.9	6.27	3.82	1.38	6.44	1.37	44.2	0.61	38.1	10	8.36	1.04	0.64	36.5	3.8	12.2
Bäckbergsgruvan	SGUR10051	6677195	488890	Magnetite-Calc silicate skarn	Skarn	257.7	243.75	13.95	114.5	1.58	0.83	1.48	2.64	0.32	85.2	0.11	26.5	9.48	3.45	0.33	0.09	9.9	0.79	0.5
Bäckbergsgruvan	SGUR10058	6677195	488890	Magnetite-Calc silicate skarn	Skarn	2432.14	2330.66	101.48	1100	21	7.37	4.86	32.8	3.52	705	0.54	331	104	52.2	4.14	0.92	59.7	4.29	0.8
Mölbergsgruvan	SGUR10060	6589962	492216	Magnetite-Calc silicate skarn	Skarn	78.28	64.24	14.04	27	2.09	0.88	0.71	2.63	0.39	14.9	0.1	11.9	3.06	2.94	0.43	0.13	9.3	0.72	1.1
Klacka-Lerberg	SGUR10062	6606739	495521	Magnetite-Calc silicate skarn	Skarn	138.48	118.92	19.56	46.3	3.12	0.96	1.1	5.31	0.49	25.8	0.14	22.2	5.32	4.99	0.63	0.12	13.3	0.8	7.9
Mogruvan	SGUR10076	6588226	493978	Magnetite-Calc silicate skarn	Skarn	21.88	12.25	9.63	3.8	1.01	0.61	0.12	1.4	0.2	2.1	0.08	2.5	0.5	1.13	0.2	0.06	6.9	0.57	0.7
Mogruvan	SGUR10077	6588226	493978	Magnetite-Calc silicate skarn	Skarn	40.96	28.64	12.32	10.2	1.75	0.76	0.2	2.18	0.28	5	0.09	6.7	1.45	2.21	0.3	0.11	8.3	0.73	0.7
Bojgruvan	SGUR10080	6551501	473426	Magnetite-Calc silicate skarn	Skarn	563.2	508.64	54.56	230	6.65	3.37	2.04	10.85	1.27	119.5	0.52	92.1	25.4	15.45	1.3	0.52	38.1	2.83	13.3
Skyttebo	SGUR10081	6566654	487319	Magnetite-Calc silicate skarn	Skarn	45.21	32.28	12.93	13.3	1.53	0.81	0.49	1.38	0.3	6.1	0.14	7.4	1.79	1.52	0.22	0.14	8.8	0.99	0.3
Glittergruvan	SGUR10093	6671906	702086	Magnetite-Calc silicate skarn	Skarn	68.93	27.75	41.18	6.3	7.13	2.72	1.24	6.15	1.23	2	0.23	7.2	1.18	3.58	1.08	0.35	26.5	1.94	0.1
Lappgruvorna	SGUR10104	6669753	703502	Magnetite-Calc silicate skarn	Skarn	23.02	19.88	3.14	9	0.38	0.2	0.14	0.32	0.05	5.8	0.01	3.1	0.89	0.53	0.06	0.01	2.2	0.23	0.1
Lappgruvorna	SGUR10106	6669753	703502	Magnetite-Calc silicate skarn	Skarn	318.66	175.88	142.78	28.4	20.1	7.44	7.31	27.3	3.43	7.6	0.72	66.8	8.27	28	3.74	1.06	100.5	5.79	2.2
Glittergruvan	SGUR10110	6671906	702086	Magnetite-Calc silicate skarn	Skarn	3.71	2.36	1.35	0.5	0.17	0.06	0.05	0.23	0.01	0.7	0.01	0.4	0.08	0.2	0.04	0.01	1	0.05	0.2
Markdalsgruvan	SGUR10113	6671295	702884	Magnetite-Calc silicate skarn	Skarn	358.71	204.5	154.21	80.8	17.1	9.27	3.45	15	3.62	14.1	0.96	60.4	13.7	14.05	2.64	1.33	112.5	6.79	3
Berggruvan, Sörviksfältet	SGUR00939	6672745	509090	Magnetite-Calc silicate skarn	Skarn	95.67	74	21.67	30.9	2.65	1.46	0.7	3.04	0.54	17.7	0.21	14.2	3.58	2.98	0.44	0.18	15	1.19	0.9
Sörviksfältet, Berggruvan	SGUR00940	6672745	509090	Magnetite-Calc silicate skarn	Skarn	124.13	94.79	29.34	38.3	3.33	2.01	0.92	3.89	0.68	21	0.26	17.7	4.5	3.88	0.6	0.29	20.4	1.77	4.6
Sörviksfältet, Berggruvan	SGUR00941	6672745	509090	Magnetite-Calc silicate skarn	Skarn	70.81	48.26	22.55	19.6	2.48	1.72	0.57	2.65	0.55	11.7	0.28	9	2.24	1.9	0.38	0.27	15.1	1.77	0.6
Källmossgruvorna	SGUR00950	6663677	509885	Magnetite-Calc silicate skarn	Skarn	41.96	29.89	12.07	12.2	1.45	0.65	0.69	1.78	0.22	6.2	0.09	5.9	1.36	1.46	0.26	0.07	8.7	0.63	0.3
Finnäset	SGUR00951	6667600	508230	Magnetite-Calc silicate skarn	Skarn	258.02	231.13	26.89	105.5	3.32	1.67	2.34	4.59	0.63	64.3	0.23	35.3	10.6	6.7	0.62	0.23	18.6	1.59	1.8
Finnäset	SGUR00952	6667600	508230	Magnetite-Calc silicate skarn	Skarn	74.86	66.98	7.88	29	0.97	0.47	0.87	1.54	0.15	15.8	0.06	11.6	3.1	2.37	0.17	0.03	5.6	0.43	2.7
Dalgruvan, Finnäsfältet	SGUR00954	6667456	508223	Magnetite-Calc silicate skarn	Skarn	333.66	317.34	16.32	146.5	2.21	1.1	1.16	3.59	0.4	108.5	0.17	38	12.55	5.24	0.41	0.18	10.7	1.15	1.8

Table 1. *Continuation.*

Locality	Sample	x	y	Type	Beskrivning	TotREE	LREE	HREE	Ce	Dy	Er	Eu	Gd	Ho	La	Lu	Nd	Pr	Sm	Tb	Tm	Y	Yb	Sc
Dalgruvan, Finnäset	SGUR00957	6667456	508223	Magnetite-Calc silicate skarn	Skarn	261.47	247.04	14.43	113	1.97	1.04	1.35	2.83	0.36	90.4	0.13	25.3	8.98	3.48	0.37	0.14	9.5	0.92	1.7
Dalgruvan, Finnäset	SGUR00959	6667456	508223	Magnetite-Calc silicate skarn	Skarn	85.91	74.27	11.64	33.4	1.46	0.81	0.53	1.87	0.27	18.7	0.13	12.2	3.31	2.26	0.26	0.11	7.8	0.8	2
Finnäset	SGUR00960	6667600	508230	Magnetite-Calc silicate skarn	Skarn	336.92	313.47	23.45	145	3.31	1.75	1.88	3.77	0.6	106.5	0.25	36.5	12.2	5.42	0.55	0.22	15	1.77	2.2
Timansberg	SGUR00974	6609890	491027	Magnetite-Calc silicate skarn	Skarn	28.49	14.82	13.67	4.7	1.75	0.92	0.44	1.64	0.3	3.1	0.19	2.6	0.59	1.35	0.28	0.12	9	1.11	0.4
Dalkarlsberg	SGUR00978	6588705	492570	Magnetite-Calc silicate skarn	Skarn	1170.52	1139.61	30.91	568	4.31	2.1	2.48	8.93	0.78	359	0.31	137	46.9	16	0.97	0.3	20.1	2.04	1.3
Dalkarlsberg	SGUR00984	6588705	492570	Magnetite-Calc silicate skarn	Skarn	682.07	665.79	16.28	328	2.41	0.88	1.09	6.6	0.38	205	0.06	85.8	28.6	10.5	0.67	0.07	11.3	0.51	0.2
Tabergsgruvorna	SGUR00990	6598013	498938	Magnetite-Calc silicate skarn	Skarn	174.95	65.12	109.83	16.8	15.45	6.78	1.71	13.65	2.8	9.3	0.75	13	2.38	8.08	2.56	0.94	75.1	5.45	0.2
Vretgruvan	SGUR00991	6593042	492335	Magnetite-Calc silicate skarn	Skarn	59.12	45.8	13.32	19.3	1.4	0.86	0.47	1.57	0.27	12.1	0.11	7.7	2	1.66	0.23	0.1	9.5	0.85	1
Långgruvan	SGUR00995	6516616	619024	Magnetite-Calc silicate skarn	Skarn	19.25	13.59	5.66	4.7	0.62	0.41	0.25	0.62	0.14	3.6	0.05	2.4	0.56	0.56	0.1	0.04	3.9	0.4	0.9
Förola	SGUR00997	6522424	623089	Magnetite-Calc silicate skarn	Skarn	48.72	41.17	7.55	17.2	0.95	0.48	0.4	1.06	0.16	11.6	0.05	6.8	1.82	1.29	0.18	0.03	5.2	0.5	1
Förola	SGUR00999	6522424	623089	Magnetite-Calc silicate skarn	Skarn	134.01	118.48	15.53	51.3	1.98	1.01	1.19	2.74	0.39	31.3	0.18	20.4	5.53	3.92	0.35	0.13	10.4	1.09	2.1
Bredsjönäs	SGUR10214	6565554	618134	Magnetite-Calc silicate skarn	Skarn	8.16	5.58	2.58	1.7	0.25	0.16	0.04	0.16	0.05	1.4	0.02	0.8	0.21	0.17	0.03	0.01	1.9	0.16	1.1
Bredsjönäs	SGUR10216	6565554	618134	Magnetite-Calc silicate skarn	Skarn	15.62	12.52	3.1	4.6	0.28	0.24	0.16	0.5	0.06	2.9	0.01	2.1	0.57	0.49	0.06	0.01	2.3	0.14	1.2
Bredsjönäs	SGUR10218	6565554	618134	Magnetite-Calc silicate skarn	Skarn	12.12	10.06	2.06	3.5	0.16	0.13	0.07	0.34	0.04	2.8	0.01	1.7	0.41	0.24	0.03	0.01	1.6	0.08	1
Bredsjönäs	SGUR10219	6565554	618134	Magnetite-Calc silicate skarn	Skarn	19.66	15.54	4.12	6.3	0.5	0.25	0.14	0.55	0.07	3.7	0.02	2.6	0.67	0.58	0.07	0.01	3	0.2	1
Gullebo	SGUR10230	6445222	564422	Magnetite-Calc silicate skarn	Skarn	931.33	671.54	259.79	270	35.2	18.1	4.64	37.7	6.65	100.5	1.78	168	37.9	39.6	5.93	2.38	176.5	13.25	13.2
Hylleled	SGUR10232	6433536	580680	Magnetite-Calc silicate skarn	Skarn	4082.76	975.26	3107.5	220	365	216	6.16	258	73.9	82.6	31.6	195	34.2	119.5	54.2	32.8	2120	214	59.8
Tjusta	SGUR10237	6440315	579150	Magnetite-Calc silicate skarn	Skarn	98.99	63.8	35.19	24.6	3.86	2.3	0.72	3.51	0.82	13.9	0.34	11.8	2.8	2.77	0.61	0.31	24.7	2.25	3.7
Tjusta	SGUR10238	6440315	579150	Magnetite-Calc silicate skarn	Skarn	76.76	42.56	34.2	16.3	3.58	2.28	0.48	3.22	0.71	8.8	0.27	8.4	1.95	2.21	0.56	0.31	24.6	1.89	1.2
Tjusta	SGUR10239	6440315	579150	Magnetite-Calc silicate skarn	Skarn	80.79	53.01	27.78	21	2.59	1.7	0.72	2.67	0.59	11.2	0.28	10.3	2.5	2.22	0.44	0.25	20.3	1.63	2.4
Nartorp	SGUR10250	6471962	591966	Magnetite-Calc silicate skarn	Skarn	99.34	81.97	17.37	36.5	1.9	1.36	0.42	1.81	0.4	26.9	0.21	10.6	3.28	2.16	0.32	0.16	11.6	1.42	0.3
Nartorp	SGUR10252	6471962	591966	Magnetite-Calc silicate skarn	Skarn	193.53	169.63	23.9	82	2.17	1.55	2.28	2.1	0.47	33.3	0.29	34.3	10.6	3.25	0.37	0.23	16.9	1.92	1.8
Petängen	SGUR10255	6463381	597709	Magnetite-Calc silicate skarn	Skarn	189.88	134.67	55.21	58.2	5.76	4.09	2.02	5.53	1.27	18.8	0.63	33.7	8.51	6.21	0.87	0.55	38	4.04	1.7
Källhagen	SGUR10256	6423597	581350	Magnetite-Calc silicate skarn	Skarn	1670.67	526.94	1143.73	122	127.5	73.1	1.44	109	25.9	35.8	9.18	141	23	66.1	20.1	10.35	814	63.6	28.6

Table 1. *Continuation.*

Locality	Sample	x	y	Type	Beskrivning	TotREE	LREE	HREE	Ce	Dy	Er	Eu	Gd	Ho	La	Lu	Nd	Pr	Sm	Tb	Tm	Y	Yb	Sc
BAST140001	Bastnäs	6634470	532926	Magnetite-Calc silicate skarn	Skarnjärnmalm	38078.37	33149.3	4929.07	10000	792	160	146.5	1000	98.8	10000	7.57	10000	1000	1000	229	13.2	3570	58.5	2.8
PNY130001	Bastnäs	6634425	533003	Magnetite-Calc silicate skarn	Bastnäs	37907.16	33134	4773.16	10000	852	150	132	1000	94.7	10000	4.11	10000	1000	1000	262	11.25	3360	39.1	2
PNY130002	Stålklockan	6635388	532811	Magnetite-Calc silicate skarn	Stålklockan	5128.66	4958.13	170.53	2170	33	5.72	9.23	129.5	3.67	1110	0.24	1065	276	198	10.9	0.52	114.5	1.98	0.4
PNY130003	Stålklockan	6635388	532811	Magnetite-Calc silicate skarn	Stålklockan	1600.17	1475.78	124.39	647	17.55	5.6	3.58	38.2	2.71	350	0.42	302	80.1	53.9	4.09	0.68	90.1	3.24	1
PNY130004	Stålklockan	6635390	532824	Magnetite-Calc silicate skarn	Stålklockan	5241.48	5013.29	228.19	2250	37.9	8.04	7.99	108	4.76	1310	0.43	925	258	154	10.4	0.78	162.5	3.38	0.3
PNY130005	Stålklockan	6635349	532852	Magnetite-Calc silicate skarn	Stålklockan	45511.94	34001.2	11510.74	10000	1000	406	1000	1000	302	10000	7.24	10000	1000	1000	890	25.8	8810	69.7	1.2
PNY130006	Persgruvan	6634264	531497	Magnetite-Calc silicate skarn	Persgruvan	2461.68	2242.61	219.07	985	32.6	10.5	7.91	66.8	4.98	523	0.58	454	119.5	84.6	6.99	1.01	157.5	4.91	1.8
PNY130007	Lerklockan	6634403	531718	Magnetite-Calc silicate skarn	Lerklockan	490.62	450.72	39.9	197.5	5.73	1.88	2.12	11.8	0.85	123.5	0.18	78.4	21.8	15	1.29	0.24	28.4	1.33	0.6
PNY130008	Lerklockan	6634460	531811	Magnetite-Calc silicate skarn	Lerklockan	381.99	128.49	253.5	28.6	33.7	11.9	3.84	37.3	5.38	16.7	0.57	21.4	4.15	16.3	5.99	1.15	189.5	5.31	0.2
PNY130011A	Malmkärra	6658328	547092	Magnetite-Calc silicate skarn	Malmkärra	4604.5	4083.55	520.95	1690	104	30.9	15.85	163.5	14.65	1180	1.82	679	183	169	22.4	3.63	326	17.55	3.2
PNY130011B	Malmkärra	6658328	547092	Magnetite-Calc silicate skarn	Malmkärra	3391.17	3015.5	375.67	1255	78.4	23.7	5.9	138.5	10.95	714	1.5	594	149.5	158	17.55	2.77	226	14.8	0.6
PNY130012	Malmkärra	6658328	547092	Magnetite-Calc silicate skarn	Malmkärra	1593.54	1032.69	560.85	383	118	48	4.59	96.2	19.4	245	3.21	188	45.2	69.9	18.95	6.09	315	32.2	0.8
PNY130013	Johanna	6658660	550883	Magnetite-Calc silicate skarn	Johanna	14007.95	12965.9	1042.05	5780	130.5	45.7	30.8	306	19.8	3370	3.59	2400	660	418	30.4	5.36	778	28.7	1.1
PNY130014	Johanna	6658683	550966	Magnetite-Calc silicate skarn	Johanna	114.79	104.03	10.76	46.3	1.66	0.59	0.43	2.77	0.21	25	0.06	19.4	5.36	4.07	0.39	0.06	7.2	0.59	0.7
PNY130015	Östanmossa	6660543	551764	Magnetite-Calc silicate skarn	Östanmossa	30318.81	28849.8	1469.01	10000	227	54.2	86.5	823	27.6	8940	3.24	7000	1000	1000	69.5	5.67	1055	26.8	0.3
PNY130016	S. Hack-spiksgr	6659832	552272	Magnetite-Calc silicate skarn	S. Hackspiksgr	519.81	422.3	97.51	196	11.5	6.45	5.8	12.45	2.28	107	0.92	67.2	19	13.85	1.91	0.88	67.4	6.17	1
Rödbergsgruvan A	Rödbergs-gruvan A	6597194	494237	Magnetite-Calc silicate skarn	Rödbergsgruvan A	30536.17	29378.5	1157.67	10000	171	39.7	28.2	583	22	9660	1.74	7150	1000	957	48.3	3.68	857	14.25	0.3
Rödbergsgruvan B	Rödbergs-gruvan B	6597194	494237	Magnetite-Calc silicate skarn	Rödbergsgruvan B	406.69	242.86	163.83	86.6	17.9	7.07	6.41	20.9	3.11	53.7	0.65	49.2	11.2	14.45	3.15	1.03	125.5	5.42	0.4
Gyttorp	Gyttorp	6597427	497660	Magnetite-Calc silicate skarn	Gyttorp	37069	33233.2	3835.8	10000	896	197	198	1000	102.5	10000	14.7	10000	1000	1000	256	22.1	2230	117.5	35.2
BAST140001	Bastnäs	6634470	532926	Magnetite-Calc silicate skarn		38078.37	33149.3	4929.07	10000	792	160	146.5	1000	98.8	10000	7.57	10000	1000	1000	229	13.2	3570	58.5	2.8
Stora Stripagruvan	TOB150041A	6631944	533732	Magnetite-hematite-quartz (BIF)	Kvartsbandad hematit-magnetitmalm	115.15	87.04	28.11	35.1	3.34	1.72	0.68	4.04	0.71	18.1	0.23	17	4.36	3.86	0.7	0.25	19.7	1.46	3.9
Stora Stripagruvan	TOB150041B	6631944	533732	Magnetite-hematite-quartz (BIF)	Kvartsbandad hematit-magnetitmalm	82.18	61.6	20.58	24.9	2.23	1.1	1.45	2.86	0.45	14.5	0.19	11.4	3.03	2.56	0.5	0.16	14.9	1.05	0.9
St. Östergruvan (Myrbacksfältet)	TOB150042A	6632944	531900	Magnetite-hematite-quartz (BIF)	Rostig kvartsrik magnetitmalm	1712.74	1663.4	49.34	794	6.49	3.2	8.4	11.7	1.2	542	0.5	209	73.7	21	1.45	0.48	32.9	3.12	3.6
St.Östergruvan (Myrbacksfältet)	TOB150042B	6632944	531900	Magnetite-hematite-quartz (BIF)	Rostig kvartsrik magnetitmalm	502.21	473.69	28.52	222	3.27	1.67	3.86	5.39	0.62	148.5	0.23	63.6	21.3	8.24	0.67	0.25	20.2	1.61	0.8

***Table 1.** Continuation.*

Locality	Sample	x	y	Type	Beskrivning	TotREE	LREE	HREE	Ce	Dy	Er	Eu	Gd	Ho	La	Lu	Nd	Pr	Sm	Tb	Tm	Y	Yb	Sc
Kanntalsgruvan	TOB150043A	6632354	530860	Magnetite-hematite-quartz (BIF)	Magnetit-kvartsmalm med kopparkis-impregnation	432.69	350.67	82.02	155	6.69	3.62	1.77	10.65	1.42	83.2	0.48	66.4	17.8	13.05	1.3	0.55	64.7	3.26	2.8
Stora Bastnäs gruvan	TOB150047A	6634413	532917	Magnetite-hematite-quartz (BIF)	Kvartsrik bandad hematit-magnetitmalm	536.24	461.75	74.49	191	7.78	3.27	9.5	11.05	1.51	159.5	0.27	60.2	18.15	11.55	1.56	0.39	57.8	1.91	0.8
Stora Bastnäs gruvan	TOB150047B	6634413	532917	Magnetite-hematite-quartz (BIF)	Kvartsrik bandad hematit-magnetitmalm	408.93	389.02	19.91	169.5	2.44	0.81	5.28	6.89	0.4	122.5	0.1	57.2	17.05	10	0.67	0.12	14.7	0.67	0.6
Östra Åtorps gruvan	TOB150052A	6635382	533631	Magnetite-hematite-quartz (BIF)	Kvarts-magnetit-hematitmalm	1081.31	991.35	89.96	442	12.1	4.8	5.65	21.2	2.18	290	0.55	155	45.1	28	2.59	0.69	63.1	3.95	4.4
Östra Åtorps gruvan	TOB150052B	6635382	533631	Magnetite-hematite-quartz (BIF)	Kvarts-magnetit-hematitmalm	385.23	355.05	30.18	161.5	4.16	1.31	2.85	8.35	0.64	102.5	0.07	53.8	16.5	9.45	0.93	0.12	22.3	0.65	0.1
Stora Högfors gruvan	TOB150053A	6636541	534267	Magnetite-hematite-quartz (BIF)	Kvarts-magnetit-hematitmalm	1133.13	1109.47	23.66	511	4.37	1.14	4.62	19.05	0.55	288	0.07	195.5	56.8	34	1.42	0.14	15.4	0.57	0.5
Stora Högfors gruvan	TOB150053B	6636541	534267	Magnetite-hematite-quartz (BIF)	Kvarts-magnetit-hematitmalm	8589.41	7995.6	593.81	3420	87.9	30.8	24	193	14.6	1695	1.84	1885	470	308	20.9	3.42	418	16.35	0.6
Munkgruvan	TOB150066A	6658783	550162	Magnetite-hematite-quartz (BIF)	Hematit-felsiskmeta-vulkanit	175.91	135.14	40.77	57.1	4.28	2.65	1	4.59	0.94	34.7	0.43	23.9	6.61	4.74	0.74	0.39	28.9	2.44	2.5
Munkgruvan	TO-B150066B	6658783	550162	Magnetite-hematite-quartz (BIF)	Hematit-kvartsgång/mjölkkvarts	12.92	9.03	3.89	3.5	0.42	0.22	0.08	0.29	0.09	2.9	0.02	1.4	0.39	0.27	0.08	0.01	2.8	0.25	0.2
Stålgruvan	TOB150067A	6663543	553710	Magnetite-hematite-quartz (BIF)	Magnetit-hematit-kvarts/metavulkanit	75.82	61.75	14.07	26.4	1.94	1	0.47	1.97	0.39	14.8	0.17	12.1	3.08	2.23	0.34	0.06	9.2	0.97	0.7
Stålgruvan	TOB150067B	6663543	553710	Magnetite-hematite-quartz (BIF)	Magnetit-hematit-kvarts/metavulkanit	201.57	180.62	20.95	78.5	2.9	0.94	1.96	4.83	0.5	51.2	0.08	29.8	8.54	5.59	0.61	0.04	15.3	0.58	0.2
Knutsbo gruvor	KNUT2	6662595	577230	Magnetite-hematite-quartz (BIF)	Kvartsbandad hematitmalm	147.73	126.65	21.08	54.4	2.96	0.81	2.32	3.86	0.5	38.7	0.07	18.1	5.46	3.71	0.63	0.05	15.5	0.56	0.1
S Gamla Bastnäsfältet	cmr150055a	6633789	532691	Magnetite-hematite-quartz (BIF)	Siltstensbandad hematitmalm	448.15	362.81	85.34	154.5	9.79	5.57	2.31	12	2.09	95.5	0.74	66.5	17.35	12.75	1.83	0.81	59.6	4.91	1.9
S Gamla Bastnäsfältet	cmr150055b	6633805	532740	Magnetite-hematite-quartz (BIF)	Skarnbandad hematitmalm, varp	404.41	343.99	60.42	144.5	7.21	3.54	2.34	11.1	1.51	98.9	0.36	58.7	16.1	11.65	1.39	0.45	43.5	2.46	0.7
Bojmossfältet, Norberg	cmr150061a	6658010	550156	Magnetite-hematite-quartz (BIF)	Hematitmalm med kvartsådra, varp	43.61	27.47	16.14	7	1.9	0.91	0.71	2.85	0.39	2.3	0.08	9.2	1.29	3.12	0.33	0.11	11.7	0.72	1
Bybergsgruvan	SGUR10042	6666790	508285	Magnetite-hematite-quartz (BIF)	Kvartsrik	111.6	101.97	9.63	38.9	1.15	0.56	1.86	1.39	0.17	43.1	0.07	9.5	3.12	1.5	0.19	0.07	6.8	0.62	2.6
Bybergsgruvan	SGUR10047	6666790	508285	Magnetite-hematite-quartz (BIF)	Kvartsrik	72.31	71.01	1.3	28.7	0.21	0.06	0.56	0.7	0.02	30.2	0.01	7.3	2.34	1.01	0.06	0.01	0.9	0.03	0.2
Bovins gruva, Sörviksfältet	SGUR00942	6672437	508762	Magnetite-hematite-quartz (BIF)	Kvartsrik	50.33	46.63	3.7	21	0.53	0.19	0.37	0.69	0.07	14.5	0.01	6	1.96	1.31	0.12	0.01	2.6	0.17	0.8
Bovinsgruvan, Sörviksfältet	SGUR00943	6672437	508762	Magnetite-hematite-quartz (BIF)	Kvartsrik	149.41	133.23	16.18	60.7	2	1.06	1.29	2.85	0.41	41.2	0.18	17.4	5.27	3.12	0.38	0.16	11	0.99	1.4
Bovinsgruvan, Sörviksfältet	SGUR00944	6672437	508762	Magnetite-hematite-quartz (BIF)	Kvartsrik	175.47	167.43	8.04	76.5	1.16	0.47	0.96	1.86	0.18	57.4	0.06	20.4	6.31	3	0.23	0.05	5.4	0.49	1
Ikorrbotten	SGUR00945	6670805	509885	Magnetite-hematite-quartz (BIF)	Kvartsrik	61.12	56.15	4.97	23.5	0.63	0.23	0.57	1.44	0.09	18.3	0.01	8	2.35	1.59	0.15	0.01	3.7	0.15	0.4
Ikorrbotten	SGUR00946	6670805	509885	Magnetite-hematite-quartz (BIF)	Kvartsrik	483.61	449.01	34.6	207	3.5	2.52	2.42	3.8	0.84	164	0.46	45.3	16.2	6.39	0.59	0.42	23.4	2.87	3.9
Stavs gruva	SGUR10209	6545499	580036	Magnetite-hematite-quartz (BIF)	Kvartsrik	286.79	227.82	58.97	100.5	5.85	4.44	1.4	4.88	1.4	67.4	0.8	32.3	9.61	5.83	0.84	0.71	40.1	4.83	5.9
Stavs gruva	SGUR10210	6545499	580036	Magnetite-hematite-quartz (BIF)	Kvartsrik	157.22	132.11	25.11	57.9	3.38	1.81	1.52	3.66	0.64	34	0.18	21.3	6.1	4.43	0.54	0.2	16.9	1.46	3.2

Table 1. Continuation.

Locality	Sample	x	y	Type	Beskrivning	TotREE	LREE	HREE	Ce	Dy	Er	Eu	Gd	Ho	La	Lu	Nd	Pr	Sm	Tb	Tm	Y	Yb	Sc
Oltorp	SGUR10247	6446783	589170	Magnetite-hematite-quartz (BIF)	Kvartsrik	66.06	41.89	24.17	16.3	2.49	1.67	0.34	2.28	0.53	8.3	0.25	8.5	1.94	1.93	0.38	0.24	17	1.61	2.3
Gränsö södra gruva	SGUR10254	6401039	601363	Magnetite-hematite-quartz (BIF)	Kvartsrik	4468.68	4322.14	146.54	2060	26.2	7.86	7.74	68.9	3.57	973	0.7	824	233	130.5	7.02	0.95	95.3	4.94	25
Lilla Högfors gruvan	TOB150054A	6636515	534067	Magnetite-Mg-silicate skarn	Talk-antofyllit-magnetitskarn	345.04	326.68	18.36	157	1.96	0.89	0.83	4.25	0.44	105	0.15	39.1	13.55	5.55	0.44	0.12	13.7	0.66	1.4
Lilla Högfors gruvan	TOB150054B	6636515	534067	Magnetite-Mg-silicate skarn	Talk-antofyllit-magnetitskarn	166.56	108.86	57.7	38.8	6.27	2.67	1.43	9.18	1.19	17.8	0.23	26.7	5.81	8.54	1.28	0.3	44.1	1.66	0.6
Eriksbergsgruvan 2	TOB150055A	6636751	533975	Magnetite-Mg-silicate skarn	Magnetit-antofyllit-skarn	121.86	62.39	59.47	22.7	7.83	3.88	0.37	6.52	1.49	10.5	0.5	13.8	3.24	4.76	1.29	0.56	40.2	3.72	0.5
Eriksbergsgruvan 2	TOB150055B	6636751	533975	Magnetite-Mg-silicate skarn	Magnetit-antofyllit-skarn	155.55	91.84	63.71	37.1	7.14	3.85	0.39	6.03	1.4	18.1	0.69	18.8	4.94	6.18	1.16	0.61	44	4.86	0.3
Morens Öster gruvan	TOB150059A	6643914	540720	Magnetite-Mg-silicate skarn	Magnetit-(hematit)-kvarts antofyllitskarn	280.77	228.94	51.83	103	5.9	3.23	0.88	5.72	1.2	55	0.36	42.8	12	7.54	0.92	0.4	37.3	2.52	2
Morens Öster gruvan	TOB150059B	6643914	540720	Magnetite-Mg-silicate skarn	Magnetit-(hematit)-kvarts antofyllitskarn	1739.71	1552.59	187.12	684	29	9.27	8.99	47.6	4.29	418	0.52	262	75.9	54.9	6.16	0.94	132.5	4.44	1.2
Svavelbergets kisförekomst	TOB150057A	6637809	536489	Magnetite-(Fe-sulphide)-Calcsilicate skarn	Massiv sulfid med magnetkis-py-kopparkis	3665.41	3472.23	193.18	1535	45.2	10.9	3.33	91.2	6.07	721	0.64	770	205	146.5	11.2	1.2	112.5	5.47	0.2
Svavelbergets kisförekomst	TOB150057B	6637809	536489	Magnetite-(Fe-sulphide)-Calcsilicate skarn	Massiv sulfid med magnetkis-py-kopparkis	1728.05	1491.99	236.06	639	49	15.4	4.69	62.6	7.6	298	0.93	329	83.6	75	9.85	1.71	143.5	8.07	0.1
ALM140001	Almunge	6642082	675436	Nephelin syenite		298.77	247.35	51.42	112.5	5.73	3.36	1.84	6.6	1.11	60.9	0.69	43.6	12.95	7.36	0.97	0.56	34.4	4.6	1.6
ALM140002	Almunge	6641542	676032	Nephelin syenite		305.66	268.14	37.52	119.5	4.84	2.48	2.1	6.85	0.81	64.2	0.37	51.3	14	8.39	0.91	0.32	25.3	2.49	1.8
ALM140003	Almunge	6641569	676292	Nephelin syenite		120.92	102.05	18.87	46.2	1.84	1.35	0.8	2.19	0.37	28.7	0.29	16.3	4.81	2.55	0.29	0.21	12.8	1.72	0.5
ALM140004	Almunge	6640771	674898	Nephelin syenite		238.48	194.61	43.87	84.5	5.2	3.25	1.05	6.81	1.02	38.7	0.59	42.1	11.3	8.25	0.91	0.47	29	3.43	1.9
Tåresåive Mo-REE	ING090076A	7421196	709317	Pegmatite/aplite	Pulver från Dick C. (granit-pegmatit)	42651.2	33055.7	9595.5	10000	1000	764	34.2	1000	250	10000	130	10000	1000	1000	207	128.5	6280	836	21.5
SVEAFALLEN	SVEAFALLEN	6563279	467518	Pegmatite/aplite	Granit	13220.28	12579.35	640.93	5870	113	33.9	11.85	259	16.9	2720	2.09	2620	689	399	27.9	3.14	428	16	10.5
REU140001	Reunavaare	7342033	697981	Pegmatite/aplite		18206.9	13158.1	5048.8	6050	575	414	0.1	463	124	2870	91	2270	707	544	89.3	73.5	3110	572	254
REU140002	Reunavaare	7342208	697840	Pegmatite/aplite		4809.89	588.59	4221.3	127.5	370	395	0.59	163	97.1	38.2	96.3	126	23.3	86	43.8	64.1	2620	535	24
YBY140001	Ytterby	6592332	690226	Pegmatite/aplite		18695.4	3801.4	14894	983	1000	1000	24.4	1000	612	397	594	687	138	455	279	409	10000	1000	117
YBY140002	Ytterby	6592332	690226	Pegmatite/aplite		30624	13624	17000	3430	1000	1000	110	1000	1000	1005	1000	6130	814	1000	1000	1000	10000	1000	135
YBY140003	Ytterby	6592332	690226	Pegmatite/aplite		26418.9	10238.9	16180	2780	1000	1000	26.9	1000	812	563	1000	4090	693	1000	493	875	10000	1000	86
FLA140001	Flakaberget	7389427	703658	Pegmatite/aplite		15555.92	1627.42	13928.5	113.5	1000	1000	2.62	796	325	28.7	225	247	28.6	344	199	179.5	10000	1000	67
HOLM140001	Holmtjärn	6691407	514383	Pegmatite/aplite		29550.45	12550.45	17000	3290	1000	1000	19.45	1000	1000	950	1000	4290	741	1000	1000	1000	10000	1000	1260
SVEAFALLEN	SVEAFALLEN	6563279	467518	Pegmatite/aplite	magnetit	13220.28	12579.35	640.93	5870	113	33.9	11.85	259	16.9	2720	2.09	2620	689	399	27.9	3.14	428	16	10.5

APPENDIX 2

Hyper spectral infrared imaging

Hyperspectral imaging, or imaging spectroscopy, combines the power of digital imaging and spectro-scopy. In collaboration with a drill core scanning project at SGU, samples from the EURARE project have been scanned for hyper spectral imaging. More details on the drill core scanning project at SGU may be found on the SGU website (http://www.sgu.se/en/mineral-resources/geological-information-for-mineral-exploration/drill-core-collection/drill-core-scanning-at-sgu/).

Samples collected for the EURARE project were scanned. The scanner measures how visible and infrared light across different wavelength ranges is reflected from the surface of the samples. The scanning captured visible and near-infrared (VNIR), short-wavelength infrared (SWIR) and long-wavelength (LWIR) spectral images as well as a high-resolution optical RGB image, all in a single scan, directly from the samples.

Our aim was to see whether it is possible to distinguish REE-bearing minerals from other rock-forming silicates/oxides and compare the results with those from petrography and geochemistry studies on the samples. Theoretically, REEs produce absorption bands in the visible spectral range. The intensity of the reflected light in different ranges is measured using spectrometers. Different elements absorb the incoming light selectively at specific wavelengths, and individual minerals may be identified by their spectral signature. Rare earth oxides usually show specific signatures in VNIR and SWIR. Samples containing REE- bearing minerals can generally be distinguished within the VNIR spectrum, but mineralscontaining HREE present a different signature from samples with a higher concentration of LREE (e.g. in xenotime).

The VNIR spectral range is largely free from interference from common rock-forming minerals (except iron oxides), and REE mineralisations are typically mixtures predominantly made up of either LREE or HREE.

Selected images of hyper spectral infrared of the samples that contain REE mineralisation are shown in this appendix (Figs. 1 –7).

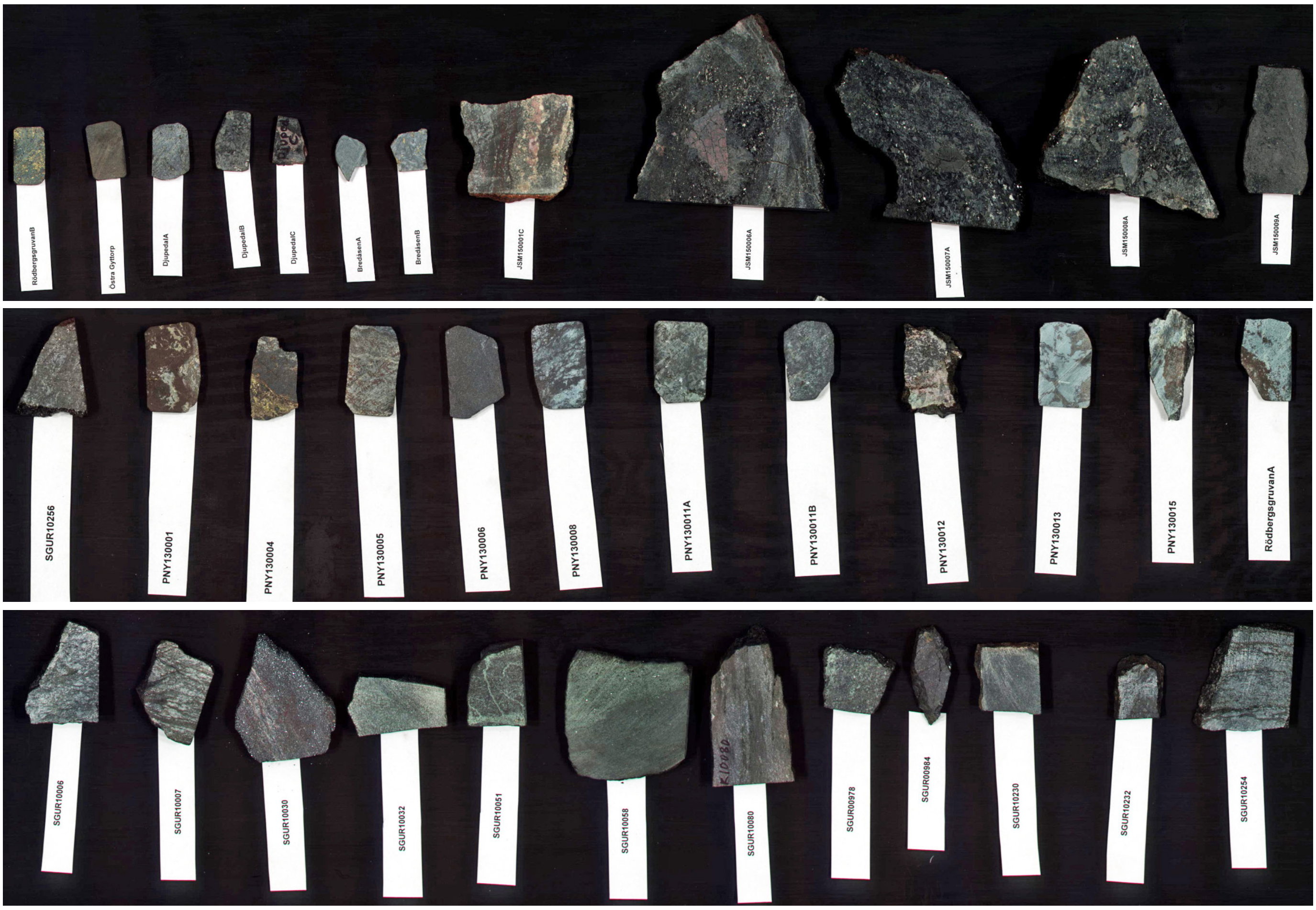

Figure 1. Optical image of the samples, pictures are take in visible light.

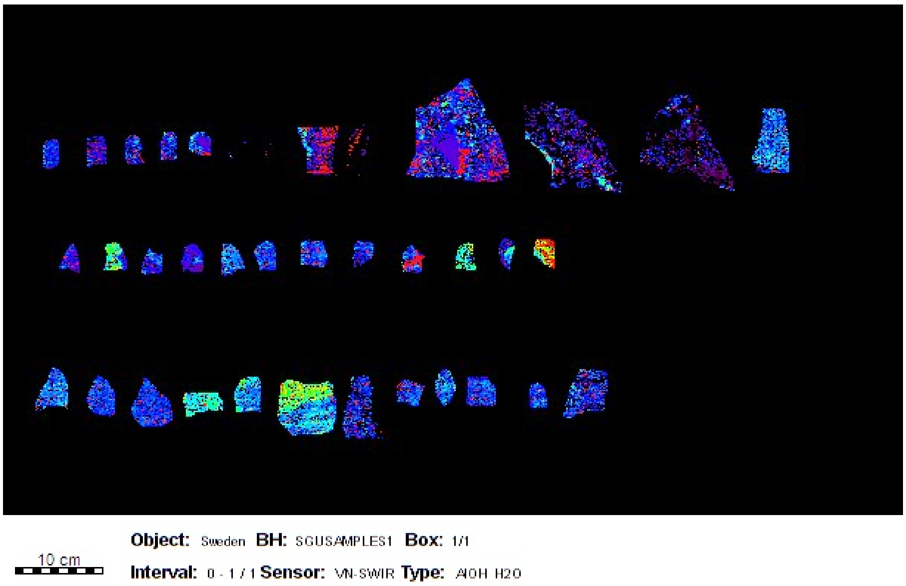

Figure 2. Spectral indices image of the samples in Figure 1. The image is complied by data from the VNIR to SWIR, representing AlOH H_2O indices which is the ratio between wavelength 1950nm and 2200nm, and provides a simpler means of evaluating bound water content with aluminous phyllosilicates.

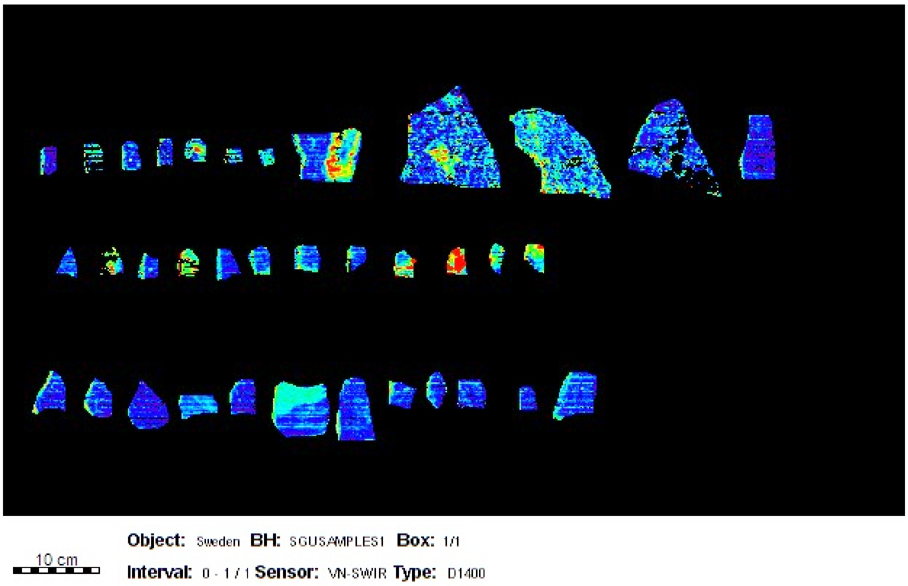

Figure 3. Spectral indices image of the samples in Figure 1. The image is complied by data from the VNIR to SWIR , representing wavelength 1400nm.

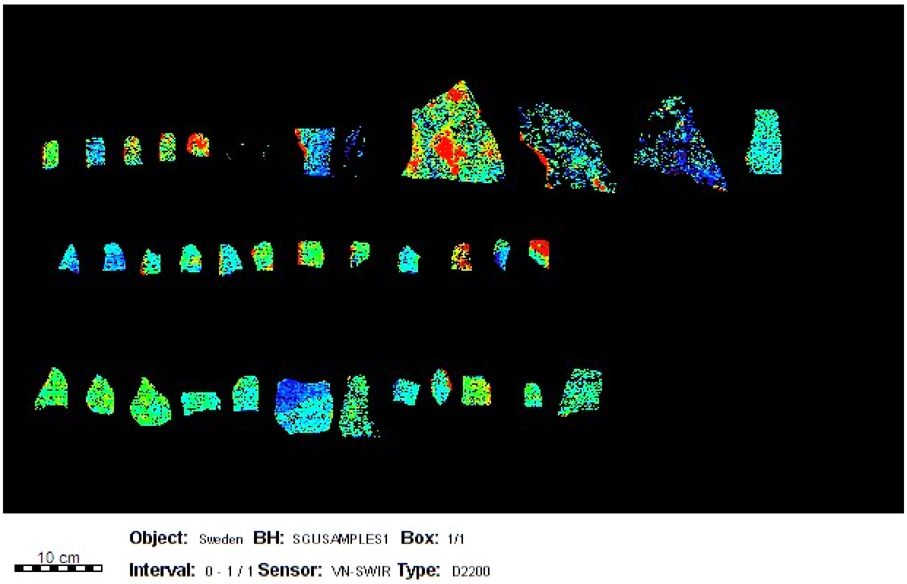

Figure 4. Spectral indices image of the samples in Figure 1. The image is complied by data from the VNIR to SWIR , representing wavelength 2200nm.

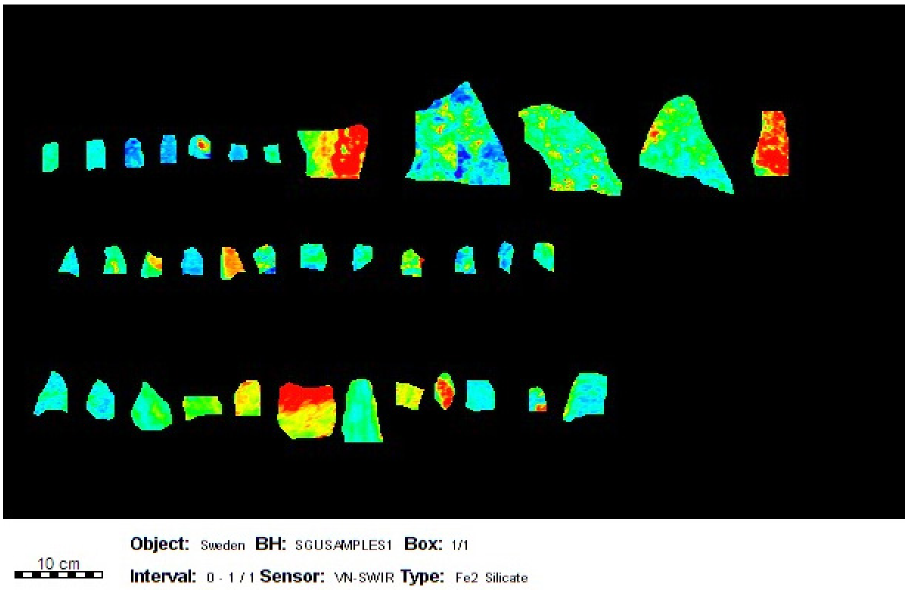

Figure 5. Spectral indices image of the samples in Figure 1. The image is complied by data from the VNIR to SWIR , representing Fe^2 Silicate indices which Is the ratio between the reflectance values at 1200 and 1600nm. Iron-bearing minerals, including iron oxides (but not magnetite) , iron carbonates (ankerite or siderite) and ferromagnesian minerals, have an absorption between 800 and 1000nm. Values >1 reflect the presence of iron-bearing minerals, while values <1 reflect their absence.

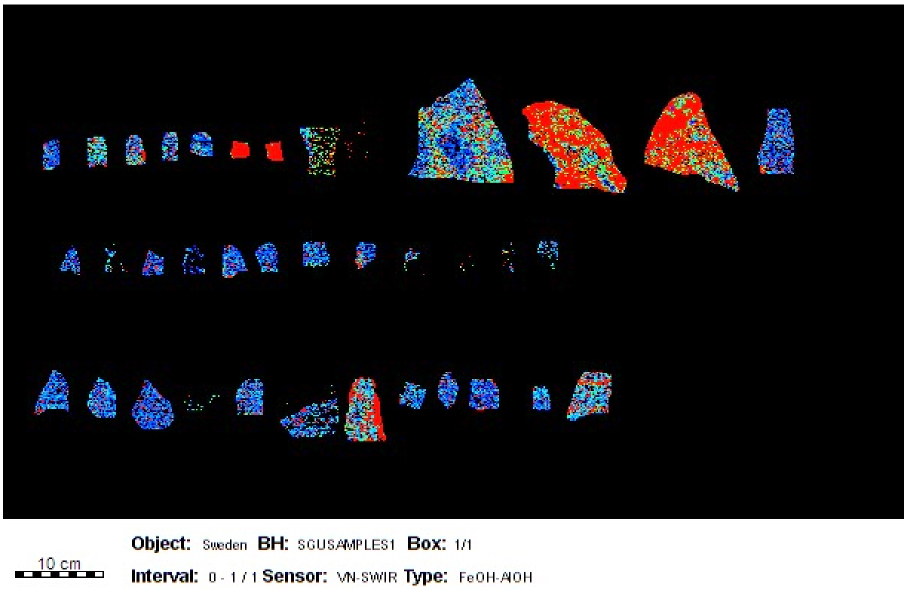

Figure 6. Spectral indices image of the samples in Figure 1. The image is complied by data from the VNIR to SWIR , representing FeOH-AlOH indices which is record of the ratio between the Fe^{2+}-OH and Mg-OH absorptions.

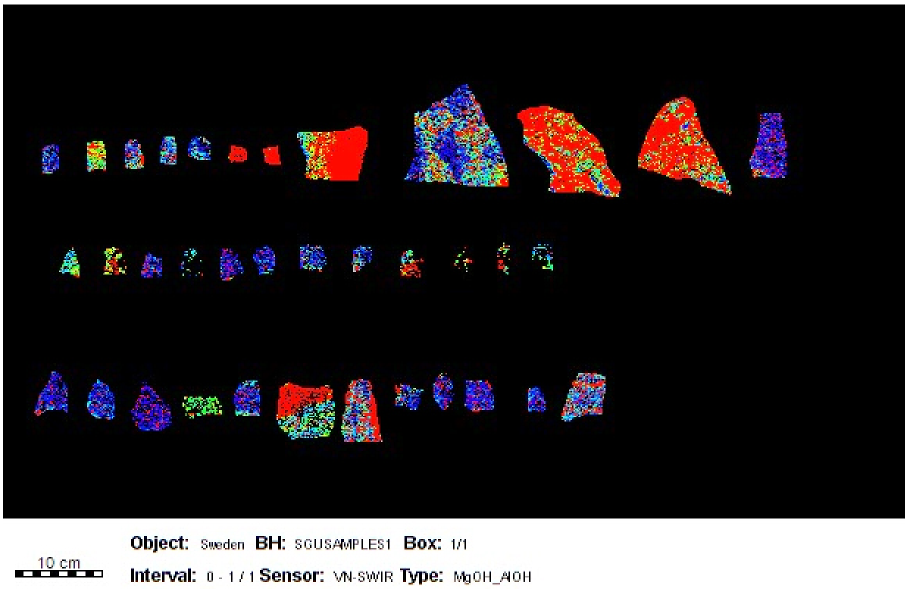

Figure 7. Spectral indices image of the samples in Figure 1. The image is complied by data from the VNIR to SWIR , representing MgOH-AlOH indices which is record of the ratio between the Al^{3+}-OH and Mg-OH absorptions.

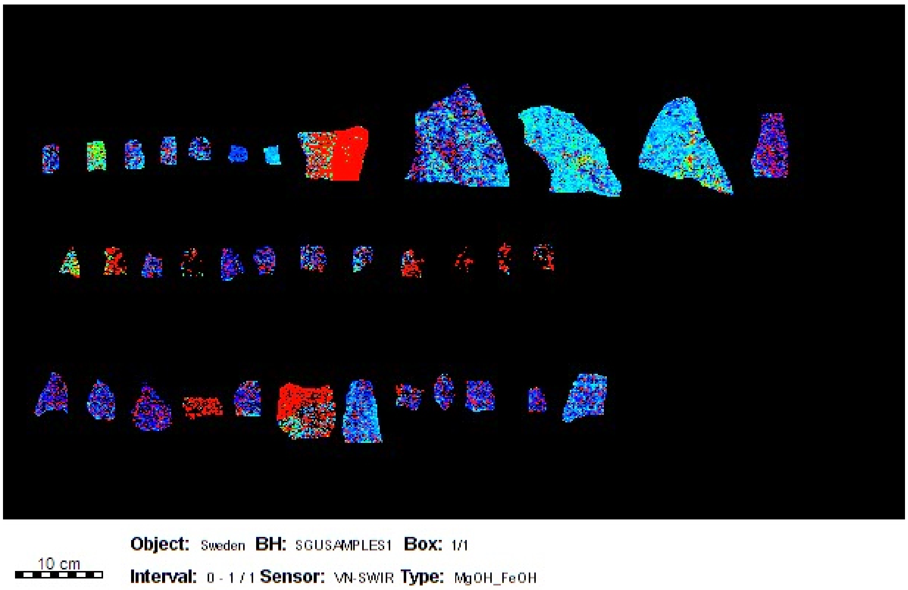

Figure 8. Spectral indices image of the samples in Figure 1. The image is complied by data from the VNIR to SWIR , representing MgOH-FeOH indices which is record of the ratio between the Fe^{2+}-OH and Mg-OH absorptions .

Geological Survey of Sweden
Box 670
SE-751 28 Uppsala
Phone: +46 18 17 90 00
Fax: +46 18 17 92 10
www.sgu.se

Uppsala 2018
ISSN 0349-2176
ISBN 978-91-7403-459-2